[Theoretical]

Astrophysics
(765649S)

II

VITALY NEUSTROEV

SPACE PHYSICS AND ASTRONOMY
RESEARCH UNIT
UNIVERSITY OF OULU

2026

Part II

Theoretical Astrophysics

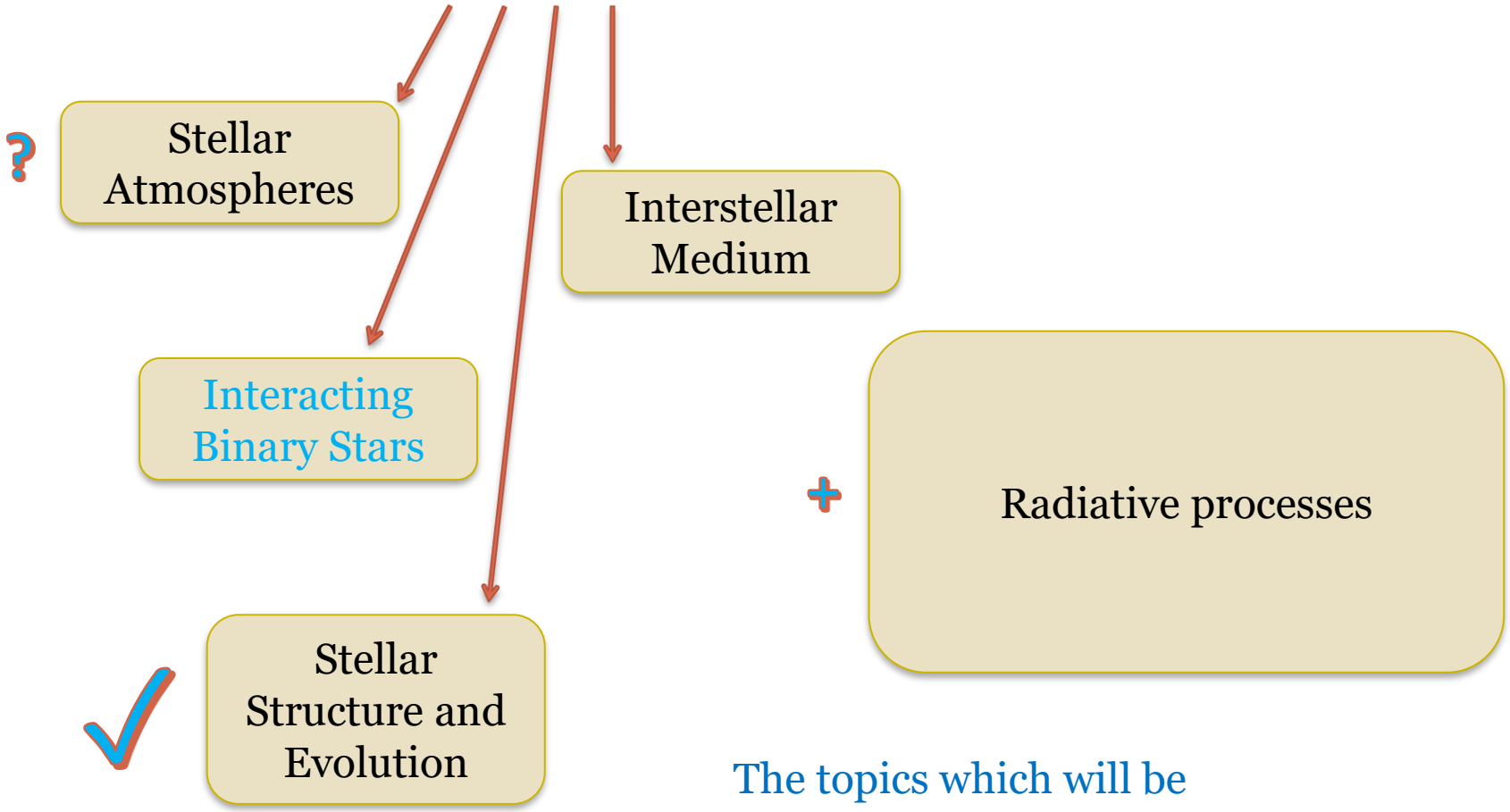

The topics which will be discussed in the given course

Stellar atmospheres

WHAT IS A STELLAR ATMOSPHERE?
WHY SHOULD WE CARE ABOUT IT?
WHAT CAN WE LEARN FROM OBSERVATIONS?

What is a stellar photosphere?

- Thin, tenuous transition zone between (invisible) stellar interior and (essentially vacuum) exterior.
- The "photosphere" is the visible disc, whilst the "atmosphere" also includes coronae and winds.
- In contrast with the interior, where convection may dominate, the energy transport mechanism of the atmosphere is radiation.
- Stellar atmospheres are primarily characterized by two parameters: ($T_{\rm eff}$, $\log g$).

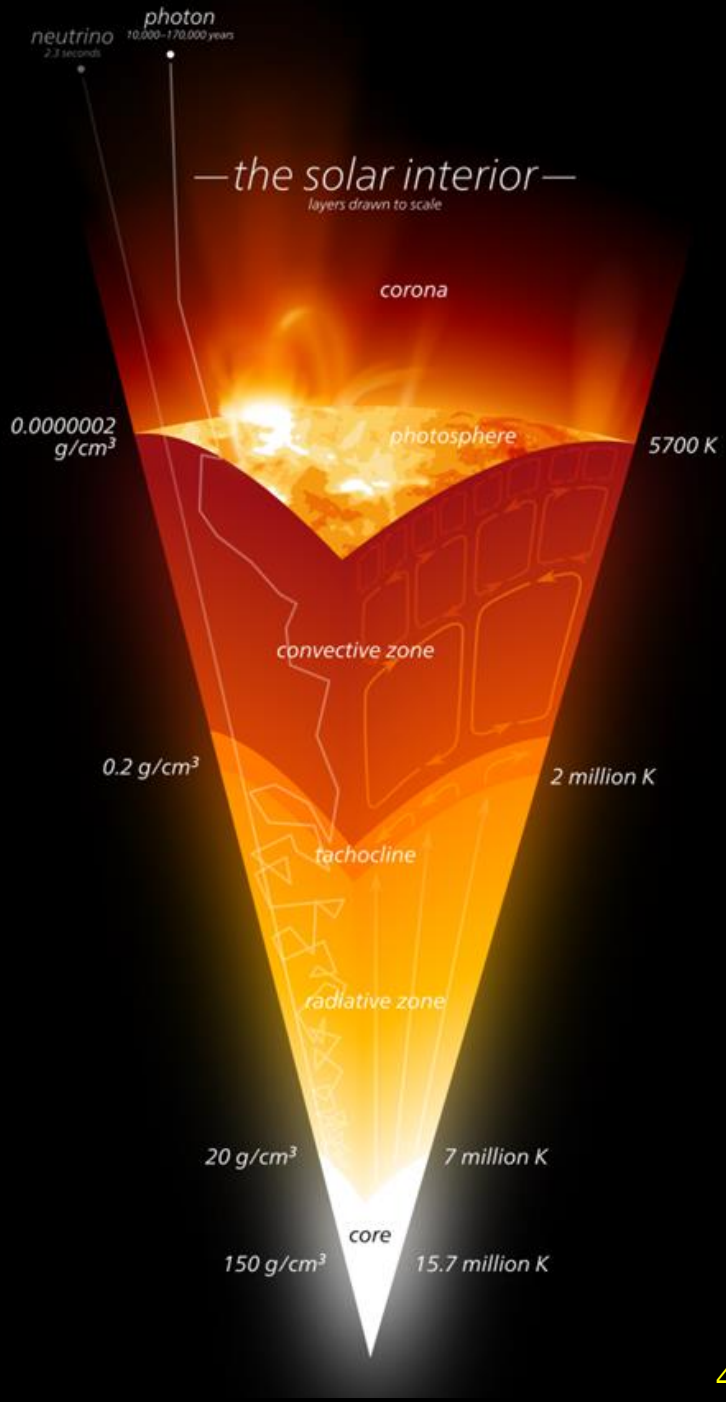

What is a stellar photosphere?

Thin zone between stellar interior and exterior:
ΔR_{sun}=a few$\times 10^{7}$ cm, $M_{atm}\sim 2\times 10^{21}$ g=$\sim 10^{-12}\ M_{\odot}$

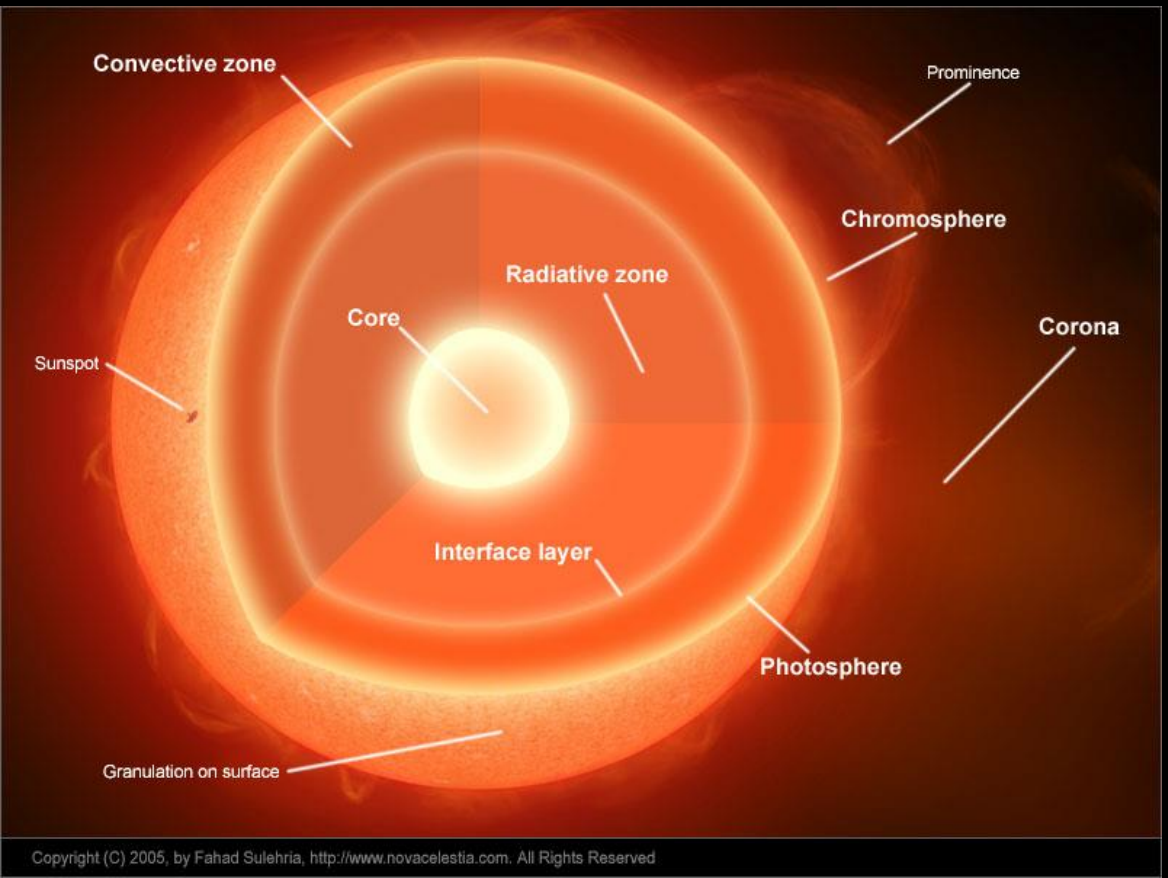

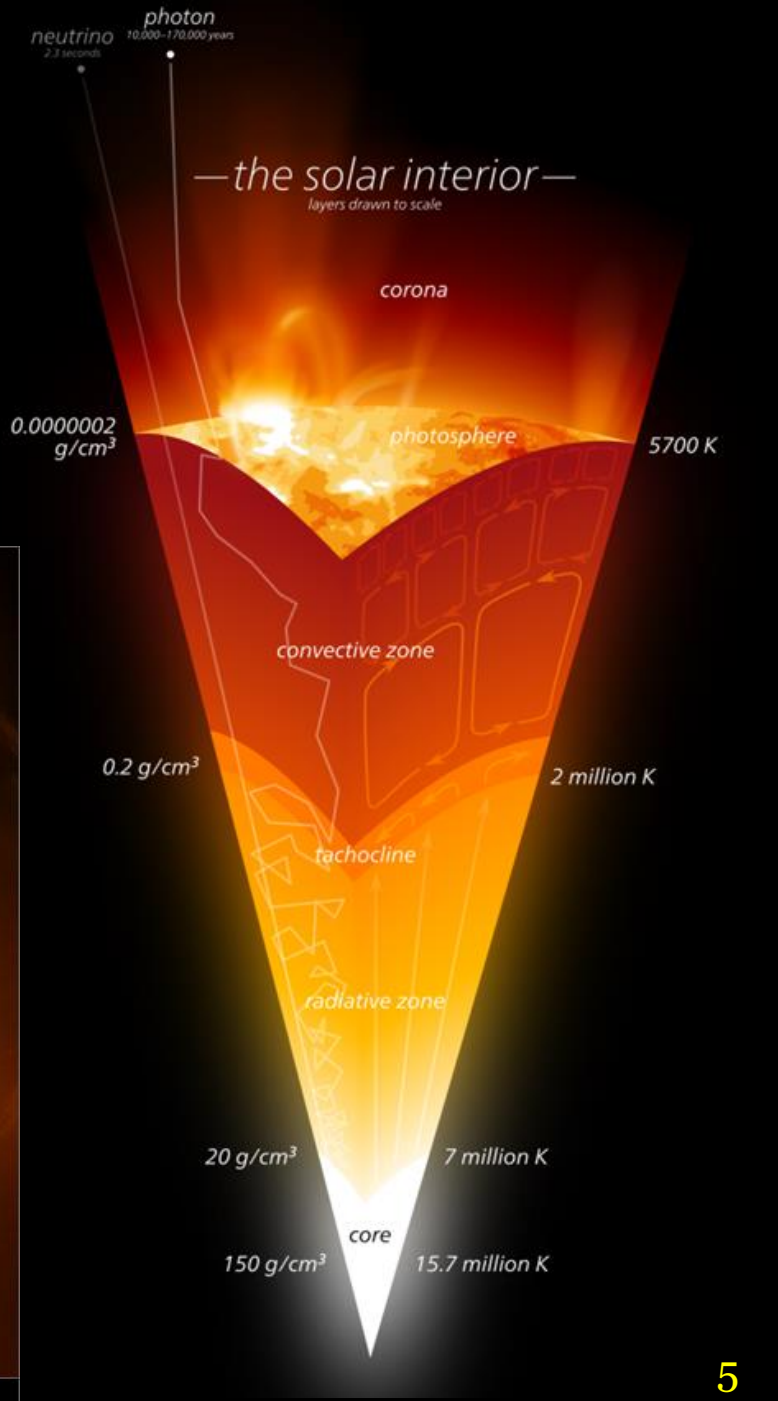

Stellar atmospheres: why should we care?

The optical depth $\tau=1$

about 2/3 of the light is absorbed

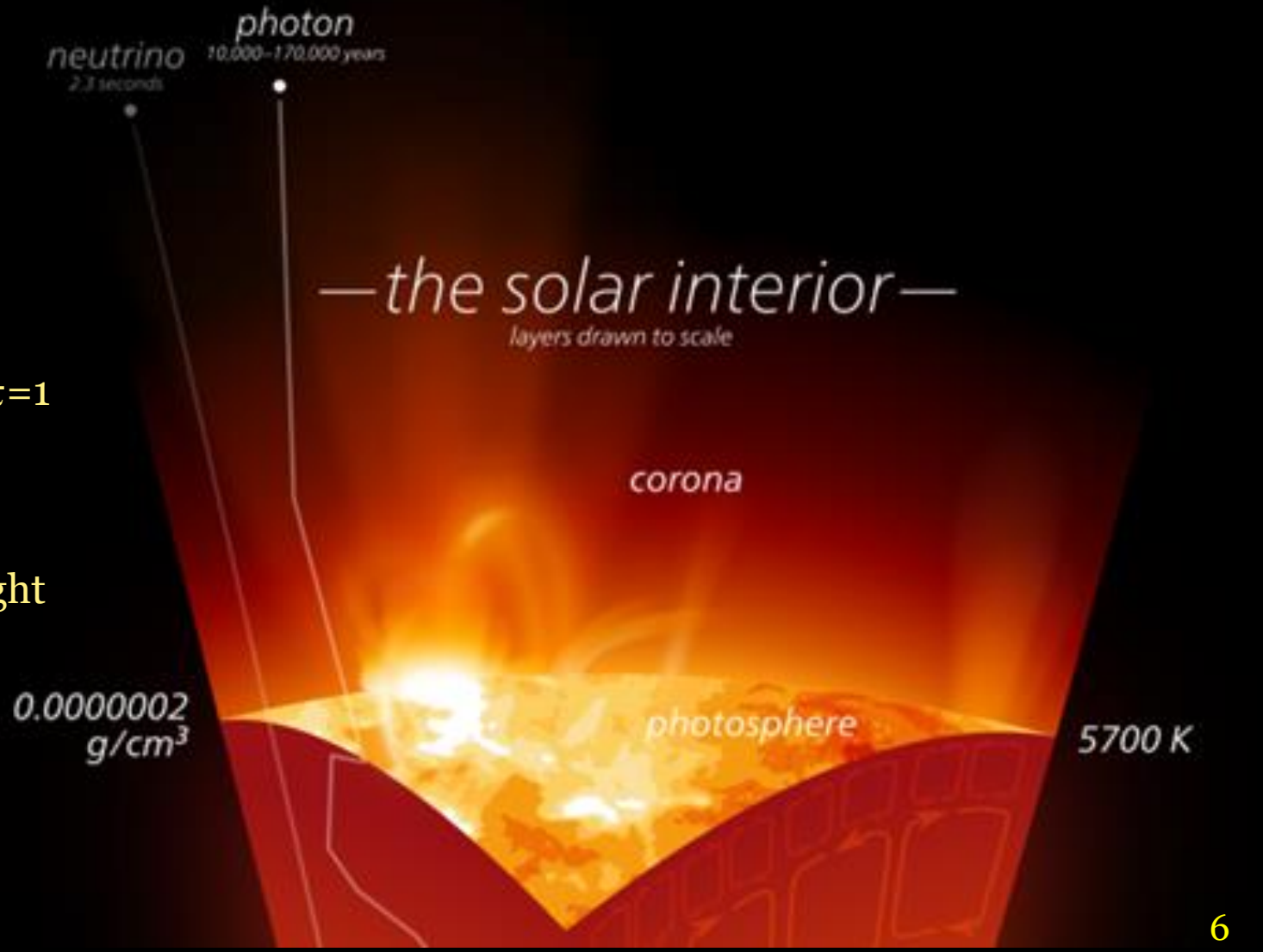

Stellar atmospheres?

- Stellar interiors are effectively invisible to external observers (apart for e.g. astroseismology) so **all** the information we receive from stars originates from their atmospheres. In particular, spectral lines also originate in a stellar atmosphere. Understanding how radiation interacts with matter affecting the emergent line and continuous spectrum is at the heart of this course.

- Knowledge of **plasma physics** (e.g. line broadening), **atomic physics** (microscopic interaction between light and matter), **radiative transfer** (macroscopic interaction between light and matter), **thermodynamics** (LTE vs non-LTE), **hydrodynamics** (velocity fields) yields stellar properties, chemical composition, outflow properties.

- Inputs for stellar/galactic evolution and structure.

Recap: what can we learn from observations?

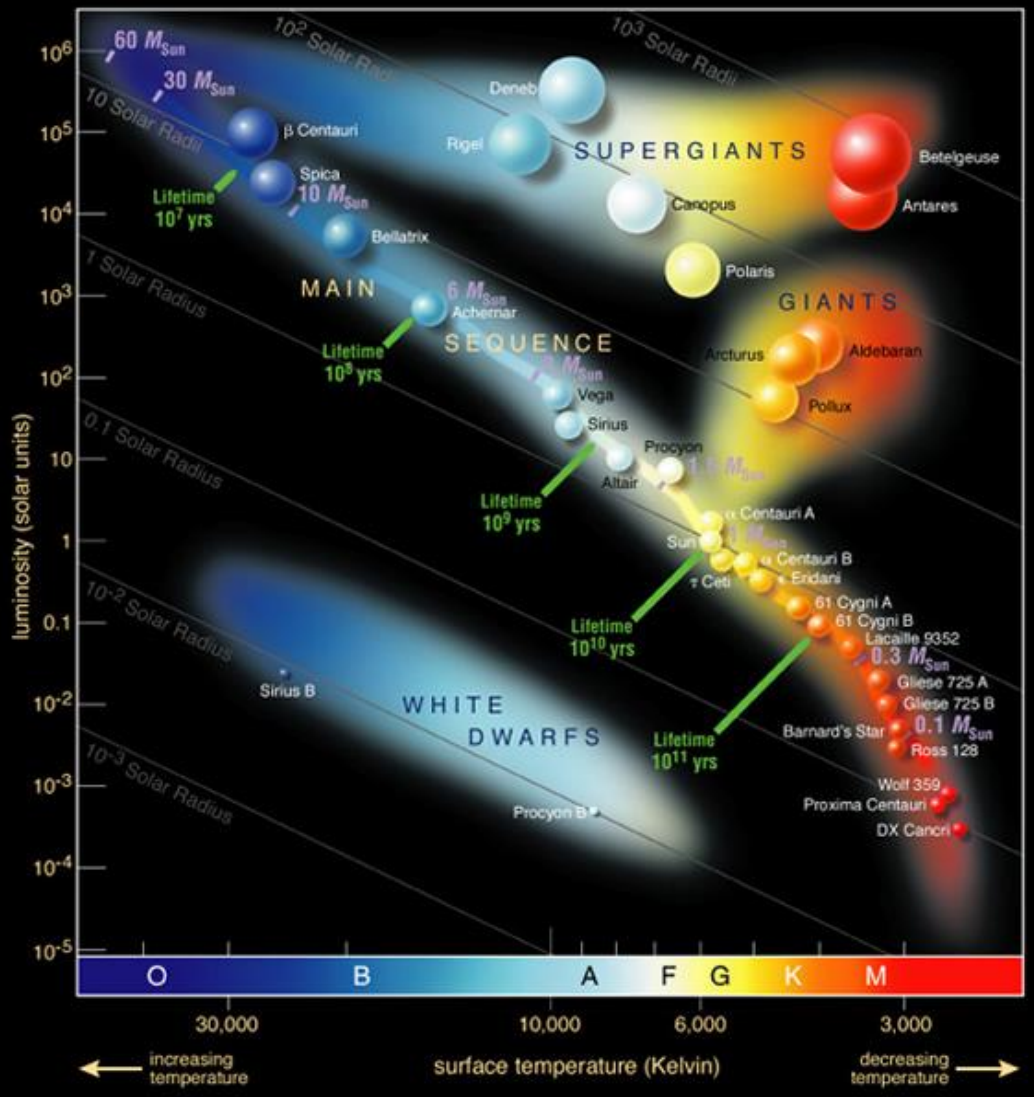

What can we learn from observations?

Please re-read Lecture 1.

Also, before the next class,

re-study Lectures 4 – 6 (slides 124 – 172)
VERY carefully.
We will be based on that material a lot.

What can we learn from observations?

10

Temperature

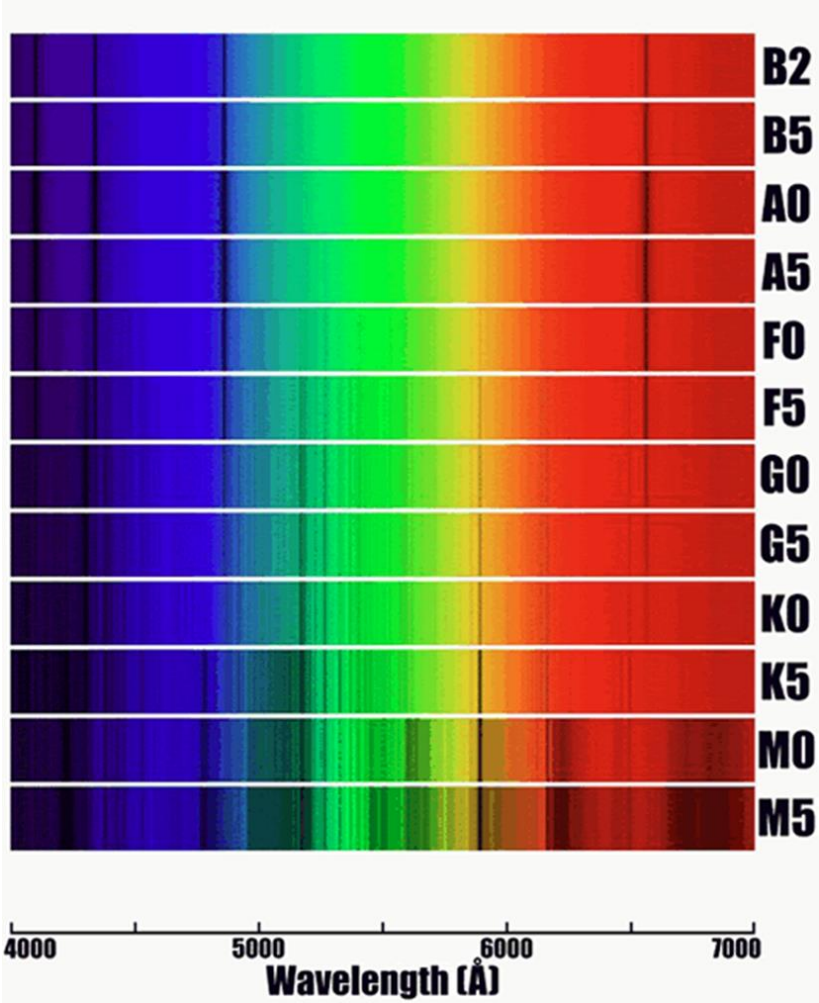

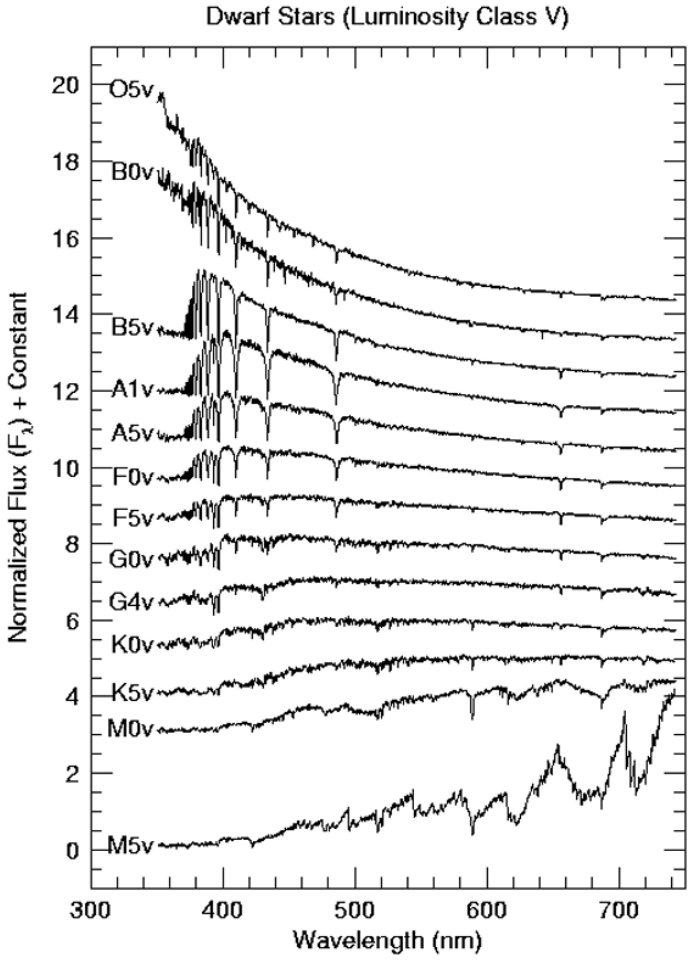

What can we learn from observations?

Surface gravity and stellar **abundances** also come from spectra:

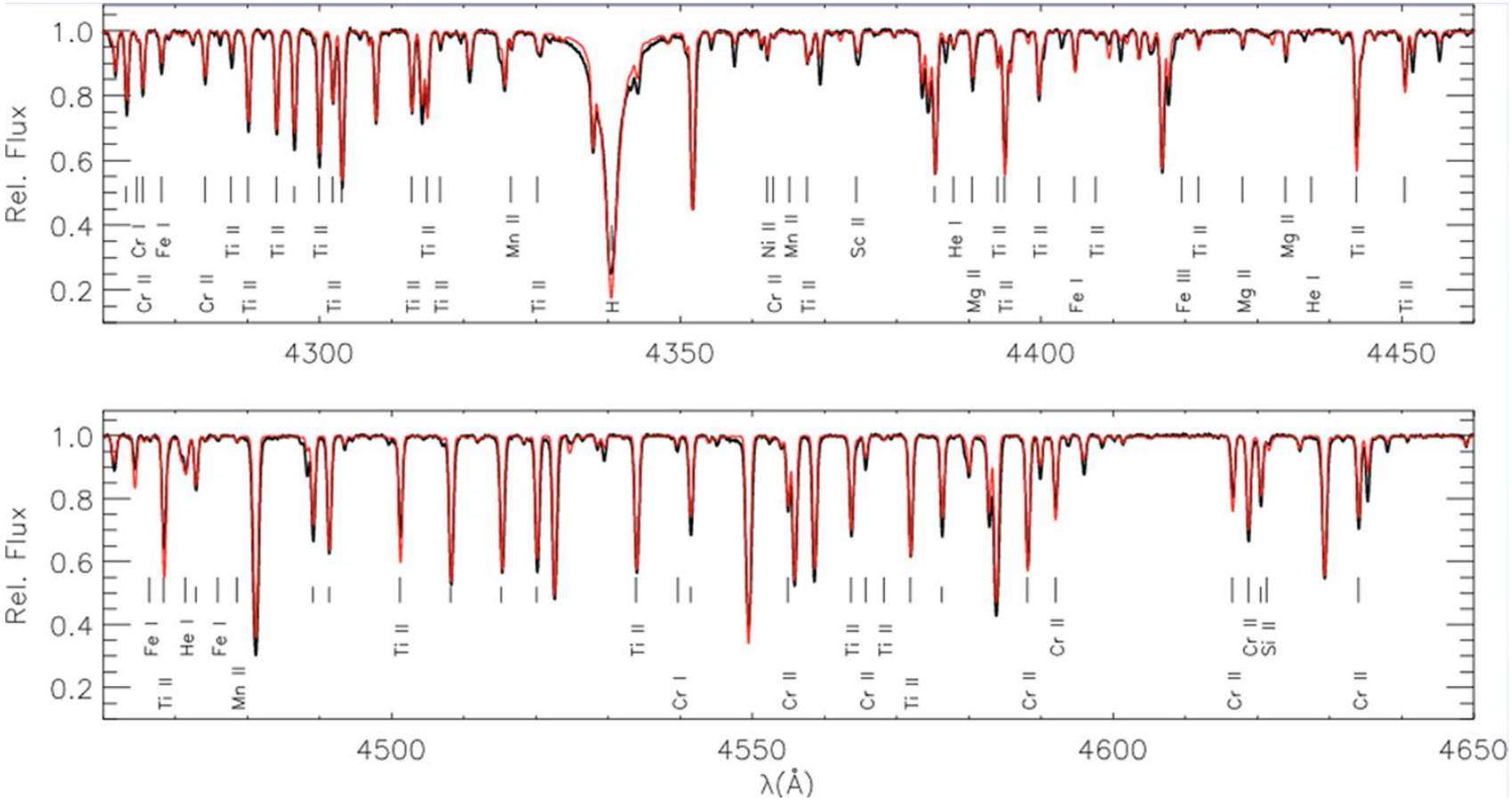

Spectral Lines

Impact of Spectral Resolution

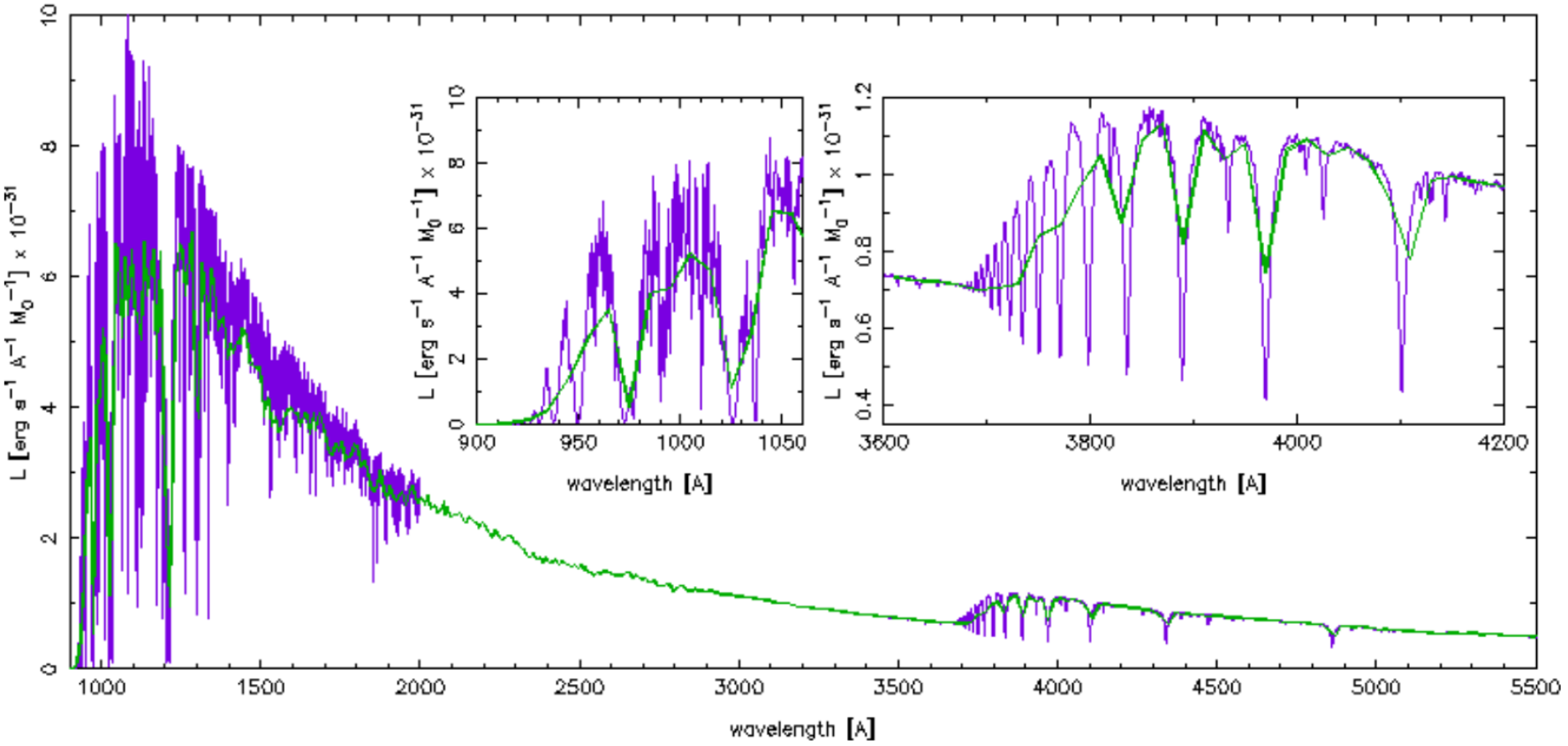

Primary star parameters (T_{eff}, $\log g$)

- Primary star parameters are effective temperature T_{eff} and surface gravity $\log g$, + chemical composition (metallicity):
  - **Effective temperature** (in K) is defined by $L=4\pi R^2 \sigma T_{eff}^4$

    (here L - luminosity, R - stellar radius), related to *ionization*.
  - **Surface gravity** (cm/s^2), $g = GM/R^2$, related to *pressure*.
- The Sun has T_{eff}=5777K, $\log g$=4.44 – its atmosphere is only a few hundred km deep, <0.1% of the stellar radius.
- A red giant has $\log g$~1 (extended atmosphere), whilst a white dwarf has $\log g$~8 (effectively zero atmosphere), and neutron stars have $\log g$~14-15

Spectral Types

Morgan-Keenan (M-K) classification scheme orders stars via "OBAFGKM" spectral classes using ratios of line strength.

Only Bad Astronomers Forget Generally Known Mnemonics

Oh, Be A Fine Girl/Guy, Kiss Me

Table 15.1. *MK spectral classes.*

MK spectral class	Class characteristics
O	Hot stars with He II absorption
B	He I absorption; H developing later
A	Very strong H, decreasing later; Ca II increasing
F	Ca II stronger; H weaker; metals developing
G	Ca II strong; Fe and other metals strong; H weaker
K	Strong metallic lines; CH and CN bands developing
M	Very red; TiO bands developing strongly

O-types have the bluest B-V & highest T_{eff}'s. OBA stars are early-type star, whilst cooler stars are late-type.

Spectral classes are each subdivided into (up to) ten divisions – e.g. O2 .. O9, B0, B1 .. B9, A0, A1 .. etc

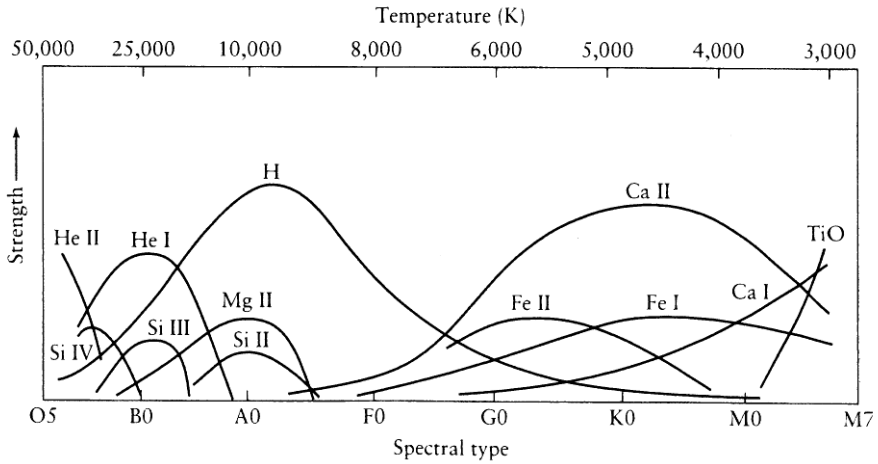

Luminosity Class classification

- Luminosity class information is often added, based upon spectral line widths:

Ia	Most luminous supergiants
Ib	Less luminous supergiants
II	Luminous giant
III	Normal giants
IV	Subgiants
V	Main sequence stars (dwarfs)
VI	Subdwarfs
VII	White dwarfs

- Dwarfs have high pressures (large line widths) and supergiants have lower pressures (smaller line widths).

Luminosity Classes and Luminosity

- Line pairs for spectral classification:

Class	Line pairs for class	Class	Line pairs for luminosity
O5 ⇔ O9	4471 He I/4541 He II	O9 ⇔ B3	4116–21 (Si IV, He I)/4144 He I
B0 ⇔ B1	4552 Si III/4089 Si IV	B0 ⇔ B3	3995 N II/4009 He II
B2 ⇔ B8	4128–30 Si II/4121 He I	B1 ⇔ A5	Balmer line wings
B8 ⇔ A2	4471 He I/4481 Mg II	A3 ⇔ F0	4416/4481 Mg II
	4026 He I/3934 Ca II		
A2 ⇔ F5	4030–34 Mn I/4128–32	F0 ⇔ F8	4172/4226 Ca I
	4300 CH/4385		
F2 ⇔ K	4300 (G band)/4340 Hγ	F2 ⇔ K5	4045–63 Fe I/4077 Sr II
F5 ⇔ G5	4045 Fe I/4101 Hδ		4226 Ca I/4077 Sr II
	4226 Ca I/4340 Hγ	G5 ⇔ M	Discontinuity near 4215
G5 ⇔ K0	4144 Fe I/4101 Hδ	K3 ⇔ M	4215/4260, Ca I increasing
K0 ⇔ K5	4226 Ca I/4325		
	4290/4300		

Continuous Energy Distribution

Stars share some properties of black-bodies

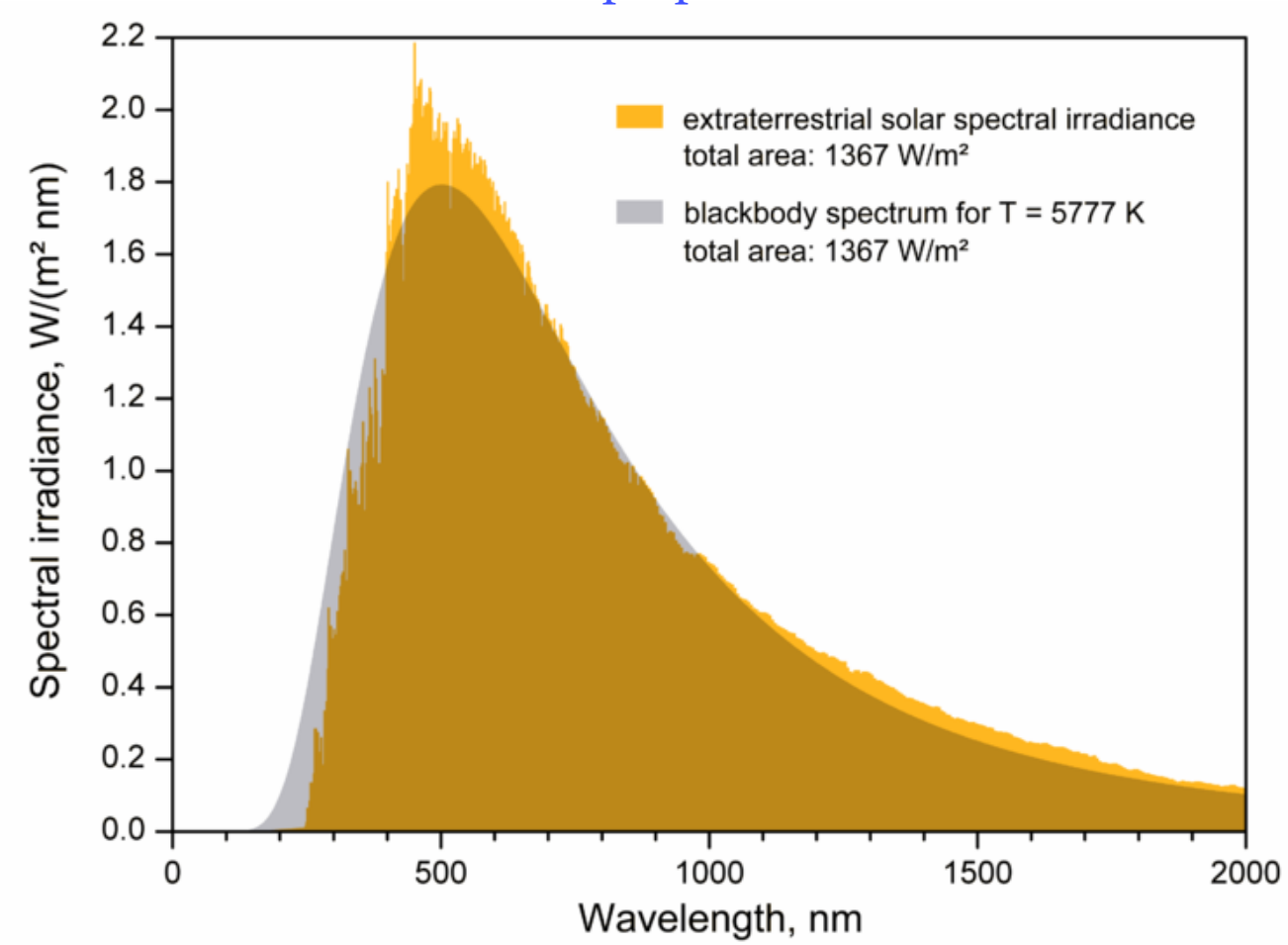

Stefan – Boltzmann Law

Blackbody radiation is continuous and isotropic whose intensity varies only with wavelength and temperature.

Following empirical (Josef Stefan in 1879) and theoretical (Ludwig Boltzmann in 1884) studies of black bodies, there is a well-known relation between Flux and Temperature known as Stefan-Boltzmann law:

$$F = \sigma T^4$$

with $\sigma = 5.6705 \times 10^{-5}$ erg/cm^2/s/K^4

(Note that Bohm-Vitense refers to "astronomical flux", $H = F/\pi$, as "flux").

We will return to "different" types of fluxes later.

Flux

19

Flux (1)

158

- From an observational point of view, we are generally more interested in the energy flux or flux (L_λ, L) and the flux density (F_λ, F).
  Flux density gives the power of the radiation per unit area and hence has dimensions of erg s^{-1} cm^{-2} Å^{-1} (or erg s^{-1} cm^{-2} Hz^{-1}).
  Observed flux densities are usually extremely small and therefore (especially in radio astronomy) flux densities are often expressed in units of the Jansky (Jy), where 1 Jy=10^{-23} erg s^{-1} cm^{-2} Hz^{-1}.
- You should be aware - and beware - that different authors define the terms flux density, flux and intensity differently, and they are sometimes used interchangeably!
- We will often call flux density as just flux.
- Standard definition:
  Flux describes any effect that appears to pass or travel through a surface or substance. In transport phenomena (radiative transfer, heat transfer, mass transfer, fluid dynamics), flux is defined as the rate of flow of a property per unit area, which has the dimensions [quantity]×[time]$^{-1}$ ×[area]$^{-1}$.
  - For example, the magnitude of a river's current, i.e. the amount of water that flows through a cross-section of the river each second is a kind of flux.

Flux (2)

159

In radiative transfer, flux is related to the intensity ("specific" is often omitted):

- Flux F_λ is a measure of the net energy flow across an area $d\sigma$, over a time dt, in a $d\lambda$. The only directional significance is whether the energy crosses $d\sigma$ from the top or from the bottom. Then we can write:

The solid angle $d\omega$ appears for I_λ but not for F_λ

$$F_\lambda = \frac{\oint dE_\lambda}{d\lambda\, d\sigma\, dt}$$

Integrated over all directions.

substitute

$$I_\lambda = \frac{dE_\lambda}{\cos\theta\, d\lambda\, d\sigma\, d\omega\, dt}$$

$$F_\lambda = \oint \underbrace{I_\lambda \cos\theta\, d\omega}_{\left[\frac{erg}{\text{Å}\, cm^2\, s}\right]}$$

Thus, flux F_λ is the projection of the specific intensity I_λ in the radial direction (integrated over all solid angles)

The amount of energy going through 1 cm² per second per 1Å into the solid angle dω in the direction inclined by the angle θ to the normal of the area.

Flux (3)

160

Expressing $d\omega$ by means of θ and φ,

$d\omega = \sin\theta\, d\theta\, d\varphi$

$$F_\lambda = \oint I_\lambda \cos\theta\, d\omega = \int_0^{2\pi} d\varphi \int_0^{\pi} I_\lambda \cos\theta \sin\theta\, d\theta$$

If there is no azimuthal dependence for I_λ then

$$F_\lambda = \oint I_\lambda \cos\theta\, d\omega = 2\pi \int_0^{\pi} I_\lambda \cos\theta \sin\theta\, d\theta$$

In the plane-parallel or spherical case, we do not find any dependence of I_λ on the longitude φ

$$F_\lambda = -2\pi \int_0^{\pi} I_\lambda \cos\theta\, d(\cos\theta)$$

Meaning of flux:

161

Radiation flux = netto energy going through area
Decomposition into two half-spaces:

$$F = -2\pi \int_0^{\pi} I_\lambda \cos\theta\, d(\cos\theta) = 2\pi \int_{-1}^{1} I(\mu)\, \mu\, d\mu \qquad \mu = \cos\theta$$

$$= 2\pi \int_0^1 I(\mu)\, \mu\, d\mu + 2\pi \int_{-1}^0 I(\mu)\, \mu\, d\mu$$

$$= 2\pi \int_0^1 I(\mu)\, \mu\, d\mu - 2\pi \int_0^1 I(-\mu)\, \mu\, d\mu = \boldsymbol{F^+ - F^-}$$

Netto = Outwards - Inwards

Special cases: at the surface of a star $F^- = 0$, so that $F = F^+$
at the centre of a star, isotropic radiation field: $F=0$

Magnitude scale

- In practice, we often (historically) measure flux densities F (erg cm^{-2} s^{-1}) from astronomical objects via a logarithmic magnitude scale (like the eye and most other human senses).
- See the course "Observational Astronomy" (765640S) for more detail (lecture 10), here we discuss it shortly.

- $m_v - m_0 = -2.5 \log(F_v/F_0)$

  In the Vega system, the star Vega (A0V) defines the photometric "zero point" m_0 at all wavelengths (U=B=V=R=I=0.0 mag etc).

Table 15.6. *Flux calibration for an A0 V star.*

Symbol	Flux (erg cm^{-2} s^{-1} Å^{-1})	λ_0 (μm)
U	4.22×10^{-9}	0.36
B	6.40×10^{-9}	0.44
V	3.75×10^{-9}	0.55
R	1.75×10^{-9}	0.71
I	8.4×10^{-10}	0.97

Standard broad-band filters

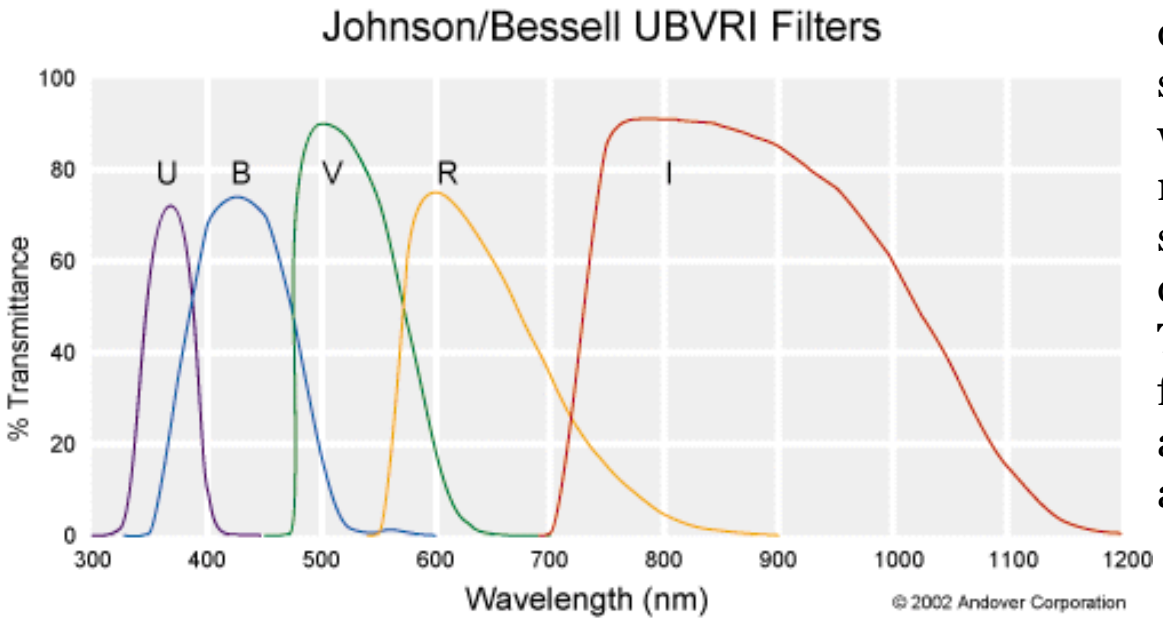

U filter (P/N JOHN-U-XX)
B filter (P/N JOHN-B-XX)
V filter (P/N JOHN-V-XX)
R filter (P/N JOHN-R-XX)
I filter (P/N JOHN-I-XX)

It is convenient to measure flux densities or magnitudes within some certain frequency or wavelength range. The total energy measured is then the integral of the source flux times some frequency dependent effective filter response. This last quantity includes all the factors that modify the energy arriving at the top of the Earth's atmosphere.

$$m = -2.5 \log \int_0^\infty F_\nu W(\nu)\, \mathrm{d}\nu + \text{constant}$$

F_ν – a star SED
$W(\nu)$ – a filter passband

Colour index

- We can define a colour index as the difference between filters relative to Vega e.g. $B - V = m_B - m_V$, such that stars bluer than A0 have a negative B-V colour and stars redder than Vega have a positive colour e.g. $(B\text{-}V)_{Sun}$=+0.65 mag.

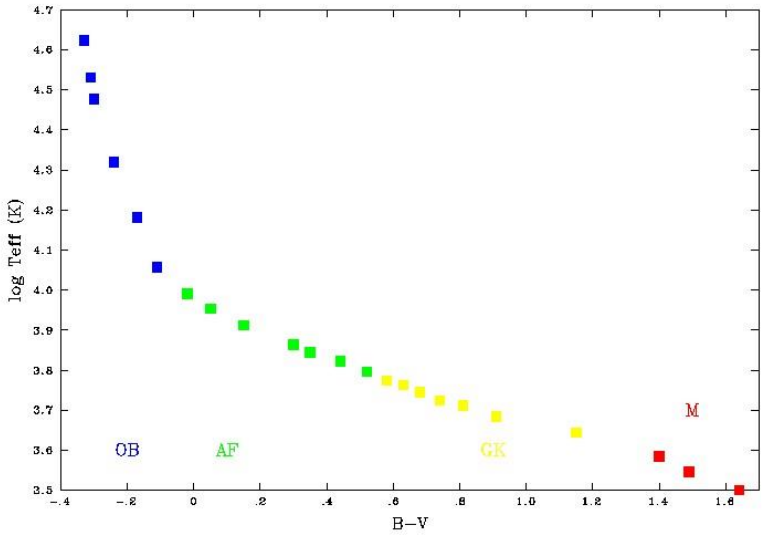

$$B - V = -2.5\log\left(\frac{\int F_\nu W_B(\nu)\,d\nu}{\int F_\nu W_V(\nu)\,d\nu}\right) + 0.710$$

$$U - B = -2.5\log\left(\frac{\int F_\nu W_U(\nu)\,d\nu}{\int F_\nu W_B(\nu)\,d\nu}\right) - 1.093.$$

e.g., for T_{eff}<10000K:

$$T = \frac{7090}{(B-V)+0.71} K$$

More on magnitudes

- We define the absolute (visual) magnitude (M_V) as the apparent (visual) magnitude of a star of m_V lying at a distance of d=10pc: $M_V = m_V\ (10\ pc)$.
- Because $F \propto d^{-2}$
  $M_V - m_V = -2.5 \log[F(10pc)/F(d)] = -5\log(d/10\ pc) = 5 - 5\log(d/pc)$
- For the Sun (d=4.85×10^{-6} pc), m_V=-26.75 and M_V=+4.82 mag.
  The "distance modulus" $M_v - m_v$=31.57 mag
- Because interstellar medium is not completely transparent, we write
  $M_V - m_V = 5 - 5\log(d/pc) - A_V$.
- The A_V term is due to interstellar extinction.
  Visually, $A_V \sim 3.1$ E(B-V) for most sight lines.
  $E(B-V) = B-V - (B-V)_o$, i.e. the difference between the observed and intrinsic B-V colour.

Interstellar Extinction

Extinction is MUCH higher at shorter wavelengths, so IR observations of e.g. Milky Way disk probe much further. The extinction to the Galactic Centre (d=8kpc) is approx A_V=30 mag (5500A) versus A_K=3 mag (2μm).

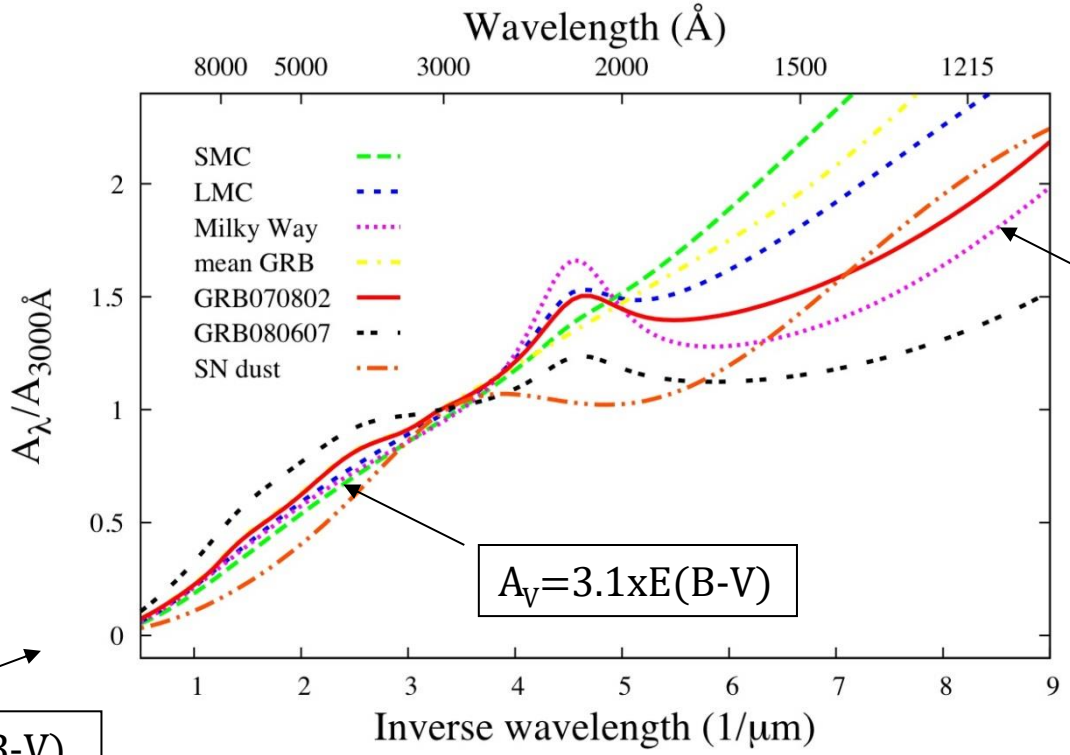

A_{1200A}=10xE(B-V)

A_V=3.1xE(B-V)

A_K=0.3xE(B-V)

Illustration of interstellar extinction

V-band (5500Å)

R-band (7000Å)

I-band (9000Å)

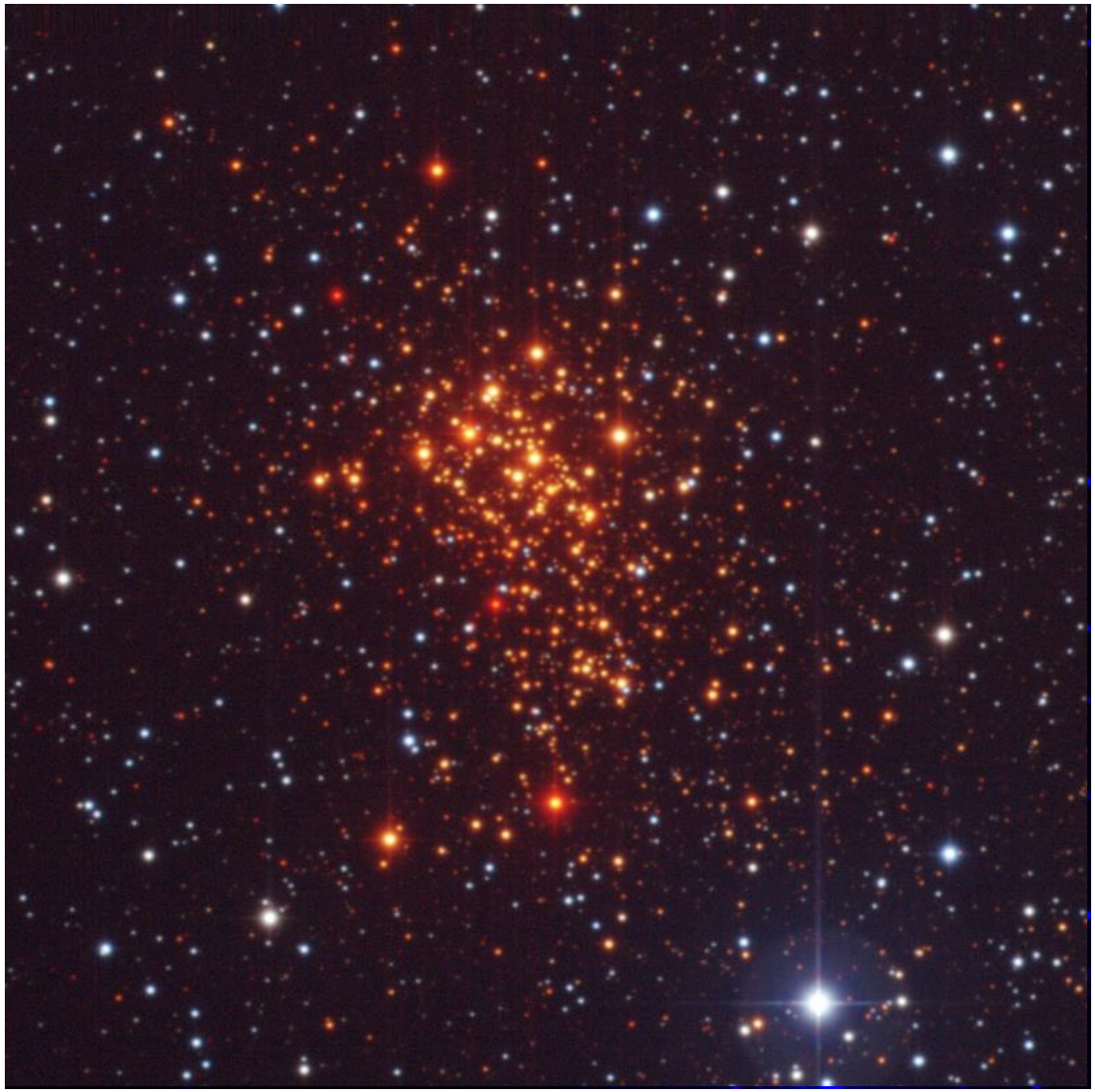

VRI-composite
of highly reddened
cluster Wd1 (E_{B-V}~4)

Bolometric Flux

- The bolometric flux (erg cm^{-2} s^{-1}) from a star received at the top of the Earth's atmosphere is the integral of the spectral flux (measured at a frequency ν or a wavelength λ) over all frequencies or wavelengths:

$$F_{Bol} = \int_0^\infty F_\nu d\nu = \int_0^\infty F_\lambda d\lambda$$

- The luminosity (erg/s) is the bolometric flux from the star integrated over a full sphere (at distance d):

$$L = 4\pi d^2 F_{Bol}$$

- Since the Earth's atmosphere is opaque to UV and some IR radiation one cannot always directly measure the bolometric flux.

Bolometric Corrections

One can calculate bolometric corrections (BC), primarily from atmospheric models to correct measured fluxes (usually in the V band) for the total (bolometric) flux. Usually expressed in magnitudes:

$$BC = M_{bol} - M_V \quad \text{with} \quad M_{bol} = 4.74 - 2.5 \log(L/L_\odot)$$

BC=-0.08 mag for the Sun is a small correction since it emits most radiation in the visual. Hot OB stars have very negative BC's, since most of the energy is emitted in the UV, as are cool M stars with most energy emitted in the IR.

BC calibrations

Bolometric corrections can be estimated from intrinsic colours $(B\text{-}V)_0$ as shown here for dwarfs:

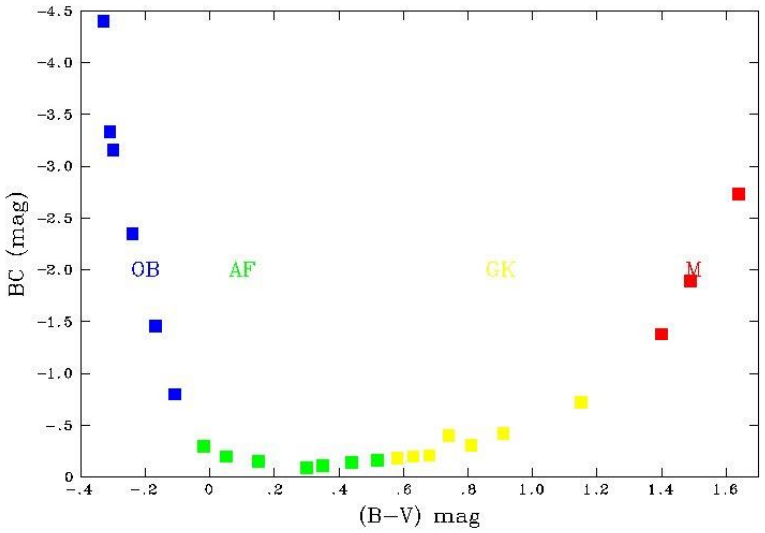

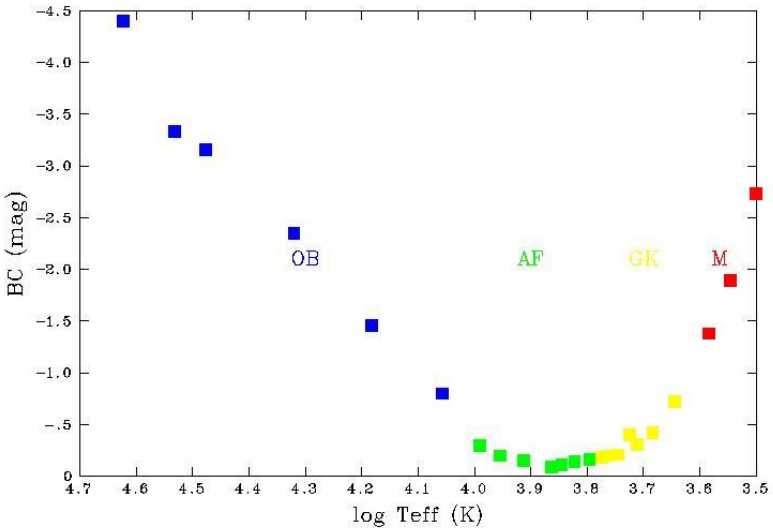

Or from the Spectral Type, using a T_{eff} – Spectral Type calibration.

See the next slide…

Properties of Main-Sequence Stars

Table 15.7. *Calibration of MK spectral types.*

Sp	*M*(*V*)	*B* − *V*	*U* − *B*	*V* − *R*	*R* − *I*	$T_{\rm eff}$	BC
MAIN SEQUENCE, V							
O5	−5.7	−0.33	−1.19	−0.15	−0.32	42 000	−4.40
O9	−4.5	−0.31	−1.12	−0.15	−0.32	34 000	−3.33
B0	−4.0	−0.30	−1.08	−0.13	−0.29	30 000	−3.16
B2	−2.45	−0.24	−0.84	−0.10	−0.22	20 900	−2.35
B5	−1.2	−0.17	−0.58	−0.06	−0.16	15 200	−1.46
B8	−0.25	−0.11	−0.34	−0.02	−0.10	11 400	−0.80
A0	+0.65	−0.02	−0.02	0.02	−0.02	9 790	−0.30
A2	+1.3	+0.05	+0.05	0.08	0.01	9 000	−0.20
A5	+1.95	+0.15	+0.10	0.16	0.06	8 180	−0.15
F0	+2.7	+0.30	+0.03	0.30	0.17	7 300	−0.09
F2	+3.6	+0.35	0.00	0.35	0.20	7 000	−0.11
F5	+3.5	+0.44	−0.02	0.40	0.24	6 650	−0.14
F8	+4.0	+0.52	+0.02	0.47	0.29	6 250	−0.16
G0	+4.4	+0.58	+0.06	0.50	0.31	5 940	−0.18
G2	+4.7	+0.63	+0.12	0.53	0.33	5 790	−0.20
G5	+5.1	+0.68	+0.20	0.54	0.35	5 560	−0.21
G8	+5.5	+0.74	+0.30	0.58	0.38	5 310	−0.40
K0	+5.9	+0.81	+0.45	0.64	0.42	5 150	−0.31
K2	+6.4	+0.91	+0.64	0.74	0.48	4 830	−0.42
K5	+7.35	+1.15	+1.08	0.99	0.63	4 410	−0.72
M0	+8.8	+1.40	+1.22	1.28	0.91	3 840	−1.38
M2	+9.9	+1.49	+1.18	1.50	1.19	3 520	−1.89
M5	+12.3	+1.64	+1.24	1.80	1.67	3 170	−2.73

From Allen's Astrophysical Quantities (4th edition)

Solve a problem

A B0V star in the LMC (distance 50kpc) has V=13.0 mag, B-V=-0.20 mag.

What is its bolometric luminosity, relative to the Sun?

Properties of the Planck law

- For increasing temperatures, the black body intensity increases for all wavelengths. The maximum in the energy distribution shifts to shorter λ (longer ν) for higher temperatures.
- $\lambda_{max}\, T = 2.98978 \times 10^{7}$ Å K

  is Wien's displacement law for the maximum I_λ providing an estimate of the peak emission (λ_{max} =5175 Å for the Sun).

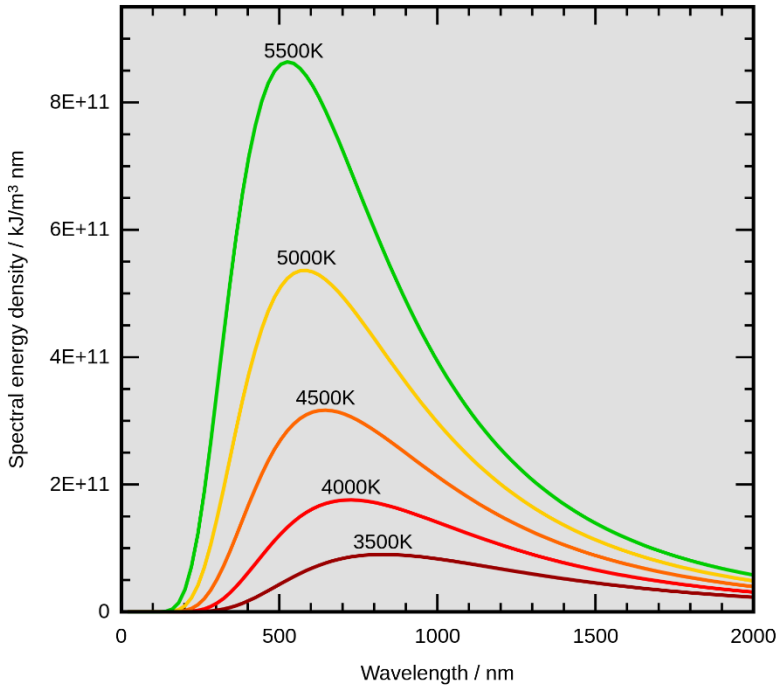

Rayleigh-Jeans and Wien approximations

At long wavelengths $\lambda >> \lambda_{max}$ (small frequencies $\nu << \nu_{max}$) the Planck formulae

$$B_\nu(T) = \frac{2h\nu^3}{c^2}\frac{1}{e^{h\nu/kT}-1} \qquad B_\lambda(T) = \frac{2hc^2}{\lambda^5}\frac{1}{e^{hc/\lambda kT}-1}$$

can be approximated by the Rayleigh-Jeans law

$$B_\nu(T) \approx 2\frac{\nu^2}{c^2}kT\,, \quad B_\lambda(T) \approx 2ckT\lambda^{-4}$$

At short wavelengths $\lambda \leq \lambda_{max}$ (large frequencies $\nu \geq \nu_{max}$), the Wien law is a good approximation

$$B_\nu(T) \approx 2\frac{h\nu^3}{c^2}e^{-\frac{h\nu}{kT}}\,, \quad B_\lambda(T) \approx 2\frac{hc^2}{\lambda^5}e^{-\frac{hc}{\lambda kT}}$$

Color and brightness temperatures

Define brightness temperature as $I_\nu = B_\nu(T_b)$

In radio band we get

$$I_\nu = 2\frac{\nu^2}{c^2}kT_b \quad , \text{ so that } T_b = \frac{c^2}{2\nu^2 k}I_\nu \text{ for } h\nu << kT$$

Colour temperature T_c is obtained by "fitting" the observed spectrum with the Planck function ignoring normalization. It gives correctly the temperature of the black body source of unknown absolute scale of the intensity.

Are stars black bodies?

(e.g. UV-optical spectrophotometry of Vega)

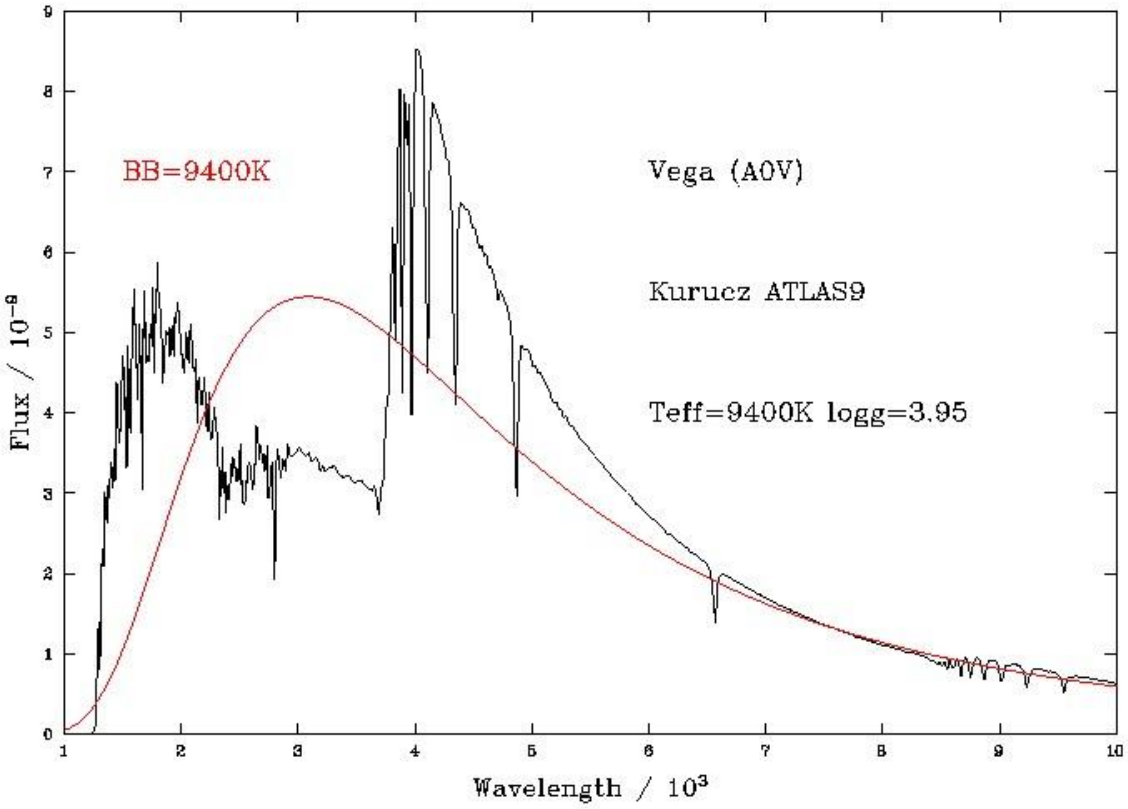

Not really

Stars do differ from black bodies

The observed flux distributions of real stars deviate from black body curves, as indicated here for the UBV colors of dwarfs and supergiants. This difference is due to sources of continuous and line opacity in the stellar photospheres and will be discussed later in this course.

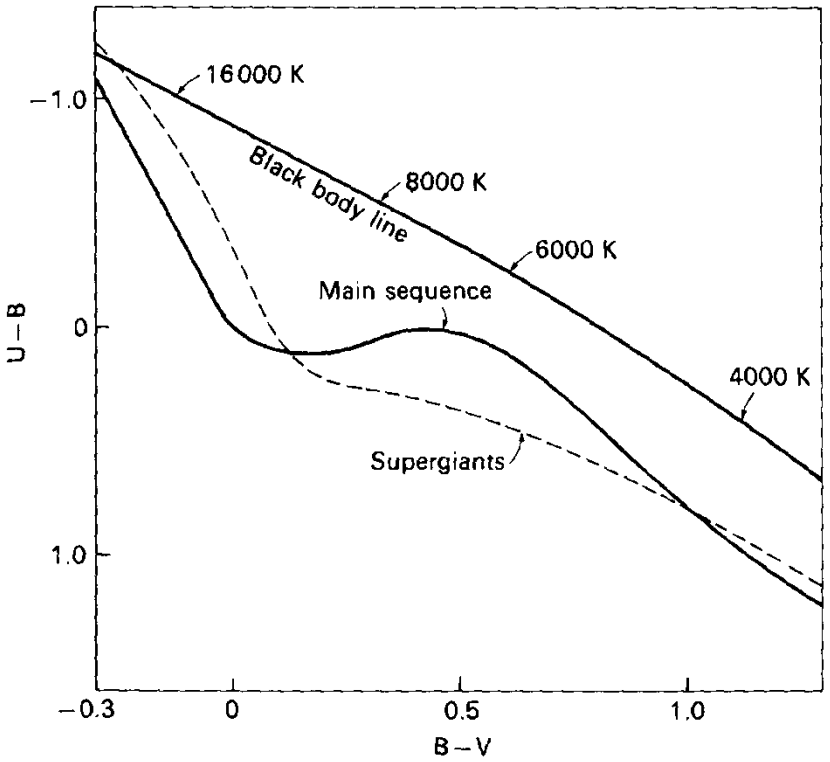

Stars do differ from black bodies

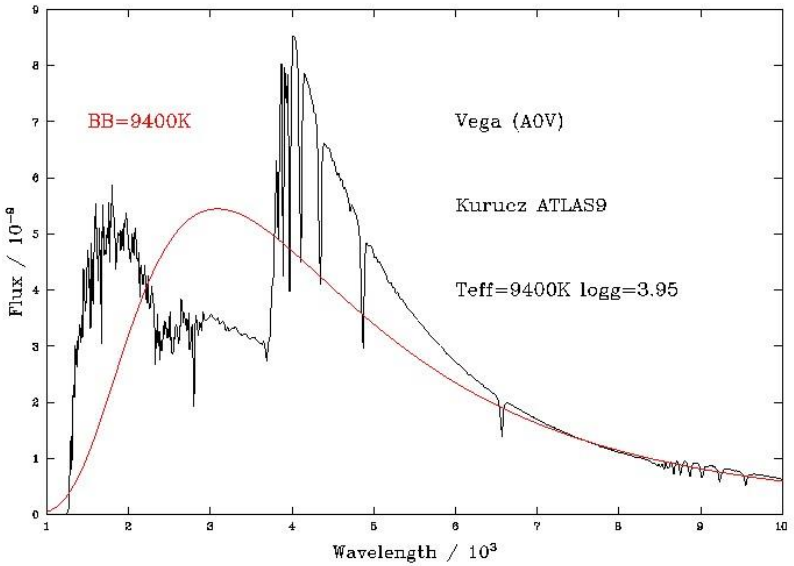

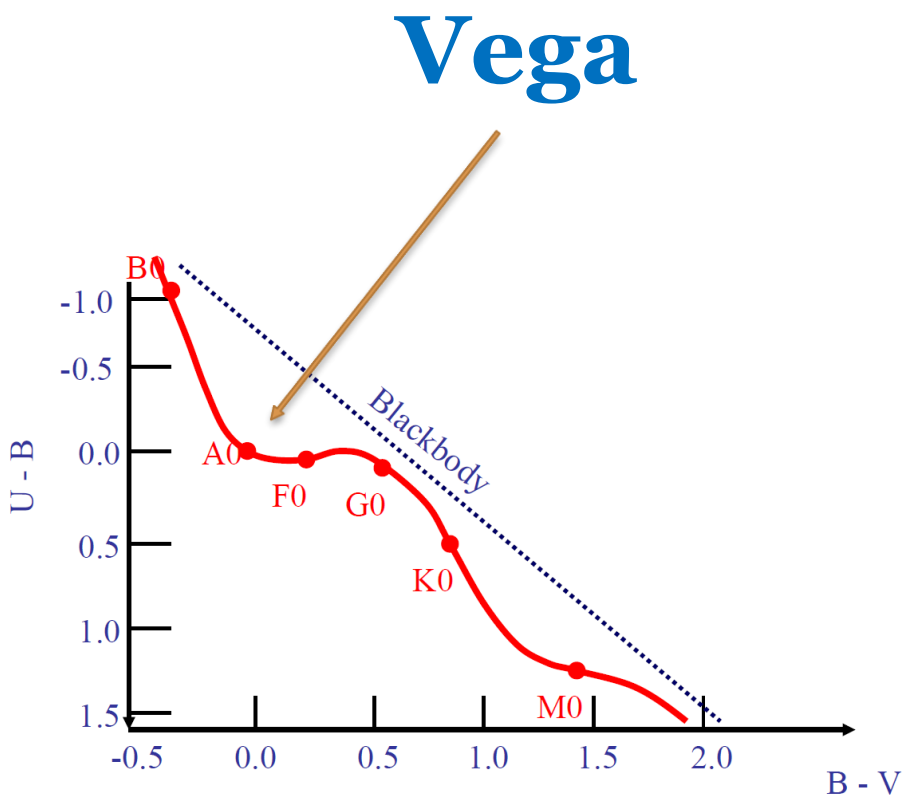

Radiative transfer III

RADIATIVE TRANSFER EQUATION IN PLANE-PARALLEL ATMOSPHERE. LIMB DARKENING.

Solar limb darkening

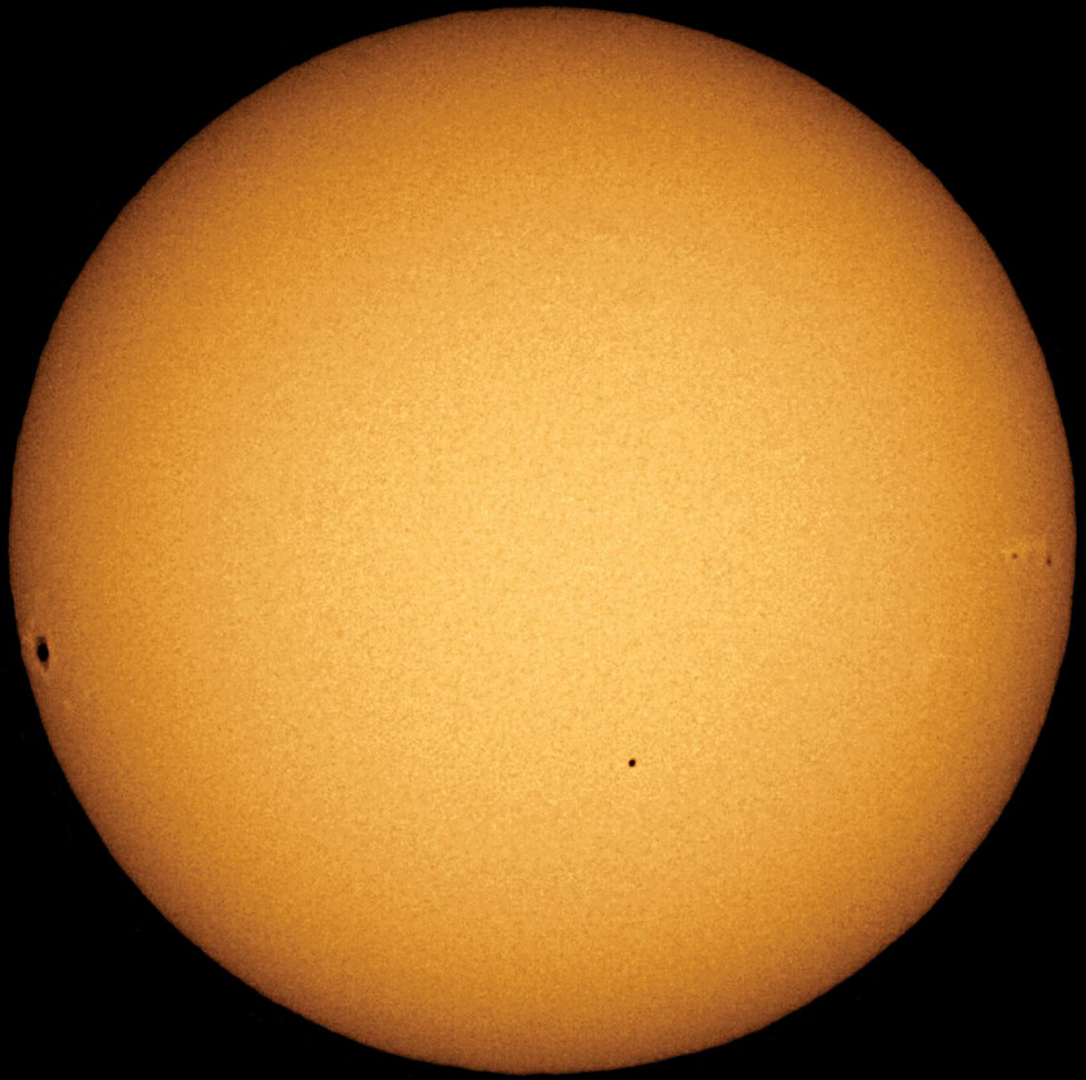

Transfer Equation for Stars

From lecture 6 (slide I-167):

The plane-parallel transfer equation
(for stars with thin photospheres)

$$\cos\theta \frac{dI_\lambda(\theta)}{d\tau_\lambda} = I_\lambda(\theta) - S_\lambda$$

The cos(θ) term is because the optical depth is measured along the radial direction *x* and not along the line of sight, i.e $d\tau_\lambda = -\kappa_\lambda \rho\, dx$

We are looking from the outside in, along direction x

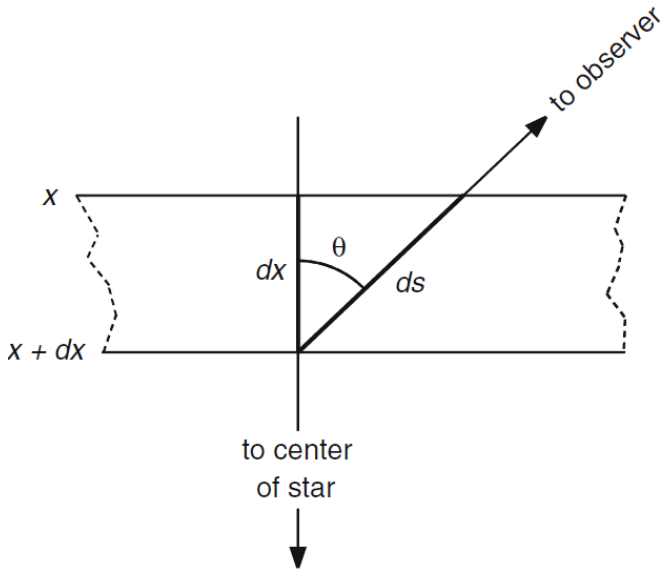

Surface Intensity

- To derive the intensity at the **surface**, we can multiply the plane-parallel transfer equation by an integrating factor $e^{-\tau/\cos\theta}=e^{-u}$, $\tau = u \cos\theta$

$$\frac{dI_\lambda(\theta)}{du}e^{-u} - I_\lambda(\theta)\ e^{-u} = -S_\lambda e^{-u}$$

- This can be written as

$$\frac{d(I_\lambda(\theta)e^{-u})}{du} = -S_\lambda e^{-u}$$

- Integrating du from 0 to infinity

$$[I_\lambda(\theta)e^{-u}]_0^\infty = -\int_0^\infty S_\lambda(\tau_\lambda)e^{-u}du$$

$$I_\lambda(0,\theta) = \int_0^\infty S_\lambda(\tau_\lambda)e^{-u}du$$

Limb darkening

Let us assume a linear source function: $S_\lambda(\tau_\lambda) = a_\lambda + b_\lambda \tau_\lambda$

We then derive: $I_\lambda(0,\theta) = \int_0^\infty S_\lambda(\tau_\lambda) e^{-u} du = \int_0^\infty a_\lambda e^{-u} du + \int_0^\infty b_\lambda \tau_\lambda e^{-u} du$

Recall $u = \tau/\cos(\theta)$, so $\tau = u\cos(\theta)$ and $I_\lambda(0,\theta) = a_\lambda \int_0^\infty e^{-u} du + b_\lambda \cos\theta \int_0^\infty u e^{-u} du$

Using the standard integral $\int_0^\infty u^n e^{-u} du = n!$

we obtain $$I_\lambda(0,\theta) = a_\lambda + b_\lambda \cos\theta = S_\lambda(\tau_\lambda = \cos\theta)$$

Thus, in the linear approximation for the Source function, the optical depth lies between 0 and 1. From the centre of the star we see radiation leaving the star perpendicular to the surface: $I_\lambda(0,0°) = a_\lambda + b_\lambda$, whilst at the limb the starlight leaves the surface at an angle $I_\lambda(0,90°) = a_\lambda$.

Limb darkening (less light from the limb versus the centre, if $b_\lambda > 0$).

Solar limb darkening

- This optical image of the Sun clearly shows limb darkening. We see into the atmosphere down to a depth of $\tau = 1$.
- Limb darkening exists because the continuum source function decreases outward: $S_\lambda(\tau_\lambda) = a_\lambda + b_\lambda \tau_\lambda$, both a_λ and $b_\lambda > 0$.
- As we look towards the limb, we see higher photospheric layers, which are less bright.

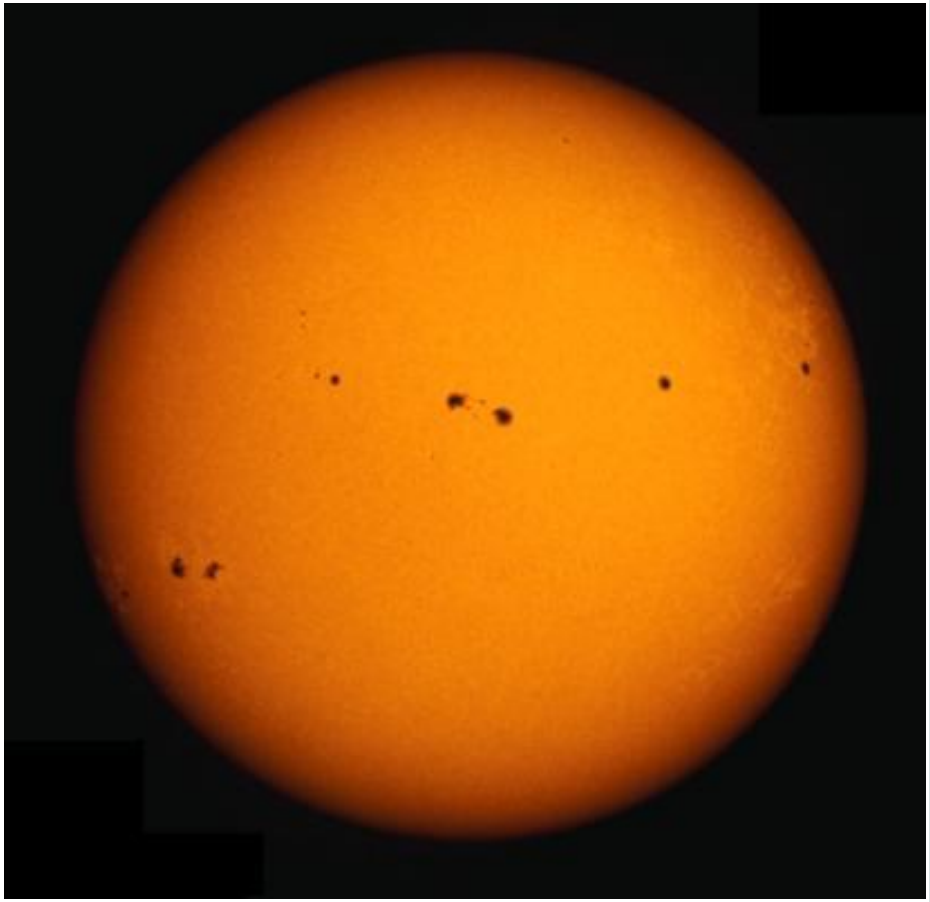

Schematic of limb darkening

Schematic illustration of limb darkening – penetration of different lines of sight (thick lines) to "unit optical depth" (dashed lines) corresponds to different depths in the photosphere, depending on θ. Radiation seen at θ_2 is characteristic of higher (cooler) layers than the radiation seen at position θ_1

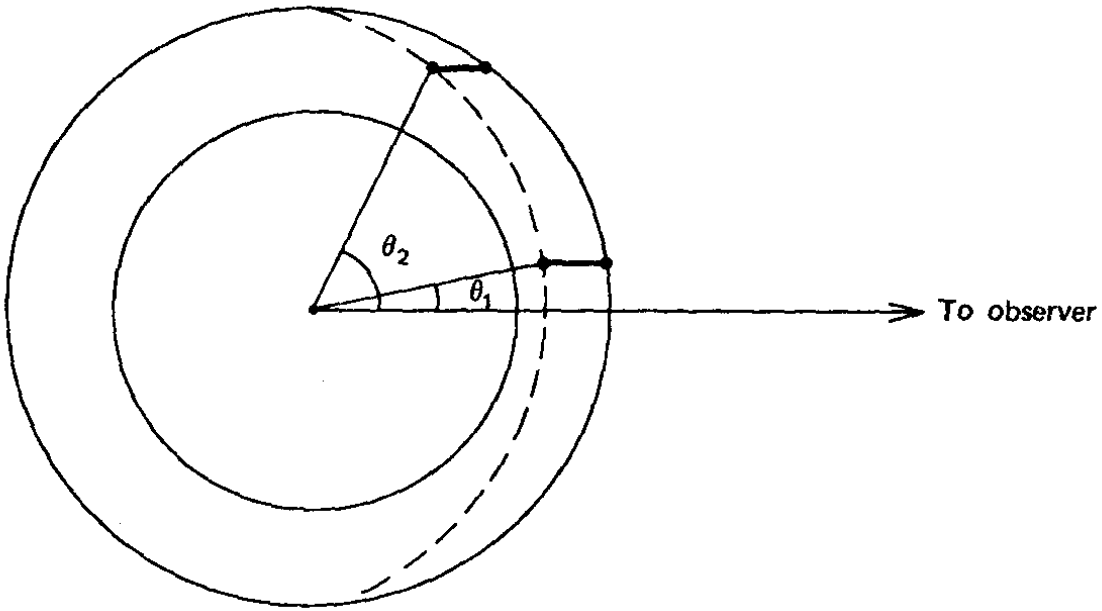

Linear vs Quadratic source function

Up to now we assumed a linear source function. More generally, if:

$$S_\lambda(\tau_\lambda) = \sum_{n=0} a_{n\lambda}\,\tau_\lambda^n$$

Then

$$I_\lambda(0,\theta) = \sum_{n=0} A_n \cos^n\theta \qquad A_n = a_{n\lambda}\int_0^\infty u^n\, e^{-u} du = a_{n\lambda} n$$

We still get $S_\lambda(0)$ at the limb, but a more complicated result at the centre.
For example, a quadratic term requires the solution of

$$S(\tau_\lambda) = a_{0\lambda} + a_{1\lambda}\tau_\lambda + a_{2\lambda}\tau_\lambda^2$$

$$I_\lambda(0,\theta) = a_{0\lambda} + a_{1\lambda}\cos\theta + 2a_{2\lambda}\cos^2\theta$$

At $\theta = 90°$, $\tau_\lambda = 0$, whilst at $\theta = 0°$, $\tau_\lambda \sim 1 + 2a_{1\lambda}/a_{2\lambda}$ providing $a_{2\lambda} << a_{1\lambda}$.
The ratio of the limb-to-centre intensity is

$$\boldsymbol{I_\lambda(0,90°)/I_\lambda(0,0°) = a_{0\lambda}/(a_{0\lambda} + a_{1\lambda} + 2a_{2\lambda})}$$

Example for Solar Case:

The measured centre to limb variation of the solar intensity is

$$I_\lambda(0,\theta)/I_\lambda(0,0) = a_{0\lambda} + a_{1\lambda}\cos\theta + 2a_{2\lambda}\cos^2\theta$$

$\lambda(\mu m)$	a_0	a_1	$2a_2$
0.3	0.06	0.74	0.20
0.4	0.14	0.91	-0.05
0.6	0.35	0.88	-0.23
0.8	0.49	0.73	-0.22
1.5	0.56	0.64	-0.20
2.0	0.70	0.48	-0.18

(Table 4.17, AQ 4th edition)

Wavelength dependence

Limb darkening is observed to be greatest at **shorter** wavelengths in the Sun. The temperature distribution of the upper atmosphere of the Sun can be obtained from limb darkening measurements, carried out via e.g. multi-filter images of the Solar continuum (between the lines).

Until recently, the Sun was the only star for which limb darkening was observed, since one needs to **spatially** resolve the disc (most other stars appear as point sources!) to measure limb darkening.

Other methods are now possible.

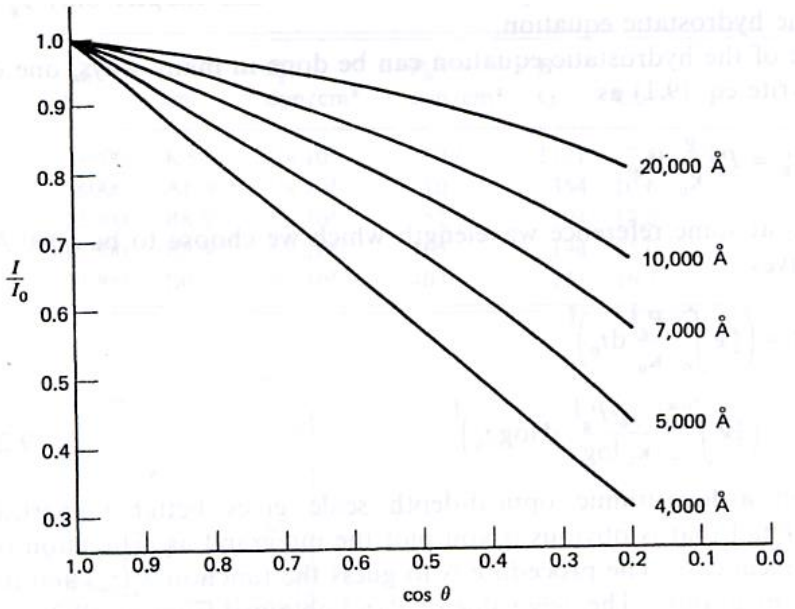

(Pierce & Waddell 1961).

Centre

Limb

Limb darkening for other stars

1. Direct interferometry, via high spatial resolution "imaging" – e.g. ESO/VLT interferometry or COAST array, providing a star is very large and nearby (a cool supergiant).

2. The light curve due to the gravitational micro-lensing of a background (generally Galactic bulge or Magellanic Cloud) star by a foreground source (e.g. PLANET team).

3. The light curve from an eclipsing binary system during secondary eclipse allows us to study limb darkening of the primary, although non-trivial! Similar approach followed by extra solar planets occulting parent star (e.g. HD209458).

Limb darkening from interferometry

COAST (Cambridge Optical Aperture Synthesis Telescope) spatial resolution of 20-30 milli-arcsec) has made limb darkening observations of M supergiant Betelgeuse at different wavelengths (using filters).

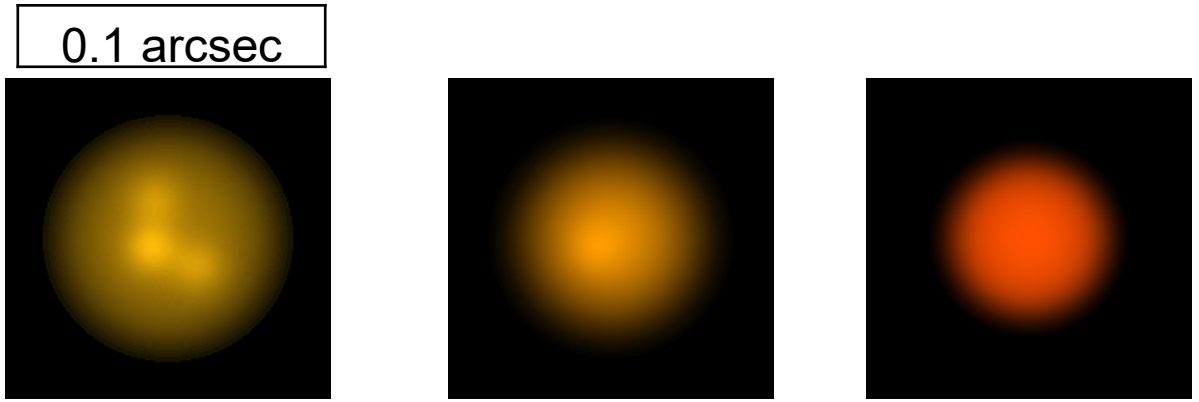

7000A 9050A 12900A

Limb darkening from interferometry

ESO's Very Large Telescope Interferometer (VLTI) is possible to achieve a resolution of 0.001 arcsec or even less. It has resolved the disc of the cepheid L Carinae.

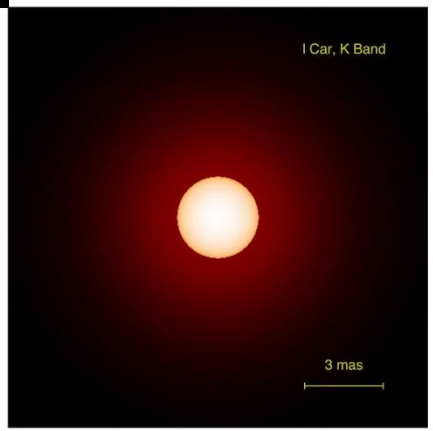

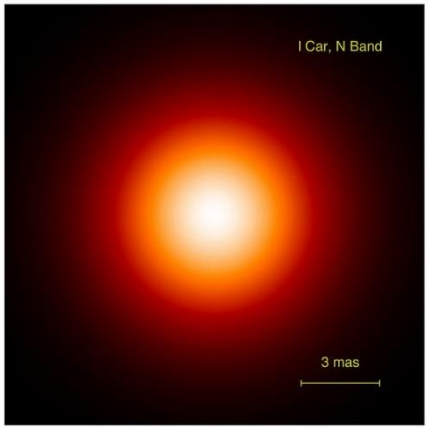

Limb darkening from microlensing

- Galactic gravitational micro-lensing occurs when a foreground object (lens) passes in front of a background star (source). The gravitational deflection of light by the lens causes the flux from the source to be amplified.
- Microlensing surveys (e.g. PLANET, MACHO) have identified hundreds of such events towards the Galactic bulge and Magellanic Clouds.
- One such event, MACHO 97-BLG-28 was studied to reveal limb darkening information for the background K giant (Albrow et al. 1999).

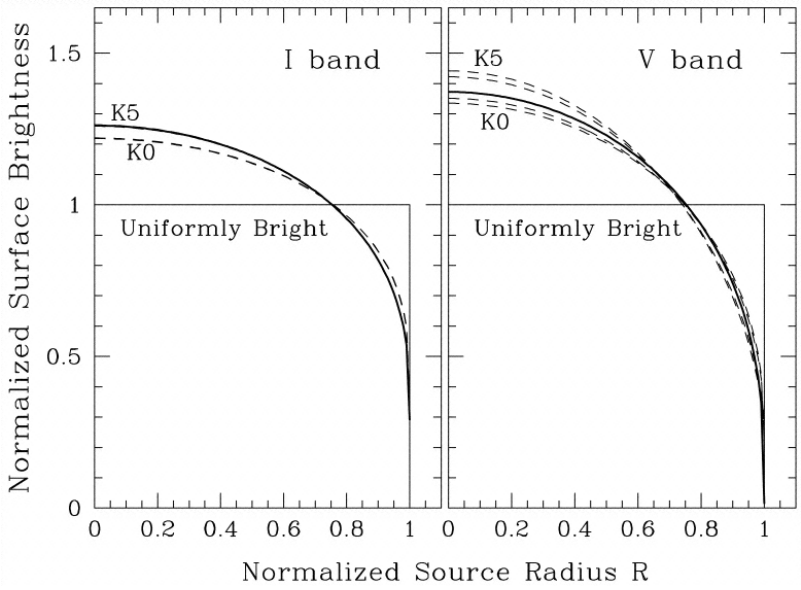

Thick lines show how much fainter the K giant becomes at its edges in the red I (left) and blue-green V filter (right). If the star emitted a uniform amount of light across its whole stellar disk, the profile would look like the straight solid black line instead

Limb darkening from eclipsing systems

- HD209458 is the first system in which extra-solar planet (P=3.5d, $0.6M_J$) has been observed to transit its (F8V) primary, allowing determination of limb darkening (Brown et al. 2001).

- More generally eclipsing binaries are problematic due to degeneracy with other parameters (Grygar et al. 1972). Accurate light curves needed for linear limb darkening parameters.

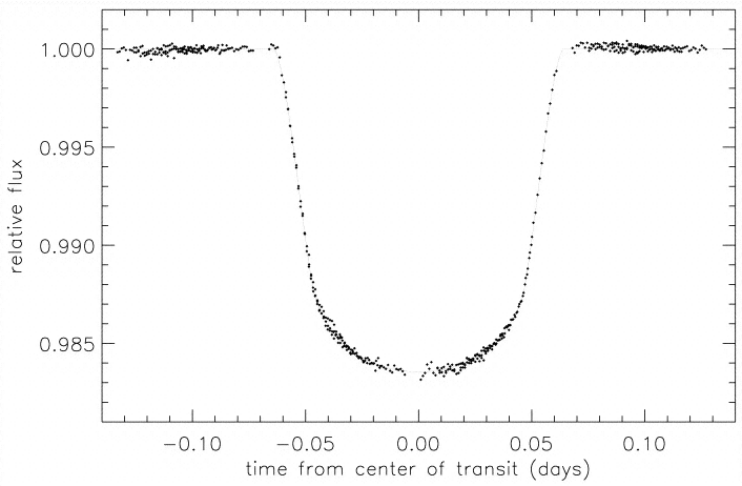

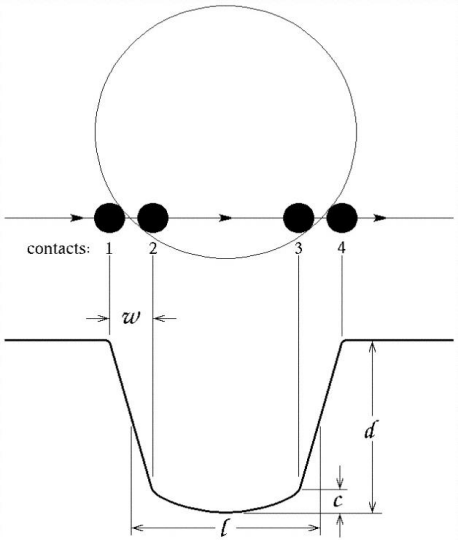

Limb darkening: current state

- Stars appear darker at their limbs than at their disk centers because at the limb we are viewing the higher and cooler layers of stellar photospheres.
- Limb darkening derived from state-of-the-art stellar atmosphere models systematically **fails** to reproduce recent transiting exoplanet light curves from the Kepler, TESS, and JWST telescopes – stellar brightness obtained from measurements drops less steeply towards the limb than predicted by models.
- Possible explanation: magnetic fields on the stellar surface are not taken into account:

  Kostogryz et al. (2024, NatAst):
  stellar atmosphere models computed with the use of a 3D radiative magneto-hydrodynamic code show that small-scale concentration of magnetic fields on the stellar surface affect limb darkening at a level allowing the authors to explain the observations.

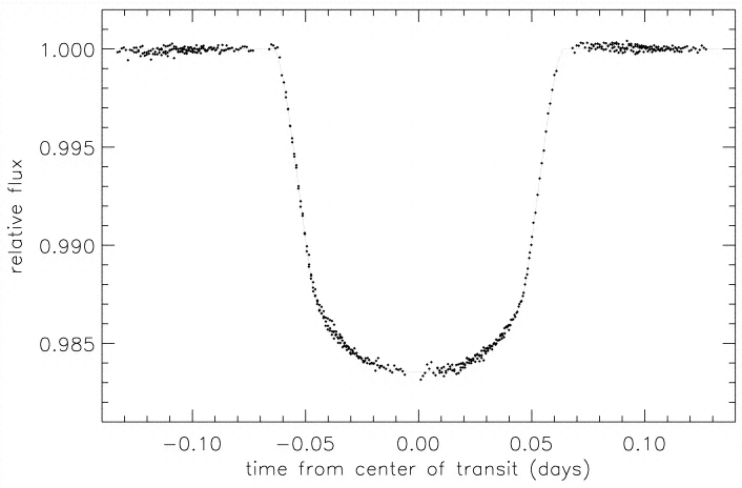

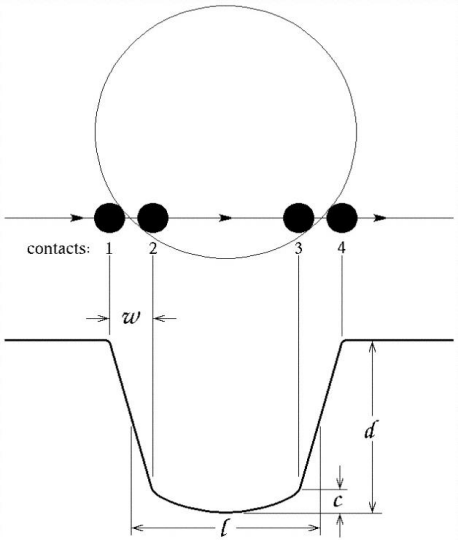

Eddington-Barbier relation

FORMAL SOLUTION TO THE PLANE-PARALLEL TRANSFER EQUATION.

EDDINGTON-BARBIER RELATION.

GREY ATMOSPHERE.

Formal Solution to RTE (1)

The **plane-parallel** transfer equation (for stars with thin photospheres)

$$\cos\theta \frac{dI_\lambda(\theta)}{d\tau_\lambda} = I_\lambda(\theta) - S_\lambda$$

The integrated form of the RTE is
[See D. Gray (page 127-129, 131) for more detail]:

$$I_\lambda(\tau_\lambda) = -\int_c^{\tau_\lambda} S_\lambda(t_\lambda) e^{-(t_\lambda - \tau_\lambda)\sec\theta} \sec\theta \, dt_\lambda$$

Here, the integration limit c (*which complicates the integral*), replaces $I_\nu(0)$ in the parallel-ray transfer equation (Lecture 5, slide I-149):

$$I_\lambda(\tau_\lambda) = \int_0^{\tau_\lambda} S_\lambda(t_\lambda) e^{-(\tau_\lambda - t_\lambda)} \, dt_\lambda + I_{\lambda 0} e^{-\tau_\lambda}$$

This is because the boundary conditions are different for radiation going in (θ>90°) and coming out (θ<90°) →

Formal Solution to RTE (2)

- The full intensity at the position τ_λ on the line of sight through the photosphere is

$$I_\nu(\tau_\nu) = I_\nu^{\text{out}}(\tau_\nu) + I_\nu^{\text{in}}(\tau_\nu)$$
$$= \int_{\tau_\nu}^{\infty} S_\nu e^{-(t_\nu - \tau_\nu)\sec\theta} \sec\theta \, dt_\nu$$
$$- \int_0^{\tau_\nu} S_\nu e^{-(t_\nu - \tau_\nu)\sec\theta} \sec\theta \, dt_\nu$$

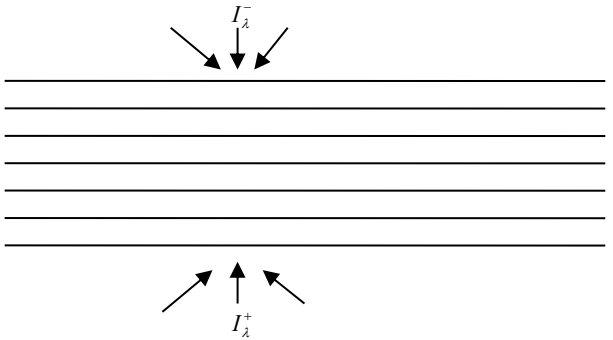

- An important special case occurs at the stellar surface. In this case

$$I_\nu^{\text{in}}(0) = 0$$
$$I_\nu^{\text{out}}(0) = \int_0^{\infty} S_\nu e^{-t_\nu \sec\theta} \sec\theta \, dt_\nu$$

where we assumed that the external radiation is **completely negligible** compared to the star's own radiation. **This Equation is the expression we need to compute the spectrum**.

- However, since the discs of most stars are spatially unresolved, we must deal with flux rather than intensity, so we will not deal with this equation any further.

Emergent Flux

From our lecture 6 (slide I-161), the flux is [If there is no azimuthal (ϕ) dependence in I_λ]:

$$F = 2\pi \int_{-1}^{1} I(\mu)\, \mu\, d\mu \qquad \mu = \cos\theta$$

Netto = Outwards – Inwards.

Decomposition into two half-spaces:

$$F = 2\pi \int_{0}^{1} I(\mu)\mu\, d\mu + 2\pi \int_{-1}^{0} I(\mu)\, \mu\, d\mu$$

$$= 2\pi \int_{0}^{1} I(\mu)\, \mu\, d\mu - 2\pi \int_{0}^{1} I(-\mu)\mu\, d\mu = \boldsymbol{F^+ - F^-}$$

Eddington-Barbier relation

Special case: at the surface of a star $F^- = 0$, so that $F = F^+$

$$F_\lambda(0) = 2\pi \int_0^1 I_\lambda\,(0,\theta)\,\mu\,d\mu$$

From earlier, assuming a linear source function $S_\lambda(\tau_\lambda) = a_\lambda + b_\lambda \tau_\lambda$ yields

$$I_\lambda(0,\theta) = a_\lambda + b_\lambda\, cos\,\theta = a_\lambda + b_\lambda \mu$$

In this case we obtain the "Eddington-Barbier" relation:

$$F_\lambda(0) = \pi(a_\lambda + 2/3\; b_\lambda) = \pi S_\lambda(\tau_\lambda = 2/3)$$

The emergent flux from the stellar surface is π times the Source function at an optical depth of $2/3$

Grey atmosphere (1)

If we assume Local TE (LTE), then

$$F_\lambda(0) = \pi S_\lambda(\tau_\lambda = 2/3) = \pi B_\lambda[T(\tau_\lambda = 2/3)]$$

Let us assume the opacity is independent of λ, i.e. $\kappa_\lambda = \kappa$. We call such a (hypothetical) atmosphere a **grey atmosphere**. Then

$$F_\lambda(0) = \pi B_\lambda[T(\tau = 2/3)]$$

The energy distribution of F_λ is that of a blackbody corresponding to the temperature at the optical depth $\tau = 2/3$.

The black body intensity is defined (following discovery by Max Planck in 1900) as either

$$B_\lambda(T) = \frac{2hc^2}{\lambda^5}\frac{1}{e^{hc/\lambda kT} - 1} \quad \text{or} \quad B_\nu(T) = \frac{2h\nu^3}{c^2}\frac{1}{e^{h\nu/kT} - 1}$$

where c=2.99x10^{10} cm, h=6.57x20^{-27} erg s, k=1.38x10^{-16} erg/s.

Let's compute the Bolometric flux.

Bolometric flux of Black Body

$$B_\nu(T) = \frac{2h\nu^3}{c^2}\frac{1}{e^{h\nu/kT}-1}$$

Note that: $$B_\nu(T)\mathrm{d}\nu = B_\lambda(T)\mathrm{d}\lambda \Rightarrow B_\lambda = B_\nu\left|\frac{\mathrm{d}\nu}{\mathrm{d}\lambda}\right| = B_\nu\frac{c}{\lambda^2}$$

Let us compute the bolometric flux:

$$F = \pi\int_0^\infty B_\nu(T)\mathrm{d}\nu = \pi\int_0^\infty \frac{2h\nu^3}{c^2}\frac{1}{e^{h\nu/kT}-1}\mathrm{d}\nu = \pi\frac{2h}{c^2}\left(\frac{kT}{h}\right)^4\int_0^\infty \frac{x^3}{e^x-1}\mathrm{d}x = \pi\frac{2h}{c^2}\left(\frac{kT}{h}\right)^4\frac{\pi^4}{15} = \sigma_{SB}T^4$$

$$\sigma_{SB} = 2\frac{\pi^5k^4}{15c^2h^3} = 5.67\ 10^{-5}\ \mathrm{erg\ cm^{-2}s^{-1}\ K^{-4}} - \text{Stefan-Boltzmann constant}$$

Planck function is monotonic with temperature: $$\frac{\partial B_\nu(T)}{\partial T} = \frac{2h^2\nu^4}{c^2kT^2}\frac{e^{h\nu/kT}}{\left(e^{h\nu/kT}-1\right)^2} > 0$$

$$F = \sigma T^4$$

Grey atmosphere (2)

If we assume Local TE (LTE), then

$$F_\lambda(0) = \pi S_\lambda(\tau_\lambda = 2/3) = \pi B_\lambda[T(\tau_\lambda = 2/3)]$$

Let us assume the opacity is independent of λ, i.e. $\kappa_\lambda = \kappa$. We call such a (hypothetical) atmosphere a grey atmosphere. Then

$$F_\lambda(0) = \pi B_\lambda[T(\tau = 2/3)]$$

The energy distribution of F_λ is that of a blackbody corresponding to the temperature at the optical depth $\tau = 2/3$.

Thus, integrating over λ

$$F(0) = \int_0^\infty F_\lambda(0) d\lambda = \pi \int_0^\infty B_\lambda(T(\tau = 2/3)] d\lambda = \sigma T^4(\tau = 2/3)$$

From Stefan-Boltzmann, $F(0) = \sigma T_{\text{eff}}^4$, by definition, we find $T_{\text{eff}} = T(\tau = 2/3)$.
The "surface" of a star, which has temperature T_{eff} (by definition) is not at the very top of the atmosphere (where τ = 0), but lies deeper down, at $\tau = 2/3$.

This can be considered as an *average* point of origin from the observed photons.

Summary

- Solution to plane-parallel transfer equation at surface explains limb darkening in Sun.
- Limb darkening in other stars can be estimated from interferometry, eclipsing binaries, microlensing.
- Eddington-Barbier relation.
- Grey atmosphere.
- Assuming a grey atmosphere , we found that the “surface” of a star, which has temperature $T_{\rm eff}$ (by definition) is not at the very top of the atmosphere (where $\tau = 0$), but lies deeper down, at $\tau = 2/3$.

Radiative Equilibrium

GREY ATMOSPHERE
THERMAL (RADIATIVE) EQUILIBRIUM
THE DEPTH DEPENDENCE OF THE SOURCE FUNCTION
EDDINGTON APPROXIMATION
TEMPERATURE STRUCTURE OF THE GREY ATMOSPHERE

Grey atmosphere

- Above we assumed that the opacity can be independent of λ, i.e. $\kappa_\lambda = \kappa$. We call such a (hypothetical) grey atmosphere.
- In the theory of stellar atmospheres, much of the technical effort goes into iteration schemes using equations of radiative equilibrium (which we will discuss today) to find the source function S_λ.
- Often, a starting point for such iterations is the **grey** case.

Thermal (radiative) equilibrium

- In stellar atmospheres, radiation dominates transfer of energy, so we can discuss (three) conditions of radiative equilibrium, which can be used to derive the temperature structure in the photosphere.

- The radiation we see from the Sun comes from a layer of geometrical height of a few hundred km.

- In a column of 100 km height and 1 cm^2 cross-section there are 10^{24} particles (since $n \sim 10^{17}/cm^3$ in Sun), each of which has a thermal energy of $3kT/2$ (10^{-12} erg). The total thermal energy of this column is therefore 10^{12} erg/cm^2. The observed radiative energy loss (per cm^2) of the solar surface is $F_\odot = 6.3 \times 10^{10}$ erg cm^{-2} s^{-1}.

- If the Sun shines at a constant rate, the energy content of the solar photosphere can only last for 15 seconds without being replenished from below.

- Exactly the same amount of energy must be supplied or else the photosphere would quickly change temperature.

First equation of radiative equilibrium

- Since this does **not** happen, $\mathrm{d}F/\mathrm{d}t=0$ or $\mathrm{d}F/\mathrm{d}x=0$ or $\mathrm{d}F/\mathrm{d}\tau=0$, i.e. the total flux must be constant at all depths of the photosphere (**conservation of energy**) – the **1st equation of radiative equilibrium**

$$F(x) = F(0) = const = \sigma T_{eff}^4$$

- When all the energy is carried by radiation, we have

$$F(x) = \int_0^\infty F_\lambda(\tau_\lambda) d\lambda = F(0)$$

Although the shape of F_λ can be expected to change very significantly with depth, its integral remains invariant.

- If other sources of energy transport are significant, then a more general expression of flux constancy must be applied:

$$\Phi(x) + \int_0^\infty F_\lambda(\tau_\lambda) d\lambda = F(0)$$

Φ(x) is, for example, the convective flux

Radiative equilibrium

- We may integrate the plane-parallel transfer equation over solid angle ω.

$$\int \cos\theta \frac{dI_\lambda(\tau_\lambda,\theta)}{d\tau_\lambda} d\omega = \int I_\lambda(\tau_\lambda,\theta)\, d\omega - \int S_\lambda(\tau_\lambda)\, d\omega$$

$$\frac{d}{d\tau_\lambda}[F_\lambda(\tau_\lambda)] = 4\pi[J_\lambda(\tau_\lambda)] - \int S_\lambda(\tau_\lambda)\, d\omega$$

Based on the definition of mean intensity and flux:

$$J_\lambda = \frac{1}{4\pi}\oint I_\lambda d\omega \quad \text{and} \quad F_\lambda = \oint I_\lambda \cos\theta\, d\omega$$

- Finally, assuming S_λ to be isotropic we obtain,

$$\frac{1}{4\pi}\frac{d}{d\tau_\lambda}[F_\lambda(\tau_\lambda)] = J_\lambda(\tau_\lambda) - S_\lambda(\tau_\lambda)$$

Second equation of radiative equilibrium

- In the grey case, for which the opacity κ is independent of wavelength

$$\frac{1}{4\pi}\frac{d}{d\tau}F(\tau) = -S(\tau) + J(\tau) = 0$$

Since $dF/d\tau = 0$, the Source function must be equal the mean intensity J.

- If the atmosphere is **not** grey, which is the situation for most stars, let's incorporate the opacity κ into the RHS, and integrating over wavelength

$$\frac{1}{4\pi\rho}\frac{d}{ds}\left[\int_0^\infty F(\tau_\lambda)d\lambda\right] = \int_0^\infty (-\kappa_\lambda S_\lambda + \kappa_\lambda J_\lambda)d\lambda = 0$$

$$\tau_\lambda = \int_0^s \kappa_\lambda \rho ds$$

Since $dF/ds = 0$, we get the **radiative balance equation (energy conservation)**

$$\int_0^\infty \kappa_\lambda S_\lambda d\lambda = \int_0^\infty \kappa_\lambda J_\lambda d\lambda$$

- This is **the second equation of radiative equilibrium** and can be understood as the total energy absorbed (RHS) must equal the total energy re-emitted (LHS) if no heating or cooling is taking place.

Third equation of radiative equilibrium

The third radiative equilibrium condition is obtained by multiplying the transfer equation by $\cos\theta$ and integrating over solid angle and then wavelength

$$\cos\theta \frac{dI_\lambda(\theta)}{d\tau_\lambda} = I_\lambda(\theta) - S_\lambda$$

$$\oint \cos^2\theta \frac{dI_\lambda(\tau_\lambda,\theta)}{d\tau_\lambda} d\omega = \oint \cos\theta\, I_\lambda(\tau_\lambda,\theta) d\omega - \oint \cos\theta\, S_\lambda(\tau_\lambda,\theta) d\omega$$

$$K_\lambda(\tau_\lambda) = \frac{1}{4\pi}\oint I_\lambda \cos^2\theta\, d\omega \qquad F_\lambda = \oint I_\lambda \cos\theta\, d\omega \qquad \mathbf{0}\ (S_\lambda \text{ is isotropic})$$

$$4\pi \int \frac{dK_\lambda}{d\tau_\lambda} d\lambda = \int F_\lambda\, d\lambda = F(\tau)$$

The third radiative equilibrium condition:

$$\int_0^\infty \frac{dK_\lambda}{d\tau_\lambda} d\lambda = \frac{F(\tau)}{4\pi}$$

Equations of radiative equilibrium

- All the three radiative equilibrium conditions are not independent. S_λ that is a solution of one will be the solution of all three.
- The flux constant $F(0)$ is often expressed in terms of an effective temperature $F(0) = \sigma T_{eff}^4$.
- When model photospheres are constructed using flux constancy as a condition to be fulfilled by the model, the effective temperature becomes one of the fundamental parameters characterizing the model.
- In real stars, energy is created or lost from the radiation field through e.g. convection, magnetic fields,
  plus in supernovae atmospheres energy conservation is not valid (radioactive decay of Ni to Fe),
  so the energy constraints are more complicated in reality.

Recap: Equations of radiative equilibrium

- **The 1st equation of radiative equilibrium:**

$$F(x) = F(0) = const = \sigma T_{eff}^4$$

i.e. the total flux must be constant at all depths of the photosphere (**conservation of energy**):
$\mathrm{d}F/\mathrm{d}t=0$ or $\mathrm{d}F/\mathrm{d}x=0$ or $\mathrm{d}F/\mathrm{d}\tau=0$

- **The 2nd equation of radiative equilibrium:**
the total energy absorbed (RHS) must equal the total energy re-emitted (LHS) if no heating or cooling is taking place:

$$\int_0^\infty \kappa_\lambda S_\lambda d\lambda = \int_0^\infty \kappa_\lambda J_\lambda d\lambda$$

- **The 3rd radiative equilibrium condition:**

$$\int_0^\infty \frac{dK_\lambda}{d\tau_\lambda} d\lambda = \frac{F(\tau)}{4\pi}$$

- All the three radiative equilibrium conditions are not independent.
S_λ that is a solution of one will be the solution of all three.

The depth dependence of the source function

- In a **grey** atmosphere, with $K(\tau) = \int_0^\infty K_\lambda \, d\lambda$, the 3rd equation implies:

  a new unknown function $K(\tau)$

$$\frac{dK(\tau)}{d\tau} = \frac{F(\tau)}{4\pi}$$

- We can differentiate this, and insert our earlier result:

$$\frac{d^2K(\tau)}{d\tau^2} = \frac{1}{4\pi}\frac{dF(\tau)}{d\tau} = J(\tau) - S(\tau) = 0 \qquad [1]$$

- Integration of the equation with respect to τ gives $K(\tau)=c_1\tau+c_2$ [2]

  where $dK/d\tau = c_1 = F/4\pi$

- For a given F, we now have two equations, [1] and [2], to determine the three unknowns: J, S and K (or c_2). We need an additional relation between two of these variables in order to determine all three.

Eddington approximation (1)

- Previously we have seen that for the determination of the flux the anisotropy in the radiation field is very important because in the flux integral the inward-going intensities are subtracted from the outward-going ones, due to the factor $\cos\theta$.
- But for K, a small anisotropy is unimportant because the intensities are multiplied by the factor $\cos^2\theta$, which does **not** change sign for inward and outward radiation.

- To evaluate K or c_2, we can approximate the radiation field by an isotropic radiation field of the mean intensity J: $I = J$ (by definition). From the definition of K_λ we obtain

$$4\pi\, K_\lambda = \oint I_\lambda(\tau_\lambda,\theta)\cos^2\theta\, d\omega = J_\lambda(\tau_\lambda)\oint \cos^2\theta\, d\omega = \frac{4\pi}{3} J_\lambda(\tau_\lambda)$$

or after division by 4π,

$$K_\lambda(\tau_\lambda) = \frac{1}{3} J_\lambda(\tau_\lambda)$$

$d\omega = \sin\theta\, d\theta\, d\varphi$

This approximation for the K-function is known as the **Eddington approximation**.

Eddington approximation (2)

- Inserting the Eddington approximation into the above equation we find

$$\frac{dK(\tau)}{d\tau} = \frac{F(\tau)}{4\pi}$$

$$\frac{dK(\tau)}{d\tau} = \frac{1}{3}\frac{dJ(\tau)}{d\tau} = \frac{F(\tau)}{4\pi} = c_1 \qquad \frac{dJ(\tau)}{d\tau} = \frac{3}{4\pi}F(\tau)$$

- Since the mean intensity J equals the source function S in a grey atmosphere, integrating the latter result we obtain

$$F(x) = F(0) = const$$

$$S(\tau) = \frac{3}{4\pi}\tau F(0) + C = J(\tau)$$

- From the conditions of radiative equilibrium, we finally obtained **the law for the depth dependence of the source function** (**for a grey atmosphere assuming the Eddington approximation**). We can evaluate C using boundary condition for the known emerging flux (there is no flux going into the star), plus we assume the outward intensity does not depend upon θ:

Eddington approximation (3)

- Boundary condition: there is no flux going into the star, i.e. $I(0,\theta) = I^- = 0$ for $\pi/2 < \theta < \pi$
- We also assume that the outward intensity does not depend upon θ, i.e. $I(0,\theta) = I^+ = \text{const}$ for $0 < \theta < \pi/2$

$J_\lambda = \frac{1}{4\pi}\oint I_\lambda d\omega$ and $F_\lambda = \oint I_\lambda \cos\theta \, d\omega$ $\quad d\omega = \sin\theta \, d\theta \, d\varphi$

- It gives $J(0) = \frac{1}{2}I^+ = \frac{1}{2\pi}F(0)$

τ=0

$S(\tau) = \frac{3}{4\pi}\tau F(0) + C = J(\tau)$

- Hence $C = J(0) = F(0)/2\pi$ so:

$$S(\tau) = \frac{1}{\pi}\left(\frac{3}{4}\tau + \frac{1}{2}\right)F(0)$$

$$S(\tau) = \frac{3}{4\pi}\left(\tau + \frac{2}{3}\right)F(0)$$

- To find the depth dependence of T, we also need to assume **LTE**.

Temperature structure of the grey atmosphere

In LTE, the source function is the Planck function, $S(\tau)=B(\tau)=\sigma T^4/\pi$

$$B(\tau)=\frac{\sigma}{\pi}T^4(\tau)=\frac{3}{4\pi}(\tau+\frac{2}{3})F(0)$$

$S(\tau)=\frac{3}{4\pi}(\tau+\frac{2}{3})F(0)$

Recall that $F(0)=\sigma T^4_{\text{eff}}$, by definition, so

$$\frac{1}{\pi}\sigma T^4(\tau)=\frac{3}{4\pi}(\tau+\frac{2}{3})\sigma T_{eff}^4 \quad \text{or} \quad T^4(\tau)=\frac{3}{4}(\tau+\frac{2}{3})T_{eff}^4$$

We derived the **temperature dependence on optical depth**.
Note $T(\tau=2/3) = T_{\text{eff}}$ as we obtained earlier, and $T^4(\tau=0)=T_{\text{eff}}^4/2$

A complete solution of the grey case, using accurate boundary conditions, without Eddington approximation, leads to a solution only slightly different from this, usually expressed as

$$T^4(\tau)=\frac{3}{4}[\tau+q(\tau)]T_{eff}^4$$

Here $q(\tau)$ is a slowly varying function (Hopf function), with
$q = 1/\sqrt{3} = 0.577$ at $\tau=0$ to $q=0.710$ at $\tau=\infty$.

Grey Temperature Structure

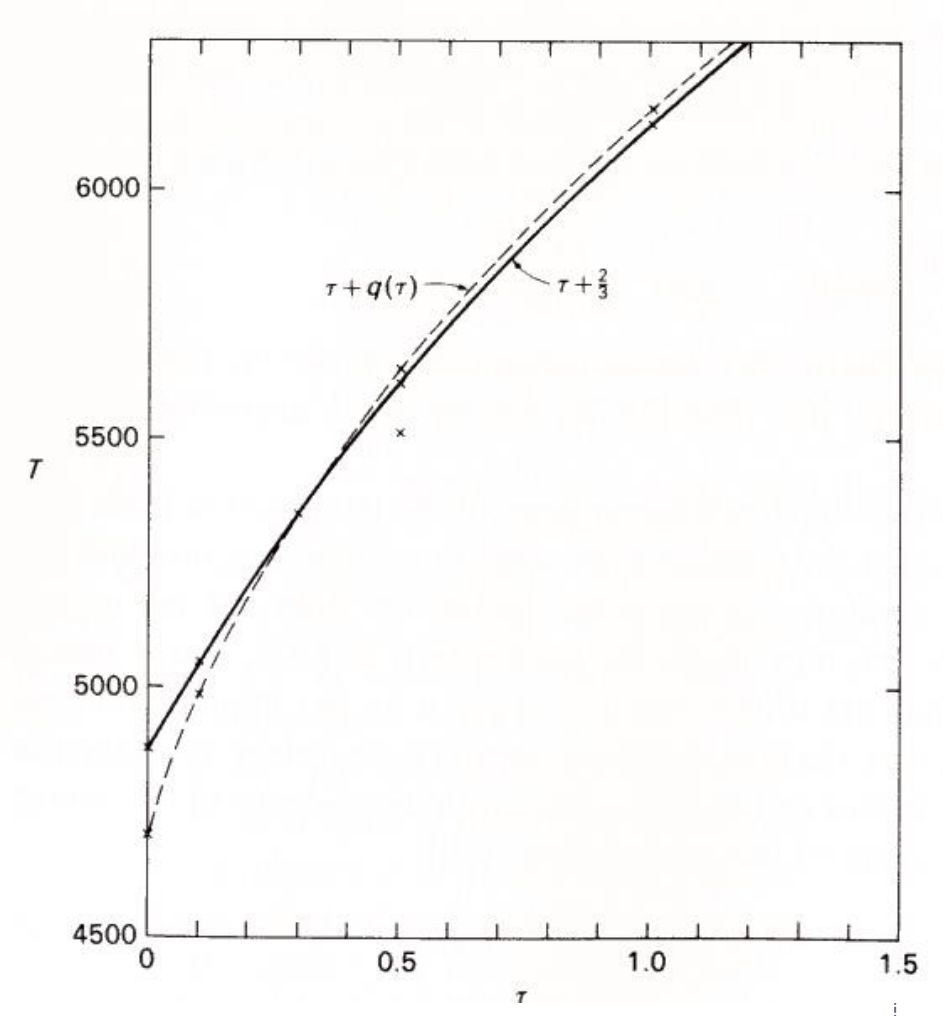

Comparison between $T(\tau)$ in the Solar atmosphere using the simplifying Eddington assumption (solid) versus the exact grey case (dashed) using the Hopf function, $q(\tau)$:

$$q(\tau) \approx 0.710 - 0.133e^{-2\tau}$$

How realistic is this?

- How good an approximate is the grey atmosphere? Next we must look at the frequency dependence of the sources of opacity.
- The grey temperature distribution is shown here versus the observed Solar temperature distribution as a function of optical depth τ at 5000Å (D. Gray, Table 9.2)
- The poor match is because the opacity is **wavelength dependent**, as we shall see next lecture.

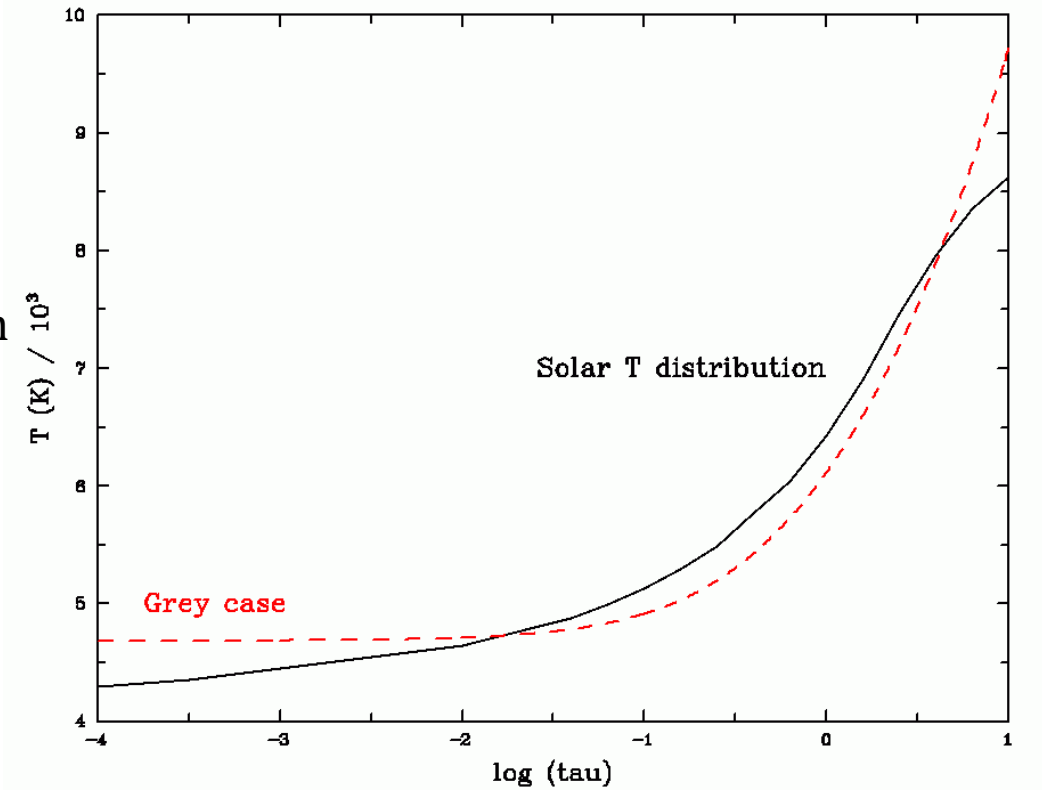

Summary

- Three equations of radiative equilibrium can be derived:
  (a) constant flux with depth;
  (b) energy absorbed equals energy emitted;
  (c) the K-integral is linear in τ.

- From these, the **grey** temperature distribution $T(\tau)$ may be derived, assuming:
  (a) the Eddington approximation and
  (b) LTE, in reasonable agreement with the exact case.

- On the next lecture, we will discuss LTE in more detail.

Local Thermodynamic Equilibrium (LTE)

MAXWELLIAN VELOCITY DISTRIBUTION
BOLTZMANN EQUATION
SAHA EQUATION

Thermodynamic Equilibrium (TE)

- Interaction of radiation and matter is the most important physical process in stellar atmospheres.
- To find $\boldsymbol{I_\lambda}$ we need to know α_λ and ε_λ (or k_λ and j_λ) – absorption and emission coefficients.
- To find α_λ and ε_λ, density ρ, temperature T, and chemical composition X are **not** enough. We need to know distributions of atoms over levels and ionization states, which depend on radiation $\boldsymbol{I_\lambda}$.

- In TE, ρ, T, and X fully determine α_λ and ε_λ.

Local Thermodynamic Equilibrium

In **Thermodynamic Equilibrium**:

1. All particles have Maxwellian distribution in velocities (with the same temperature T).
2. Atom populations follow Boltzmann law (same T).
3. Ionization is described by Saha formula (same T).
4. Radiation intensity is given by the Planck function (same T).
5. The principle of detailed equilibrium is valid (the number of direct processes = number of inverse processes).

In **Local thermodynamic equilibrium (LTE)**, 1-3 are applied **locally**.

The radiation spectrum can in principle be very far from Planck function.

LTE

In the study of stellar atmospheres, the assumption of Local Thermodynamic Equilibrium (**LTE**) is described by:

1. Electron and ion velocity distributions are Maxwellian.
2. Excitation equilibrium is given by Boltzmann equation (introduced today).
3. Ionization equilibrium is given by Saha equation (introduced today).
4. The source function is **given** by the Planck function

   $S_\lambda = I_\lambda = B_\lambda(T)$ i.e. Kirchoff's law $j_\lambda = \kappa_\lambda B_\lambda(T)$

Is LTE a valid assumption?

- For LTE to be valid, the photon and particle mean free paths need to be much smaller than the length scale over which these temperature changes significantly.
- Radiation cannot play a role in defining atom populations and ionization state. Collisions should dominate.
- Generally, when **collisional** processes dominate over radiative processes in the excitation and ionization of atoms, the state of the gas is close to LTE.
- Consequently, **LTE is a good assumption in stellar interiors, but may break down in the atmosphere**. If LTE is no longer valid, all processes need to be calculated in detail via **non-LTE**. This is much more complicated, but needs to be considered in some cases (see later in course).

Mean Free Path

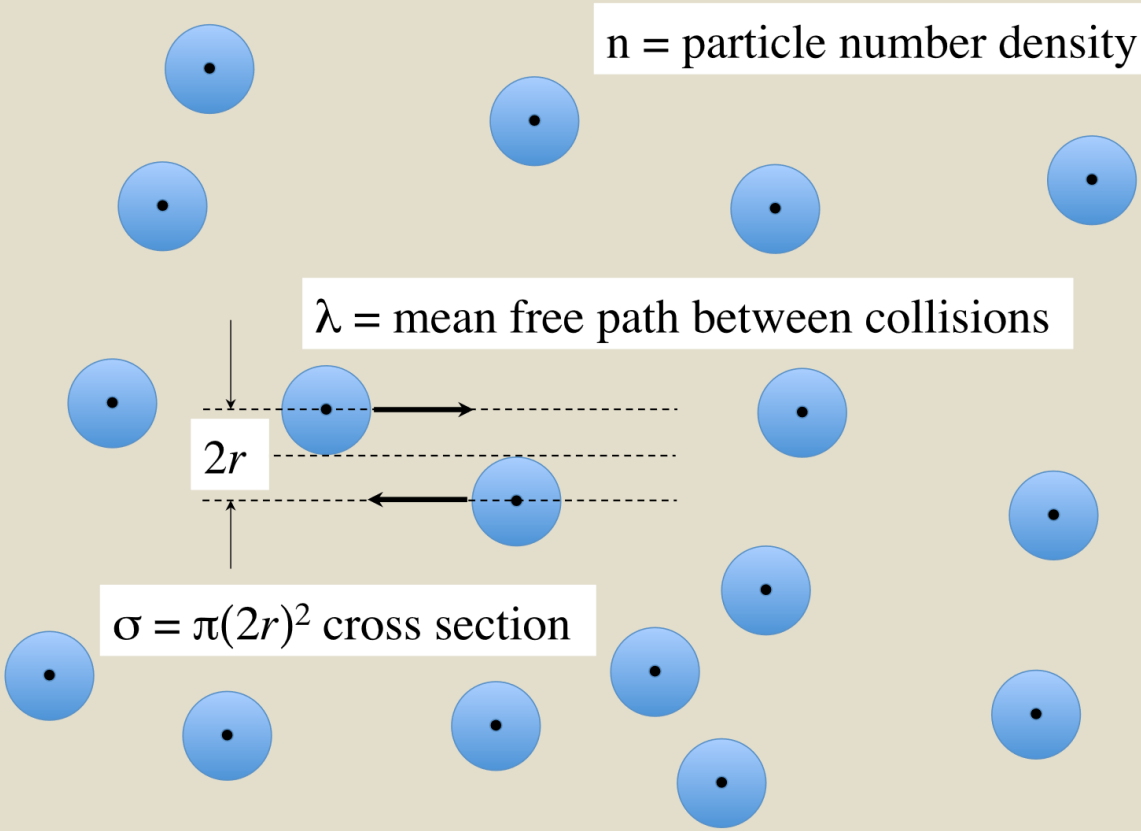

- In the Sun, the characteristic distance over which the temperature varies (the temperature scale height) is ~500km.
- **How does this scale compare with the average distance travelled by an atom before hitting another atom?**
- Two hydrogen atoms will collide if their centres pass within a radius of 2 Bohr radii ($2a_0$) of each other. The collision cross-section of the H atom is $\sigma=\pi(2a_0)=3.5\times10^{-16}$ cm^2.
- The mean free path between collisions is $\lambda=1/(\sigma n(\mathrm{H}))$.

Mean free path in the solar photosphere

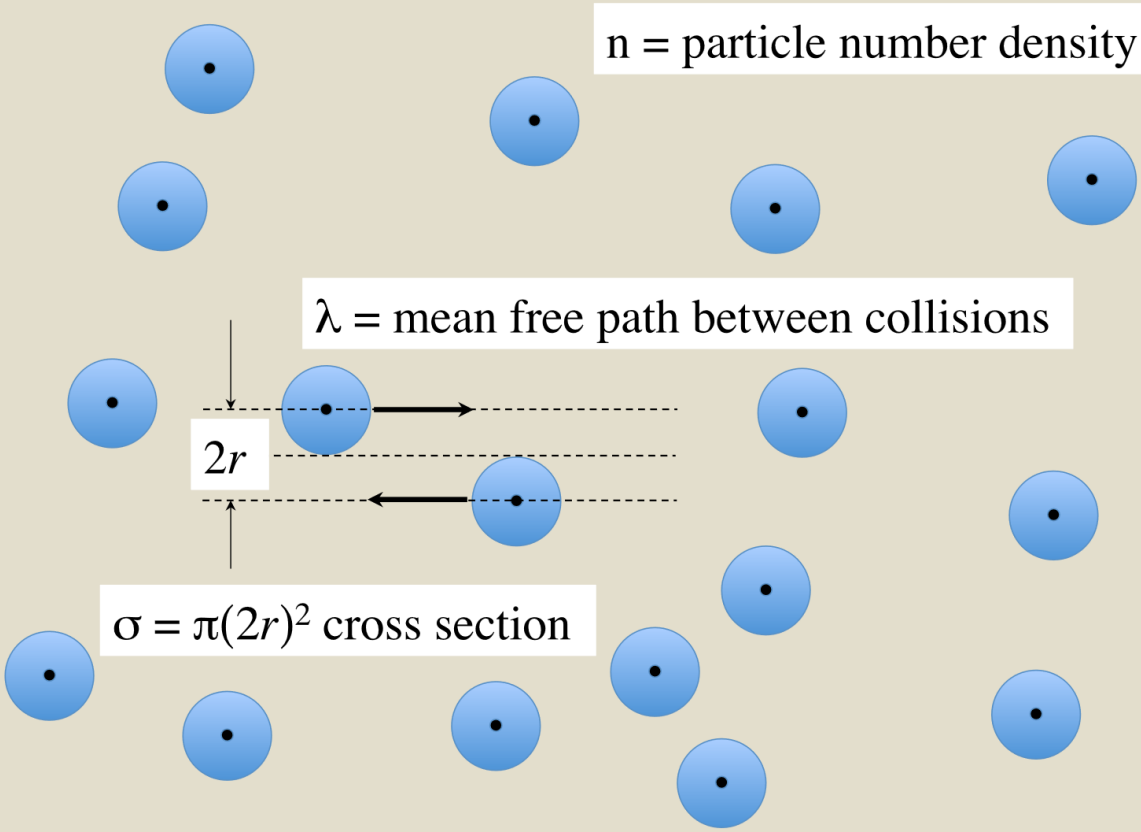

- The density of the Solar photosphere is $\rho = 2.5 \times 10^{-7}$ g/cm^3 so the number of H atoms/cm^3 is $n(\mathrm{H}) = \rho / m_{\mathrm{H}} = 1.5 \times 10^{17}$ cm^3 where m_{H} is the mass of the H atom.
- Then the mean free path between collisions is $\lambda = 1/(\sigma n(\mathrm{H})) = 0.02$ cm. i.e. atoms are confined within a limited volume of space in the photosphere at effectively fixed temperature (relative to the temperature scale height).

In the upper layers, $\rho \rightarrow 0$, $\lambda \uparrow$, radiation dominates over collisions → **out of LTE**

Mean Free Path in the Sun

Since the photosphere is the layer visible from Earth, photons must be able to escape freely into space. After ~10^{21} scatterings and re-emissions (thousands years!) from the centre.
Calculate the time needed for a photon to escape!

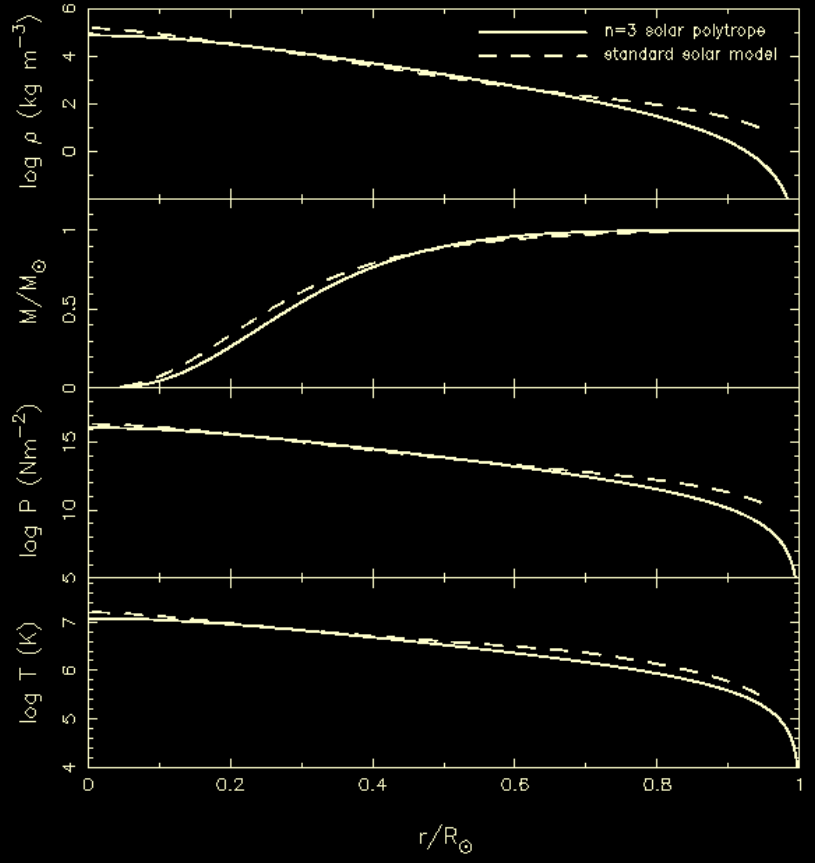

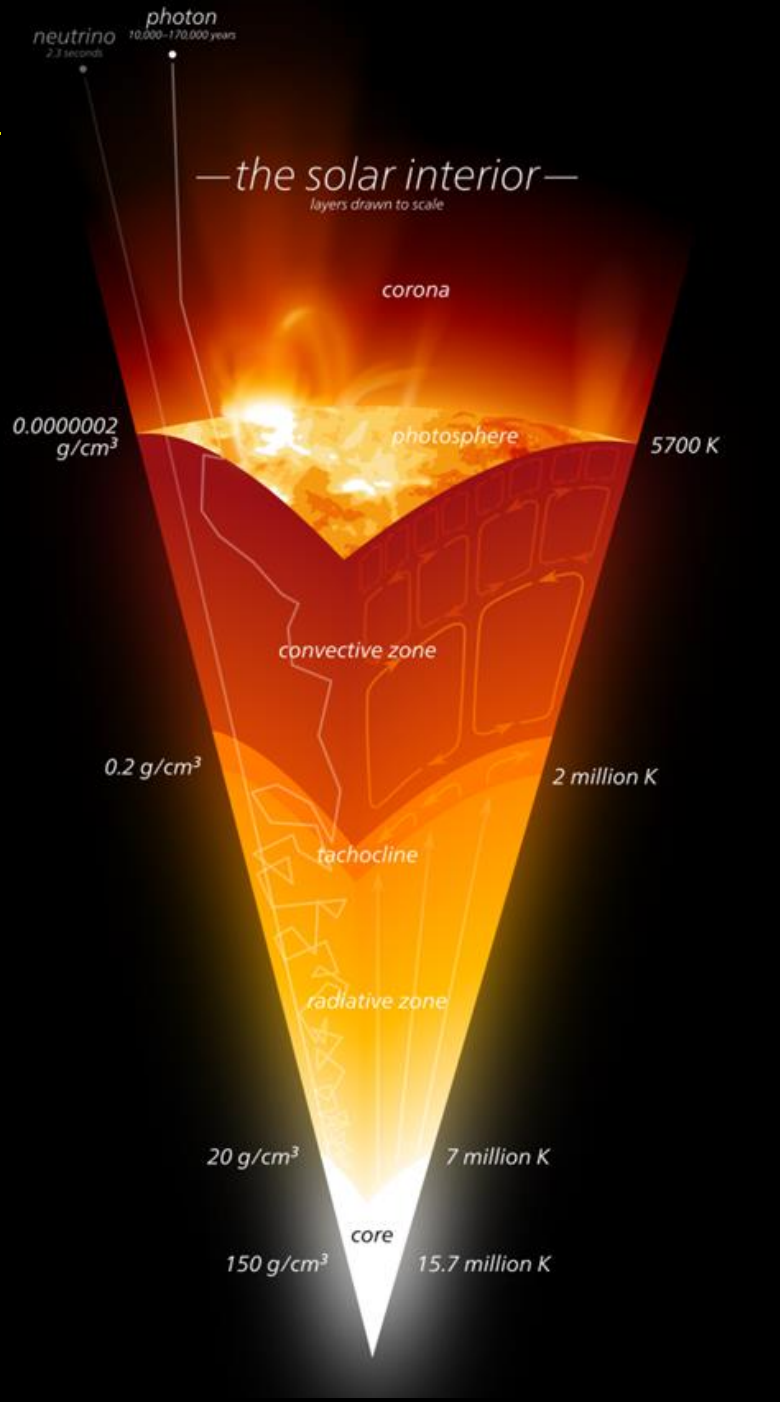

The Random Walk

- As the photons diffuse upward through the stellar material, they follow a haphazard path called a random walk. Figure shows a photon that undergoes a net vector displacement d as the result of making a large number N of **randomly** directed steps, each of length l (=λ, the mean free path).
- It can be shown that for a random walk, the displacement d is related to the size of each step, l, by

$$d = l\sqrt{N}.$$

- This implies that the distance from the centre of a star to the surface is

$$D = l \times N$$

- This is why the transport of energy through a star by radiation may be extremely **inefficient**.

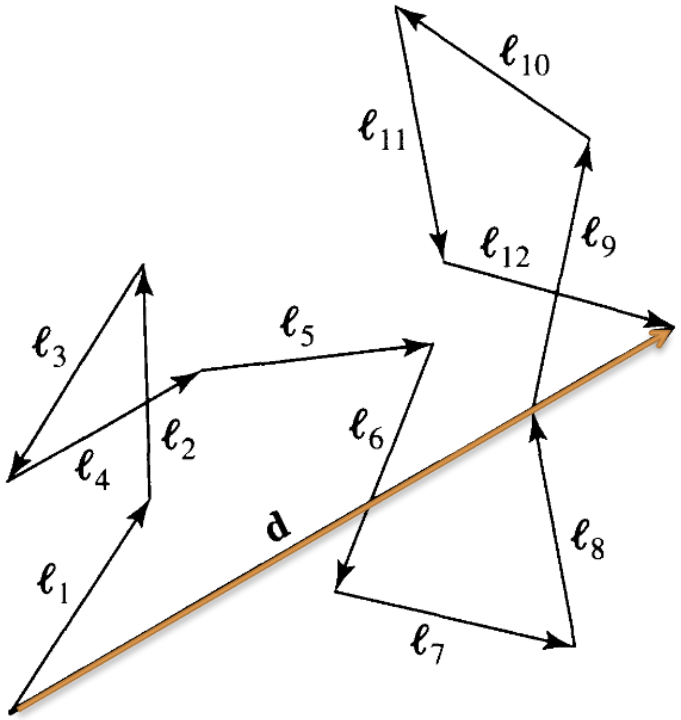

LTE

As noticed above, **LTE** is described by:

1. Maxwellian electron and ion velocity distributions.
2. Excitation equilibrium given by Boltzmann equation.
3. Ionization equilibrium given by Saha equation.

Let's discuss them.

Maxwellian velocity distribution

Gas pressure is produced by the motions of the gas particles. The velocities of particles are distributed in a Maxwellian distribution (also called the Maxwell–Boltzmann distribution).

$$\frac{dN(v)}{N_{\text{total}}} = \left(\frac{2}{\pi}\right)^{1/2}\left(\frac{m}{kT}\right)^{3/2} v^2 e^{-mv^2/2kT}\, dv$$

Because the particles produce Doppler shifts, the line-of-sight velocities have a distribution that is an important special case for spectroscopy:

$$\frac{dN(v_R)}{N_{\text{total}}} = \left(\frac{m}{2\pi kT}\right)^{3/2} e^{-mv_R^2/2kT}\, dv_R$$

where v_R is the radial (line of sight) velocity component.

Maxwellian velocity distribution

The maximum of the speed distribution occurs at v_1 (the most probable velocity):

$$v_1 = \left(\frac{2kT}{m}\right)^{1/2}$$

The average velocity, v_2, is

$$v_2 = \left(\frac{8}{\pi}\frac{kT}{m}\right)^{1/2} = 1.128v_1$$

The root mean square velocity, v_3, is

$$v_3 = \left(\frac{3kT}{m}\right)^{1/2} = 1.225v_1$$

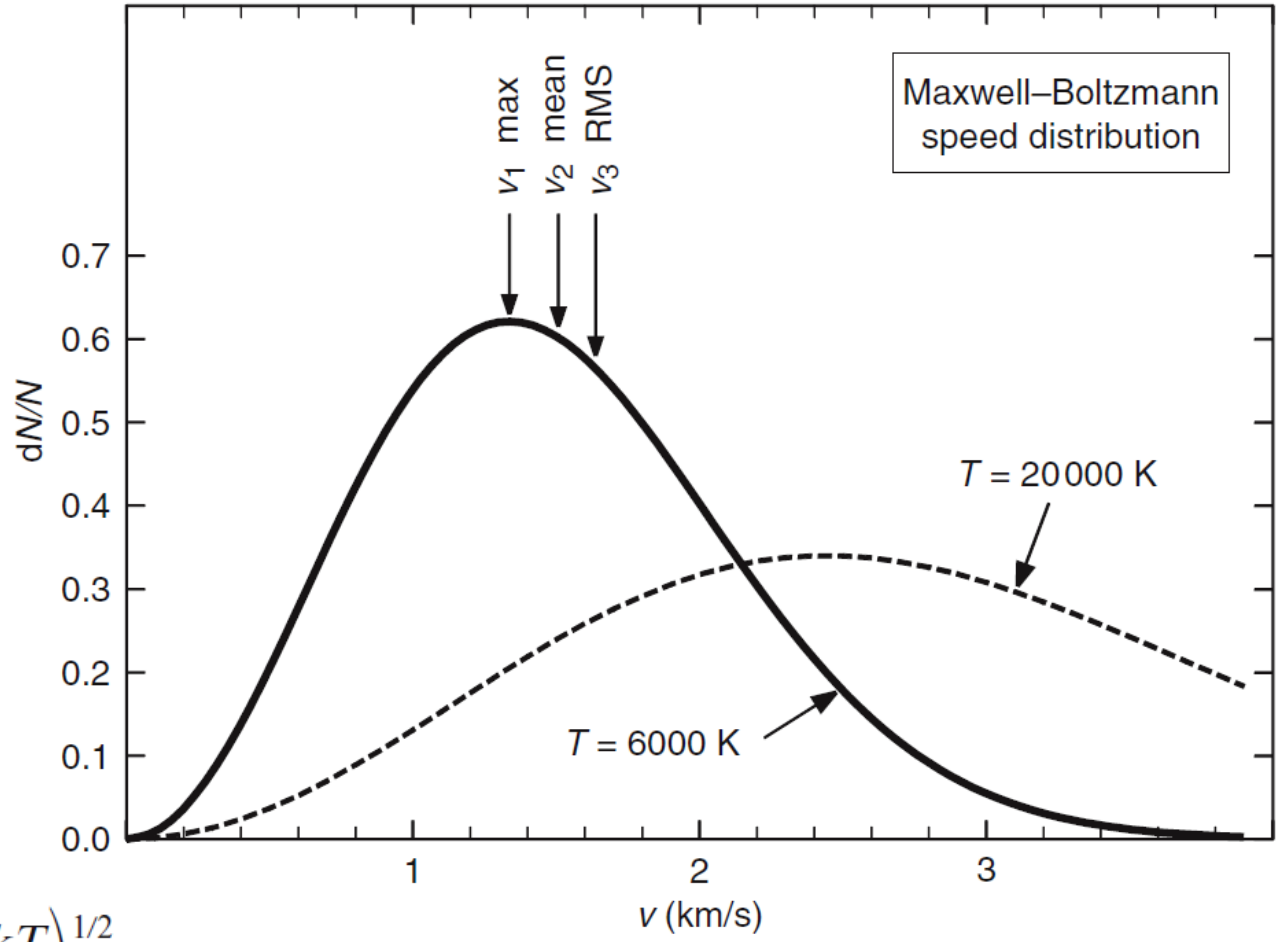

Boltzmann equation

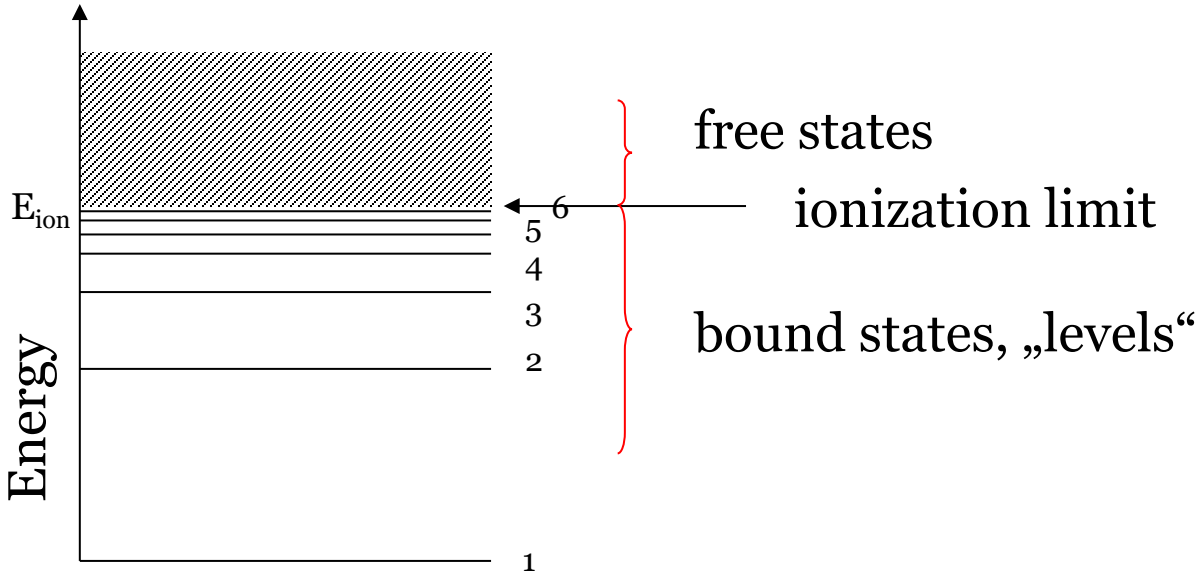

For excited levels u and l of e.g. atomic hydrogen, the **Bolzmann equation** relates their population (occupation) numbers as follows:

$$\frac{N_u}{N_l} = \frac{g_u}{g_l} e^{-(E_u - E_l)/kT}$$

where $\chi_{ul} = E_u - E_l$ is the energy difference between the levels, g_u & g_l are their statistical weights (see next slide), k=8.6174x10^{-5} eV/K is the Boltzmann constant.

Boltzmann equation may also be written as:

$$\log\frac{N_u}{N_l} = \log\frac{g_u}{g_l} - \frac{5040}{T}\chi_{ul}(eV)$$

$\Theta = 5040/T$

In the "ground state" (n=1), "first excited state" (n=2), and all other excited states of H more than one quantum state may have the same energy.

The number of these for orbital n is the statistical weight, g_n, (also known as the degeneracy).

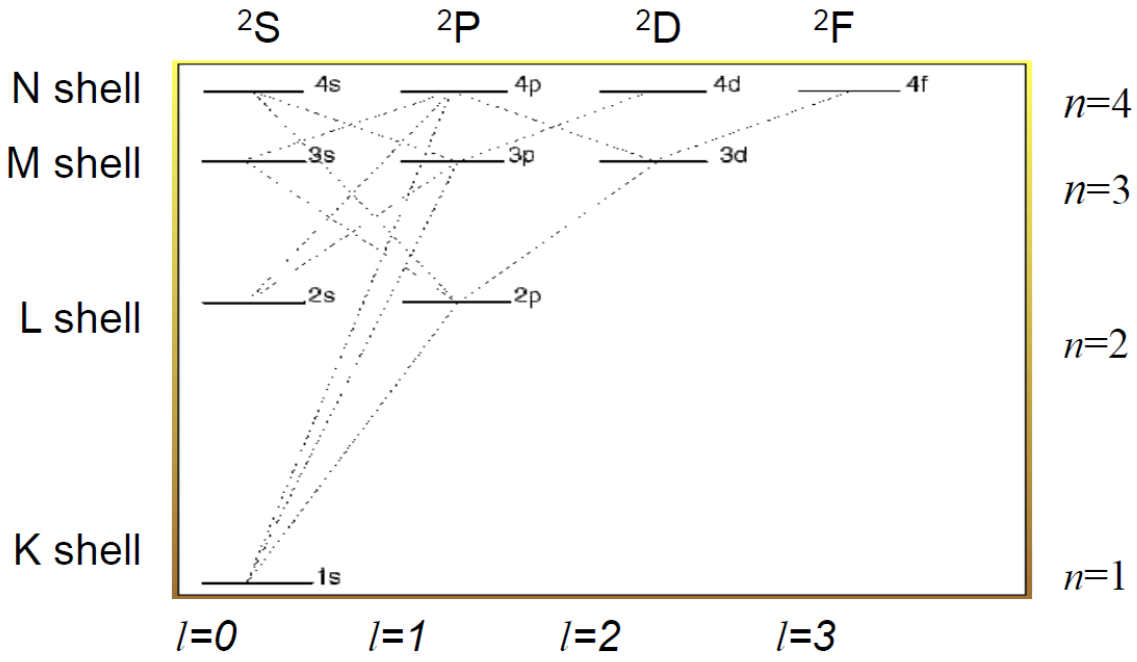

Hydrogen

For H, orbital n has a statistical weight of $g_n=2n^2$ – the various permutations for n=1 and n=2 are listed here, with statistical weights g_1=2 and g_2=8, respectively.

l=0…n-1 azimuthal quantum number
m_l=magnetic quantum number with $-l \le m_l \le l$
m_s=electron "spin" angular momentum $\pm 1/2$

Transition energy between levels u and l:

$$\chi_{ul} = C\left(\frac{1}{u^2} - \frac{1}{l^2}\right)$$

where $C=\chi_{\text{ion}}$=-13.6 eV

Ground States s_1				Energy E_1
n	ℓ	m_ℓ	m_s	(eV)
1	0	0	$+1/2$	-13.6
1	0	0	$-1/2$	-13.6
First Excited States s_2				Energy E_2
n	ℓ	m_ℓ	m_s	(eV)
2	0	0	$+1/2$	-3.40
2	0	0	$-1/2$	-3.40
2	1	1	$+1/2$	-3.40
2	1	1	$-1/2$	-3.40
2	1	0	$+1/2$	-3.40
2	1	0	$-1/2$	-3.40
2	1	-1	$+1/2$	-3.40
2	1	-1	$-1/2$	-3.40

Balmer lines

An exceptionally high T is required for a significant number of H atoms to have electrons in their 1st excited states. The Balmer lines (involving an upward transition from n=2 orbital) reach a peak strength at spectral class A (≈10000K)

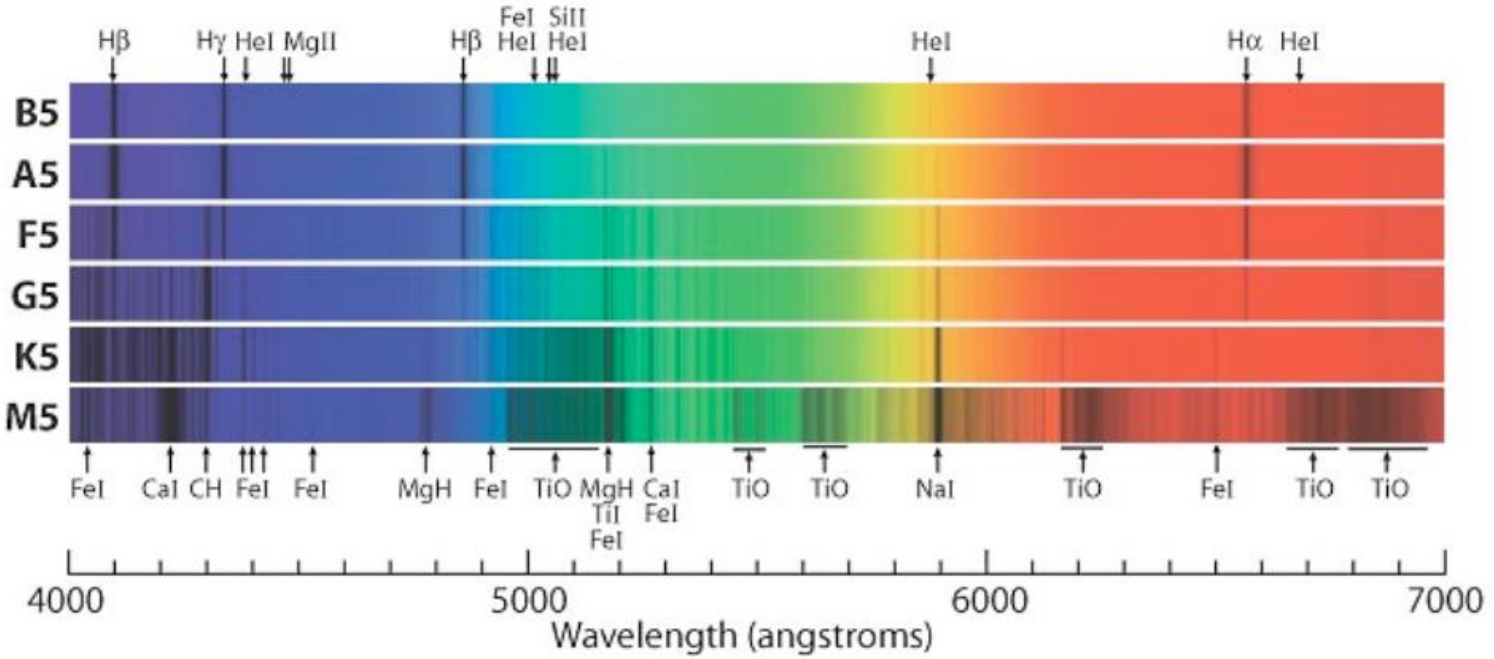

so why do the Balmer lines **diminish** in strength at higher temperatures?

We need Saha equation to answer this question.

Balmer lines

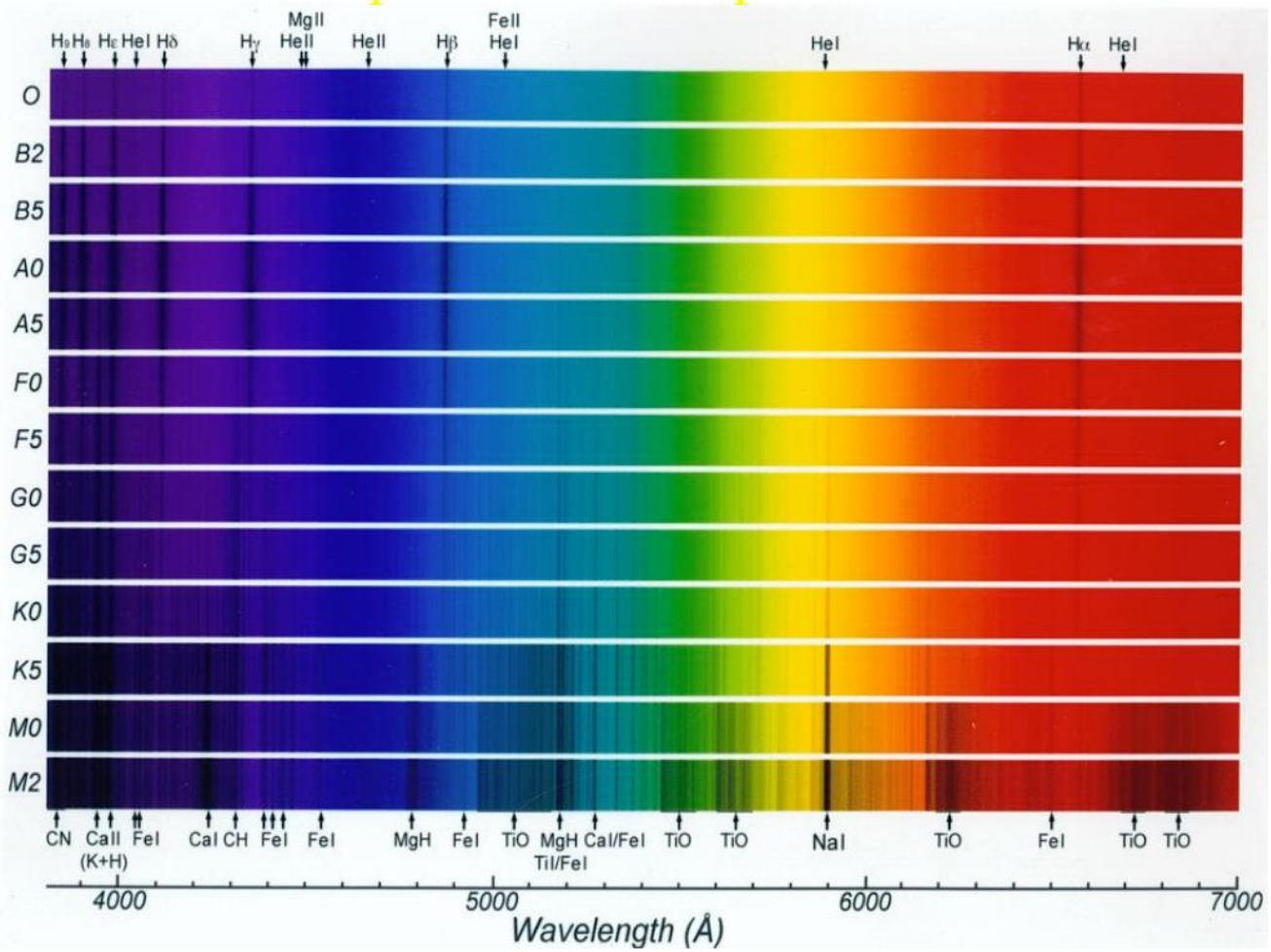

The degree of ionization of an atom

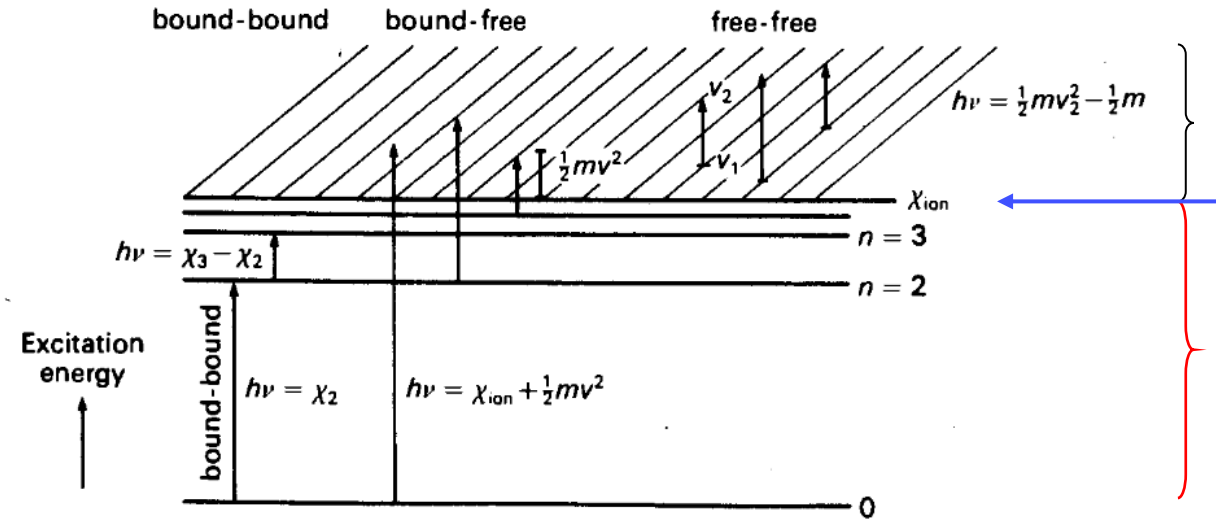

ionization limit

The degree of ionization of any atom or ion can be obtained from the Saha equation, which can be derived from the Boltzmann formula if we extend it to states with positive energies, i.e., to free electrons with the appropriate statistical weights (the upper state is now an ion plus free electron, with energy $\chi_{ion}+1/2m_e v^2$).

The statistical weight of the ion in the ground state plus electron is the product of the statistical weight of the ion g_1^+ and the statistical weight of the electron g_e: $g_{ion+e} = g_1^+ g_e$

The Saha Equation

The statistical weight of the ion in the ground state plus electron is the product of the statistical weight of the ion $g_1{}^+$ and the statistical weight of the electron g_e:

$$g_{\text{ion+e}} = g_1{}^+ g_e$$

The (differential) statistical weight of the electron, g_e, i.e. the number of available states in interval (v,$v+dv$) is (from quantum mechanics)

$$g_e = \frac{1}{N_e} \frac{8\pi m_e^3 v^2 dv}{h^3}$$

The $1/N_e$ factor comes from the space volume element. It is the volume per electron.

Inserting this into Boltzmann's equation, we arrive at **the Saha equation:**

$$\frac{N_1^+}{N_1} = \frac{2g_1^+}{N_e g_1} \frac{(2\pi m_e kT)^{3/2}}{h^3} e^{-\chi_{ion}/kT}$$

This relates the **ground** state populations of the atom and ion.

The Saha Equation

The Saha equation (Meghnad Saha 1920):

$$\frac{N_1^+}{N_1} = \frac{2g_1^+}{N_e g_1} \frac{(2\pi m_e kT)^{3/2}}{h^3} e^{-\chi_{ion}/kT}$$

This relates the **ground** state populations of the atom and ion.

To derive the ratio of the total number of ions (N^+) to the total number of atoms (N^0) we can use the conventional Boltzmann formula for each level n of the atom and ion, N_n/N_1 and N_n^+/N_1^+ i.e.

$$\frac{N_n}{N_1} = \frac{g_n}{g_1} e^{-\chi_n/kT} \qquad \frac{N_n^+}{N_1^+} = \frac{g_n^+}{g_1^+} e^{-\chi_n^+/kT}$$

Partition function (1)

If N^0 is the sum of *all neutral* particles in their different quantum states:

$$N^0 = N_1^0 + \sum_{n=2}^{\infty} N_n^0 = N_1^0 + \frac{N_1^0}{g_1} \sum_{n=2}^{\infty} g_n \, e^{-\chi_n / kT}$$

We find:

$$N^0 = \frac{N_1^0}{g_1} \left(g_1 + \sum_{n=2}^{\infty} g_n \, e^{-\chi_n / kT} \right) = \frac{N_1^0}{g_1} u^0(T)$$

where we have introduced ***u⁰***, the partition function of the atom.
This is the weighted sum of the number of ways it can arrange its electrons with the same energy, and can be used to calculate the probability that at the given temperature, the atom is on the given energy level.

Similarly for the ion,

$$N^+ = N_1^0 + \frac{N_1^+}{g_1^+} u^+(T) \qquad u^+(T) = g_1^+ + \sum_{n=2}^{\infty} g_n^+ \, e^{-\chi_n^+ / kT}$$

For H^+, $u^+=1$, since no electrons left.

Partition function (2)

If we multiply N_1^+/N_1^0 from earlier by N^+/N_1^+ and N_1^0/N^0 we again obtain the **Saha equation**:

$$\frac{N^+ N_e}{N^0} = \frac{2u^+}{u^0}\frac{(2\pi m_e kT)^{3/2}}{h^3} e^{-\chi_{ion}/kT} = 4.83 \times 10^{15} \frac{u^+}{u^0} T^{3/2} e^{-\chi_{ion}/kT}$$

In logarithmic form Saha equation can be written as:

$$\log \frac{N^+}{N^0} = \log \frac{u^+}{u^0} + \log 2 + \frac{5}{2}\log T - \chi_{ion}\Theta - \log P_e - 0.48$$

where χ_{ion} is measured in eV, Θ=5040/T and the electron pressure P_e is related to the electron density via the ideal gas law (P_e=$N_e kT$). In stellar atmospheres, P_e lies in the range 1 dyn/cm^2 (cool stars) to 1000 dyn/cm^2 (hot stars).

High temperature favours ionization, high pressure favours recombination.

Note that 1dyn/cm^2=0.1N/m^2 (SI units), so for SI calculations the final constant is -1.48 instead of -0.48

Partition functions (Gray App D2)

Table D.2. *Partition functions, log u(T).*

	θ										
	0.2	0.4	0.6	0.8	1.0	1.2	1.4	1.6	1.8	2.0	log g_0
H	0.368	0.303	0.301	0.301	0.301	0.301	0.301	0.301	0.301	0.301	0.301
He	0.000	0.000	0.000	0.000	0.000	0.000	0.000	0.000	0.000	0.000	0.000
He^+	0.301	0.301	0.301	0.301	0.301	0.301	0.301	0.301	0.301	0.301	0.301
Li	–	0.987	0.488	0.359	0.320	0.308	0.304	0.302	0.302	0.302	0.301
Be	–	0.328	0.087	0.025	0.007	0.002	0.001	0.000	0.000	0.000	0.000
Be^+	0.541	0.334	0.307	0.302	0.301	0.301	0.301	0.301	0.301	0.301	0.301
B	1.191	0.831	0.786	0.778	0.777	0.777	0.777	0.777	0.777	0.776	0.778
B^+	0.435	0.051	0.006	0.000	0.000	0.000	0.000	0.000	0.000	0.000	0.000
C	1.163	1.037	0.994	0.975	0.964	0.958	0.954	0.951	0.950	0.948	0.954
C^+	0.853	0.782	0.775	0.774	0.773	0.772	0.771	0.770	0.769	0.767	0.778
C^{++}	0.143	0.010	0.000	0.000	0.000	0.000	0.000	0.000	0.000	0.000	0.000
N	1.060	0.729	0.645	0.616	0.606	0.603	0.602	0.602	0.602	0.602	0.602
N^+	1.073	0.993	0.965	0.953	0.946	0.942	0.939	0.937	0.934	0.932	0.954
O	1.095	0.991	0.964	0.953	0.947	0.944	0.941	0.939	0.937	0.935	0.954
O^+	0.895	0.655	0.614	0.604	0.602	0.602	0.602	0.602	0.602	0.602	0.602
F	0.788	0.772	0.768	0.765	0.762	0.759	0.756	0.753	0.750	0.747	0.778
F^+	1.034	0.968	0.949	0.940	0.935	0.930	0.926	0.923	0.919	0.915	0.954
Ne	0.002	0.000	0.000	0.000	0.000	0.000	0.000	0.000	0.000	0.000	0.000
Ne^+	0.771	0.766	0.760	0.754	0.748	0.743	0.737	0.732	0.727	0.723	0.778
Na	4.316	1.043	0.493	0.357	0.320	0.309	0.307	0.306	0.306	0.306	0.301
Na^+	0.000	0.000	0.000	0.000	0.000	0.000	0.000	0.000	0.000	0.000	0.000
Mg	2.839	0.478	0.110	0.027	0.007	0.002	0.001	0.001	0.001	0.000	0.000

$\Theta = 5040/T$

Partition functions (Gray, old edition)

$$\log u\,(T) = c_0 + c_1 \log \Theta + c_2 \log^2 \Theta + c_3 \log^3 \Theta + c_4 \log^4 \Theta$$

$\Theta = 5040/T$

Element		c_0	c_1	c_2	c_3	c_4
H	1	0.30103	−0.00001			
He	2	0.00000	0.00000			
He^+		0.30103	0.00000			
Li	3	0.31804	−0.20616	0.91456	−1.66121	1.04195
Be	4	0.00801	−0.17135	0.62921	−0.58945	
Be^+		0.30389	−0.00819			
B	5	0.78028	−0.01622			
B^+		0.00349	−0.01035			
C	6	0.96752	−0.09452	0.08055		
C^+		0.77239	−0.02540			
N	7	0.60683	−0.08674	0.30565	−0.28114	
N^+		0.94968	−0.06463	−0.01291		
O	8	0.05033	−0.05703			
O^+		0.60405	−0.03025	0.04525		
F	9	0.76284	−0.03582	−0.05619		
Ne	10	0.00000	0.00000			
Ne^+		0.74847	−0.06562	−0.07088		
Na	11	0.30955	−0.17778	1.10594	−2.42847	1.70721
Mg	12	0.00556	−0.12840	0.81506	−1.79635	1.26292
Mg^+		0.30257	−0.00451			
Al	13	0.76786	−0.05207	0.14713	−0.21376	
Al^+		0.00334	−0.00995			
Si	14	0.97896	−0.19208	0.04753		
Si^+		0.75647	−0.05490	−0.10126		
P	15	0.64618	−0.31132	0.68633	−0.47505	
P^+		0.93588	−0.18848	0.08921	−0.22447	
S	16	0.95254	−0.15166	0.02340		
S^+		0.61971	−0.17465	0.48283	−0.39157	
Cl	17	0.74465	−0.07389	−0.06965		
Cl^+		0.92728	−0.15913	−0.01983		
K	19	0.34419	−0.48157	1.92563	−3.17826	1.83211
Ca	20	0.07460	−0.75759	2.58494	−3.53170	1.65240
Ca^+		0.34383	−0.41472	1.01550	0.31930	
Sc	21	1.08209	−0.77814	1.78504	−1.39179	
Sc^+		1.35894	−0.51812	0.15634		
Ti	22	1.47343	−0.97220	1.47986	−0.93275	
Ti^+		1.74561	−0.51230	0.27621		
V	23	1.68359	−0.82055	0.92361	−0.78342	
V^+		1.64112	−0.74045	0.49148		
Cr	24	1.02332	−1.02540	2.02181	−1.32723	
Cr^+		0.85381	−0.71166	2.18621	−0.97590	−2.72893
Mn	25	0.80810	−0.39108	1.74756	−3.13517	1.93514
Mn^+		0.88861	−0.36398	1.39674	−1.86424	−2.32389
Fe	26	1.44701	−0.67040	1.01267	−0.81428	
Fe^+		1.63506	−0.47118	0.57918	−0.12293	
Co	27	1.52929	−0.71430	0.37210	−0.23278	
Ni	28	1.49063	−0.33662	0.08553	−0.19277	
Ni^+		1.03800	−0.69572	0.53893	0.28861	

Ionization Potentials

Atom		Stage of ionization												
		I	II	III	IV	V	VI	VII	VIII	IX	X	XI	XII	XIII	XIV
1	H	13.598 44													
2	He	24.587 41	54.417 78												
3	Li	5.391 72	75.640 18	122.454											
4	Be	9.322 63	18.211 16	153.897	217.713										
5	B	8.298 03	25.154 84	37.931	259.366	340.22									
6	C	11.260 30	24.383 32	47.888	64.492	392.08	489.98								
7	N	14.534 14	29.601 3	47.449	77.472	97.89	552.06	667.03							
8	O	13.618 06	35.117 30	54.936	77.413	113.90	138.12	739.29	871.41						
9	F	17.422 82	34.970 82	62.708	87.140	114.24	157.17	185.19	953.91	1 103.1					
10	Ne	21.564 54	40.963 28	63.45	97.12	126.21	157.93	207.28	239.10	1 195.8	1 362.2				
11	Na	5.139 08	47.286 4	71.620	98.91	138.40	172.18	208.50	264.25	299.9	1 465.1	1 648.7			
12	Mg	7.646 24	15.035 28	80.144	109.265	141.27	186.76	225.02	265.96	328.1	367.5	1 761.8	1 963		
13	Al	5.985 77	18.828 56	28.448	119.99	153.83	190.49	241.76	284.66	330.1	398.8	442.0	2 086	2 304	
14	Si	8.151 69	16.345 85	33.493	45.142	166.77	205.27	246.49	303.54	351.1	401.4	476.4	523	2 438	2 673
15	P	10.486 69	19.769 4	30.203	51.444	65.03	220.42	263.57	309.60	372.1	424.4	479.5	561	612	2 817
16	S	10.360 01	23.337 9	34.79	47.222	72.59	88.05	280.95	328.75	379.6	447.5	504.8	564	652	707
17	Cl	12.967 64	23.814	39.61	53.465	67.8	97.03	114.20	348.28	400.1	455.6	529.3	592	657	750
18	Ar	15.759 62	27.629 67	40.74	59.81	75.02	91.01	124.32	143.46	422.5	478.7	539.0	618	686	756
19	K	4.340 66	31.63	45.806	60.91	82.66	99.4	117.56	154.88	175.8	503.8	564.7	629	715	787
20	Ca	6.113 16	11.871 72	50.913	67.27	84.50	108.78	127.2	147.24	188.5	211.3	591.9	657	727	818
21	Sc	6.561 44	12.799 67	24.757	73.489	91.65	111.68	138.0	158.1	180.0	225.2	249.8	688	757	831
22	Ti	6.828 2	13.575 5	27.492	43.267	99.30	119.53	140.8	170.4	192.1	215.9	265.1	292	788	863
23	V	6.746 3	14.66	29.311	46.71	65.28	128.1	150.6	173.4	205.8	230.5	255.1	308	336	896
24	Cr	6.766 64	16.485 7	30.96	49.16	69.46	90.64	161.18	184.7	209.3	244.4	270.7	298	355	384
25	Mn	7.434 02	15.639 99	33.668	51.2	72.4	95.6	119.20	194.5	221.8	248.3	286.0	314	344	404
26	Fe	7.902 4	16.187 8	30.652	54.8	75.0	99.1	124.98	151.06	233.6	262.1	290.2	331	361	392
27	Co	7.881 0	17.083	33.50	51.3	79.5	103	131	160	186.2	276.2	305	336	379	411
28	Ni	7.639 8	18.168 84	35.19	54.9	75.5	108	134	164	193	224.6	321	352	384	430
29	Cu	7.726 38	20.292 40	36.841	55.2	79.9	103	139	167	199	232	266	369	401	435
30	Zn	9.394 05	17.964 40	39.723	59.4	82.6	108	136	175	203	238	274	311	412	454

Degree of ionization of H in stars

We can use the Saha equation to study the degree of ionization of H in general in stellar photospheres. The fraction of ionized hydrogen to the total is defined below. We find that H switches from mostly neutral below 7000K to mostly ionized above 11000K for typical N_e. This allows us to understand why hydrogen lines are strongest in A-type stars, with temperatures of 7500-10000K.

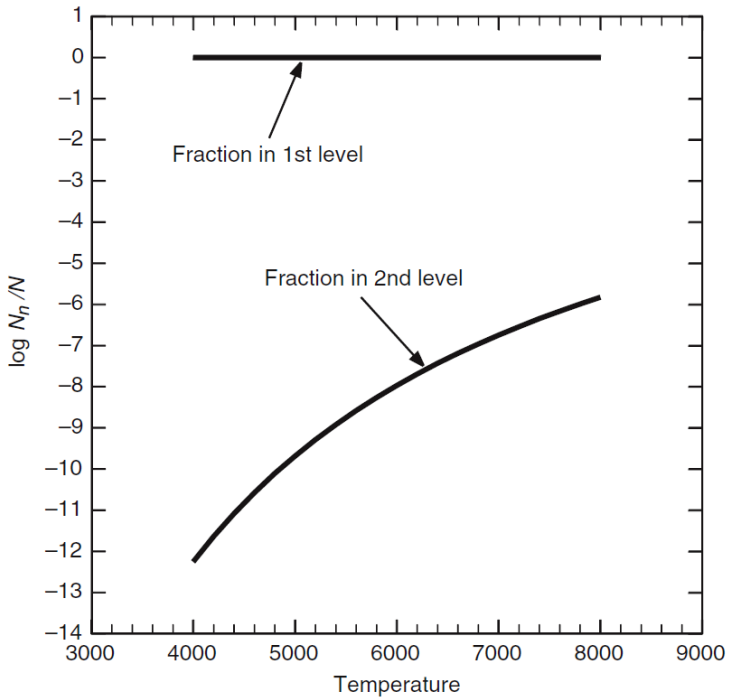

$$\frac{H^+}{H} = \frac{H^+}{H^0 + H^+} = \frac{H^+/H^0}{1 + H^+/H^0}$$

$$\frac{N^+ N_e}{N^0} = 2.4 \times 10^{15}\, T^{3/2} e^{-158000/T}$$

Using 1eV per particle, the hydrogen is heated from 0 to 10^4 K. Supplying 13.6 eV more, the temperature increases only up to 2×10^4 K. Ionization is an extremely energy consuming process. Ionization happens within a very small temperature interval.

Degree of ionization in stars

Hydrogen:

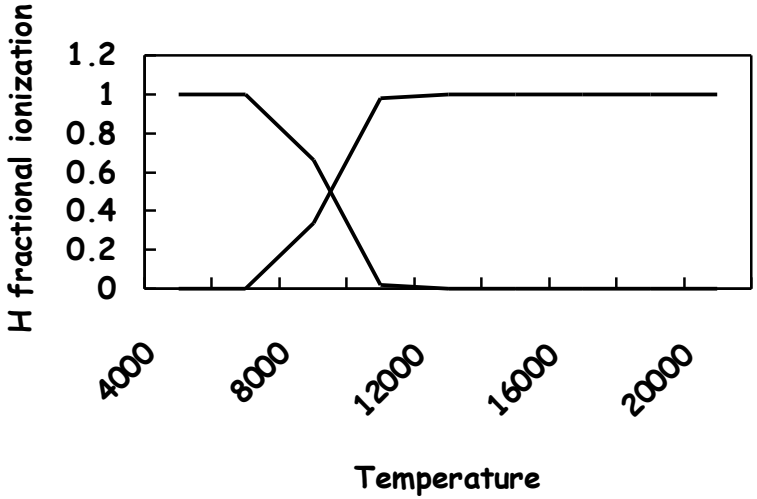

Iron:

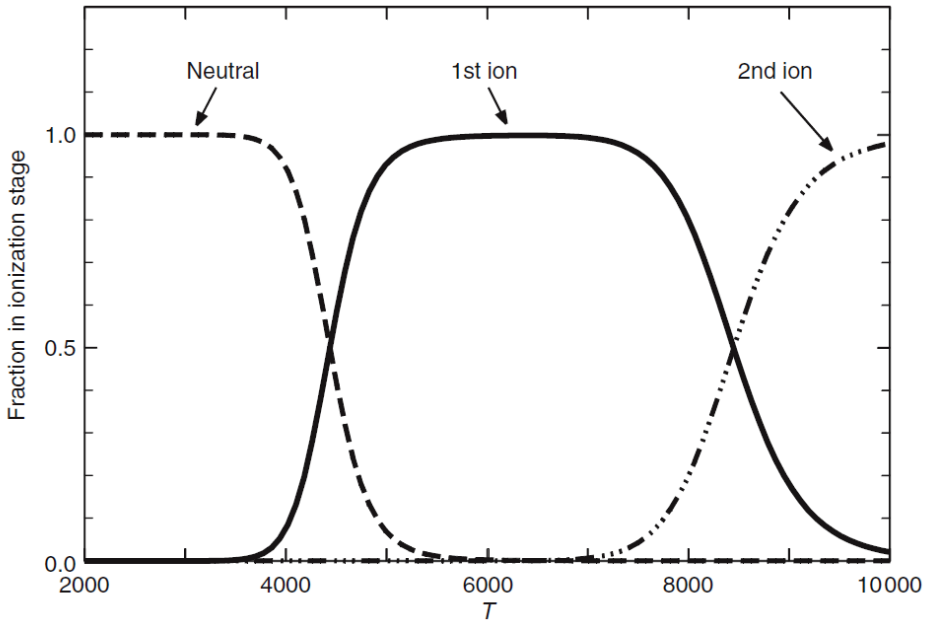

As temperature increases, ionization occurs rather abruptly. In a stellar photosphere, elements exist mainly in just two ionization stages.

Strong Balmer lines in A stars – why?

From recent example, a very high T was required to populate level n=2 of H relative to the ground state. We can now use the Boltzmann & Saha equations to measure H(n=2)/H(total) as a function of T. For increasing T, the n=2 population increases due to the Boltzmann equation, reaching a maximum value around 10,000K (equivalent to A spectral type) and then reduces as H becomes mostly ionized. This is why A stars have strong Balmer lines.

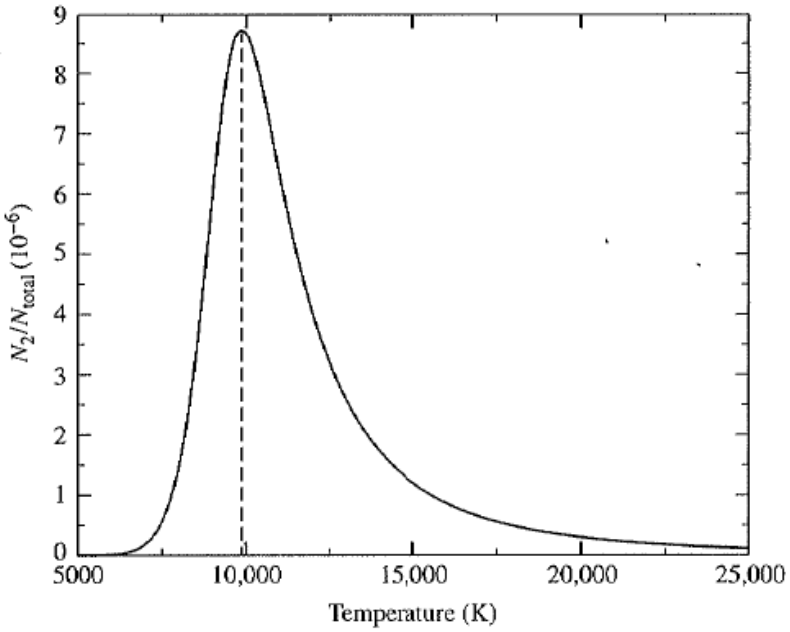

Note: He in stellar atmospheres complicates this calculation since ionized He provides excess electrons with which H ions can recombine, so it takes higher temperatures to achieve the same degree of ionization.

Strong lines in Solar photosphere

λ	Element	W(Å)	Name	λ	Element	W(Å)	Name
3581.21	Fe I	2.14	N	4920.51	Fe I	0.43	
3719.95	Fe I	1.66		4957.61	Fe I	0.45	
3734.87	Fe I	3.03	M	5167.33	Mg I	0.65	b_4
3749.50	Fe I	1.91		5172.70	Mg I	1.26	b_2
3758.24	Fe I	1.65		5183.62	Mg I	1.58	b_1
3770.63	H_{11}	1.86		5232.95	Fe I	0.35	
3797.90	H_{10}	3.46		5269.55	Fe I	0.41	
3820.44	Fe I	1.71	L	5324.19	Fe I	0.32	
3825.89	Fe I	1.52		5238.05	Fe I	0.38	
3832.31	Mg I	1.68		5528.42	Mg I	0.29	
3835.39	H_9	2.36		5889.97	Na I	0.63	D_2
3838.30	Mg I	1.92		5895.94	Na I	0.56	D_1
3859.92	Fe I	1.55		6122.23	Ca I	0.22	
3889.05	H_8	2.35		6162.18	Ca I	0.22	
3933.68	Ca II	20.25	K	6562.81	H_α	4.02	C
3968.49	Ca II	15.47	H	6867.19	O_2	tell	B
4045.82	Fe I	1.17		7593.70	O_2	tell	A
4101.75	H_δ	3.13	h	8194.84	Na I	0.30	
4226.74	Ca I	1.48	g	8498.06	Ca II	1.46	
4310 ± 10	—	—	G	8542.14	Ca II	3.67	
4340.48	H_γ	2.86		8662.17	Ca II	2.60	
4383.56	Fe I	1.01		8688.64	Fe I	0.27	
4861.34	H_β	3.68		8736.04	Mg I	0.29	
4891.50	Fe I	0.31					

Ca II in the Sun

The photosphere of the Sun has only two calcium atoms for every million H atoms, yet the Ca II **H and K lines** (produced by the ground state of singly ionized calcium, Ca^+) are ***stronger*** than the Balmer lines of H (produced by the 1st excited state of neutral H). Why?

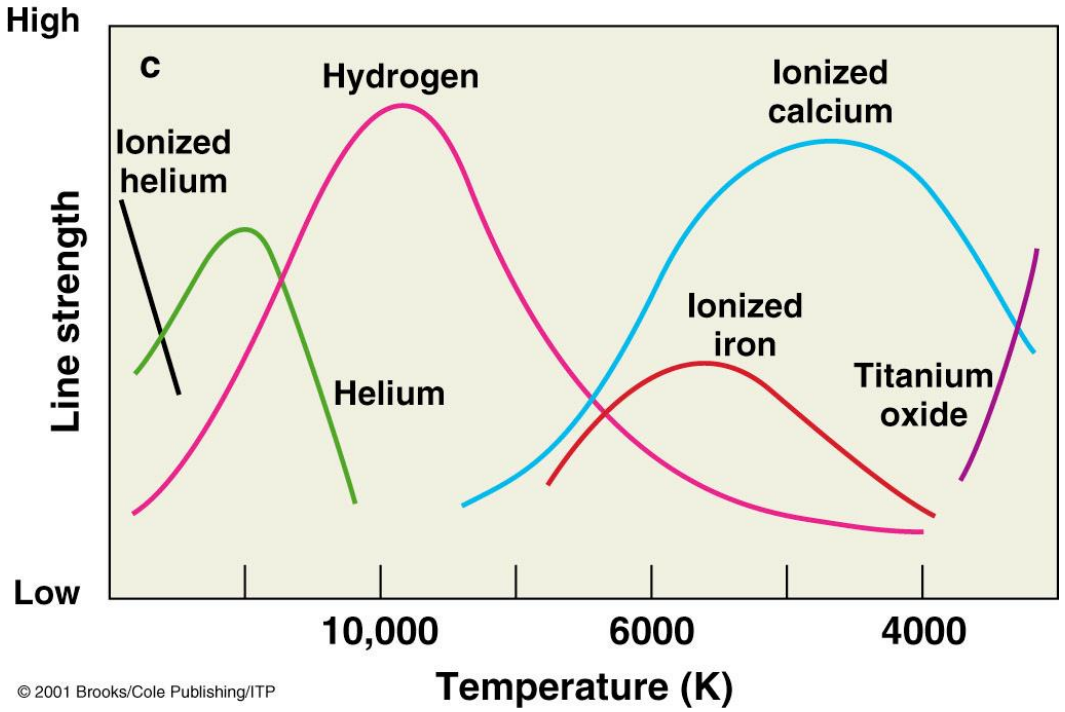

Saha-Boltzmann applied to Ca

From the Saha equation we can find that H is essentially neutral in the Solar photosphere:

P_e=200 dyn/cm^2, χ_{ion}=13.6 eV, Θ=5040/($T_{=5777}$)=0.872, the partition function u^0=2, u^+=1 (i.e. log u^+=0)

$$\log\frac{N^+}{N^0} = \log u^+ - \log u^0 + \log 2 + \frac{5}{2}\log T - \chi_{ion}\Theta - \log P_e - 0.48 = -5.235 \rightarrow N^+/N^0 \approx 0.0006\%$$

yet from the Boltzmann formula $\log\frac{N_u}{N_l} = \log\frac{g_u}{g_l} - \frac{5040}{T}\chi_{ul}(eV)$: H(n=2)/H(n=1)=5x10^{-9}

i.e. **very little** H is available to produce Balmer absorption lines.

For Ca, χ_{ion}=6.1 eV, and partition functions may be determined from tables (Slide 103) via

$$\log u\,(T) = c_0 + c_1 \log\Theta + c_2 \log^2\Theta + c_3 \log^3\Theta + c_4 \log^4\Theta$$

For Θ=5040/T=0.872, the partition function of neutral Ca

$$\log u^0\,(T) = 0.075 - 0.757\log\Theta + 2.58\log^2\Theta + 3.53\log^3\Theta - 1.65\log^4\Theta$$

i.e. u^0=1.3. Similarly, u^+=2.3.

$$\log\frac{Ca^+}{Ca^0} = \log\frac{2.3}{1.3} + \log 2 + 9.40 - 5.34 - 1.18 - 0.48 = +2.95 \rightarrow Ca^+/Ca^0 \approx 900$$

Essentially ***all*** Calcium is singly ionized.

Saha-Boltzmann applied to Ca

Essentially ***all*** Calcium is singly ionized.

$N(Ca^+)$ in the first excited state relative to the ground state (g_1=2, g_2=4, χ=3.12eV) is 1/265 from Boltzmann eqn, so nearly all Calcium in the Sun's photosphere is in the ground state of Ca^+.

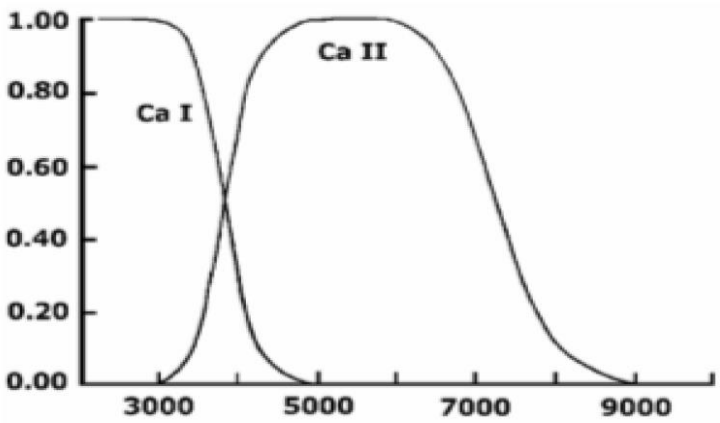

Combining these results:

$$N(Ca^+_{g.s.})/N(H_{n=2}) = N(Ca^+_{g.s.})/N(Ca) \times N(Ca)/N(H) \times N(H)/N(H_{n=2}) = 400$$

There are 400 times more Ca^+ ions with electrons in the ground-state (which produce the Ca II H&K lines) than there are neutral H atoms in the first excited state (which produce Balmer lines).

The Ca II lines in the Sun are so strong due to *T* dependence of excitation and ionization (**not** high Ca/H abundance).

More from Saha

- Another observational effect that can be understood using the Saha equation is that supergiants and giants have *lower temperatures* than dwarfs of the same spectral type.
- Spectral classes are defined by line ratios of different ions, e.g. He II 4542A / He I 4471 for O stars. At higher temperatures the fraction of He II will increase relative to He I, so the above ratio will increase.
- However, supergiants have lower surface gravities (or pressure) than main-sequence stars, so from Saha equation a lower P_e at the same temperature will give a higher ion fraction, N^+/N^0
- Assuming a given spectral class corresponds to a fixed ratio N^+/N^0, a star with a lower pressure can have a lower $T_{\rm eff}$ for the same ratio and spectral class

Summary

- LTE = Maxwell + Boltzmann + Saha.
- Boltzmann equation describes degree of excitation of an atom or ion, e.g. $N\,(\mathrm{H}_{n=2})/N\,(\mathrm{H}_{n=1})$.
- Saha equation describes degree of ionization of successive ions, e.g. $N\,(\mathrm{He}^{+})/N(\mathrm{He}^{0})$ or $N\,(\mathrm{He}^{2+})/N\,(\mathrm{He}^{+})$.
- The Partition function is the weighted sum of the number of ways an atom or ion can arrange its electrons with the same energy.
- Ionization is an extremely energy consuming process. Ionization happens within a very small temperature interval.
- Saha-Boltzmann explains the spectral type (or temperature) dependence of lines in stellar atmospheres, e.g. Strongest Balmer series at spectral type A and strong CaII lines in Solar-type stars.

Boltzmann equation & Saha Equation

- Bolzmann equation:

$$\frac{N_u}{N_l} = \frac{g_u}{g_l} e^{-(E_u - E_l)/kT}$$

Boltzmann constant
k=8.6174x10^{-5} **eV/K**

$$\log \frac{N_u}{N_l} = \log \frac{g_u}{g_l} - \frac{5040}{T} \chi_{ul}(eV)$$

- Saha Equation

$$\frac{N_1^+}{N_1} = \frac{2g_1^+}{N_e g_1} \frac{(2\pi m_e kT)^{3/2}}{h^3} e^{-\chi_{ion}/kT}$$

$\Theta = 5040/T$

$$\log \frac{N^+}{N^0} = \log \frac{u^+}{u^0} + \log 2 + \frac{5}{2} \log T - \chi_{ion}\Theta - \log P_e - 0.48$$

Stellar Opacity

ROSSELAND MEAN OPACITY

ROSSELAND DEPTH

BOUND-BOUND (LINE) ABSORPTION

BOUND-FREE AND FREE-FREE (CONTINUOUS) ABSORPTION

Opacity

- We first introduced the concept of opacity when deriving the equation of radiative transport.
- Opacity is the resistance of material to the flow of heat, which in most stellar interiors is determined by all the processes which scatter and absorb photons.
- The removal of energy from a beam of photons as it passes through matter is governed by
  - line absorption (**bound-bound**),
  - photoelectric absorption (**bound-free**),
  - inverse bremsstrahlung (**free-free**), and
  - photon scattering.
- Stimulated emission acts as negative opacity by creating photons that add to the beam.
- Stellar atmospheres are predominantly hydrogen (90% by number), whilst helium makes up almost all the rest. These two elements provide most of the opacity over most wavelengths for most (hot) stars.

Absorption coefficient

- The monochromatic absorption coefficient specifies the energy fraction taken from a light beam. It may be defined per particle, per gram, or in terms of a geometrical cross-section in cm^2:

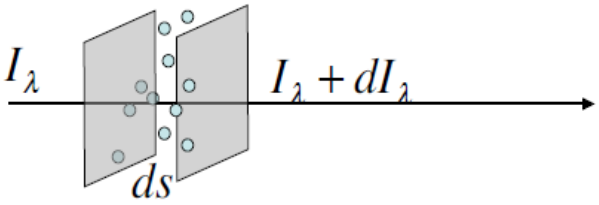

- Per gram: $\boldsymbol{dI_\lambda \equiv -\kappa_\lambda \rho I_\lambda ds}$, where κ_λ is the mass absorption coefficient [$cm^2\ g^{-1}$], ρ is the density [$g\ cm^{-3}$].

- Per cm path length: $\boldsymbol{dI_\lambda \equiv -\alpha_\lambda I_\lambda ds}$, where $\boldsymbol{\alpha_\lambda}$ is the absorption coefficient [cm^{-1}]

$$\alpha_\lambda = \kappa_\lambda \rho$$

- Per particle: $\boldsymbol{dI_\lambda \equiv -\sigma_\lambda n I_\lambda ds}$, where $\boldsymbol{\sigma_\lambda}$ is the absorption cross-section per particle for individual transitions and $\boldsymbol{n}$ is the number density [particles cm^{-3}]

$$\boldsymbol{\alpha_\lambda = \sigma_\lambda n = \kappa_\lambda \rho}$$

$$\boldsymbol{d\tau_\lambda = \alpha_\lambda ds = \sigma_\lambda n\, ds = \kappa_\lambda \rho\, ds}$$

The mean absorption coefficient

- The grey approximation (α, κ =const) is very coarse but can still be useful. Is there a sensible mean value $\bar{\alpha}$ to use? What choice to make for a mean value?
- We demand flux conservation and hope to keep the temperature structure.

- **From the third radiative equilibrium condition:** $\int_0^\infty \frac{dK_\lambda}{d\tau_\lambda} d\lambda = \frac{F(\tau)}{4\pi}$

$$F = \int F_\lambda \, d\lambda = 4\pi \int \frac{dK_\lambda}{d\tau_\lambda} d\lambda = 4\pi \int \frac{dK_\lambda}{\alpha_\lambda ds} d\lambda = \frac{4\pi}{3} \int \frac{dB_\lambda}{\alpha_\lambda ds} d\lambda$$

$$F = \frac{4\pi}{3} \frac{1}{\alpha_R} \int \frac{dB_\lambda}{ds} d\lambda = \frac{4\pi}{3} \frac{1}{\alpha_R} \frac{dB}{ds}$$

$$\frac{1}{\alpha_R} = \frac{\int \frac{dB_\lambda}{\alpha_\lambda ds} d\lambda}{\frac{dB}{ds}}$$

$K_\lambda(\tau_\lambda) = \frac{1}{3} J_\lambda(\tau_\lambda) = \frac{1}{3} B_\lambda$

the Eddington approximation

Rosseland mean opacity

$F = \pi B$

$$\frac{1}{\alpha_R} = \frac{\int \frac{1}{\alpha_\lambda}\frac{dB_\lambda}{ds}\,d\lambda}{\frac{dB}{ds}}$$

$$\frac{dB}{ds} = \frac{dB}{dT}\frac{dT}{ds} \quad \text{and} \quad \frac{dB}{dT} = \frac{d}{dT}\left(\frac{\sigma}{\pi}T^4\right) = \frac{4\sigma}{\pi}T^3$$

$$\frac{1}{\alpha_R} = \frac{\int_0^\infty \frac{1}{\alpha_\lambda}\frac{dB_\lambda}{dT}\,d\lambda}{\frac{4\sigma}{\pi}T^3}$$

Definition of Rosseland mean opacity

The Rosseland mean $1/\alpha_R$ is a weighted (harmonic) mean of opacity, for which there is a corresponding optical depth (Rosseland depth):

$$\tau_{Ross}(s) = \int_0^s \alpha_R(z)dz$$

We hoped for the temperature structure:

$$T^4(\tau) = \frac{3}{4}(\tau + \frac{2}{3})T_{eff}^4 = \frac{3}{4}(\tau_{Ross} + \frac{2}{3})T_{eff}^4$$

Eddington approximation

The grey approximation is very good for $\tau_{Ross} \gg 1$.

However, the atmosphere is NOT grey

- Opacity depends strongly on wavelengths → the atmosphere is **NOT** grey.

- Non-greyness changes the temperature structure.

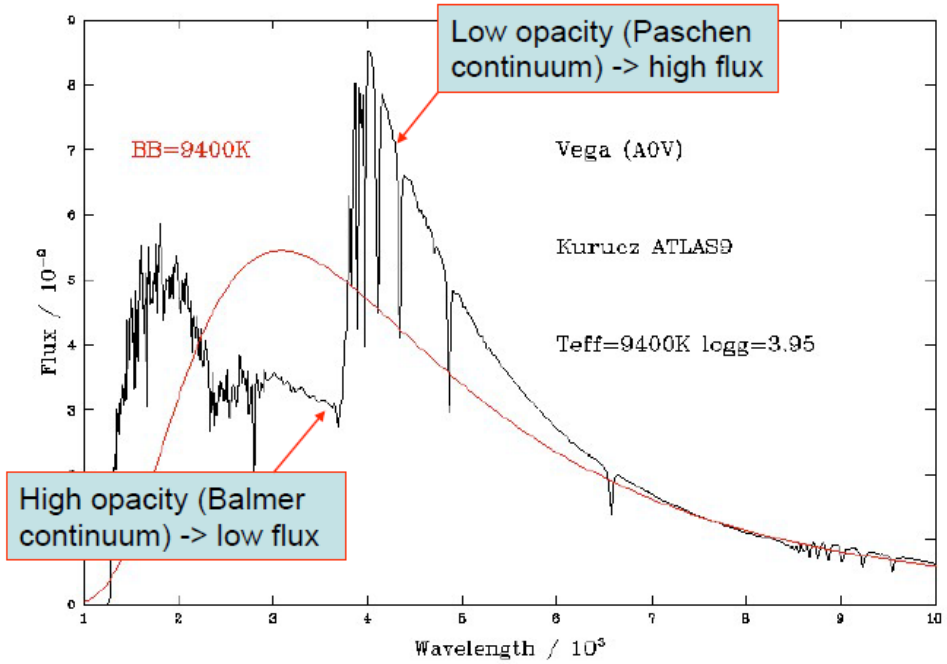

Dominant sources of opacity

- The most important transitions for the continuous absorption are those which ionise atoms (with a continuum of final states).
- For H and He the line spectra do not greatly affect radiative transport. Some metals, with very complex line spectra do contribute to the continuum.
- New stellar opacities have been recalculated in the past 20-30 years by two groups – OPAL (Iglesias et al., 1996) and The Opacity Project/OP (Seaton et al., 1994; Badnell et al., 2005) which have led to a factor of 3 increase in opacity under some temperature-density conditions via improved treatment of atomic data.

Chemical composition (Population I)

- Stellar atmosphere = mixture, composed of many chemical elements, present as atoms, ions, or molecules
- Abundances, e.g., given as mass fractions β_k
- **Solar abundances**

$$\beta_H = 0.71 \longrightarrow \mathbf{X}$$

$$\beta_{He} = 0.28 \longrightarrow \mathbf{Y}$$

"Metals" (**Z**):

$$\beta_C = 0.004$$
$$\beta_N = 0.001$$
$$\beta_O = 0.009$$
$$\vdots$$
$$\beta_{Fe} = 0.001$$
$$\vdots$$

Universal abundance for Population I stars

X+Y+Z=1

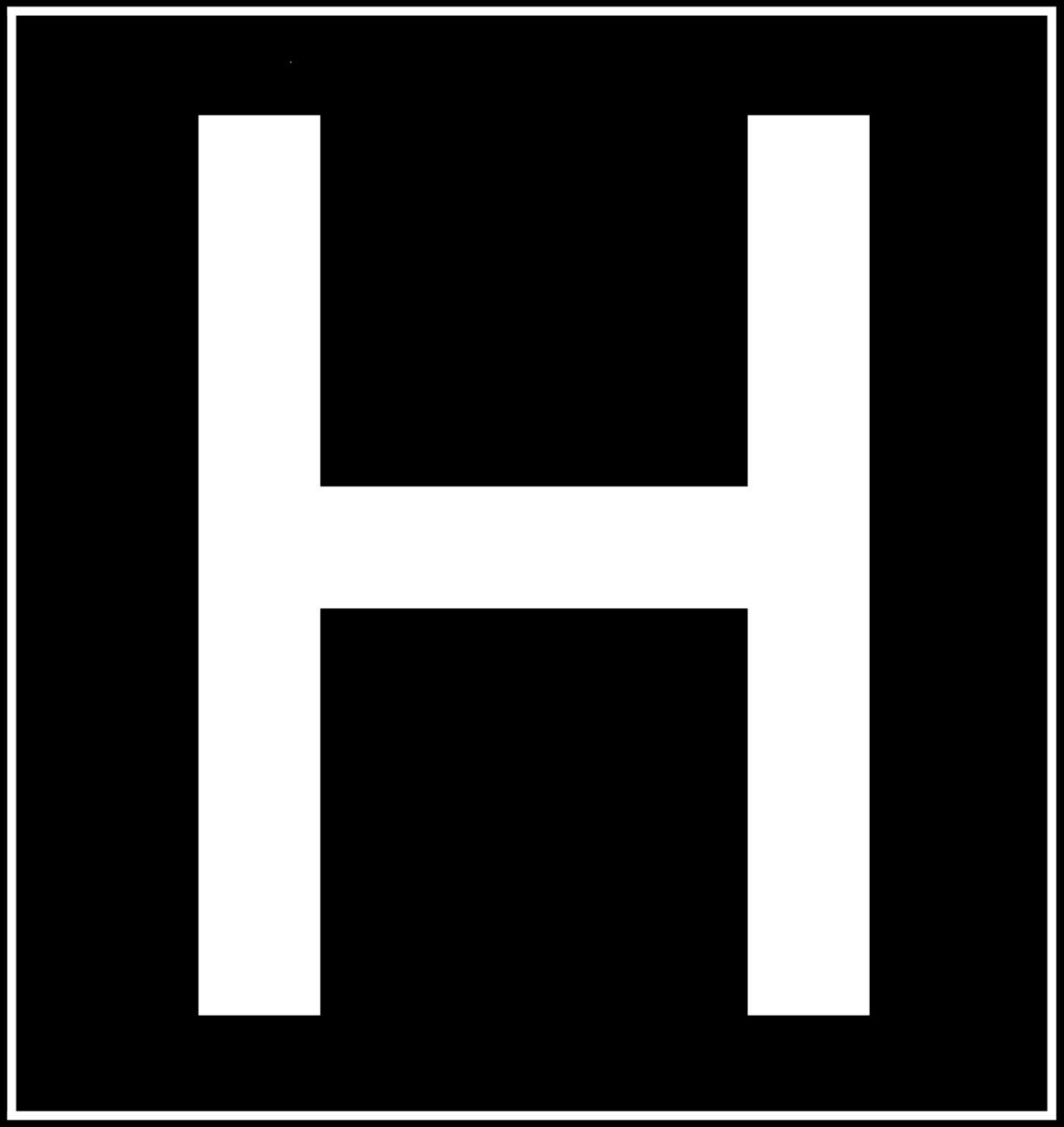

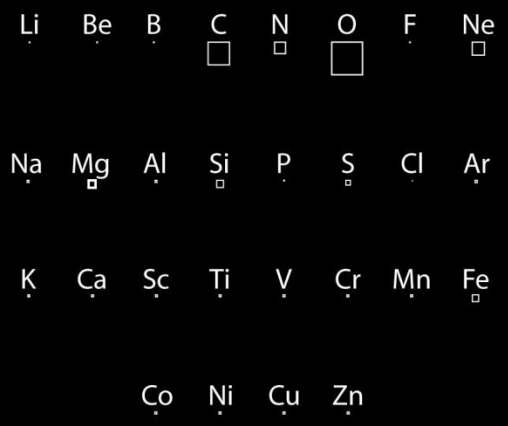

Square Area
$\propto$ Cosmic
Abundance

Chemical composition (Population II)

- Population II stars

$$\beta_H = \beta_H^{\odot}$$
$$\beta_{He} = \beta_{He}^{\odot}$$
$$\beta_Z = 0.1 \cdots 0.00001\ \beta_Z^{\odot}$$

- Chemically peculiar stars, e.g., helium stars

$$\beta_H \leq 0.002 << \beta_H^{\odot}$$
$$\beta_{He} = 0.964 >> \beta_{He}^{\odot}$$
$$\beta_C = 0.029 >> \beta_C^{\odot}$$
$$\beta_N = 0.003 \approx \beta_N^{\odot}$$
$$\beta_O = 0.002 < \beta_O^{\odot}$$

- Chemically peculiar stars, e.g., PG1159 stars

$$\beta_H \leq 0.05 << \beta_H^{\odot}$$
$$\beta_{He} = 0.25 >> \beta_{He}^{\odot}$$
$$\beta_C = 0.55 >> \beta_C^{\odot}$$
$$\beta_N < 0.02$$
$$\beta_O = 0.15 >> \beta_O^{\odot}$$

Other definitions

- Particle number density N_k = number of atoms/ions of element k per unit volume. Relation to mass density:

$$\beta_k \rho = A_k m_H N_k$$

with A_k = mean mass of element k in atomic mass units (AMU)
m_H = mass of hydrogen atom

- Particle number fraction $\frac{N_k}{\sum N_{k'}}$
- Logarithmic $\varepsilon_k = \log(N_k/N_H) + 12.00$

- Iron(Fe)-to-Hydrogen(H) ratio, for the Sun: $\log\left(\frac{N_{Fe}}{N_H}\right) \cong -4.3$

For other stars: $[\mathrm{Fe/H}] = \log\frac{(\mathrm{Fe/H})_*}{(\mathrm{Fe/H})_\odot} = \log(\mathrm{Fe/H})_\odot - \log(\mathrm{Fe/H})_*$

$$[\mathrm{Fe/H}]_\odot \equiv 0$$

Line absorption

- A bound-bound transition absorbs or emits at $h\nu = hc/\lambda = \chi_u - \chi_l$ where χ is the excitation of the upper and lower levels above the ground state. Such transitions contribute to the **line** absorption. We will discuss spectral lines later.

- The cumulative effect of many lines can behave much as continuous opacity in the upper photosphere. Problems associated with line opacity are due to the large numbers of lines involved.

- Data for millions of atomic line transitions have been calculated by Kurucz and more recently by the OP (Opacity Project).

Here is the effect of many lines (Fe and Ni) on the emergent UV continuum of the subdwarf O star Feige 67.

(From Deetjen 2000)

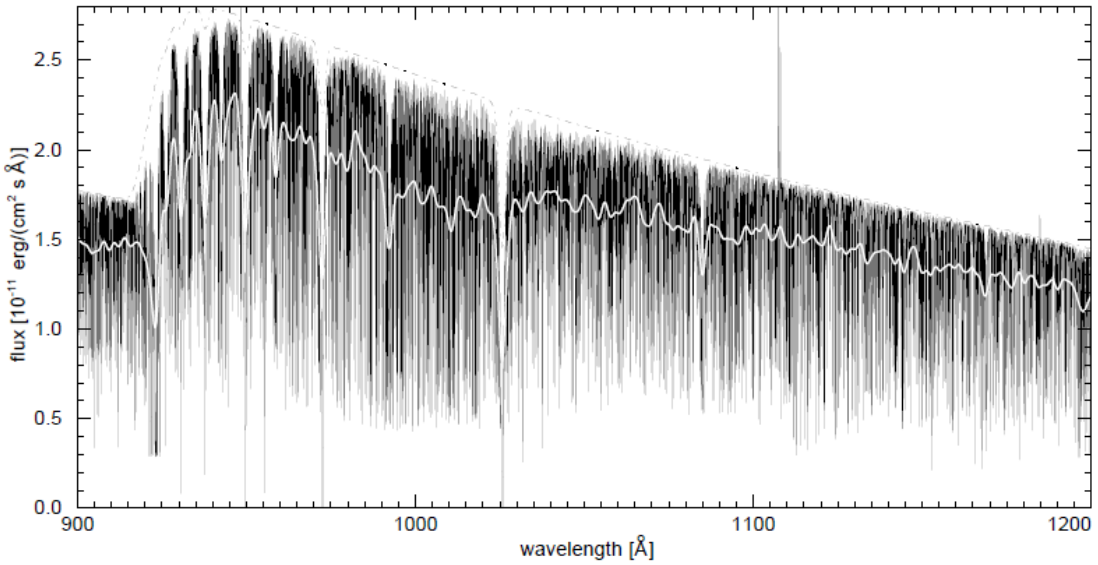

Observations

Here is the effect of many lines (Fe II and Ni) on the emergent UV continuum of the subdwarf O star Feige 67.

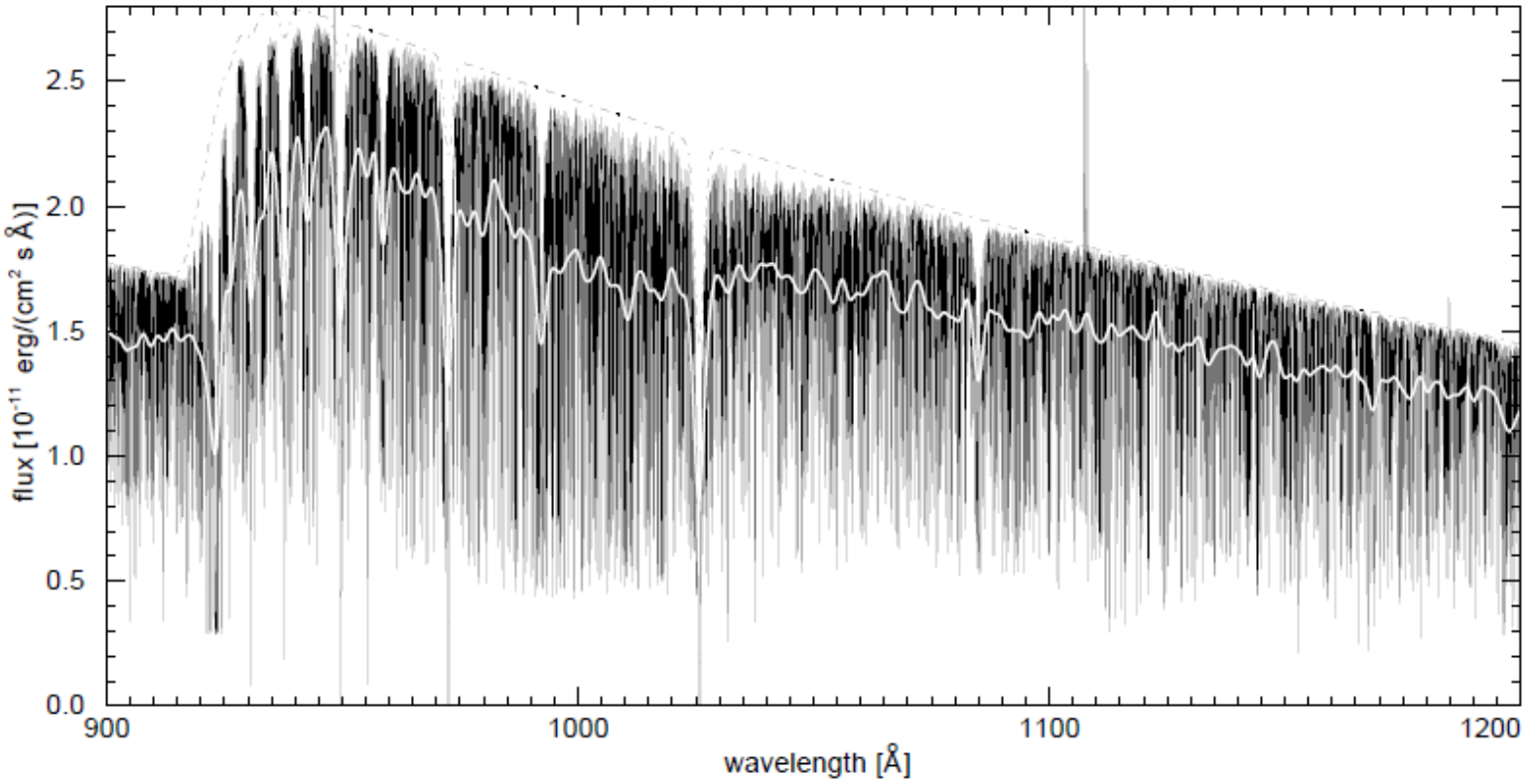

(From Deetjen 2000)

Continuous absorption

For **continuous** sources of absorption, there must be a continuum of energy levels, i.e. at least one end of the transition involving a free state of the electron (at an energy above χ_{ion}). Two possibilities…

1. A transition from a bound state (level n) to a free state with velocity v. The energy of the absorbed bound-free photon is given by

   $$h\nu = hc/\lambda = (\chi_{ion} - \chi_n) + mv^2/2$$

   Each bound-free transition corresponds to an ionization process (since the electron is free afterwards). The emission of a photon by a free-bound transition corresponds to a recombination process.
2. Finally, one can get a continuum of transitions if the electron goes from one free-state (with velocity v_1) to another free-state (with velocity v_2) . The energy of the free-free transition is

   $$h\nu = \frac{hc}{\lambda} = \frac{mv_2^2}{2} - \frac{mv_1^2}{2}$$

Lyman, Balmer, Paschen continua

- For hydrogen, transitions occurring between n=1 and another bound state n=2, 3, 4, etc. are known as the Lyman series (observed in the UV), between n=2 and higher members are the Balmer series (seen in the optical), with higher series observed in the IR: Paschen (n=3), Brackett (n=4), Pfund (n=5), etc.

- The Lyman continuum refers to a bound-free transition between n=1 and the H^+ continuum.
  Accordingly, the Balmer continuum between n=2 and the H^+ continuum, Paschen (n=3), Brackett (n=4), etc.

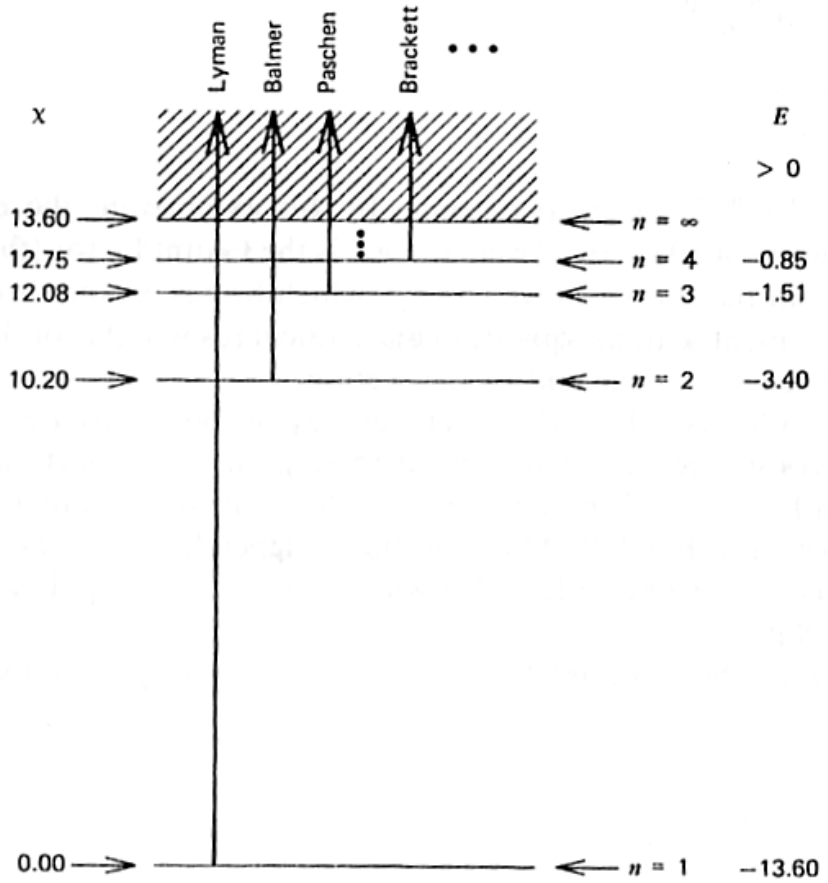

bb, bf, ff-processes

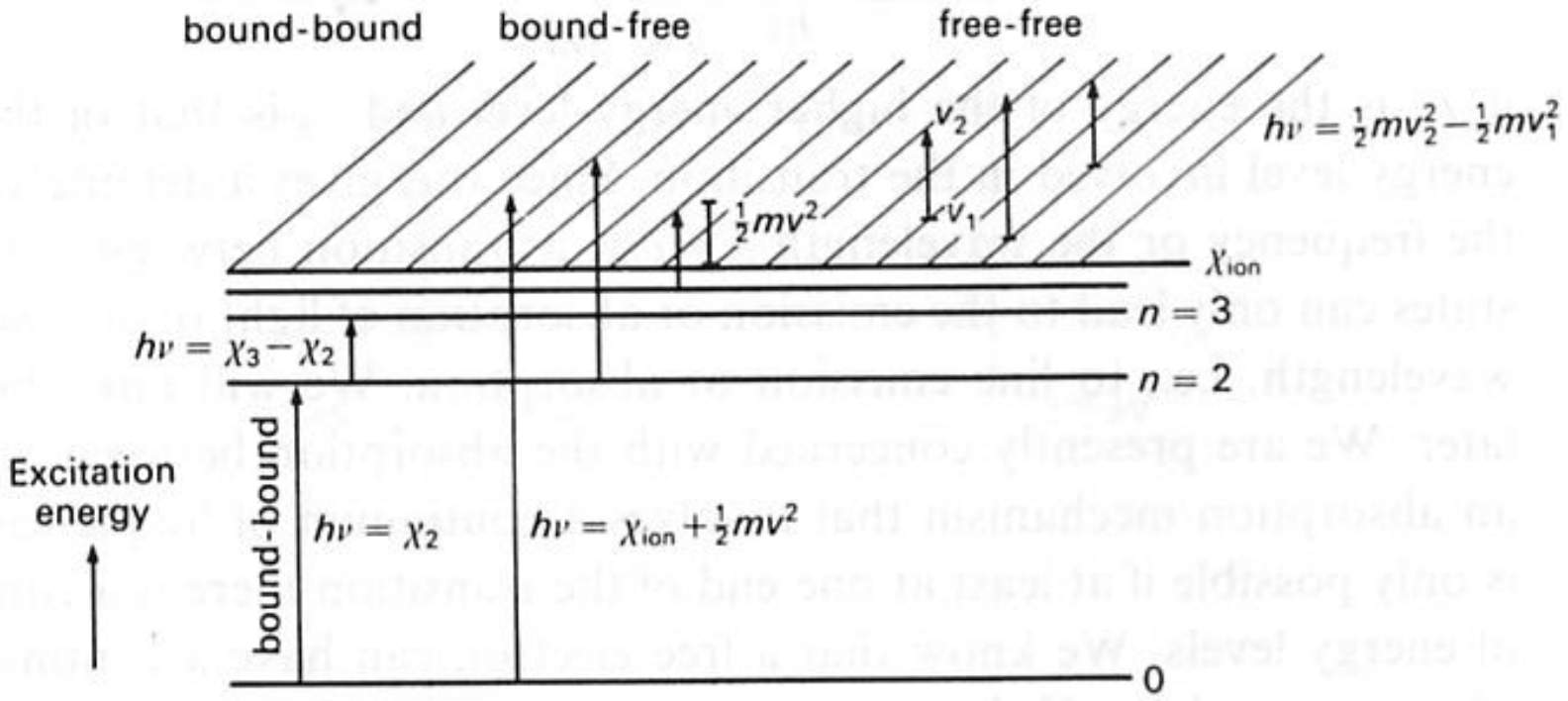

1 eV=11604 K =1.602 10^{-12} erg

χ_{ion}=13.6 eV, χ_{ion}/k=157820 K

k=8.6174x10^{-5} eV/K

Continuous absorption

Which states contribute at a given wavelength?

- Photons need an energy great enough to overcome the ionization energy i.e. $h\nu > \chi_{ion} - \chi_n$ or $\lambda < hc/(\chi_{ion} - \chi_n)$. At long wavelengths only energy levels with very large χ_n can contribute to $\boldsymbol{\alpha}$, so most continuous opacity is from mainly free-free transitions.
- The contribution of level n will start at $\lambda_n = hc/(\chi_{ion} - \chi_n)$ and continue for shorter λ. There is a **discontinuity** at λ_n because of a sudden change in the number of absorbing atoms, e.g.

  Lyman jump (912Å) due to the contribution of **n=1**.
  Balmer jump (3647Å) due to the contribution of **n=2**.

- To derive α_λ, the total absorption at wavelength λ, we have to multiply σ_n by the number of atoms in this state and sum up all states n that contribute at this wavelength.
  For this we need to use the Boltzmann formula. $\boldsymbol{\alpha_\lambda = \sigma_\lambda n}$

Bound-free absorption coefficient

Kramers approximation for continuous cross-section for level n for H-like nucleus of charge Z:

Gaunt factor ≈ 1

$$\sigma_{bf}(\mathrm{H}) = \frac{32\pi^2}{3\sqrt{3}} \frac{e^6}{c^3 h^3} R \frac{\lambda^3}{n^5} Z^4 G_{bf} = a_0 \frac{\lambda^3}{n^5} G_{bf} \ [\mathrm{cm}^2 \text{ per neutral H atom}]$$

Rydberg constant

$R=2\pi^2 me^4/h^3c$

$a_0=1.0449\times10^{-26}$ for λ in angstroms

The photoionization threshold is $E_n=h\nu_{nc}$, so σ_n decreases with ν (increases with λ).

$$h\nu_{nc} = \chi_{ion} - \chi_n$$

For H, at the threshold $\sigma_{1c}=6.3\times10^{-18}$ cm^2
The total absorption coefficient for H is:

$$\alpha_{bf}^{H}(\lambda) = \sum_{n>\sqrt{\chi_{ion}/hc}}^{\infty} \sigma_{nc}(\lambda) N_n$$

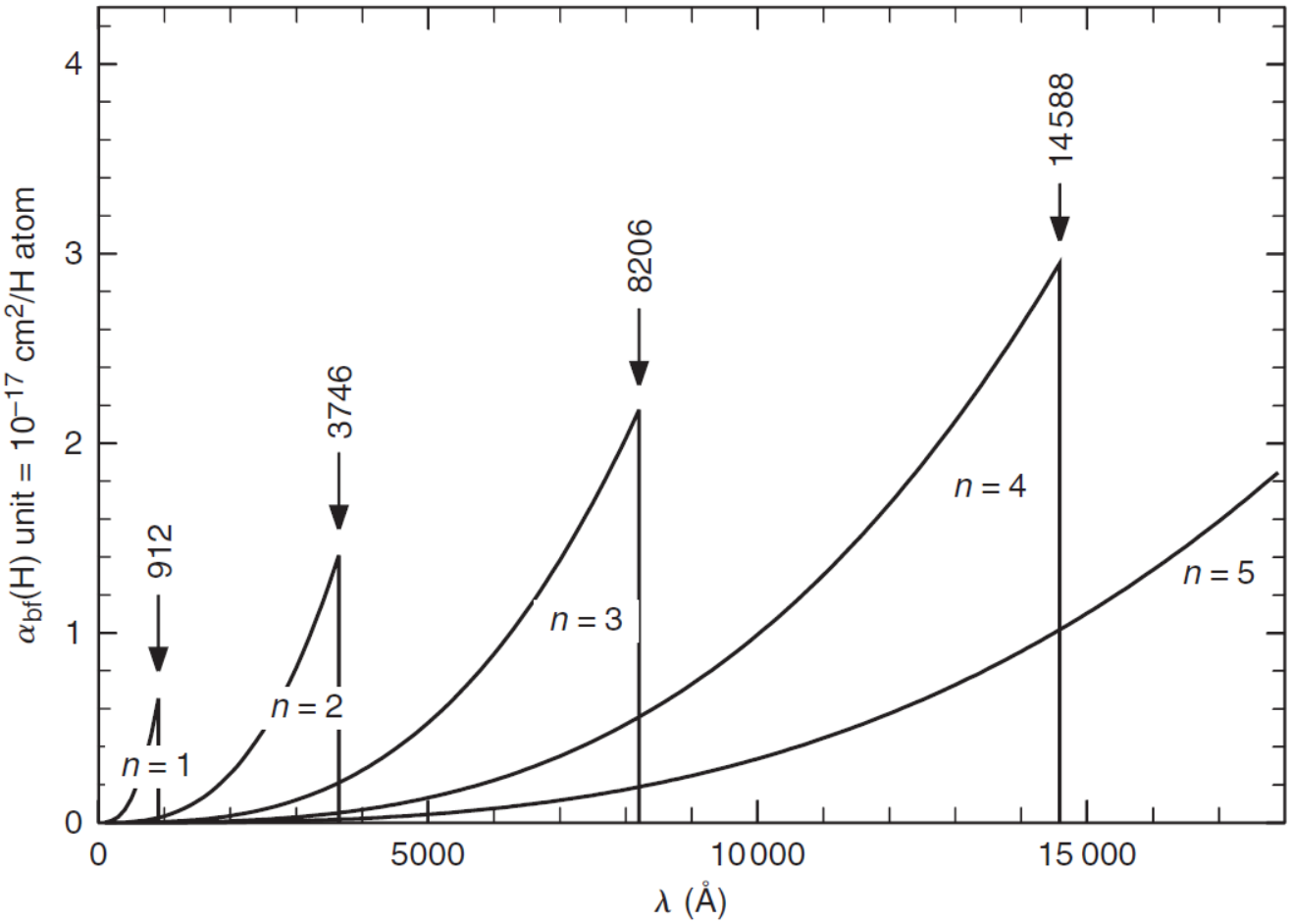

The bound–free absorption coefficient for hydrogen increases with n.

Example: Lyman continuum

Gaunt factor ≈ 1

$\sigma_{bf}(\mathrm{H}) = a_0 \frac{\lambda^3}{n^5} G_{bf}$ cm^2 per neutral H atom a_0=1.0449×10^{-26} for λ in angstroms

For H, at the photoionization threshold, σ_{1c}=6.3x10^{-18} cm^2

$$\tau_\lambda = \int_0^S \kappa_\lambda \rho ds = \int_0^S \sigma_\lambda n ds$$

Absorption by interstellar medium (ISM) at the Lyman edge:

$$\tau_\lambda = \int_0^S \sigma_{1c}(\lambda)\, N_{ISM} ds = \bar{N}_{ISM}\, \sigma_{1c} S$$

$\bar{N}_{ISM} \approx$ 1cm^3 but **all** the H atoms are in the ground state.

$$\tau_\lambda = 1 \text{ at } S = \frac{1}{\bar{N}_{ISM}\ \sigma_{1c}} = 1.5 \times 10^{17}\text{cm} = \frac{1}{20}\text{pc}$$

Impossible to observe distant objects at λ< 912Å

Free-free absorption coefficient (1)

- The free-free continuous absorption coefficient for H is much smaller than the bound-free coefficient.
- When a free electron collides with a proton, its orbit (**unbound**) is altered. A photon may be absorbed during such a collision, the orbital energy of the electron being increased by the photon energy.
- The strength of the absorption depends on the electron velocity (slower electrons are more likely to absorb a photon because a slow encounter increases the probability of a photon passing by during the collision.
- We adopt a Maxwellian distribution.
- Kramers (1923):

Rydberg constant

$$d\sigma_{ff}(\mathrm{H}) = \frac{2}{3\sqrt{3}} \frac{h^2 e^2 R}{\pi m_e^3} \frac{\lambda^3}{c^3 v} dv$$

Cross section for the fraction of electrons in the velocity interval

Free-free absorption coefficient (2)

- Integrate over velocity:

$$\sigma_{ff}(\mathrm{H}) = \frac{2}{3\sqrt{3}} \frac{h^2 e^2 R}{\pi m_e^3} \frac{\boldsymbol{\lambda^3}}{c^3} \left(\frac{2m_e}{\pi \kappa \boldsymbol{T}} \right)^{1/2}$$

Gaunt factor

- The total absorption coefficient for H is: $\kappa_{ff}^{H} = \frac{\sigma_{ff} G_{ff} N_i N_e}{N}$

  where the number density of electrons, ions and neutral Hydrogen are N_e, N_i and N, respectively.

- $N_i N_e / N$ can be substituted:

$$\kappa_{ff}^{H} = \sigma_{ff} G_{ff} \lambda^3 \frac{\log e}{2\Theta \mathrm{I}} 10^{-\Theta \mathrm{I}}$$

  where $\mathrm{I} = hcR$, $R = 2\pi^2 m e^4 / h^3 c$

- This absorption process is the inverse of Bremsstrahlung emission.

Wavelength dependence of α(H)

- Consider the H absorption coefficient α (per atom) for T=5040K (Θ=5040/T=1). Let us compare the value of α in the Balmer (n=2) to Lyman (n=1) continua at 912Å:

$$\frac{\alpha(Balmer)}{\alpha(Lyman)} = \frac{\sigma_{i2}}{\sigma_{i1}}\frac{N_2}{N_1} = \frac{\sigma_{i2}g_2}{\sigma_{i1}g_1}e^{-(10.2eV/kT)} = \frac{\sigma_{i2}g_2}{\sigma_{i1}g_1}10^{-(10.2\times5040/T)}$$

- From above, $\sigma_n \propto n^{-5}$ and $g_n = 2n^2$ so $\frac{\alpha(Balmer)}{\alpha(Lyman)} = \frac{2^{-5}\times 8}{1\times 2}6.3\times10^{-11} \approx 8\times10^{-12}$

- There is a huge difference in hydrogen absorption coefficient at 912Å (Lyman edge) at T=5040K.
- Similar calculations at T=25200K (Θ=5040/T=0.2) give

$$\frac{\alpha(Balmer)}{\alpha(Lyman)} = \frac{2^{-5}\times 8}{1\times 2}0.009 = 0.001$$

- Hydrogen absorption coefficient is very T sensitive!

Wavelength dependence of α(H)

- Consider the H absorption coefficient α (per atom) for T=5040K (Θ=5040/T=1). What about the value of α in the Paschen (n=3) to Balmer (n=2) continua at 3647Å?

$$\frac{\alpha(+)}{\alpha(-)} = \frac{\sigma_u}{\sigma_l}\frac{N_u}{N_l} = \frac{\sigma_u g_u}{\sigma_l g_l} e^{-(\chi_{ul}/kT)} = \frac{\sigma_u g_u}{\sigma_l g_l} 10^{-(\chi_{ul}\times 5040/T)}$$

Transition between levels u and l:

$$\chi_{ul} = C\left(\frac{1}{u^2} - \frac{1}{l^2}\right)$$

where $C=\chi_{ion}$=-13.6 eV

- From above, $\sigma_n \propto n^{-5}$ and $g_n = 2n^2$ so $\frac{\alpha(Paschen)}{\alpha(Balmer)} = ? 0.004$

- There is a huge difference with Lyman edge (8×10^{-12}). Still, Balmer jump is notable.
- Obviously, all the following jumps will be less and less prominent.

Wavelength dependence of α(H)

- There is a huge difference between Lyman edge (8×10^{-12}) and Balmer jump (0.004). Still, Balmer jump is notable.
- Obviously, all the following jumps are less and less prominent.

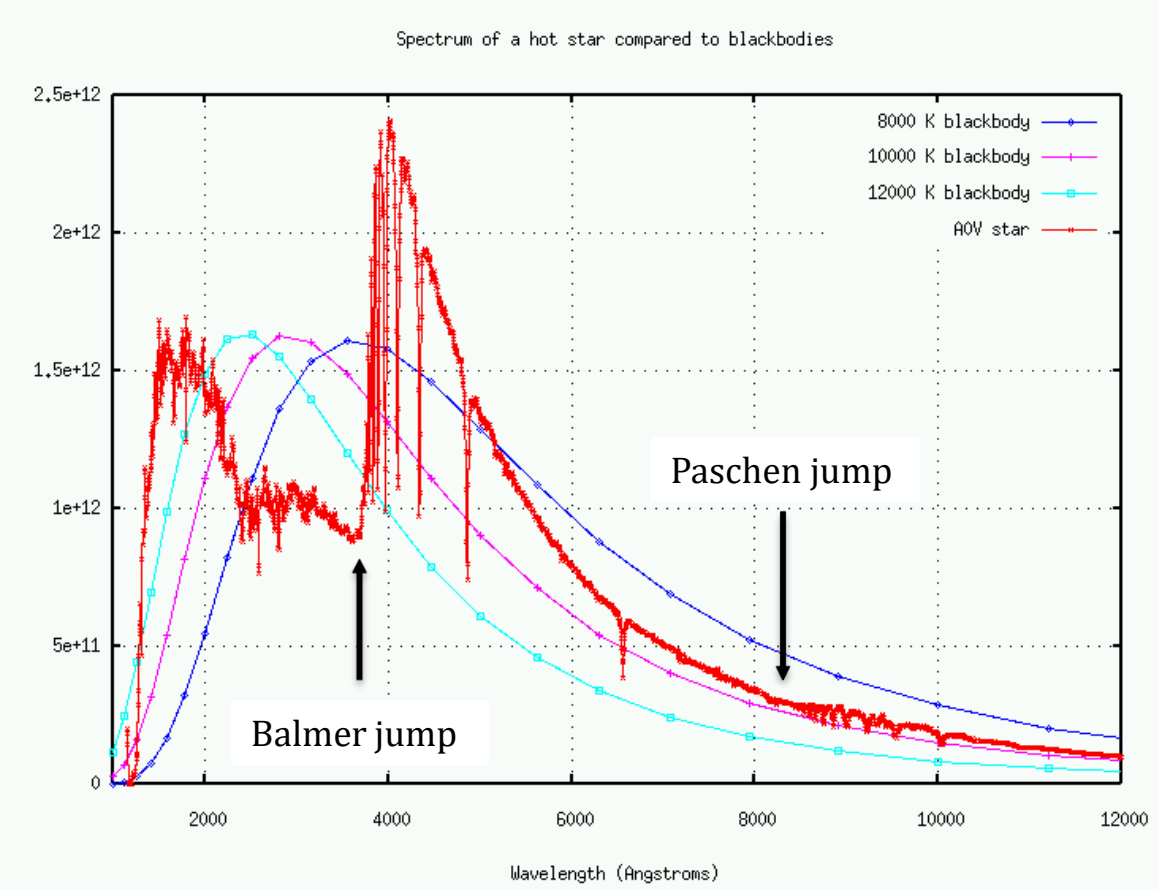

Wavelength dependence of α(H)

- Primarily, the Paschen continuum (absorption from n=3) determines the H absorption coefficient in the visual (3647Å<λ<8205Å).
- For He^+, the ionization energy is larger by a factor of $Z^2=4$ than that of the H atom. All discontinuities occur at wavelengths shorter by a factor of 4, i.e. 228Å instead of 912Å for the He^+ Lyman continuum.

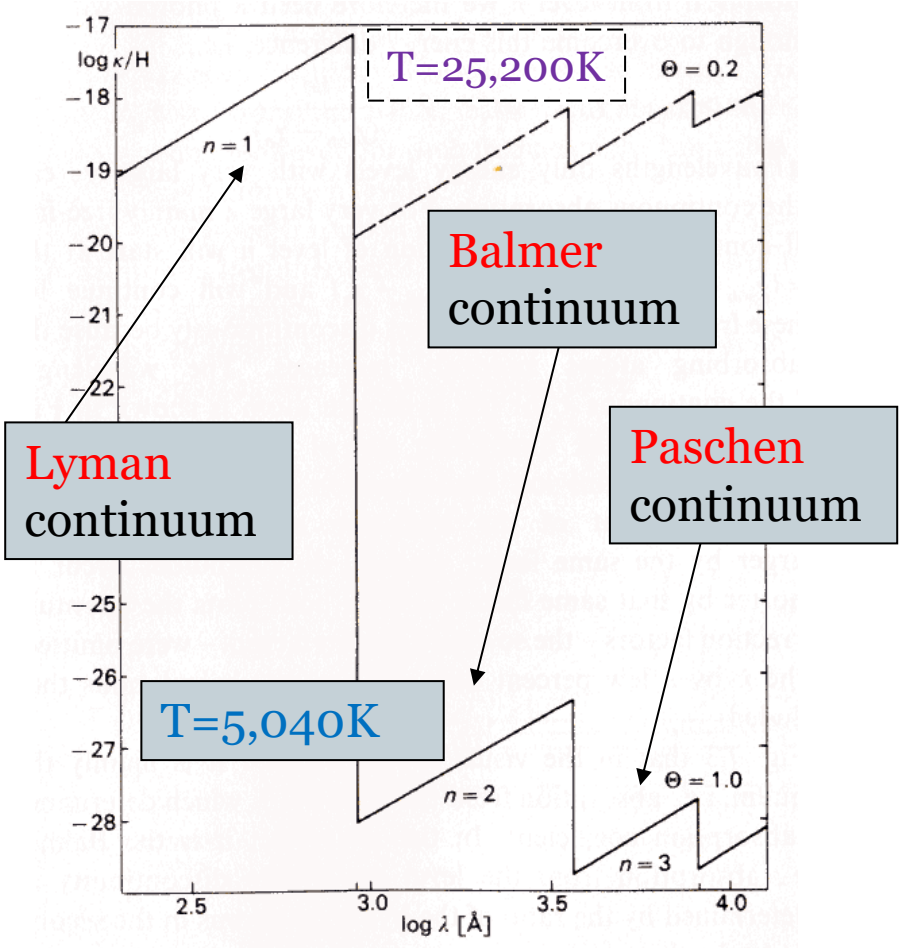

Negative hydrogen ion H^-

- The H atom is capable of holding a second electron in a bound state (binding energy 0.754eV). All photons with $\lambda < 1.64\mu m$ have sufficient energy to ionize the H^- ion back to neutral H atom plus a free electron. The extra electrons needed to form H^- come from ionized metals (such as Ca^+).
- For Solar-like stars, it turns out that H^- is the dominant continuum opacity source at optical wavelengths. In early-type stars H^- is too highly ionized to play a role, whilst in late-type stars there are too few free electrons (since no ionized metals).

Importance of H^- in the Sun (1)

We can use the Saha equation to derive the relative population of N(H^-) in the Sun (u^-=1, T=5777K, χ_{ion}=0.754 eV),

$$\log\frac{N^+}{N^0} = \log\frac{u^+}{u^0} + \log 2 + \frac{5}{2}\log T - \chi_{ion}\Theta - \log P_e - 0.48$$

$$\log\frac{N(H^0)}{N(H^-)} = \log\frac{2}{1} + \log 2 + 9.40 - 0.66 - 1.18 - 0.48 = +7.68$$

So, only **2 out of 10^8** hydrogen atoms is in the form of H^-.

Why then the H^- absorption coefficient so important?
Recall, only H atoms in the 3rd quantum level (n=3, Paschen continuum) can contribute to the visual continuous opacity. From the Boltzmann formula

$$\log N(H_{n=3})/N(H_{n=1}) = \log 2(3)^2/2(1)^2 - 5040/5777 \times 12.1 = -9.6$$

i.e. $N_H(n=3)/N_H(n=1)$=2.4x10^{-10} for the Sun. We can now compare the number of H^- ions and H atoms in the Paschen continuum:

$$\log N(H_{n=3})/N(H^-) = 2.4 \times 10^{-10}/2.1 \times 10^{-8} = 0.01$$

Importance of H^- in the Sun (2)

The atomic absorption coefficients per absorbing atom are comparable, so we expect H^- b-f absorption to be 100 times more important than the H Paschen continuum for the Sun.

The Balmer continuum (n=2) cannot so easily be neglected and does contribute to the opacity at shorter wavelengths.

Note: For early type stars (A and earlier) we find $N_H(n=3)/N(H^-) \gg 1$ so absorption of neutral H is much more important than H^-. This is why such stars have very strong discontinuities in the Balmer & Paschen limits. We will discuss the importance of the Balmer jump shortly.

H^- continuous opacity

The bound-free H^- absorption can occur for $\lambda < 16500$Å, with a different behaviour from H, reaching a maximum at 8000Å, and decreasing towards the ultraviolet. At longer wavelengths, there is only free-free H^- absorption (with a $\nu^{-3} \propto \lambda^3$ dependence).

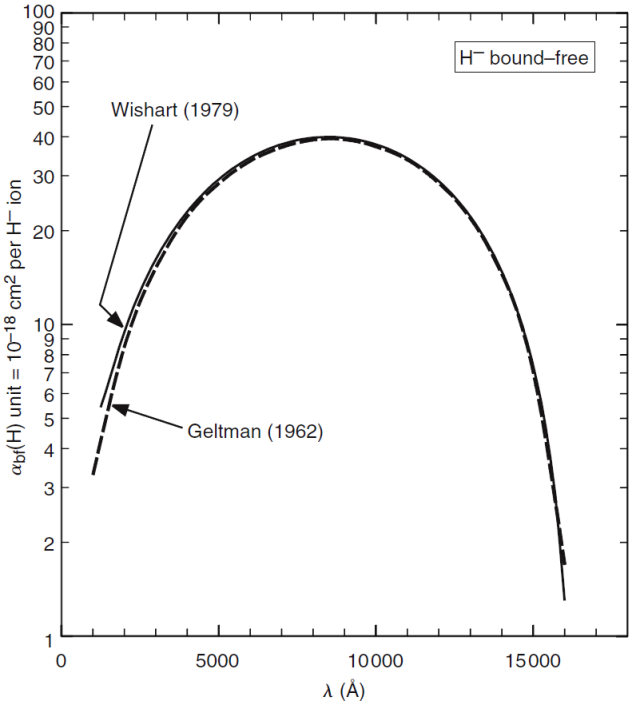

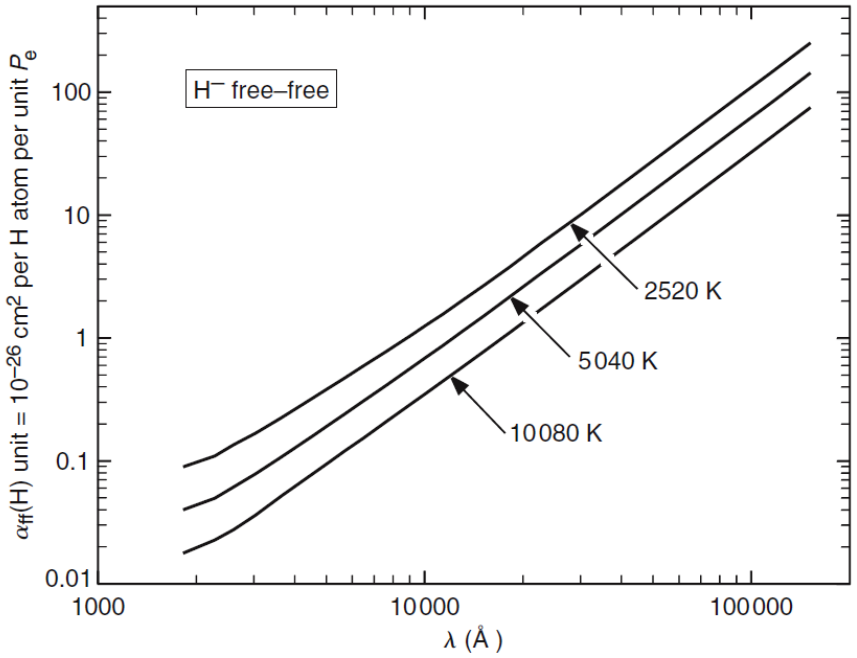

Hydrogen continuous opacity

- We have identified H^- (bound-free) in the visual and H^- (free-free) in the IR as principal sources of opacity in the Sun.
- The H Balmer continuum shortward of the 3647Å Balmer jump is an additional contributor.
- What observational evidence is there that this is true for the Sun, and what other forms of opacity play a role in other stars?

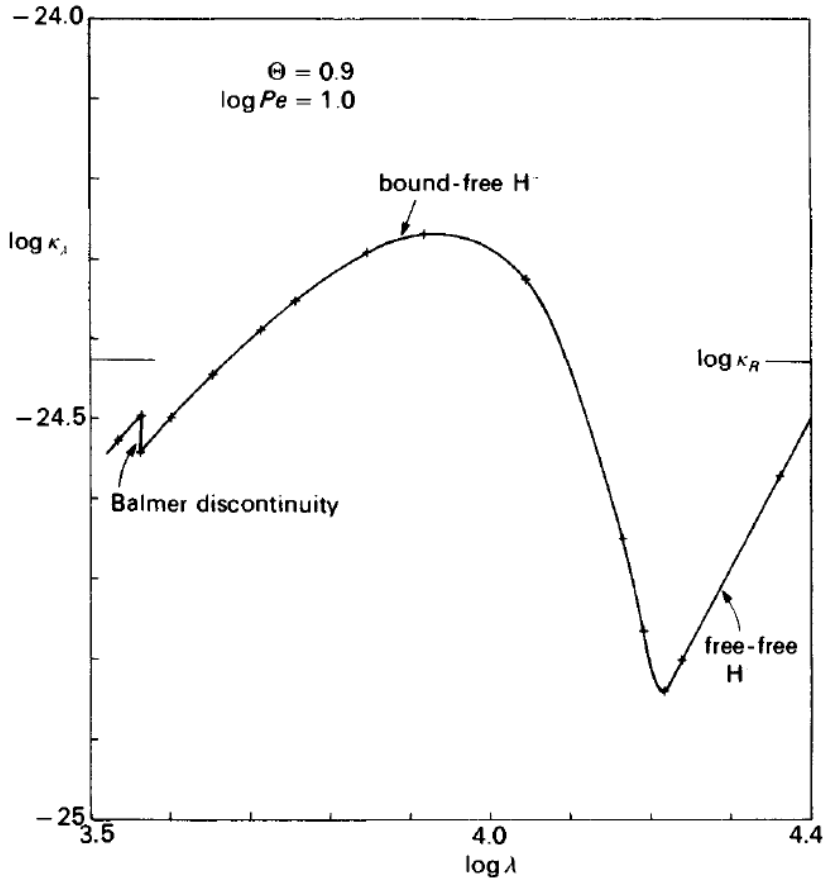

$T(\tau_\lambda)$ from Eddington approximation

We can use the observed limb darkening of the Sun at different λ to derive the depth dependence of the source function, $S_\lambda(\tau_\lambda)$.

Assuming LTE, $S_\lambda(\tau_\lambda)=B_\lambda[T(\tau_\lambda)]$ we can obtain the temperature as a function of τ_λ.

Recall from radiative equilibrium (assuming the Eddington approximation), $T(\tau_\lambda)$ can be obtained for a **grey** atmosphere.

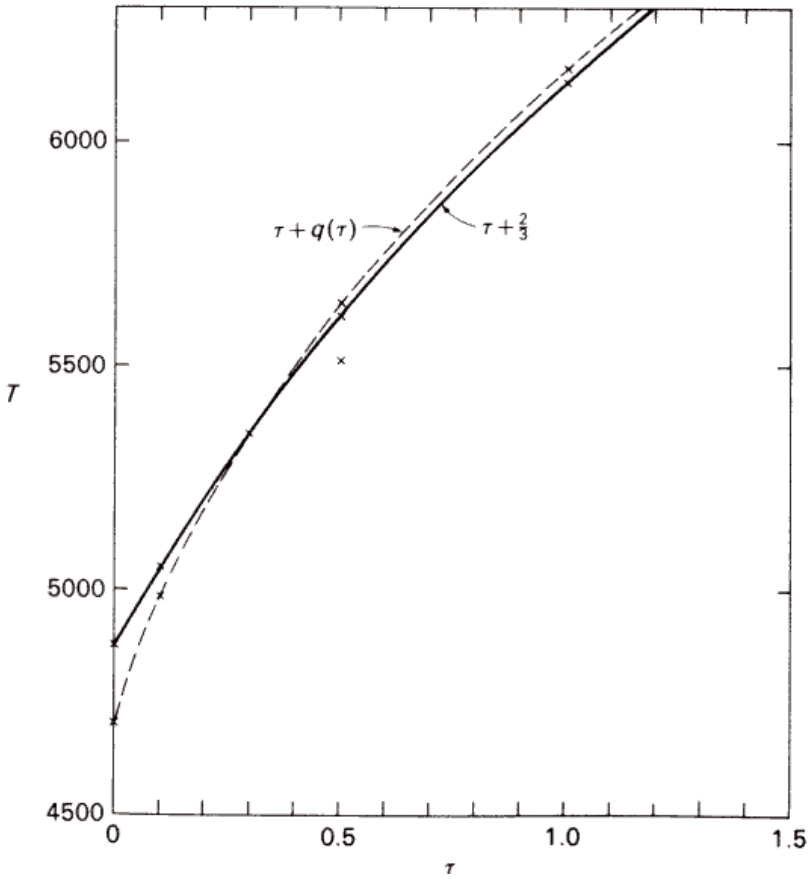

$T(\tau_\lambda)$ from limb darkening

Limb darkening observations of the Sun at different wavelengths (via imaging using suitable filters) to derive $T(\tau_\lambda)$ at various wavelengths (e.g. 3737, 5010 & 8660 Å shown here).

The horizontal line shown at T=6300 K connects points which correspond to the same ***geometrical*** depth, so it is possible to derive the wavelength dependence of τ_λ.

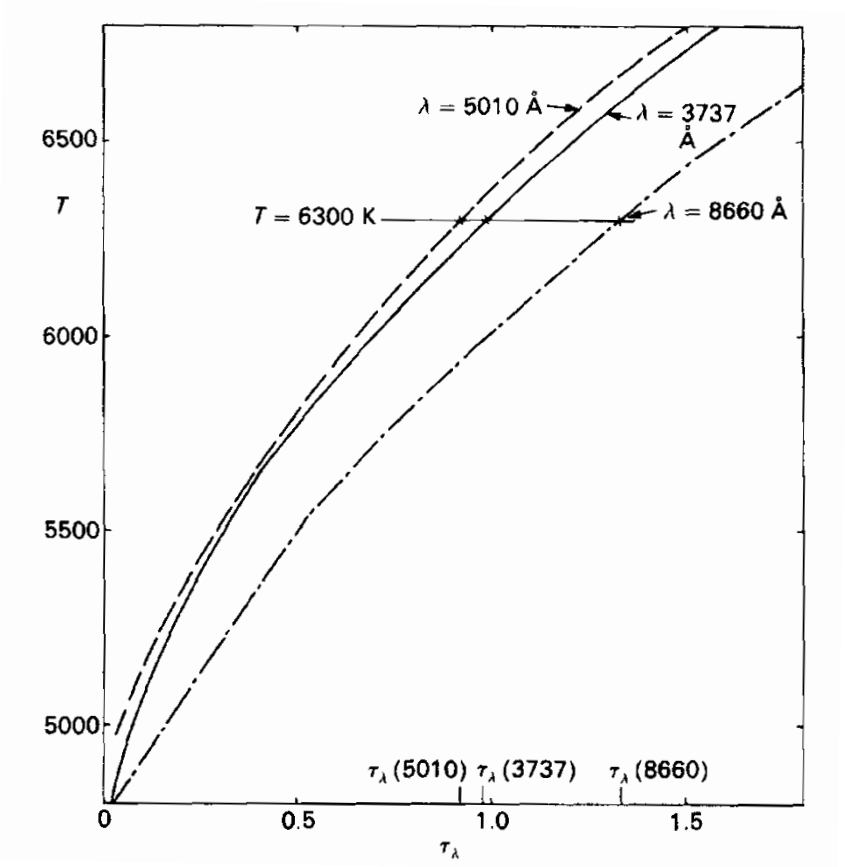

Confirmation of H^-

The wavelength dependence of τ_λ (and hence κ_λ **or** α_λ) can be observationally derived for the Sun – the optical and IR dependence **agrees** remarkably well with the theoretical absorption coefficient for b-f and f-f H^-.

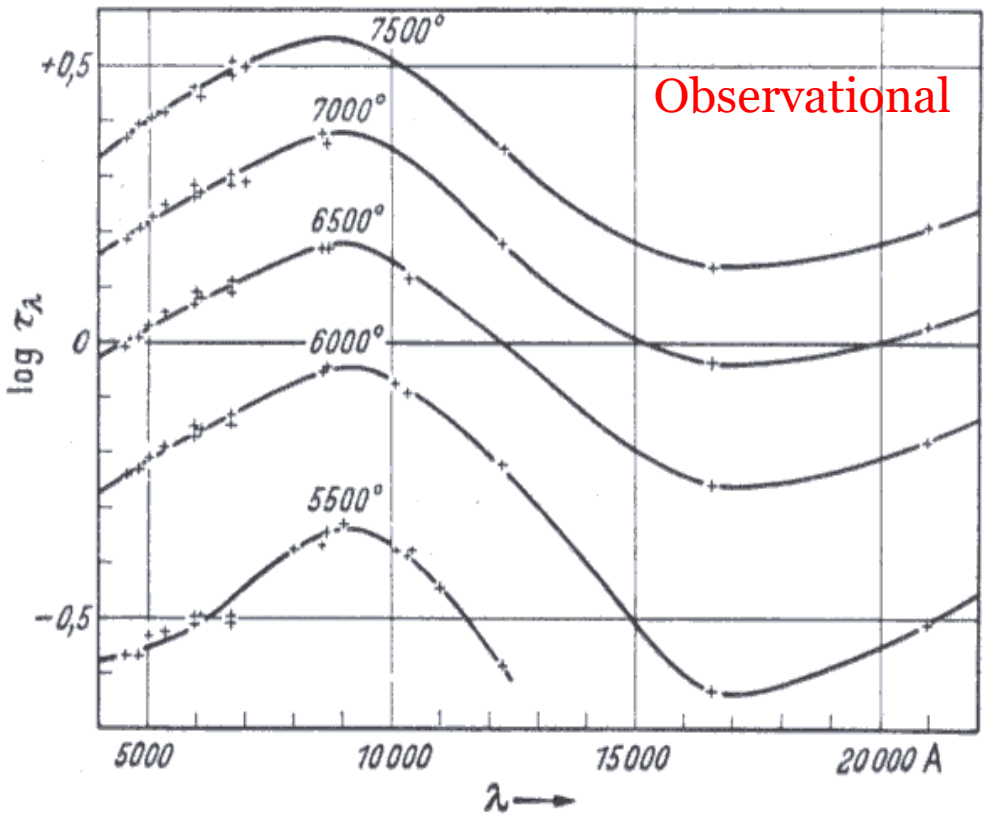

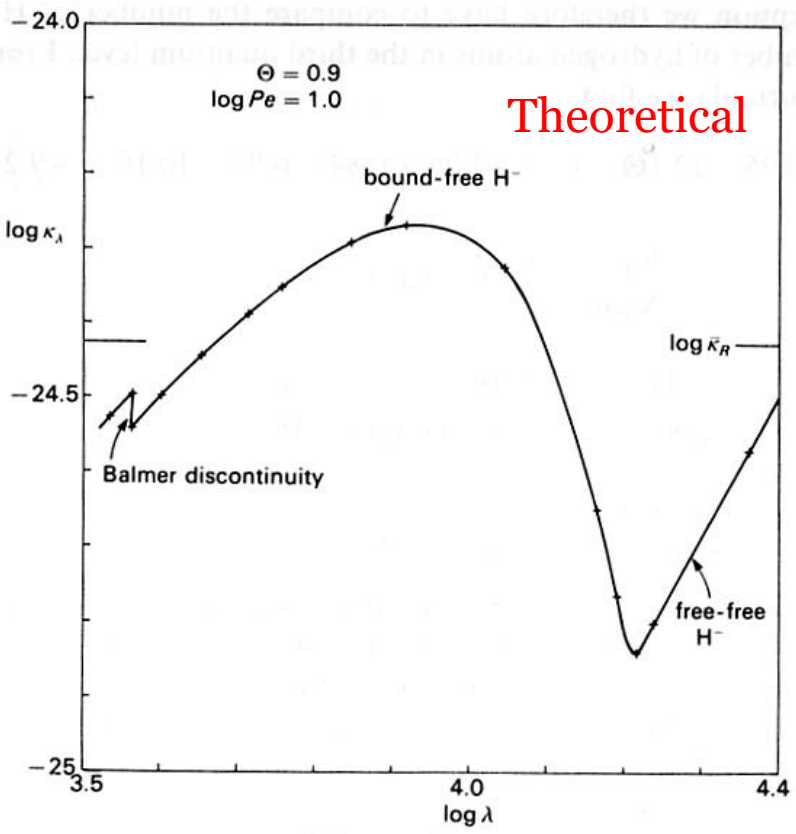

Other sources of opacity

He ABSORPTION
METALLIC ABSORPTION
SCATTERING
EFFECT OF NONGREYNESS OF THE TEMPERATURE STRUCTURE

Many physical processes contribute to opacity

- **Bound-Bound Transitions** – absorption or emission of radiation from electrons moving between bound energy levels.
- **Bound-Free Transitions** – the energy of the higher level electron state lies in the continuum or is unbound.
- **Free-Free Transitions** – change the motion of an electron from one free state to another.
- **Electron Scattering** – deflection of a photon from its original path by a particle, without changing its wavelength.
  - **Rayleigh scattering** – photons scatter off **bound** electrons (varies as λ^{-4}).
  - **Thomson scattering** –photons scatter off **free** electrons (independent of wavelength).
- **Photodissociation** may occur for molecules.

What can various particles do?

- Free electrons – Thomson scattering
- Atoms and Ions –
  - Bound-bound transitions
  - Bound-free transitions
  - Free-free transitions
- Molecules –
  - BB, BF, FF transitions
  - Photodissociation
- Most continuous opacity is due to hydrogen in one form or another

He opacity?

Helium is the next most abundant element after H, so
is it important for the continuous absorption in the Sun or other stars?

Ionization of He to He^+ requires an energy of 24.6eV ($\lambda<504$Å are needed). Indeed, even the first excited level lies 19.8eV above the ground state, which can contribute only below 600 Å where there is very little radiation coming from the Sun. From the Boltzmann formula ($g_1=1$, $g_2=3$):

$$\log(N_{He}(2s^3S) / N_{He}(1s^1S)) = 0.48-19.8\times(5040/5777) = -16.8$$

So, only 10^{-17} of the He atoms can contribute to the absorption, and since He is 10% as abundant as H, only one in 10^{-18} atoms are He atoms in the 1st excited state.

Consequently, He opacity plays a **negligible** role for the Sun. The bound-free absorption from He^- is generally negligible, whilst free-free He^- (with a form similar to free-free H^-) can be significant at long wavelengths in cool stars.
Photoionization (bound-free processes) from He only plays a significant role for the hottest, O-type, stars.

Metal (Iron) opacity

- If He only plays a role for very hot stars, do any metals contribute to the continuous opacity in cools stars?
- **Iron** (Fe/H=10^{-4}) is generally the dominant metal continuous opacity source in stellar atmospheres.
- In the Sun, let's consider absorption by atomic Fe in the ultraviolet (2000 Å) for which an excitation energy of ~1.7 eV is required. The fraction of excited Fe atoms is 4×10^{-2} relative to the ground-state (from Boltzmann formula), whilst the fraction of ionized to neutral Fe is approximately 6 (from Saha equation).
- Accounting for the abundance of Fe, we obtain the fraction of atomic Fe atoms absorbing at 2000 Å relative to the total number of H atoms to be $4 \times 10^{-2} \times 10^{-4} \times 1/6 = 6 \times 10^{-7,}$
- We previously obtained 2×10^{-8} for H^-, so metallic lines in the UV are much more important for the absorption than the H^- ion, or the neutral H atom. Even more important is the absorption by the metal atoms in the ground level, which is <1570 Å for Fe, <1520 Å for Si.

Molecular opacity

- CN^-, C_2^-, H_20^- , CH_3, TiO are important sources of opacity in late (K-type) & very late (M-type) stars.
- Molecular Hydrogen (H_2) is more common than atomic H in stars cooler than mid-M (brown dwarfs!)
- H_2 does not absorb in the visible spectrum, so only plays a role in the IR.
- H_2^+ does absorb in the visual but is less than 10% of H^-. H_2^+ is a significant absorber in the UV for such very cool stars.

Scattering

In the classical picture of an atom, we can consider the electron as being bound to the atom. Any force trying to remove it will be counteracted by an opposing force. If a force were to pull on the electron and then let go, it would oscillate with eigenfrequencies $\omega = 2\pi\nu$.

The scattering cross-section for a *classical oscillator* can be written as

$$\sigma_s = \frac{8\pi}{3}\frac{e^4}{m_e^2 c^4}\left[\frac{\nu^4}{(\nu^2-\nu_0^2)^2+\gamma^2\omega^2}\right] \qquad \omega = 2\pi\nu$$

where ν_0 is the eigenfrequency of an atom and γ is the damping constant.

Thomson & Rayleigh Scattering

Two cases are of interest:

1. **Thompson (electron) scattering** ($\nu_o=0$, $\gamma=0$) (photons scatters off a free electron, no change in λ, just direction):

classical electron radius

$$\sigma_T = \frac{8\pi}{3}\frac{e^4}{m_e^2 c^4} = \frac{8\pi}{3} r_e^2 = 6.65 \times 10^{-25}\ \mathrm{cm}^2/\mathrm{electron}$$

2. **Rayleigh scattering** by atoms/molecules ($\nu \ll \nu_o$, $\gamma \ll \nu_o$)

$$\sigma_R(\nu) \propto \sigma_T \nu^4 = \sigma_T \lambda^{-4}$$

Electron scattering vs. f-f transition

- Electron scattering (Thomson scattering) – the path of the photon is altered, but not the energy.

- Free-Free transition – the electron emits or absorbs a photon. A free-free transition **can only occur in the presence of an associated nucleus**.
  An electron in free space cannot gain the energy of a photon.

Thompson Scattering

Since an electron is tiny it makes a poor target for an incident photon so the cross-section for Thomson scattering is very small (σ_T=6.65x10^{-25} cm^2) and has the same value for photons of all wavelengths: **As such electron scattering is the only grey opacity source.**

Although e^- are very abundant in the Solar photosphere, the small cross-section makes it unimportant.

Electron scattering is most effective as a source of opacity at high temperatures. In atmospheres of OB stars where most of the gas is completely ionized, other sources of opacity involving bound electrons are excluded. In this regime, α_T **dominates** the continuum opacity.

Rayleigh Scattering

- Rayleigh scattering by H atoms in Solar-type is more relevant than e^- scattering since atoms are much more common (recall $N(H) \gg N(H^+)$).
- In M stars, H_2 becomes the dominant form for hydrogen, with strong electronic transitions in the UV, so Rayleigh scattering by molecular H_2 can be important.
- The cross-section for Rayleigh scattering is much smaller than σ_T, and is proportional to λ^{-4} so increases steeply towards the blue. (In the same way the sky appears blue, due to a steep increase in the scattering cross-section of sunlight scattered by molecules in our atmosphere).
- The cross-section is sufficiently small relative to metallic absorption coefficients that Rayleigh scattering only plays a dominant role in extended envelopes of supergiants.

Total extinction coefficient κ

- The total extinction coefficient is given by:

$$\kappa_\nu = (1 - e^{-h\nu/kT}) \sum_j x_j (\kappa_j^{bb} + \kappa_j^{bf} + \kappa_j^{ff}) + \kappa^s$$

where the sum is over all elements j of number fraction x_j.

Here the $(e^{-\frac{h\nu}{kT}})$ term accounts for stimulated emission (incident photon stimulates electron to de-excite and emit photon with identical energy, as in a laser). We shall discuss it later.

- What is the total extinction coefficient for different types of star?

G-type (optical depth unity)

For G stars, the H^- ion (bound-free) dominates for optical.

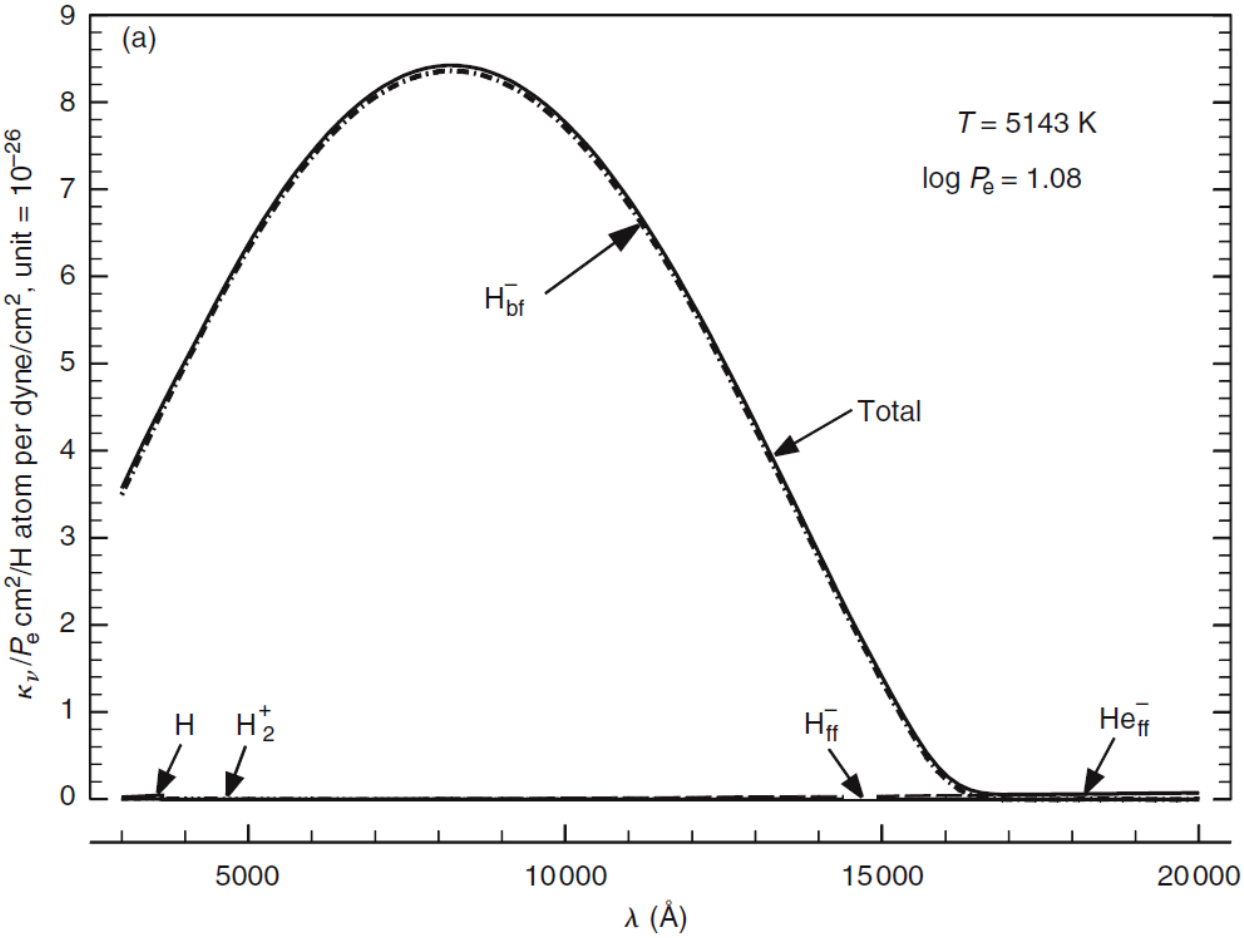

F-type (optical depth unity)

For F stars, the absorption is dominated by the two components of the H^- ion (bound-free) and (free-free), with a contribution from the Balmer continua below 3647Å.

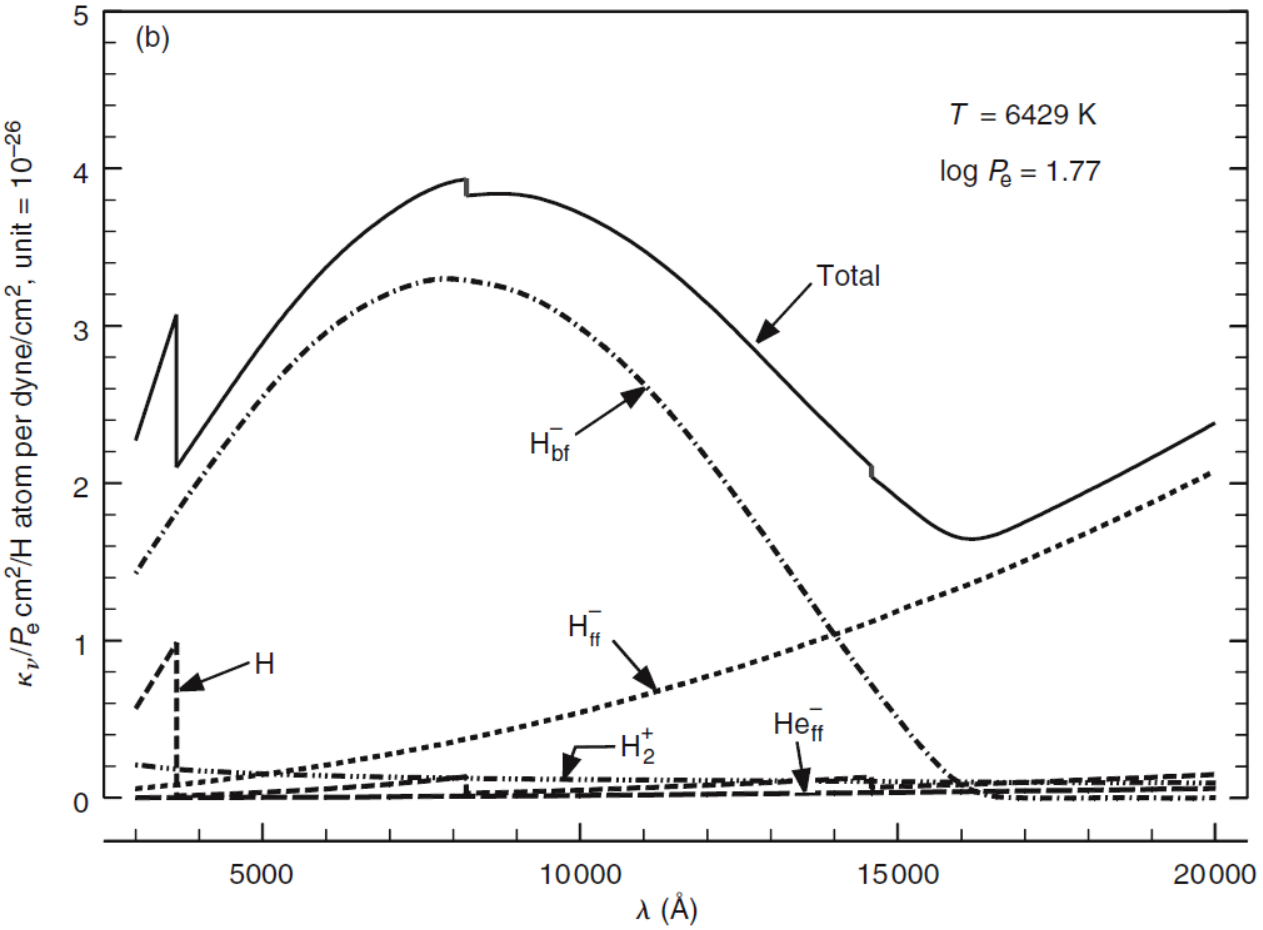

A-type (optical depth unity)

For a late A star, absorption from the H^- ion is dropping back compared to the cooler cases, while neutral hydrogen has grown with increasing temperature. H (bound-free) Balmer, Paschen and Brackett continua start to dominate.

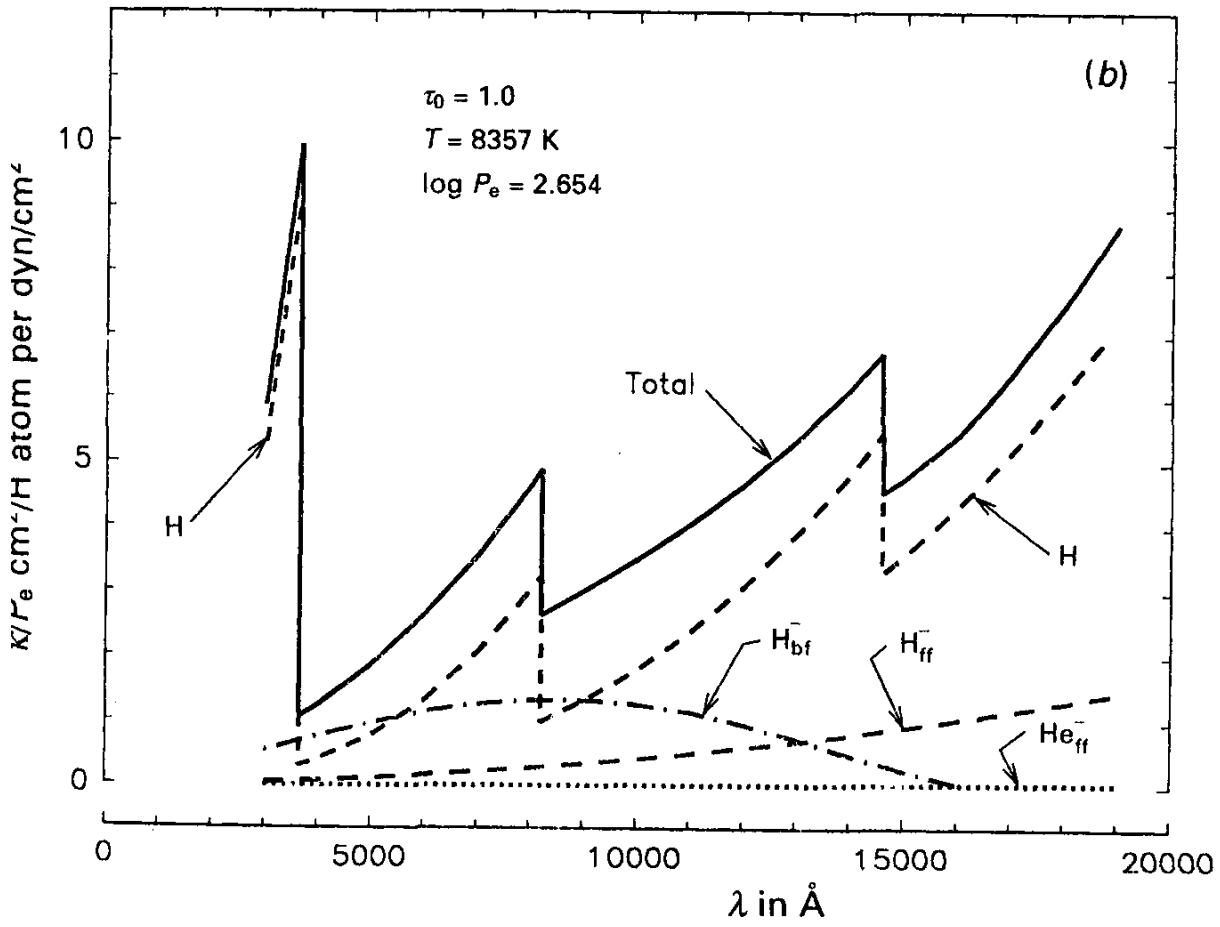

B-type (optical depth unity)

At late B, the H (bound-free) Balmer, Paschen & Brackett continua completely dominate.

For O stars electron scattering is the primary opacity source.

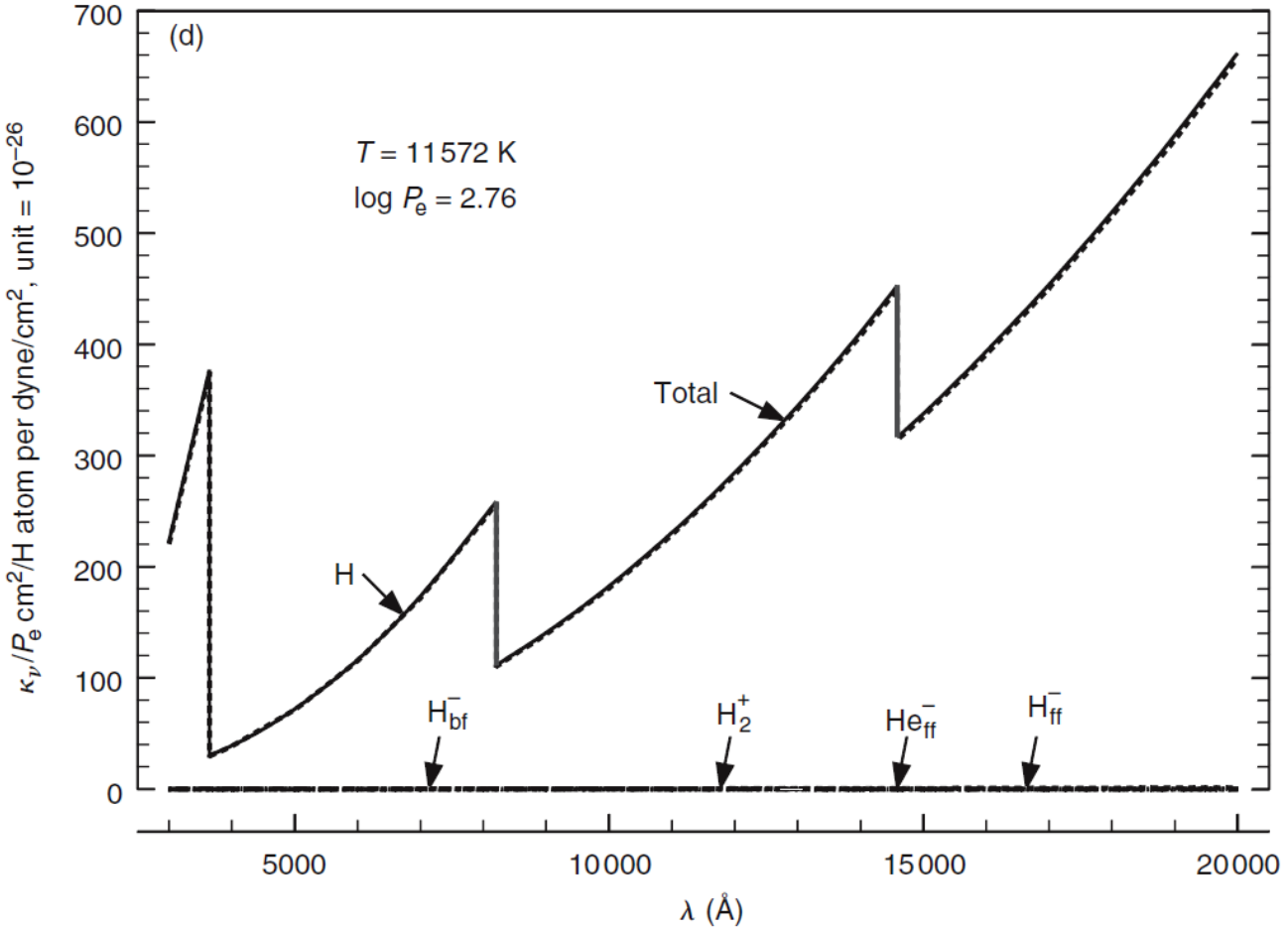

Dominant Opacity vs. Spectra Type

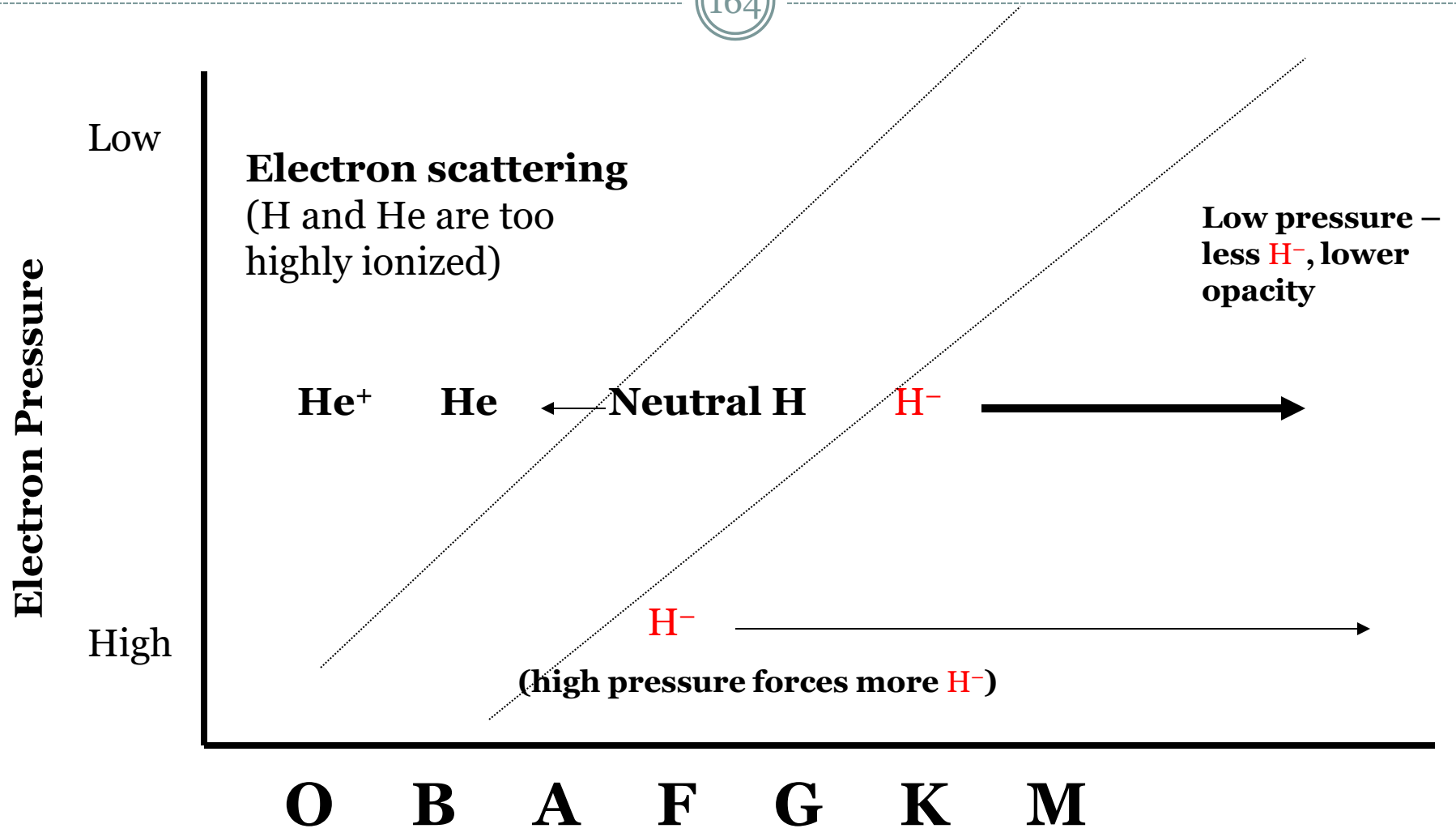

Continuum Energy Distribution

What is the effect of the λ dependence of α_λ on the emergent spectrum?

Consider the Balmer discontinuity at 3647Å. Immediately above the discontinuity (3647^+), the opacity α_λ is **lower** than average (shown as $\bar{\alpha}$), so we probe **deeper** than average into the atmosphere, where S_λ (and F_λ) is **higher** than the grey case, so F_λ exceeds the Planck function.

For 3647^-, the opacity is **higher** than average, so we probe **less deep** into the atmosphere (where T is smaller), and so receive a lower F_λ.

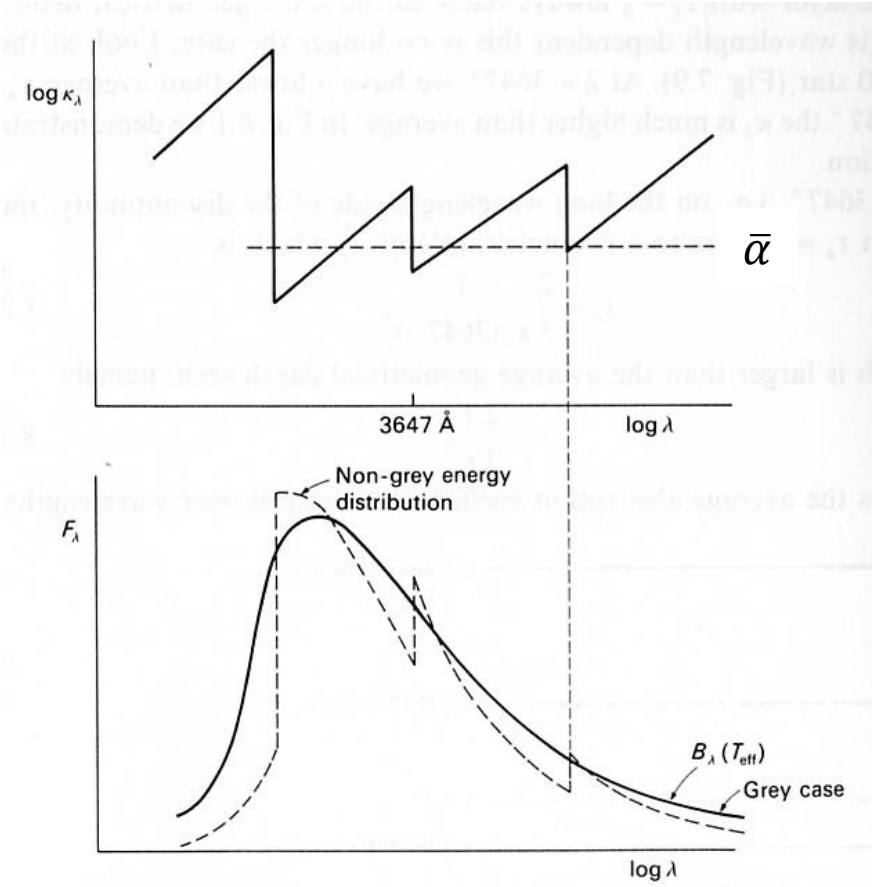

Balmer jump. Why is important?

- In hot stars, T>9000K, H^- negligible, only H contributes to opacity.

$$\frac{\alpha^+}{\alpha^-} = \frac{\sigma^+(\mathrm{H})}{\sigma^-(\mathrm{H})} \frac{N_H(n=3)}{N_H(n=2)}$$

Function of *T* only

"observed" known From Boltzmann law(T)

Thus, we can obtain the temperature.

In cooler stars (Solar-type)

$$\frac{\alpha^+}{\alpha^-} = \frac{\sigma(H^-)N(H^-) + \sigma^+(H)N_H(n=3)}{\sigma(H^-)N(H^-) + \sigma^-(H)N_H(n=2)}$$

small

$$N(H^-) = N_H(n=1)n_e f(T) \quad \text{Saha eq} \Rightarrow \quad \frac{\alpha^+}{\alpha^-}(n_e, T)$$

One of n_e or T can be determined

$$\text{if } n_e \uparrow \text{ then } \frac{\alpha^+}{\alpha^-} \to 1$$

Balmer jump in Vega

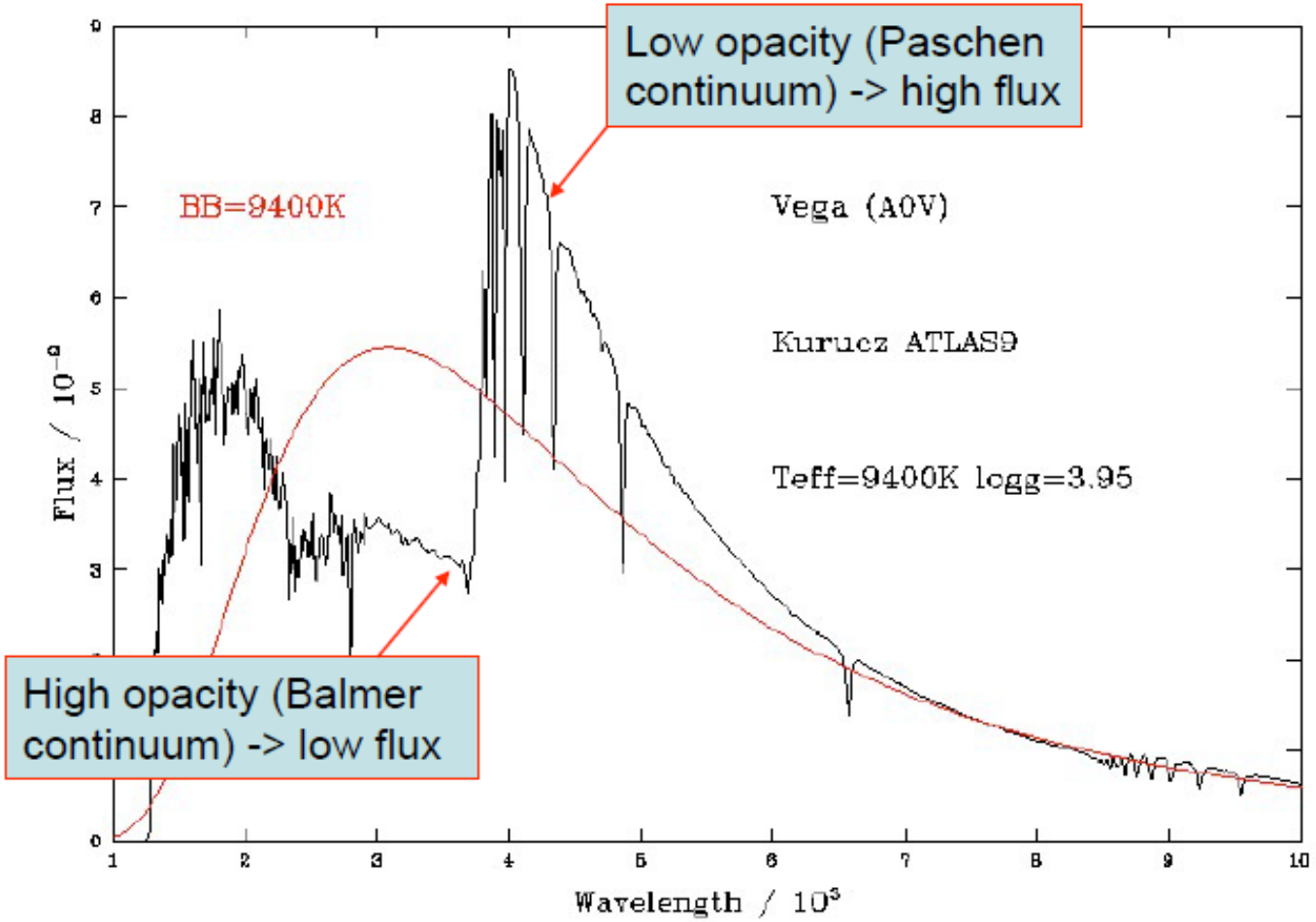

Summary

- Bound-bound transitions contribute to the line absorption. Bound-free and free-free transitions (plus scattering) contribute to the continuous absorption, mostly by H & He.
- Atomic H absorption coefficient highly T sensitive. For late-type stars in the optical and IR, bound-free and free-free transitions of the H^- ion dominate the continuous opacity, since the population of atomic H in n=3 (Paschen series) is so low.
- For early-type stars, atomic H dominates, producing strong jumps in the opacity at the Lyman, Balmer & Paschen edges.
- Negative H ion confirmed as dominant Solar optical & IR opacity source from limb darkening.
- He b-f opacity relevant only for very hot stars. Metal (Fe) opacity contributes to opacity in Solar-type stars in ultraviolet.
- Thompson (electron) scattering is grey & dominates continuum opacity in hot stars. Rayleigh scattering most important for late-type supergiants in UV
- Observed form of e.g. Balmer jump in A stars can be understood from the discontinuity in continuous H b-f opacity.
- Nongreyness changes the temperature structure.

Spectral lines

EQUIVALENT WIDTH

FWHM

FWZI

Spectral Lines

(e.g. 2D echelle image of optical Solar spectrum)

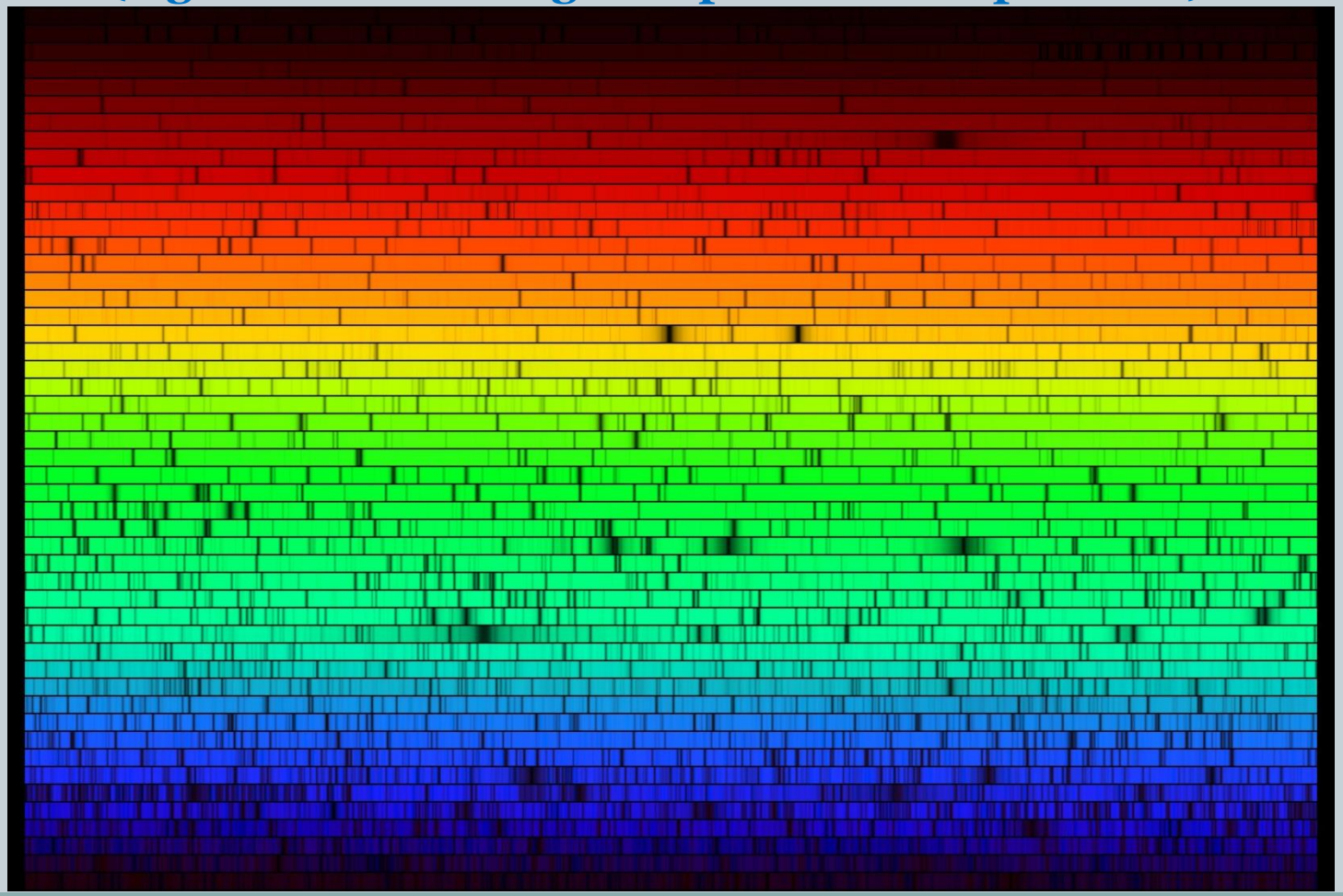

Continuous Energy Distribution

Dwarf Stars

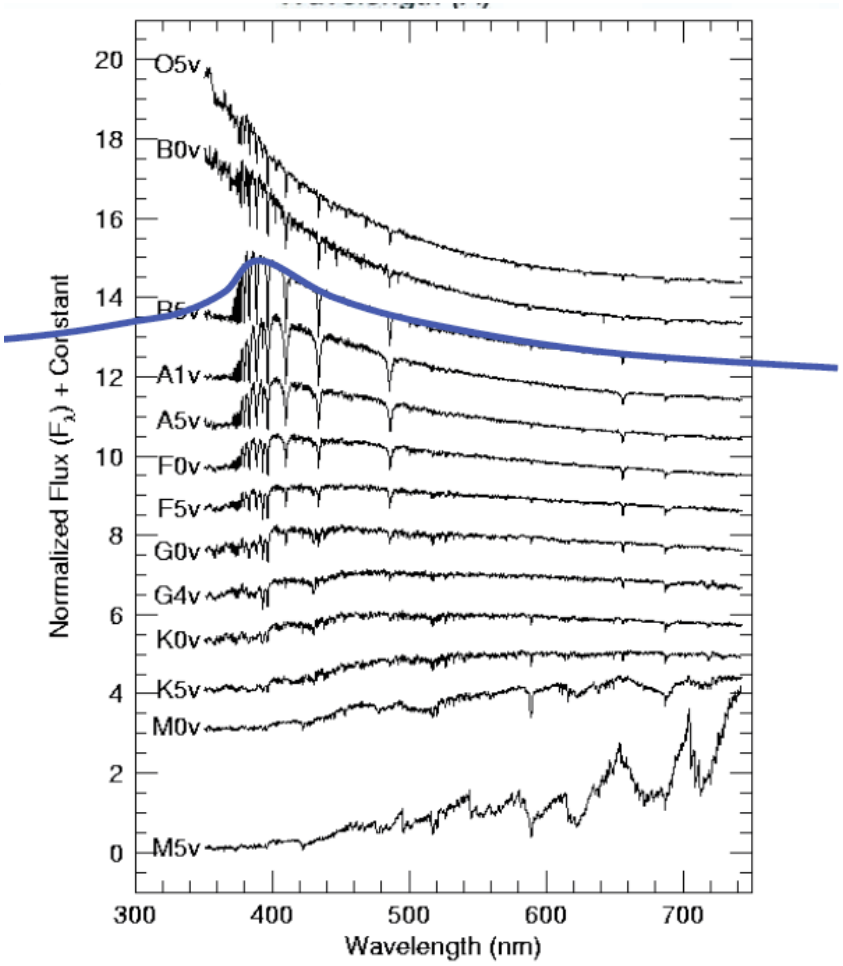

Vega

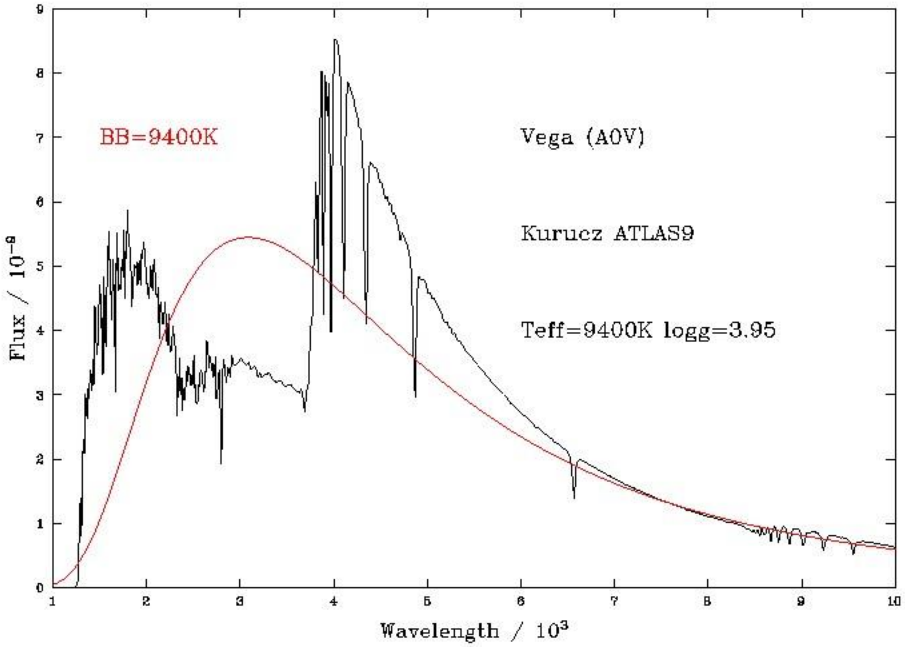

Spectra of stars, clusters, galaxies…

Spectral lines and continuum energy distributions provide temperatures and metallicity of individual stars, plus ages of clusters & galaxies (since the highest mass stars are visually the brightest).

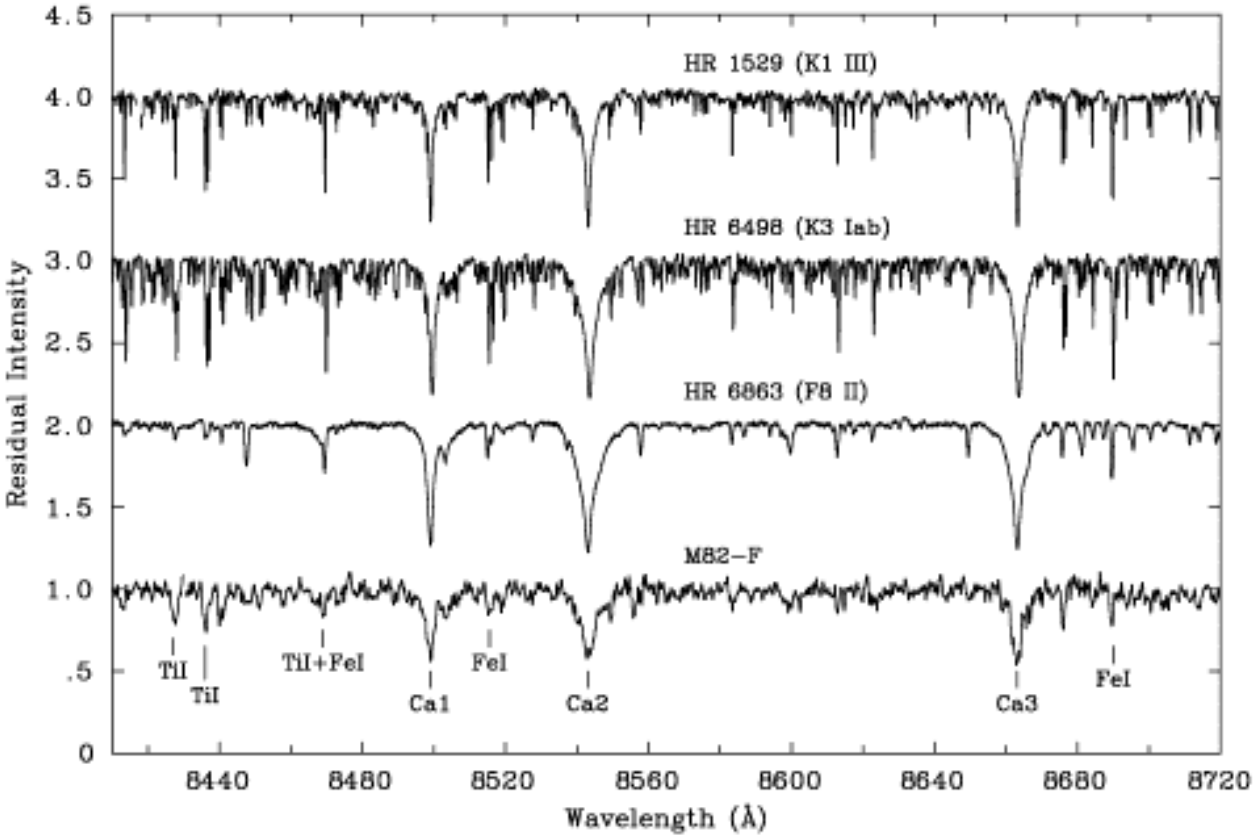

Spectral Lines

Impact of Spectral Resolution

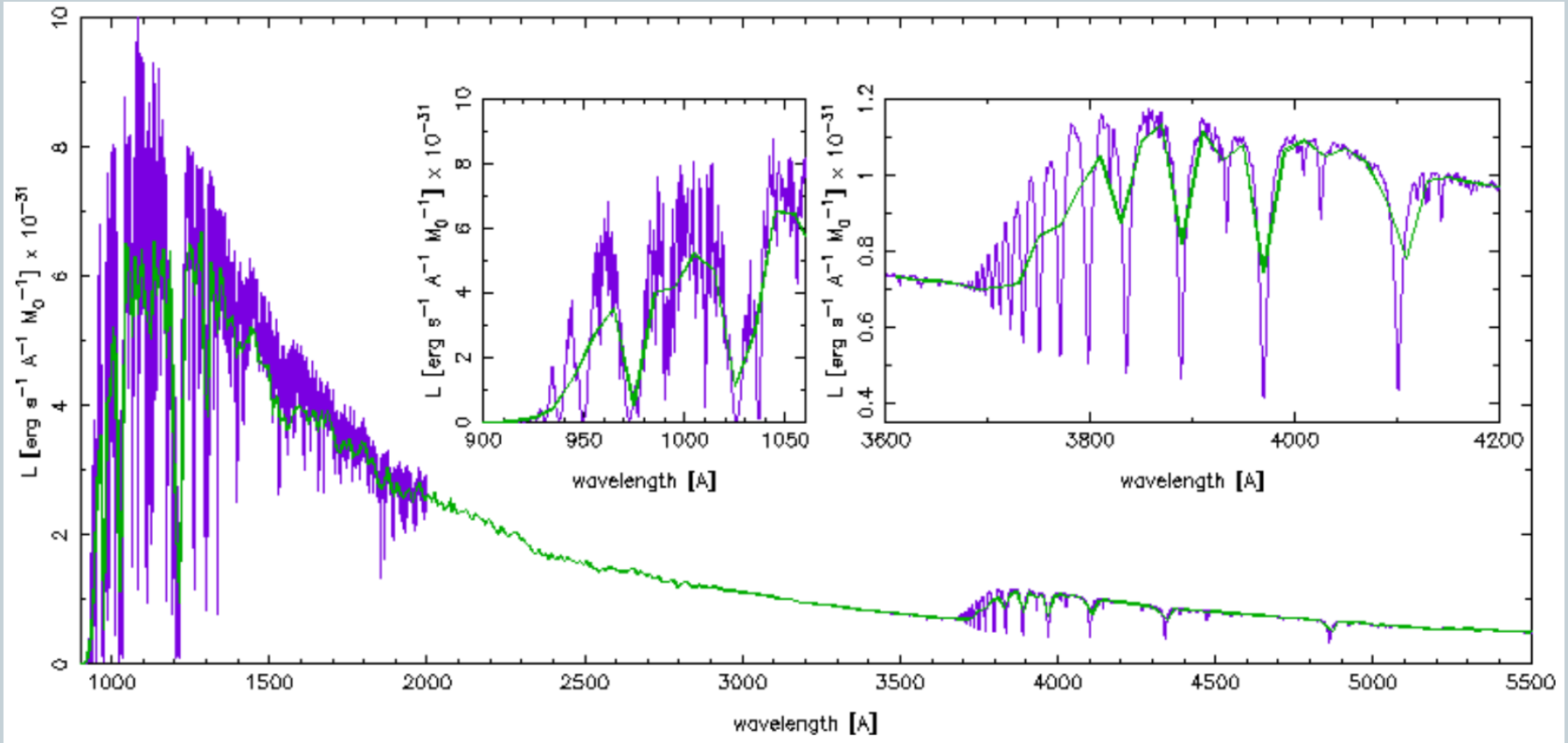

Line depth

We now turn from the continuous energy distribution to the line spectrum.

Relative intensity r_λ (*not very common term, usually applied to emission lines*):

$$r_\lambda = \frac{F_\lambda}{F_c}$$

The line depth R_λ:

$$R_\lambda = \frac{F_c - F_\lambda}{F_c} = 1 - \frac{F_\lambda}{F_c}$$

The largest $R_{\lambda,0}$— the central line depth

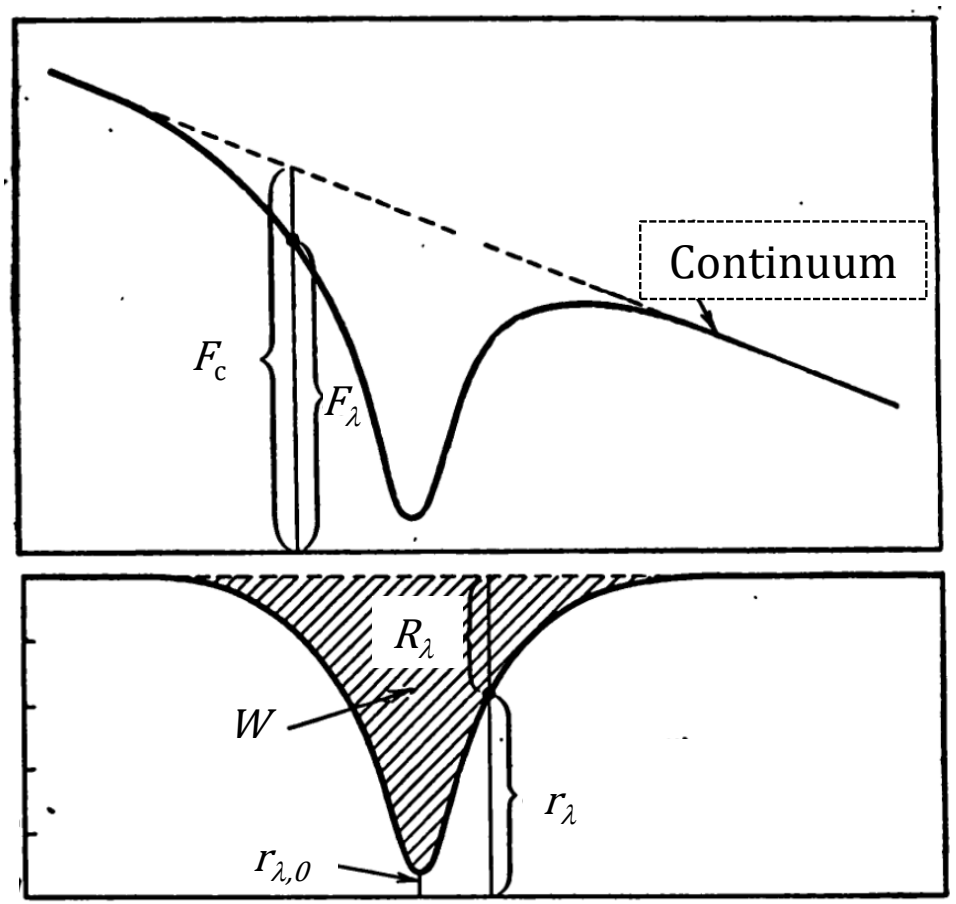

Equivalent Width

- The total area in a spectral line divided by the continuum flux F_c is called the line **equivalent width**, i.e. an integral over a line **depth R_λ**

$$W_\lambda = \int \frac{F_c - F_\lambda}{F_c} d\lambda = \int R_\lambda d\lambda$$

- The division by the continuum flux means that this is a measurement of the flux in units of the continuum – the equivalent width is identical to a rectangular line of width W_λ.
- EW of absorption lines is positive, emission lines have negative EWs, and are measured in Ångströms (at optical wavelengths).

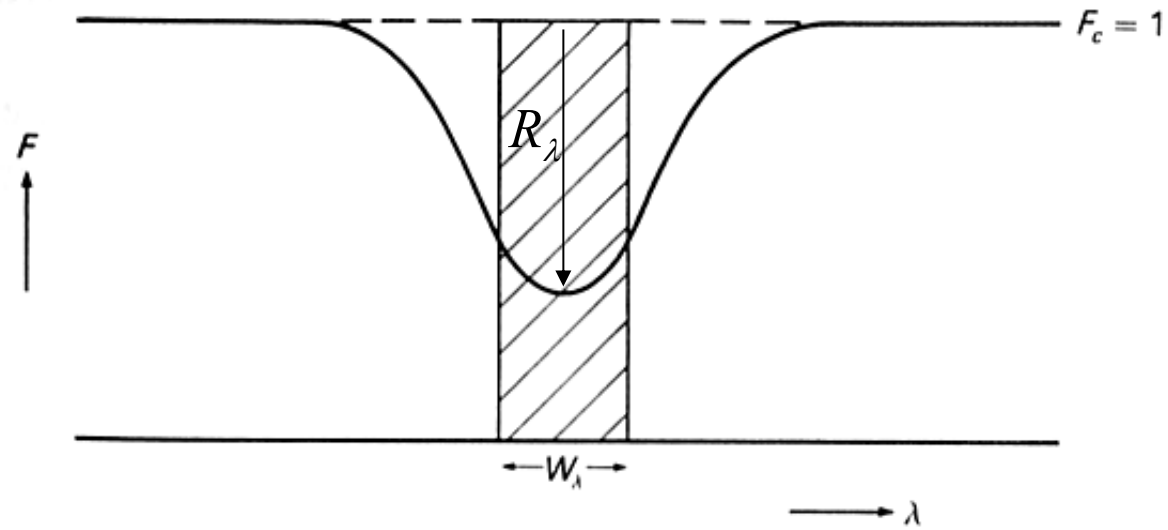

FWHM and FWZI

- Other measures of the line width are the **Full Width at Half Maximum (FWHM)**, the distance between the half line depth from blue to red, i.e. $(\Delta\lambda)_{1/2}$, and the **Full Width at Zero Intensity (FWZI)**,

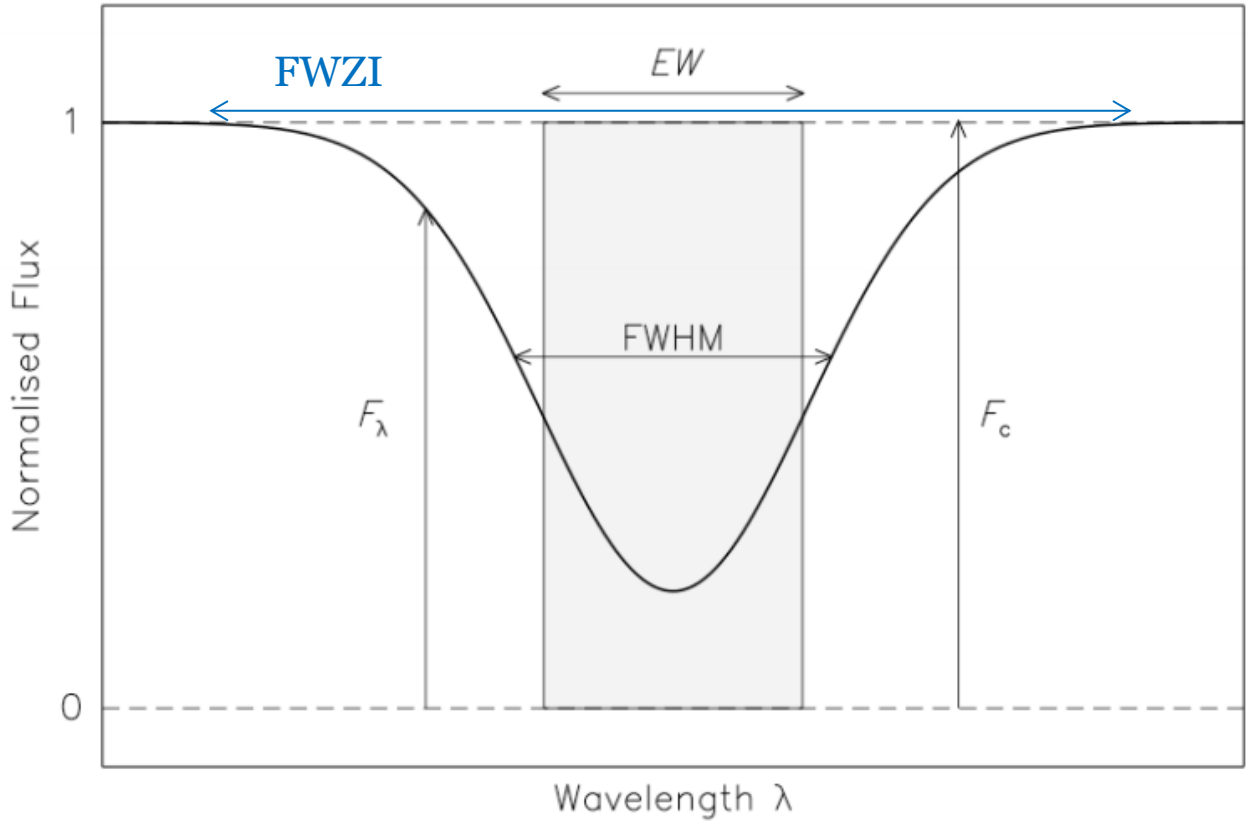

Line core and the wings

- We denote optically (thin) thick lines as those in which the line core is (not) saturated, i.e. reaching zero intensity. In reality, zero intensity is only reached for lines in non-LTE.
- The region close to the centre of the spectral line is referred to as the line core, whilst the wings sweep up the local continuum.

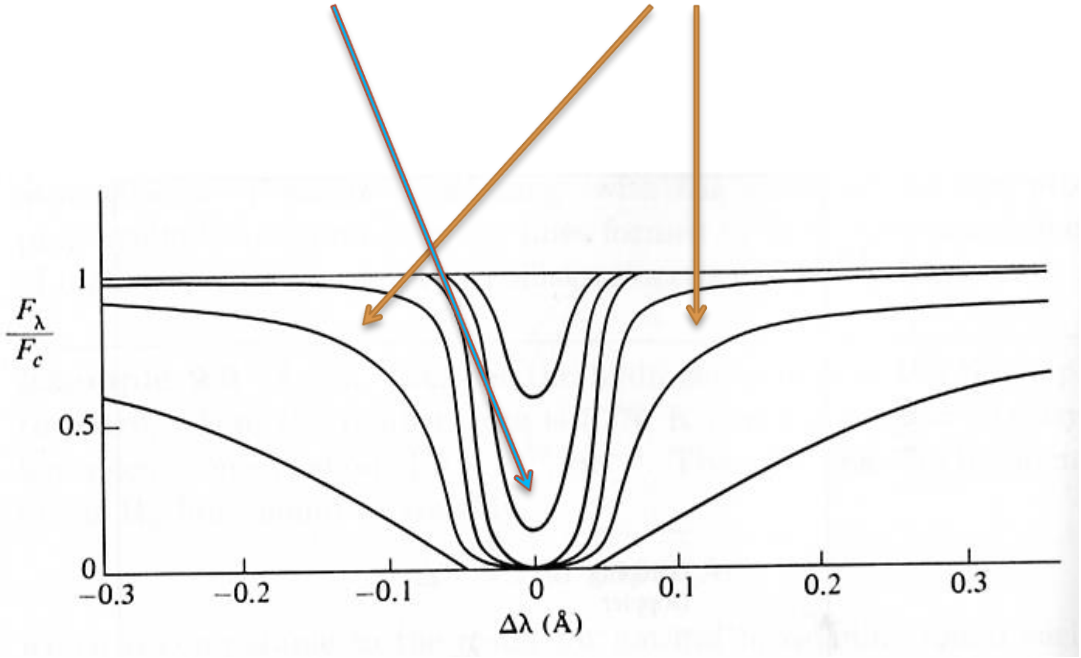

Example: Solar spectrum

λ	Element	W(Å)	Name
4920.51	Fe I	0.43	
4957.61	Fe I	0.45	
5167.33	Mg I	0.65	b_4
5172.70	Mg I	1.26	b_2
5183.62	Mg I	1.58	b_1
5232.95	Fe I	0.35	
5269.55	Fe I	0.41	
5324.19	Fe I	0.32	
5238.05	Fe I	0.38	
5528.42	Mg I	0.29	
5889.97	Na I	0.63	D_2
5895.94	Na I	0.56	D_1
6122.23	Ca I	0.22	
6162.18	Ca I	0.22	
6562.81	H_α	4.02	C
6867.19	O_2	tell	B
7593.70	O_2	tell	A
8194.84	Na I	0.30	
8498.06	Ca II	1.46	
8542.14	Ca II	3.67	
8662.17	Ca II	2.60	
8688.64	Fe I	0.27	
8736.04	Mg I	0.29	

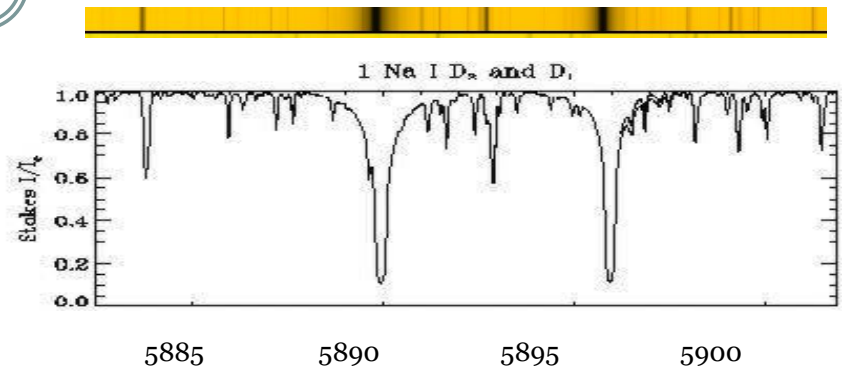

Strong spectral lines in the Solar spectrum typically have equivalent widths $W_\lambda \approx 1$Å, such as the Na I D lines in the yellow. In other stars, line equivalent widths can reach tens or even hundreds of Angstroms. EWs are by definition measured relative to the continuum strength, unlike line fluxes.

Formation of absorption lines

- We obtained earlier that the emergent flux from the stellar surface is π times the Source function at an optical depth of 2/3:

$$F_\lambda(0) = \pi S_\lambda(\tau_\lambda = 2/3) = \pi B_\lambda(T(\tau_\lambda = 2/3))$$

↑ **LTE**

- In spectral lines, the opacity is much larger, thus we see much higher layers at these wavelengths. These layers have a lower temperature and so B_λ is smaller, leading to a smaller F_λ in the line than F_c, the continuum flux in the neighbourhood of the line.

- In the following few lectures, we will study theory of line formation.

Spectral line formation

EINSTEIN COEFFICIENTS

LINE PROFILES: NATURAL BROADENING

BROADENING OF SPECTRAL LINES

NATURAL LINE BROADENING

THERMAL (DOPPLER) BROADENING

CONVOLUTION OF DIFFERENT BROADENING PROCESSES

PRESSURE BROADENING

INGIS-TELLER RELATION

ROTATIONAL AND INSTRUMENTAL BROADENING

Bound-Bound (free-free) transitions

There are 3 basic kinds of line processes associated with bound-bound transitions of atoms or ions:

1. **Direct Absorption**, in which the absorbed photon induces a bound electron to go into a higher energy level.
2. **Spontaneous Emission**, in which an electron in a higher energy level spontaneously decays to lower level, emitting the energy difference as a photon.
3. **Stimulated Emission**, in which an incoming photon induces an electron in a higher energy level to decay to a lower level, emitting in effect a second photon that is nearly identical in energy (and even phase) to the original photon.

The probability that the atom will emit (or absorb) its quantum of energy is described by **Einstein probability coefficients**, written as B_{ij} , A_{ji}, and B_{ji}.

Einstein coefficients

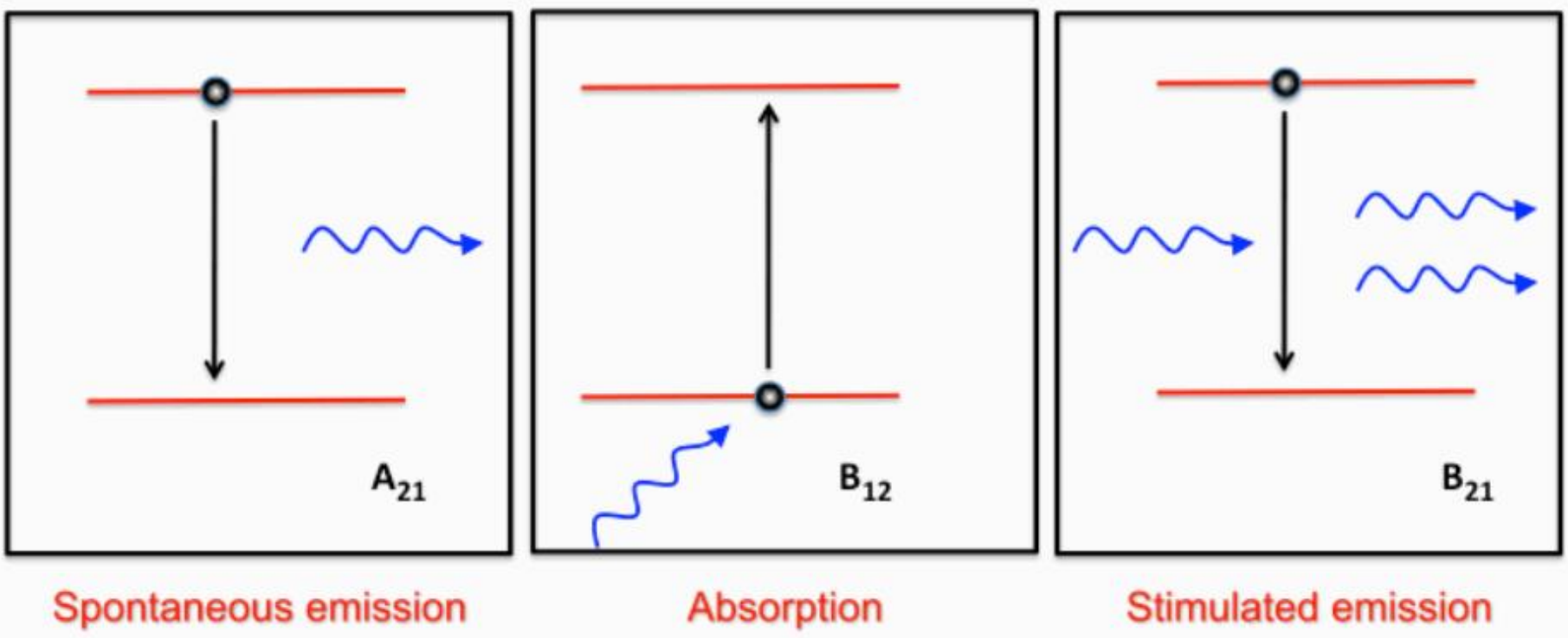

Einstein coefficients concern the probability that a particle spontaneously emits a photon, the probability to absorb a photon, and the probability to emit a photon under the influence of another incoming photon. Einstein's coefficients are valid for all radiation fields.

Spontaneous emission

Consider an upper level u and a lower level l separated by an energy $h\nu$.

- The probability that the atom will spontaneously emit its quantum of energy within a time $\mathrm{d}t$ and in a solid angle $\mathrm{d}\omega$ is $A_{ul}\,\mathrm{d}t\,\mathrm{d}\omega$.
- The proportionality constant, A_{ul}, is the Einstein probability coefficient for spontaneous emission [s^{-1}].
- Occurs independently of the radiation field.
- Emits **isotropically**.

For Hα, $A_{32}=4.4\times10^{7}$ s^{-1}. If at time $t_0=0$ there are $N_u(0)$ atoms in level u, then at time t the population is $N_u(t)=N_u(0)\exp(-A_{ul}\,t)$.

Lifetime = $1/A_{ul}$

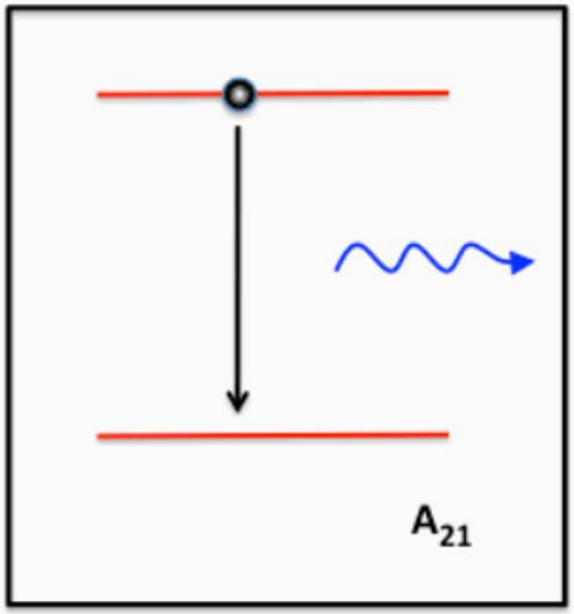

Spontaneous emission

Absorption

Consider an upper level u and a lower level l, separated by an energy $h\nu$.

- Photons with energies *close* to $h\nu$ cause transitions from levels l to u.
- The probability per unit time for this process will evidently be proportional to the mean intensity J_ν at the frequency ν.
- $B_{lu} J$: transition probability of absorption per unit time.
- The proportionality constant B_{lu} is one of the Einstein B-coefficients.

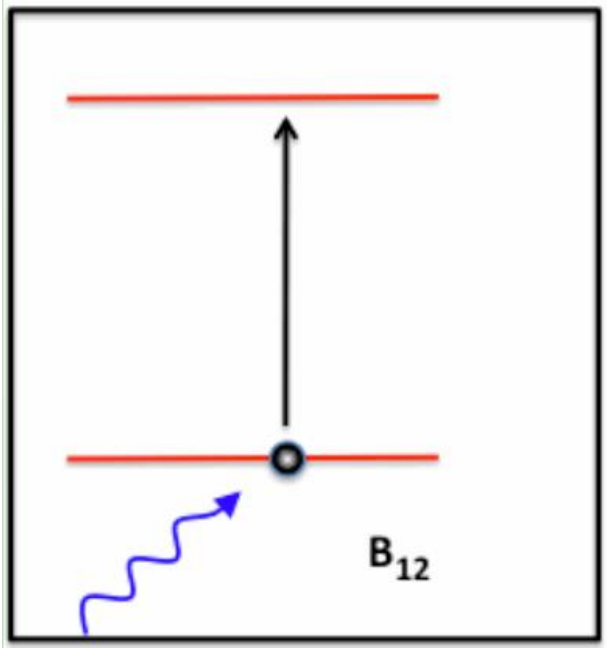

Stimulated emission

Planck's law does **not** follow from considering only spontaneous emission and absorption. Must also include stimulated emission, which like absorption is proportional to the mean intensity J.

- The system goes from an upper level u to a lower level l stimulated by the presence of a radiation field ($h\nu$ corresponding to the energy difference between levels u and l).
- The energy of the emitted photon is the **same** as of the incoming photon (also direction and phase are the same).
- $B_{ul} J$: transition probability of stimulated emission per unit time.
- The proportionality constant B_{ul} is a second Einstein B-coefficient.
- The process of stimulated emission is sometimes referred to as a process of *negative absorption*.
- Stimulated emission occurs into the **same** state (frequency, direction, polarization) as the photon that stimulated the emission.

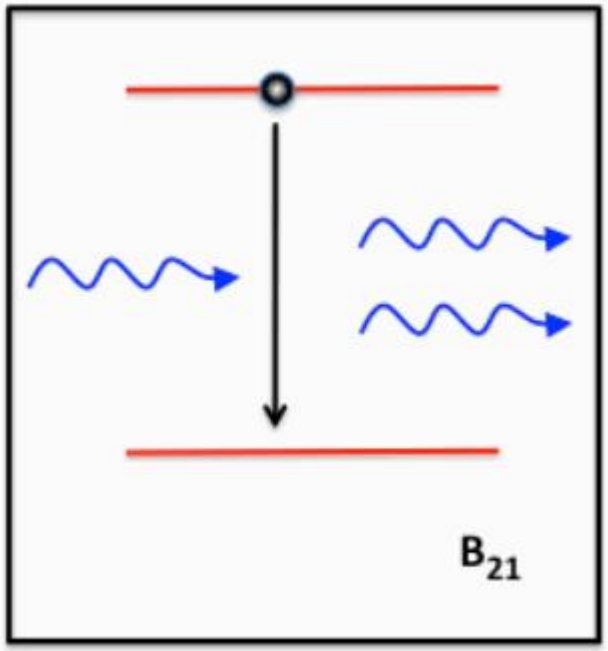

Stimulated emission

Relation between Einstein coefficients

Einstein's Coefficients are not independent. To find a relation between them, let's assume strict Thermodynamic Equilibrium (TE), and, for simplicity, adopt a 2-level approximation.

In TE, each process is in equilibrium with its inverse, i.e., within one line there is no netto destruction or creation of photons (detailed balance)

$$n_1 B_{12} J_\nu = n_2 A_{21} + n_2 B_{21} J_\nu$$

Transitions 1→2 equal to 2→1
n_1, n_2: number density of e^- in levels 1,2

$$J_\nu = \frac{A_{21}/B_{21}}{\left(\frac{n_1}{n_2}\right)\left(\frac{B_{12}}{B_{21}}\right) - 1}$$

Thermodynamic equilibrium:
Boltzmann, $J = B_\nu(T)$

$$\frac{n_1}{n_2} = \frac{g_1}{g_2} e^{h\nu_{21}/kT}$$

Relation between Einstein coefficients

TE: blackbody, J=B$_\nu(T)$

$$B_\nu(T) = \frac{A_{21}/B_{21}}{\left(\frac{g_1 B_{12}}{g_2 B_{21}}\right) e^{h\nu_{21}/kT} - 1}$$

Comparison with Planck blackbody radiation:

$$B_\nu(T) = \frac{A_{21}}{B_{21}}\left(\frac{g_1 B_{12}}{g_2 B_{21}} e^{\frac{h\nu_{21}}{kT}} - 1\right)^{-1} = \frac{2h\nu_{21}^3}{c^2}\left(e^{\frac{h\nu_{21}}{kT}} - 1\right)^{-1}$$

$$\frac{A_{21}}{B_{21}} = \frac{2h\nu_{21}^3}{c^2} \rightarrow A_{21} = B_{21}\frac{2h\nu_{21}^3}{c^2}$$

$$\frac{g_1 B_{12}}{g_2 B_{21}} = 1 \rightarrow g_1 B_{12} = g_2 B_{21}$$

Einstein coefficients

Thus, if one of the Einstein Coefficients is known then two other can be calculated.

Important: The Einstein's coefficients are **atomic constants.**
Although the above relations were derived under the conditions of TE, these relations hold in any non-TE state.

Total amount of absorbed photons per unit time at a given frequency is

$$n_1 B_{12} J_\nu - n_2 B_{21} J_\nu = n_1 B_{12} J_\nu \left(1 - \frac{n_2 B_{21}}{n_1 B_{12}}\right) = n_1 B_{12} J_\nu \underbrace{\left(1 - \frac{g_1 n_2}{g_2 n_1}\right)}$$

Thus, to take into account negative absorption (stimulated emission), one must multiply the number of absorbed photons by

$$\left(1 - e^{-h\nu_{12}/kT}\right)$$

(we already did it before)

Comparison of induced and spontaneous emission

Home work:

- When (at what temperatures, wavelengths) is spontaneous or induced emission stronger?

  Assume LTE (blackbody)

Lifetime of atom in excited state

In the absence of collisions and of any other transitions than the ***ul*** one, the mean lifetime of particles in state ***u*** is **Lifetime = $1/A_{ul}$**

If at time t_0=0 there are $N_u(0)$ atoms in level u, then at time t the population is

$$N_u(t) = N_u(0)e^{-A_{ul}t}.$$

Typical value of A_{ij} is 10^7- 10^8 s^{-1} (for Hα, A_{32}=4.4×10^7 s^{-1}), so lifetime is ~10^{-8} s.

However, not all transitions are allowed, some are strictly ~~forbidden~~!

In practice, strictly forbidden means **very low probability of occurrence** ➔ **Metastable states** at which a lifetime is much longer than of the ordinary excited states but shorter than of the ground state.

Lifetimes at metastable states can reach several hours and even longer!

Forbidden line transitions are noted by placing square brackets around the atomic species in question, e.g. [O III] or [S II]. A semi-forbidden line, designated with a single square bracket, such as C III], occurs where the transition probability is about a thousand times higher than for a forbidden line.

Einstein A-coefficients for Hydrogen

k \ i	1	2	3	4	5	6	7
2	$4{,}67 \cdot 10^8$	—	—	—	—	—	—
3	$5{,}54 \cdot 10^7$	$4{,}39 \cdot 10^7$	—	—	—	—	—
4	$1{,}27 \cdot 10^7$	$8{,}37 \cdot 10^6$	$8{,}94 \cdot 10^6$	—	—	—	—
5	$4{,}10 \cdot 10^6$	$2{,}52 \cdot 10^6$	$2{,}19 \cdot 10^6$	$2{,}68 \cdot 10^6$	—	—	—
6	$1{,}64 \cdot 10^6$	$9{,}68 \cdot 10^5$	$7{,}74 \cdot 10^5$	$7{,}67 \cdot 10^5$	$1{,}02 \cdot 10^6$	—	—
7	$7{,}53 \cdot 10^5$	$4{,}37 \cdot 10^5$	$3{,}34 \cdot 10^5$	$3{,}03 \cdot 10^5$	$3{,}24 \cdot 10^5$	$4{,}50 \cdot 10^5$	—
8	$3{,}85 \cdot 10^5$	$2{,}20 \cdot 10^5$	$1{,}64 \cdot 10^5$	$1{,}42 \cdot 10^5$	$1{,}38 \cdot 10^5$	$1{,}55 \cdot 10^5$	$2{,}26 \cdot 10^5$

Spectral line formation

EINSTEIN COEFFICIENTS

LINE PROFILES: NATURAL BROADENING

BROADENING OF SPECTRAL LINES

NATURAL LINE BROADENING

THERMAL (DOPPLER) BROADENING

CONVOLUTION OF DIFFERENT BROADENING PROCESSES

PRESSURE BROADENING

INGIS-TELLER RELATION

ROTATIONAL AND INSTRUMENTAL BROADENING

Line profiles

All the spectral lines are not monochromatic but have a finite width and a particular profile. Width and shape of a line depend directly on atomic transitions and plasma environment

Energy levels are **not** infinitely sharp. An unavoidable source of broadening is due to the Heisenberg uncertainty principle:

$$dE\ dt \sim h/2\pi$$

dt being the timescale of decay (finite lifetime of energy levels).

In each spectral line, photons of different frequencies (but close to central frequency ν_0) can be absorbed.

Let us call $\varphi(\nu)$ the probability that the transition occurs by emitting or absorbing a photon with energy $h\nu$ (emission or absorption line, $\int \varphi(\nu) d\nu \equiv 1$).

This natural broadening has the form of a Lorentzian function.

Natural Line Width

- A spectral line of an atom is formed by a transition of electron between two energy levels, whose difference yields the frequency of the line.
- The bound-bound absorption problem is analogous to the mechanical system of a damped, driven harmonic oscillator.
- In the classical picture of an atom, we can consider the electron as being bound to the atom. Any force trying to remove it will be counteracted by an opposing force. If a force were to pull on the electron and then let go, it would oscillate with eigenfrequencies $\omega_0=2\pi\nu_0$.
- The scattering cross-section for a *classical oscillator* can be written as

$$\sigma = \frac{8\pi}{3}\frac{e^4}{m_e^2c^4}\left[\frac{\omega^4}{(\omega^2-\omega_0^2)^2+\gamma^2\omega^2}\right] \qquad \omega=2\pi\nu$$

where the classical damping constant $\gamma=2e^2\omega_0{}^2/3m_ec^3=(8\pi^2e^2/3m_ec^3)\nu_0{}^2$

- This is the **Lorentz function** which is sharply peaked around $\omega=\omega_0$.

Lorentz function (1)

$$\sigma_\nu = \frac{8\pi}{3}\frac{e^4}{m_e^2 c^4}\left[\frac{\omega^4}{(\omega^2-\omega_0^2)^2+\gamma^2\omega^2}\right] \qquad \omega=2\pi\nu \quad \gamma = \frac{8\pi^2 e^2}{3m_e^2 c^3}\nu_0^2$$

$$\sigma_\nu = \frac{e^2}{m_e c}\left[\frac{\gamma/4\pi}{(\nu^2-\nu_0^2)^2+(\gamma/4\pi)^2}\right] = \left[\frac{A}{(\nu-\nu_0)^2+(\gamma/4\pi)^2}\right]$$

Note that γ defines the width of the line.

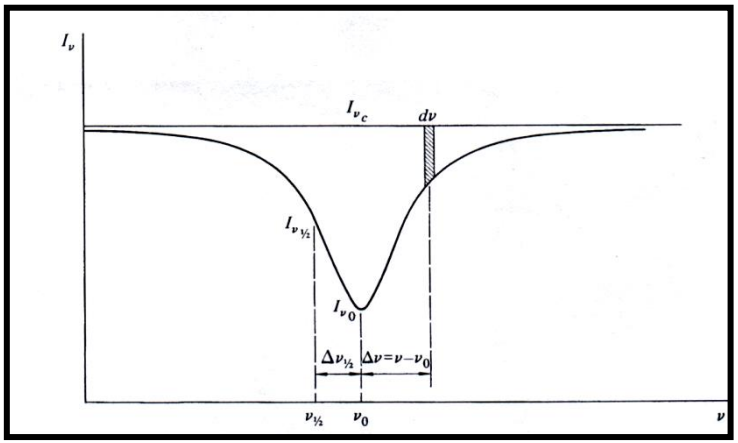

The Classical Damping Line Profile

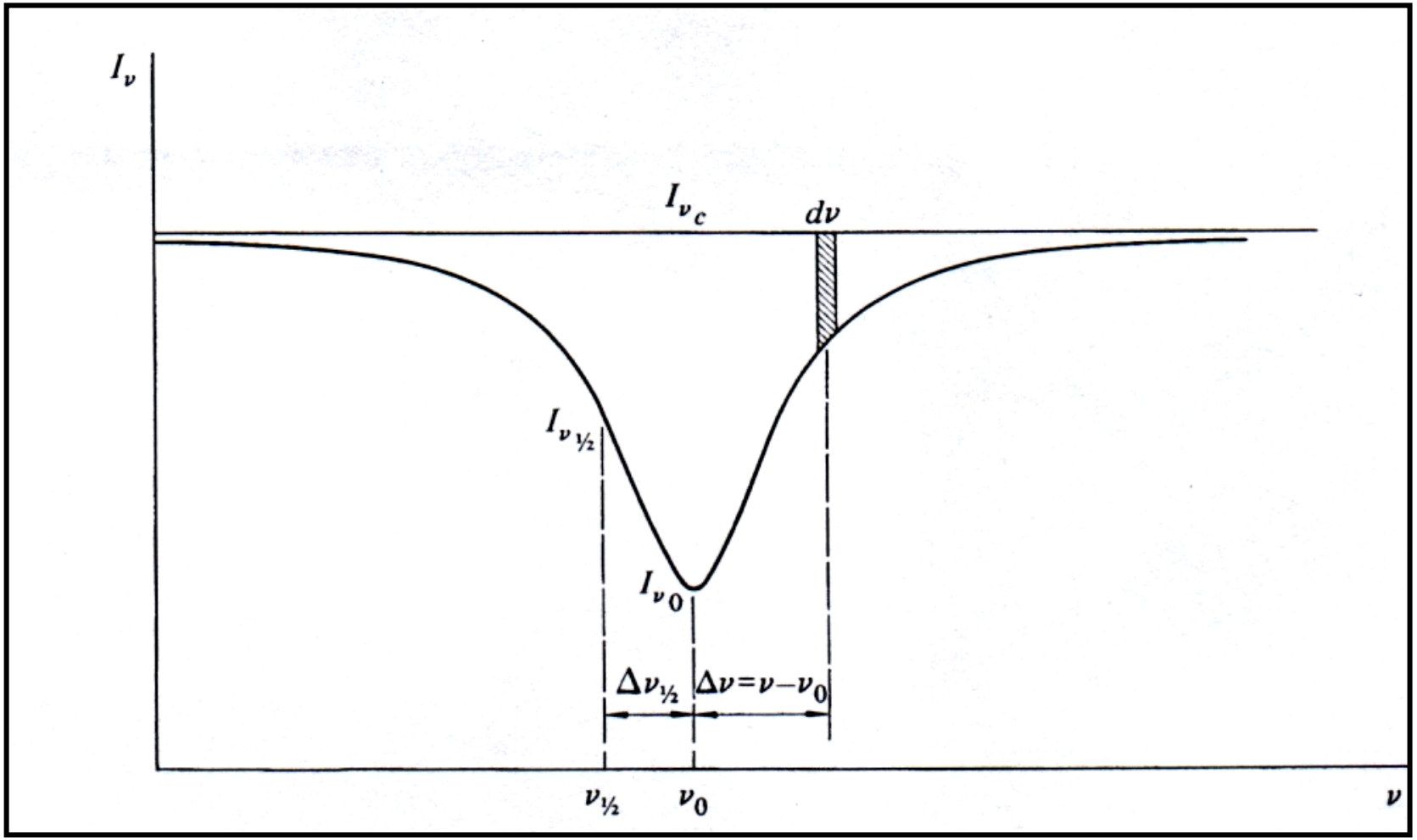

Lorentz function (2)

$\gamma = \frac{8\pi^2 e^2}{3m_e^2 c^3}\nu_0^2$

The Lorentz function $\varphi(\nu) = \left[\frac{A}{(\nu-\nu_0)^2+(\gamma/4\pi)^2}\right]$

is sharply peaked around $\nu = \nu_0$ with a maximum of $\varphi(\nu_0) = A/(\gamma/4\pi)^2$.

To find the full-width at half maximum (FWHM) we find the value of $\nu_{1/2}$ at which the function is ½ its maximum, i.e. $\varphi(\nu_{1/2}) = 1/2\ \varphi(\nu_0)$ and then solve for the FWHM $= \Delta\nu_{1/2} = 2(\nu_{1/2} - \nu_0)$:

$$\frac{1}{2}\frac{A}{(\gamma/4\pi)^2} = \left[\frac{A}{(\nu-\nu_0)^2+(\gamma/4\pi)^2}\right] \qquad (\nu-\nu_0)^2 + (\gamma/4\pi)^2 = 2(\gamma/4\pi)^2$$

we obtain $|\nu_{1/2} - \nu_0| = (\gamma/4\pi)$ $\qquad \Delta\nu_{1/2} = 2(|\nu_{1/2} - \nu_0|) = \boldsymbol{\gamma/2\pi}$

i.e. $(\Delta\lambda)_{1/2} = \frac{\lambda_0^2}{c}(\Delta\nu)_{1/2} = \frac{\lambda_0^2}{c}\frac{\gamma}{2\pi} = \frac{4\pi e^2}{3mc^2} = \frac{4\pi}{3}r_e = 0.00012$ Å

Classical electron radius

FWHM

$$\Delta\nu_{FWHM} = 2(|\nu_{1/2} - \nu_0|) = \gamma/2\pi$$

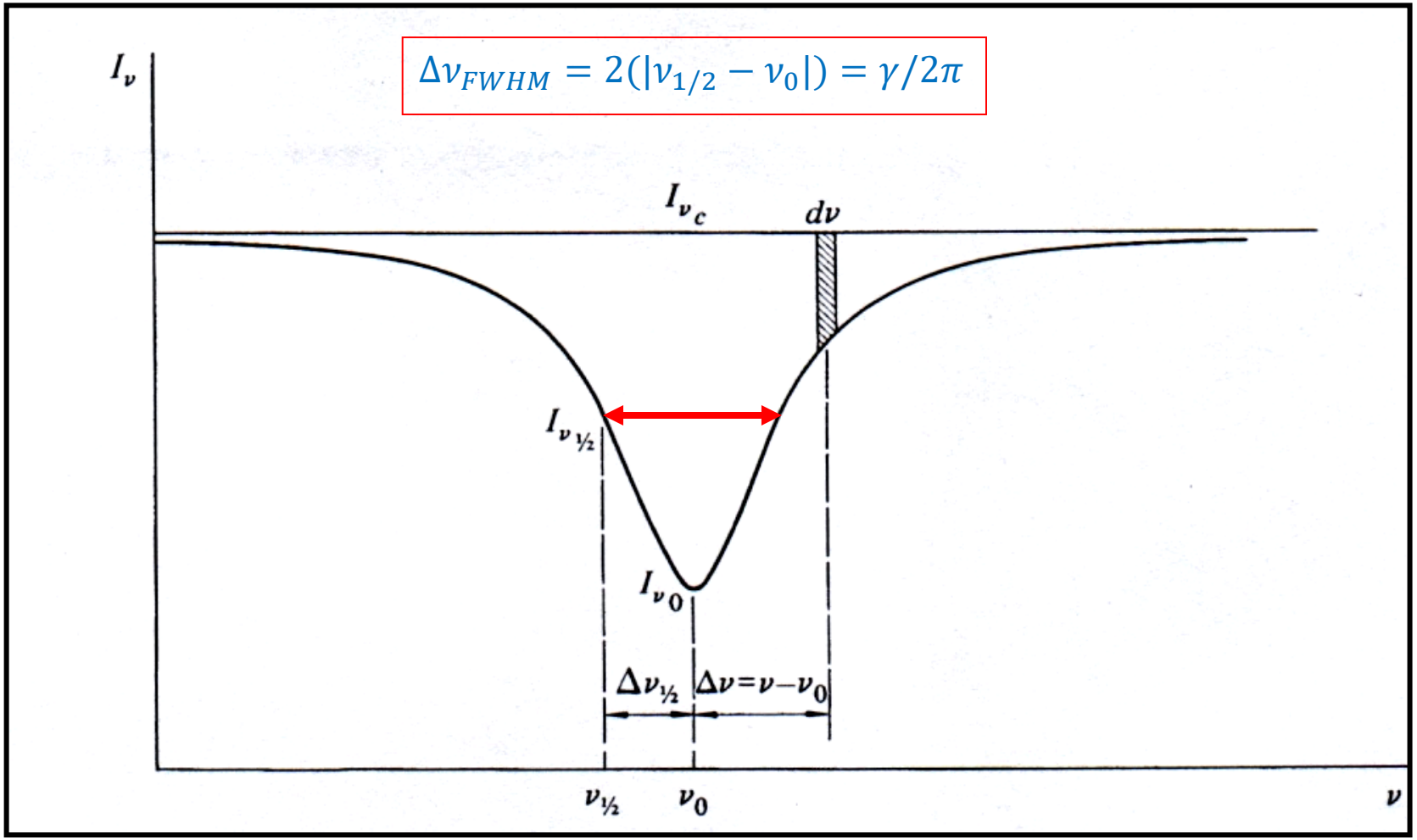

Oscillator Strength

We obtain the "integrated line scattering cross-section" by integrating over all frequencies

$$\sigma_{total} = \int_0^\infty \sigma_\nu d\nu = \frac{e^2}{m_e c} \int_0^\infty \frac{\gamma/4\pi}{(\nu - \nu_0)^2 + (\gamma/4\pi)^2} d\nu = \frac{\pi e^2}{m_e c}$$

This **classical** result predicts a **unique** scattering relation for **all** transitions.

The **quantum-mechanical** treatment shows that line scattering cross-sections may in fact **differ** greatly. The customary way of writing this result is via

$$\sigma_{total} = \frac{\pi e^2}{m_e c} f_{ij}$$

where f_{ij} is the (dimensionless) **oscillator strength** of the transition.

Obtained from lab measurements, the Solar spectrum or quantum mechanical calculations (e.g. Opacity Project), f_{ij} and Einstein A coefficient are related via:

$$A_{ij} = \frac{6.67 \times 10^{15}}{\lambda_{ij}^2(\text{Å})} \frac{g_i}{g_j} f_{ij}$$

f_{ij} for Lyman and Balmer lines

Only for the strongest transitions does f_{ij} approach unity. An electron in the n=2 orbit of H is about 5 times more likely to absorb an Hα photon and make a transition to the n=3 orbit, than it is to absorb an Hβ photon and jump to the n=4 orbit.
For **forbidden** lines, $f_{ij} \ll 1$.

λ (Å)	Line	f_{lu}	g_{low}	g_{up}
1215.7	Ly α	0.41	2	8
1025.7	Ly β	0.07	2	18
972.5	Ly γ	0.03	2	32
6562.8	H α	0.64	8	18
4861.3	H β	0.12	8	32
4340.5	H γ	0.04	8	50

Spectral line formation

201

EINSTEIN COEFFICIENTS

LINE PROFILES: NATURAL BROADENING

BROADENING OF SPECTRAL LINES: THERMAL (DOPPLER) BROADENING

CONVOLUTION OF DIFFERENT BROADENING PROCESSES

PRESSURE BROADENING

INGIS-TELLER RELATION

ROTATIONAL AND INSTRUMENTAL BROADENING

Broadening of spectral lines

There are numerous broadening mechanisms which influence the apparent shape of spectral lines:

microscopic

1. Natural broadening √
2. Thermal broadening √
3. Microturbulence (treated like extra thermal broadening)
4. Collisions (important for strong lines)
5. Isotopic shift, hyperfine splitting (hfs) Zeeman effect

macro

6. Macroturbulence
7. Rotation
8. Instrumental broadening

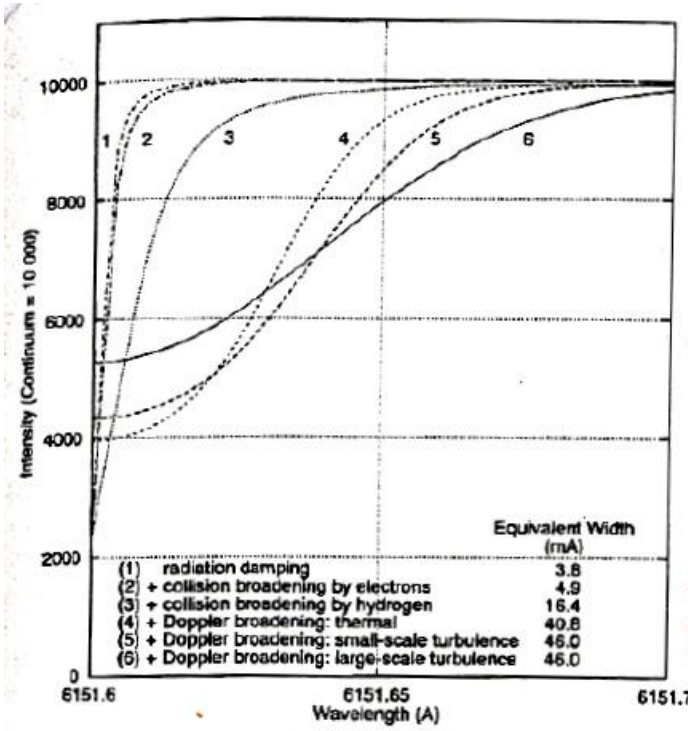

Holweger 1996

Natural Line Broadening (1)

As just noticed above, energy levels of atoms are intrinsically broadened due to the **Heisenberg uncertainty principle**. A decaying state j does not have a perfectly defined energy E_j, but rather a superposition of states spread around E_j.

$$\left.\begin{aligned} \Delta E \Delta t &= h/2\pi \\ E &= h\nu = h\omega/2\pi \end{aligned}\right\} \Rightarrow \Delta\omega\Delta t = 1$$

The longer the atom is in a state (dt high), the more precisely its energy can be measured (dE low).

A large transition probability leads to a short life in the state (low dt) and a large energy uncertainty (high dE).

Thus, the spectral lines are broadened. This type of broadening is called **natural broadening**.

Natural Line Broadening (2)

- The resulting absorption coefficients have the same form as the classical case, except that the classical damping coefficient **γ** is replaced by **Γ**, the Quantum Mechanical damping constant, the sum of all transition probabilities A_{ij} for spontaneous emission.

$$\varphi_\nu = \frac{\Gamma/4\pi}{(\nu - \nu_0)^2 + (\Gamma/4\pi)^2}$$

- φ is the natural or Lorentz profile with FWHM (as before)

$$\Delta\lambda_{1/2} = \frac{\lambda_0^2}{c}\Delta\nu_{1/2} = \frac{\lambda_0^2}{c}\frac{\Gamma}{2\pi} \approx f_{ij} \times 7 \times 10^{-4}\ \text{Å}$$

- Still very small, since f is at most of order unity!

- Clearly other line broadening mechanisms should dominate.

Thermal (Doppler) broadening

- The light emitting atoms in a stellar atmosphere are not at rest but have a thermal motion → Maxwellian velocity distribution.

- Because the particles produce Doppler shifts, the line-of-sight velocities have a distribution that is an important special case for spectroscopy:

$$\frac{dN}{N} = \frac{1}{\sqrt{\pi}} e^{-(v_r/v_{th})^2} \frac{dv_r}{v_{th}}$$

where v_r is the radial (line of sight) velocity component, and v_{th} is the most probable velocity $v_{th} = \sqrt{2kT/m}$

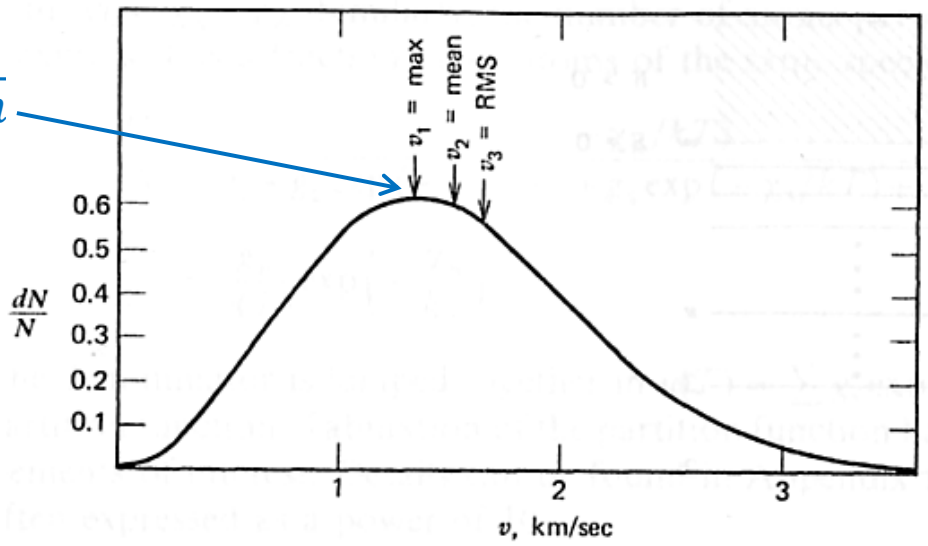

- The frequency (wavelength) shift (linear Doppler effect) is related to v_r:

$$\frac{\Delta\lambda}{\lambda_0} = \frac{\Delta\nu}{\nu_0} = \frac{v_r}{c}$$

Doppler broadening

- The distribution of $\Delta\lambda$ or $\Delta\nu$ values gives us the shape of the absorption coefficient.
- Integrating the Maxwell distribution over all velocities, we obtain

$$\varphi(\nu) = \frac{\nu_0}{c\sqrt{\pi}\Delta\nu_D}\exp[-(\nu-\nu_0)^2/\Delta\nu_D^2]$$

substituting $v_r = \frac{\nu-\nu_0}{\nu_0}c$ and $\Delta\nu_D = \frac{\nu_0}{c}v_{th} = \frac{\nu_0}{c}\sqrt{\frac{2kT}{m}}$ (the Doppler width)

- With $\int_0^\infty \phi(\nu) = 1$, we obtain the Gaussian line profile in terms of the Doppler width :

$$\varphi(\nu) = \frac{1}{\sqrt{\pi}\Delta\nu_D}e^{-(\nu-\nu_0)^2/\Delta\nu_D^2}$$

Again, the maximum is at ν_0. Temperature dependency: $\Delta v_{\text{th}} \sim \sqrt{T}$

Doppler broadening (FWHM)

- We can again obtain the line FWHM via $\nu=\nu_{1/2}$ where

  $\varphi\ (\nu_{1/2})=1/2\ \varphi\ (\nu_0)$ and then solve for the FWHM $= \Delta\nu_{1/2}=2(\nu_{1/2}-\nu_0)$

- This implies that $2 = \exp[\ (\nu_{1/2}-\nu_0)^2/\Delta\nu_D^2]$ or $(\nu_{1/2}-\nu_0)^2 = \Delta\nu_D^2 \ln 2$

- Finally,
  $\Delta\nu_{1/2} = 2(\nu_{1/2}-\nu_0) = 2\Delta\nu_D\sqrt{\ln 2} = 1.67\Delta\nu_D = 2.139\times10^{12}\sqrt{(T/\mu)}/\lambda_0(\text{Å})$ Hz

  (μ is the atomic mass)

- In wavelength units $\Delta\lambda_{1/2} = \frac{\lambda_0^2}{c}\Delta\nu_{1/2} = 7.1\times10^{-7}\lambda_0(\text{Å})\sqrt{(T/\mu)}$ Å

Doppler broadening (example)

- For the Sun, with T~6000K at Hα:

$$\Delta\nu_{1/2} = 2.139 \times 10^{12}\sqrt{(T/\mu)}/\lambda_0(\text{Å}) =$$

μ=1

i.e. in wavelength units $\Delta\lambda_{1/2} = \frac{\lambda_0^2}{c}\Delta\nu_{1/2} = 7.1 \times 10^{-7}\lambda_0(\text{Å})\sqrt{(T/\mu)}$ Å=

Doppler broadening (example)

- For the Sun, with T~6000K at Hα:

$$\Delta\nu_{1/2} = 2.139\times10^{12}\sqrt{(T/\mu)}/\lambda_0(\text{Å}) = 2.139\times10^{12}\sqrt{6000/1}/6563 = 25.2\ \text{GHz}$$

i.e. in wavelength units $\Delta\lambda_{1/2} = \frac{\lambda_0^2}{c}\Delta\nu_{1/2} = \frac{(6563\times10^{-8})^2}{3\times10^8}25.2\times10^9 = 0.36\ \text{Å}$

or velocity units: $\Delta v_{1/2} = c\frac{\Delta\lambda_{1/2}}{\lambda_0} = 3\times10^5\ \text{km/s}\frac{0.36}{6562} = 16.5\ \text{km/s}$

- This is much larger than the natural damping width of the line (10^{-4} Å), but still relatively small relative to some pressure broadening mechanisms (will discuss later).
- The atomic mass dependence in the denominator implies **smaller** line widths for metallic lines, e.g. a factor of $(56)^{1/2}$ smaller for iron lines having wavelengths close to Hα.

Spectral line formation

EINSTEIN COEFFICIENTS

LINE PROFILES: NATURAL BROADENING

BROADENING OF SPECTRAL LINES

NATURAL LINE BROADENING:

THERMAL (DOPPLER) BROADENING

CONVOLUTION OF DIFFERENT BROADENING PROCESSES

PRESSURE BROADENING

INGIS-TELLER RELATION

ROTATIONAL AND INSTRUMENTAL BROADENING

Natural and Thermal Broadenings

From above:

- Natural Line Broadening: $\varphi_\nu = \dfrac{\Gamma/4\pi}{(\nu-\nu_0)^2 + (\Gamma/4\pi)^2}$ $\qquad \Gamma = \sum_{i<j} A_{ji}$

Lorentzian profile with FWHM $\qquad \Delta\lambda_{1/2} = \dfrac{\lambda_0^2}{c}\Delta\nu_{1/2} = \dfrac{\lambda_0^2}{c}\dfrac{\Gamma}{2\pi} \approx f_{ij} \times 7 \times 10^{-4}\text{Å}$

- Doppler broadening $\qquad \varphi(\nu) = \dfrac{1}{\sqrt{\pi}\Delta\nu_D} e^{-(\nu-\nu_0)^2/\Delta\nu_D^2}$ $\qquad \Delta\nu_D = \dfrac{\nu_0}{c} v_{th} = \dfrac{\nu_0}{c}\sqrt{\dfrac{2kT}{m}}$

Gaussian line profile with FWHM $\qquad \Delta\lambda_{1/2} = \dfrac{\lambda_0^2}{c}\Delta\nu_{1/2} = 7.1 \times 10^{-7}\lambda_0(\text{Å})\sqrt{(T/\mu)}$ Å

$$\Delta\nu_{1/2} = 1.67\Delta\nu_D$$

Comparing broadenings

- Thermal (Doppler):
  - $\Delta\lambda_{th}$=0.02 Å (at λ_o=5000 Å, T=6000K, Fe)
  - $\Delta\lambda_{th}$=0.5 Å (at λ_o=5000 Å, T=50000K, H)
- Radiation damping:
  - $\Delta\lambda_{FWHM}$=a few $\times 10^{-4}$ Å

- **But:** decline of Gauss profile in wings is much steeper than for Lorentz profile:

$$\text{Gauss}\,(10\Delta\lambda_{th}) \quad : \quad e^{-10^2} \approx 10^{-43}$$

$$\approx$$

$$\text{Lorentz}\,(1000\Delta\lambda_{rad}) : \; 1/1000^2 \approx 10^{-6}$$

- In the line **wings** the **Lorentz** profile is **dominant**

Broadening mechanisms profiles

- Different broadening mechanisms have the form of
  - A Lorentzian function (natural profile and broadening, some pressure brodenings)
  - A Gaussian function (thermal broadening, instrumental broadening, etc.)
  - Other functions are possible (e.g., Linear Stark broadening)
- Generally, we have to consider both (all) types of profiles. For example, the pressure damping profile is negligible in the line core, but the Doppler profile decreases very steeply in the wings, whilst the damping profile decreases only as $1/\Delta\lambda^2$
- The Gaussian dominates the line core (or is confined to it), while the Lorentzian profile dominates in the line wings out to several times the FWHM.

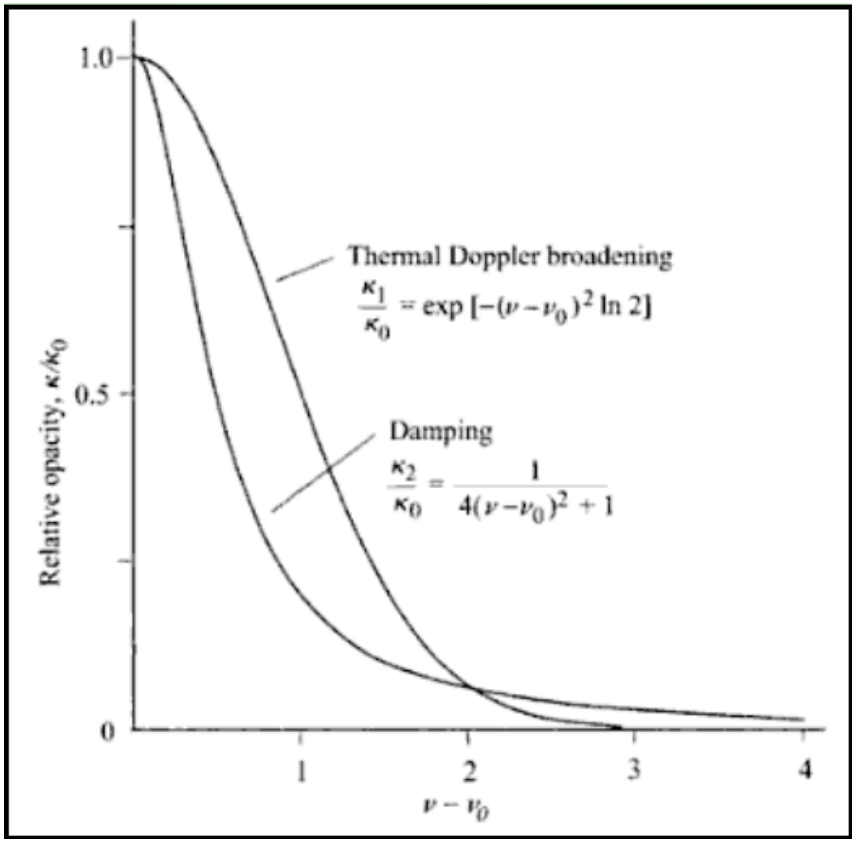

Joint effect of different mechanisms

Mathematically: **convolution**

$$(f_A * f_B)(x) = \int_{-\infty}^{\infty} f_A(y) f_B(x-y) dy$$

Properties:

- commutative: $f_A * f_B = f_B * f_A$

- Fourier transformation: $F(f_A * f_B) = normfactor \cdot F(f_A) \cdot F(f_B)$
  where F denotes the Fourier transform of f.

i.e., in Fourier space the convolution is a multiplication

Application to profile functions

Convolution of two Gaussian profiles

$$G_A(x) = \frac{1}{A\sqrt{\pi}}\ e^{-\frac{x^2}{A^2}} \qquad G_B(x) = \frac{1}{B\sqrt{\pi}}\ e^{-\frac{x^2}{B^2}}$$

$$G_C(x) = G_A(x) * G_B(x) = \frac{1}{C\sqrt{\pi}}\ e^{-\frac{x^2}{C^2}} \quad \text{with} \quad C^2 = A^2 + B^2$$

Result: Gauss profile with **quadratic summation** of half-widths.

Convolution of two Lorentzian profiles (e.g., radiation + collisional damping)

$$L_A(x) = \frac{A/\pi}{x^2 + A^2} \qquad L_B(x) = \frac{B/\pi}{x^2 + B^2}$$

$$L_C(x) = L_A(x) * L_B(x) = \frac{C/\pi}{x^2 + C^2} \quad \text{with} \quad C = A + B$$

Result: Lorentz profile with **sum** of half-widths

Voigt profile

Convolving Gauss and Lorentz profile (e.g. thermal + natural broadening)

$$G(\nu) = \frac{1}{\Delta\nu_D\sqrt{\pi}}\, e^{-\frac{(\nu-\nu_0)^2}{\Delta\nu_D{}^2}} \qquad L(\nu) = \frac{\gamma/4\pi^2}{(\nu-\nu_0)^2 + (\gamma/4\pi)^2}$$

$V = G * L$ depends on $\nu, \Delta\nu, \gamma, \Delta\nu_D$: $V(\nu) = \int_{-\infty}^{\infty} G(\nu')\, L(\nu-\nu')d\nu'$

Transformation: $\mathrm{v} := \frac{(\nu-\nu_0)}{\Delta\nu_D}$ $\quad a := \gamma/(4\pi\Delta\nu_D)$ $\quad y := \frac{(\nu'-\nu_0)}{\Delta\nu_D}$

$$G(y) = \frac{1}{\Delta\nu_D\sqrt{\pi}}\, e^{-y^2} \qquad L(y) = \frac{a/\Delta\nu_D\pi}{y^2+a^2} \qquad V = \frac{1}{\Delta\nu_D\sqrt{\pi}}\frac{a}{\pi}\int_{-\infty}^{\infty}\frac{e^{-y^2}}{(\mathrm{v}-y)^2+a^2}dy$$

Def: $\boldsymbol{V = \frac{1}{\Delta\nu_D\sqrt{\pi}}H(a,\mathrm{v})}$ with $H(a,\mathrm{v}) = \frac{a}{\pi}\int_{-\infty}^{\infty}\frac{e^{-y^2}}{(\mathrm{v}-y)^2+a^2}dy$

Voigt function, no analytical representation possible.
(approximate formulae or numerical evaluation)

Normalization: $\int_{-\infty}^{\infty} H(a,\mathrm{v})d\mathrm{v} = \sqrt{\pi}$

The Voigt func for various *a* (1)

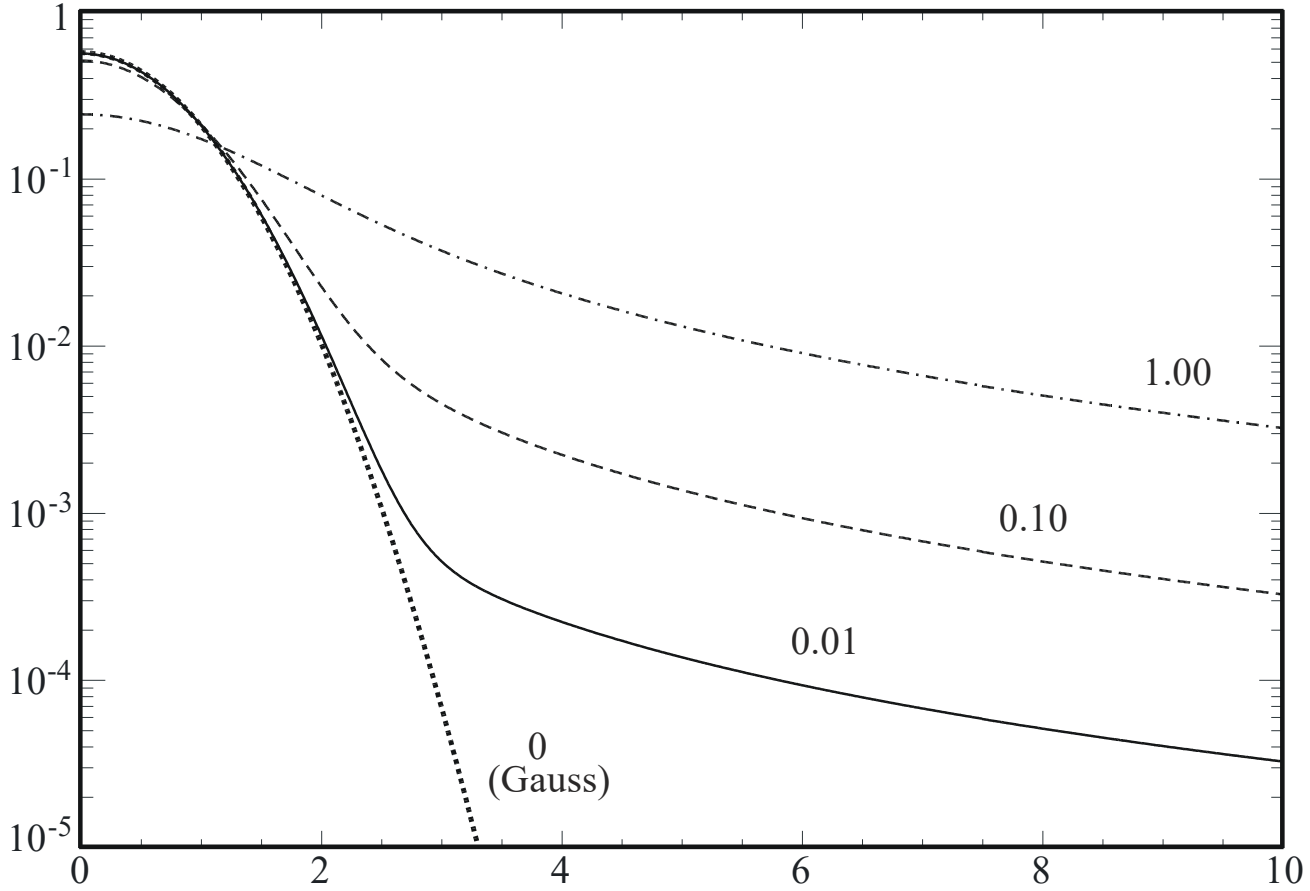

The final form of the combined **Voigt** profile depends on $\alpha = 2\pi a = \gamma/2\Delta\nu_D$, the ratio of the damping widths $\gamma/2$ to the Doppler width $\Delta\nu_D$

As **a rule of thumb**, the damping wings start to contribute a distance $-(\log \alpha)\Delta\lambda_D$ from the line centre

The Voigt func for various *a* (2)

Voigt profiles

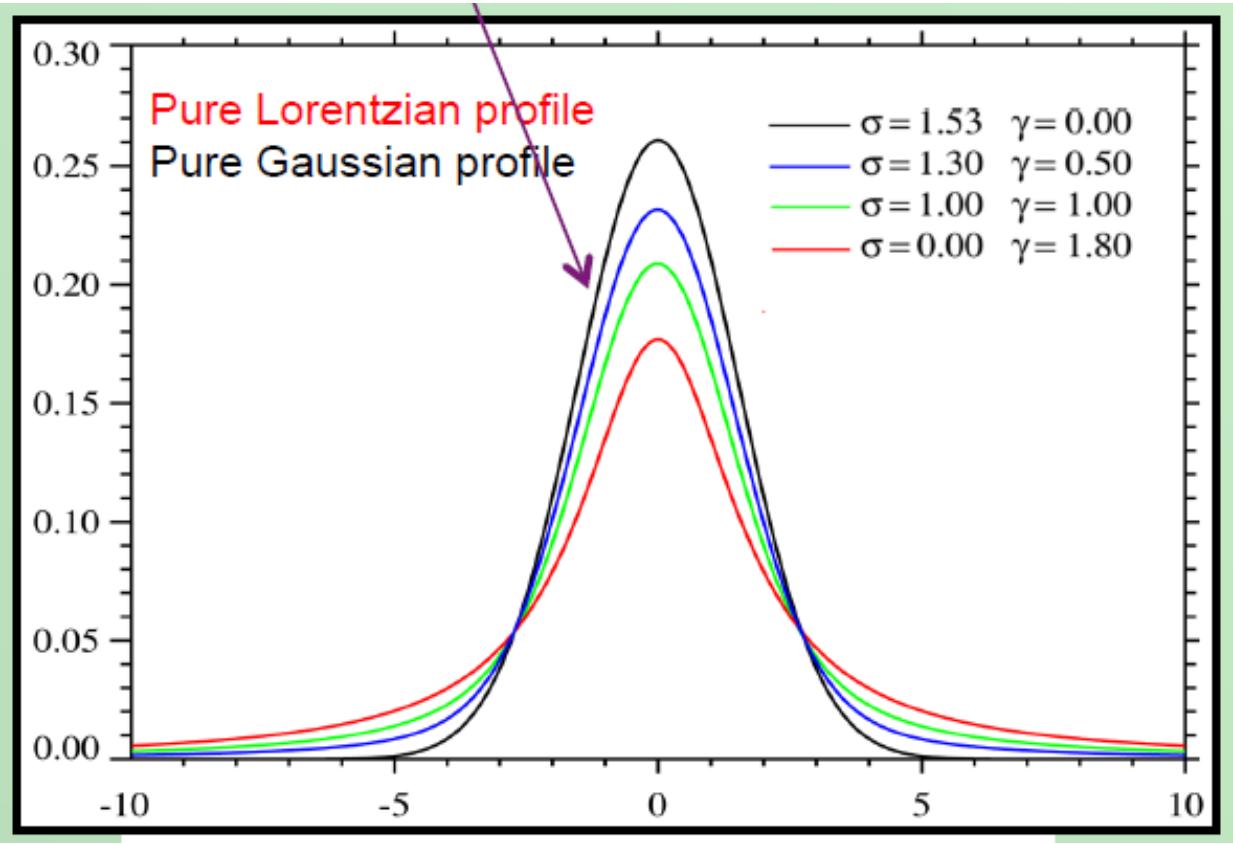

The final form of the combined **Voigt** profile depends on $\alpha = 2\pi a = \gamma/2\Delta\nu_D$, the ratio of the damping widths $\gamma/2$ to the Doppler width $\Delta\nu_D$

As **a rule of thumb**, the damping wings start to contribute a distance $-(\log \alpha)\Delta\lambda_D$ from the line centre

Calculation of a Voigt profile

No analytical representation is possible, but…

- IDL:
  IDL> u=findgen(201)/40.-2.5
  IDL> v=voigt(0.5,u)
  IDL> plot,u,v

- Python

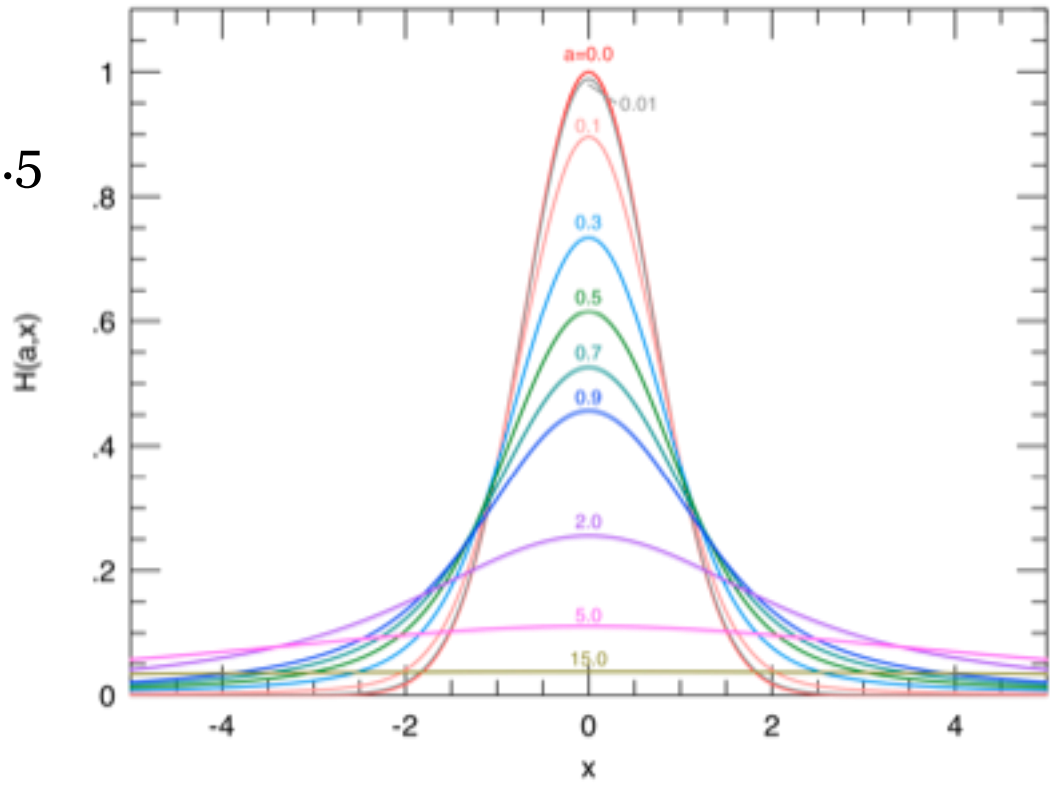

Spectral line formation

220

EINSTEIN COEFFICIENTS
LINE PROFILES: NATURAL BROADENING
BROADENING OF SPECTRAL LINES
NATURAL LINE BROADENING:
THERMAL (DOPPLER) BROADENING
CONVOLUTION OF DIFFERENT BROADENING PROCESSES
PRESSURE BROADENING
INGIS-TELLER RELATION
ROTATIONAL AND INSTRUMENTAL BROADENING

Other broadening mechanisms

There are numerous broadening mechanisms which influence the apparent shape of spectral lines:

microscopic

1. Natural broadening √
2. Thermal broadening √
3. Microturbulence √
   (treated like extra thermal broadening)
4. Collisions (important for strong lines)
5. Isotopic shift, *hfs*, Zeeman effect

macro

6. Macroturbulence
7. Rotation
8. Instrumental broadening

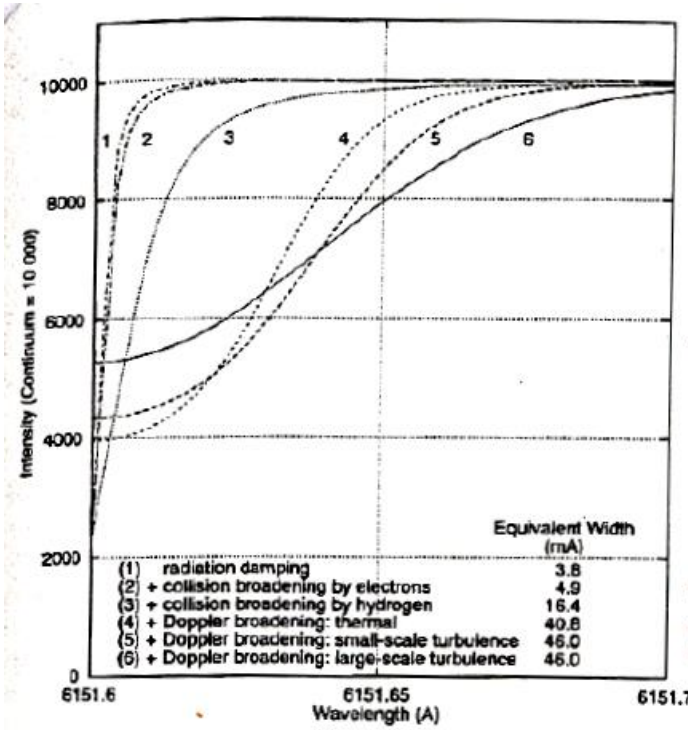

Holweger 1996

Collisional and Pressure broadening

- The orbitals of an atom can be perturbed in a collision with a neutral atom (collisional broadening) or encounter with the electric field of an ion (pressure broadening).

Direct collisions?

- Collisions in the gas de-excite atoms before they naturally decay, shortening its lifetime.
- The resulting line profile is Lorenzian (as with natural broadening) with a width of $\nu_{1/2}=1/(\pi t)$ where t is the time between collisions.
- The number of collisions (per second) is the number of perturbers in the volume swept out by the atom, i.e. $N\sigma v$. Since $\frac{1}{2}mv^2=3/2\ kT$, the time between collisions is

$$t \approx 1/(N\sigma\sqrt{3kT/m})$$

- So, the FWHM in terms of pressure ($P=NkT$) is:

$$\Delta\nu_{1/2}(\mathrm{Hz}) = P\sigma/\pi\sqrt{3/kTm} = 3.6\times10^{19}P\sigma/\sqrt{mT/m_H}$$

- For the Sun (T=5800K, P=10^5 dyne/cm^2),
  H atom *direct* collisions ($\sigma=\pi a_0^2=8\times10^{-17}$ cm^2) cause $\Delta\nu_{1/2} = 4$ MHz
  i.e. **less than the natural width**

$$\Delta\lambda_{1/2} = \frac{\lambda_0^2}{c}\Delta\nu_{1/2} = 5\times10^{-5}\ \text{Å}$$

Impact broadening

- Nevertheless, the impact approximation can be used for some broadening mechanisms, which are important since atoms can interact without direct collision.

- The change in energy induced by the collision is a function of the separation $\boldsymbol{r}$ between the absorber and perturbing particle, and can be approximated by a power law of the form $\Delta E \sim \text{Constant} \times r^{-n}$ where n is an integer, such that the change in frequency is $\Delta\nu = \Delta E/h = C_n r^{-n}$

  Constants C_n are determined by laboratory measurements, or calculations.

Pressure broadening (1)

$$\Delta\nu = \frac{C_n}{r^n}$$

n =	name	interaction of
2	linear Stark effect	hydrogen-like ions + p, e
3	resonance broadening	neutral atoms with each other, H+H
4	quadratic Stark effect	ions + e, p
6	van der Waals broadening	metals + H

Two approximations exist – impact broadening for $n>2$ (n=3 resonance, n=4 quadratic Stark effect, n=6 van der Waals) and a quasi-static approximation (i.e. surrounding particles are nearly at rest; for linear Stark broadening, n=2).

Pressure broadenings…

The orbitals of an atom can be perturbed in a collision with a neutral atom or encounter with the electric field of an ion.

n =	name	interaction of
2	linear Stark effect	hydrogen-like ions + p, e
3	resonance broadening	neutral atoms with each other, H+H
4	quadratic Stark effect	ions + e, p
6	van der Waals broadening	metals + H

resonance broadening (n=3)
quadratic Stark effect (n=4)
van der Waals broadening (n=6)

} impact broadening approximations

Lorentz profile

$$\Delta\nu = \frac{C_n}{r^n}$$

(Ansatz): constants C_n are determined by laboratory measurements, or calculations → Let‘s discuss in a bit more detail

Additional material for self-study

Collisional Broadening

- Frequency of collisions = $1/T_0$
- Suppose collisions occur if particles pass within distance = impact parameter ρ_0

$$\frac{1}{T_0} = N\pi\rho_0^2 v$$

N = #perturbers/cm^3, v = relative velocity cm/s

- Then damping parameter is

$$\Gamma = 2N\pi\rho_0^2 v$$

We used $\sigma=\pi a_0^2$ for direct collisions

Weisskopf approximation (1)

- perturber is a classical particle
- path is a straight line
- no transitions caused in atom
- interaction creates a phase shift or frequency shift given by

$$\Delta\omega = \frac{C_p}{r^p}$$

- p exponents of astronomical interest: 3,4,6

Weisskopf approximation (2)

Total phase shift

$$\eta(\rho) = C_p \int_{-\infty}^{+\infty} \frac{dt}{r^p} = C_p \int_{-\infty}^{+\infty} \frac{dt}{[\rho^2 + v^2 t^2]^{p/2}} = \frac{C_p}{v\rho^{p-1}} \psi_p$$

$$\psi_p = \sqrt{\pi}\, \frac{\Gamma[(p-1)/2]}{\Gamma[p/2]}$$

p	ψ_p
2	π
3	2
4	π/2
6	3π/8

$$r(t) = [\rho_0^2 + v^2 t^2]^{1/2}$$

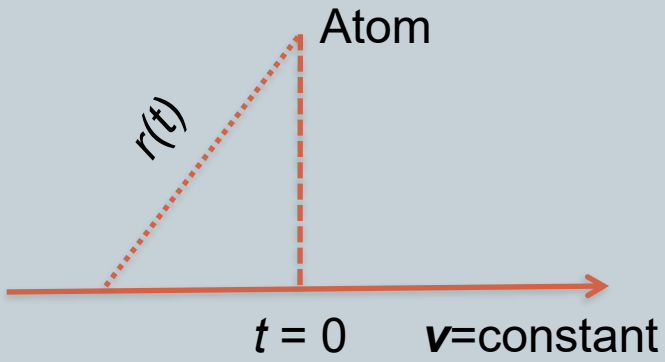

perturber path

Weisskopf approximation (3)

- Assume that only collisions that produce a phase shift $> \eta_0$ are effective in broadening:
  then impact parameter is

$$\rho_0 = \left(\frac{C_p \psi_p}{\eta_0 v} \right)^{\frac{1}{p-1}}$$

- Weisskopf assumed $\eta_0 = 1$, yields damping

$$\Gamma_W = 2\pi N v \left(\frac{C_p \psi_p}{v} \right)^{\frac{2}{p-1}}$$

  depends on ρ, T

- Ignores weak collisions $\eta < \eta_0$

Better Impact Model: Lindholm-Foley

- Includes effects of multiple weak collisions, which introduce a phase shift $\Delta\omega_o$; $\Gamma_{LF} > \Gamma_W$

$$I(\omega) = \frac{\Gamma/(2\pi)}{(\omega - \omega_0 - \Delta\omega_0)^2 + (\Gamma/2)^2}$$

p	3	4	6
Γ	$2\pi^2 C_3 N$	$11.37\, C_4^{2/3} v^{1/3} N$	$8.08\, C_6^{2/5} v^{3/5} N$
$\Delta\omega_0$	0	$9.85\, C_4^{2/3} v^{1/3} N$	$2.94\, C_6^{2/5} v^{3/5} N$

- Impact theory fails for small ρ

Additional material for self-study

Impact broadenings (n=3,4,6)

- **Resonance Broadening** (n=3) occurs between identical species, restricted to upper/lower level having an electric dipole transition to ground state (resonance line):

$$\Delta\lambda_{1/2} = 8.6\text{x}10^{-30}(g_i / g_k)^{1/2}\lambda^2\lambda_{res}f_{res}N_i$$

- **Quadratic Stark broadening** (n=4): Interaction of electron or proton with a system without dipole moment. The frequency shift depends on the square of the local electric field generated by passing electrons. With C_4 a constant obtained from laboratory data,

$$\log\gamma_4 = 19 + \frac{2}{3}\log C_4 + \log P_e - \frac{5}{6}\log T$$

- **Van der Waals broadening** (n=6): A momentary dipole on one neutral atom induces a change in lifetime, by inducing a dipole on the other. Because of its overwhelming abundance, **neutral H** acts as a perturber. For C_6 a constant (excitation and ionization dependent),

$$\log\gamma_6 = 19.6 + \frac{2}{5}\log C_6 + \log P_g - \frac{7}{10}\log T$$

Additional material for self-study

Example

A comparison of quadratic Stark and van der Waals broadening for the Na I 5890 line at various optical depths in the Sun.

The latter dominates here, and greatly exceeds the natural width by a factor of about 30.

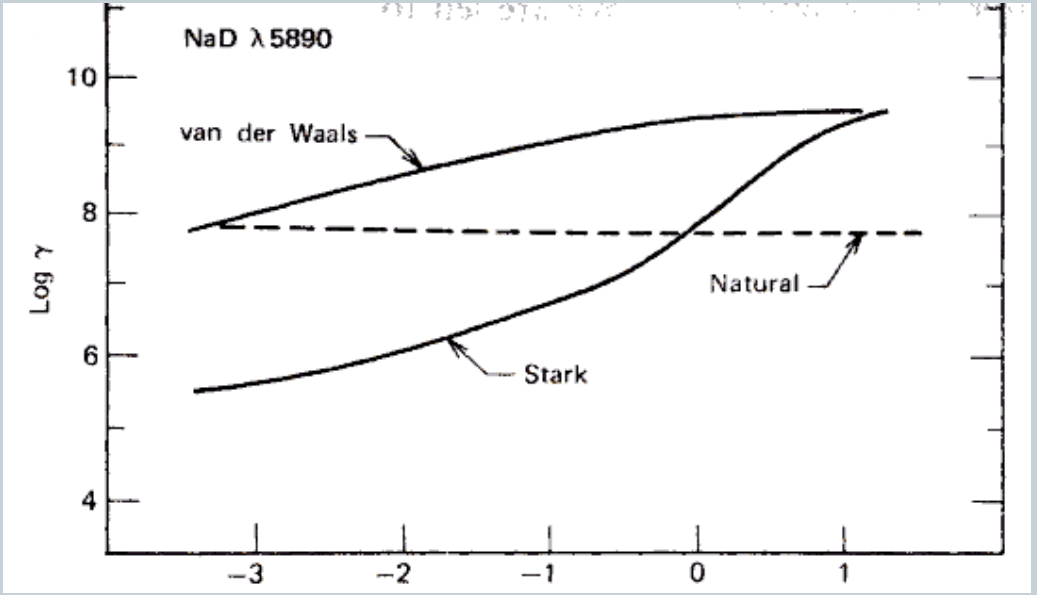

In general,

- **Quadratic Stark broadening** (n=4) affects most lines in **hot stars** since **electron** pressure approaches gas pressure.
- **Van der Waals broadening** (n=6) affects most lines in **cool stars** since this involves interactions between **neutral atoms**

Linear Stark broadening (n=2)

- Atoms do **not** generally have permanent electric dipole moments. If there were such a moment, the Stark effect would be *linear*. Such a moment can occur only for two or more levels of the same energy (they are degenerate) but different orbital quantum numbers. This happens only for single electron atoms (H, He^{+}, Li^{2+}, ...).

- The frequency shift depends on the local electric field generated by passing electrons.

- Unfortunately, impact theory is no longer satisfactory and we have to consider the distribution of electric fields. In the star there is no a uniform field – there is an average field distribution felt by an average atom (**statistical** Stark effect). This distribution is called the Holtsmark distribution.

Holtsmark Statistical Theory

- Ensemble of perturbers instead of single
- more particles, more chances for strong field
- e- attracted to ions, reduce perturbation by Debye shielding
- in stellar atmospheres density is low, number of perturbers is large, and Holtsmark distribution is valid

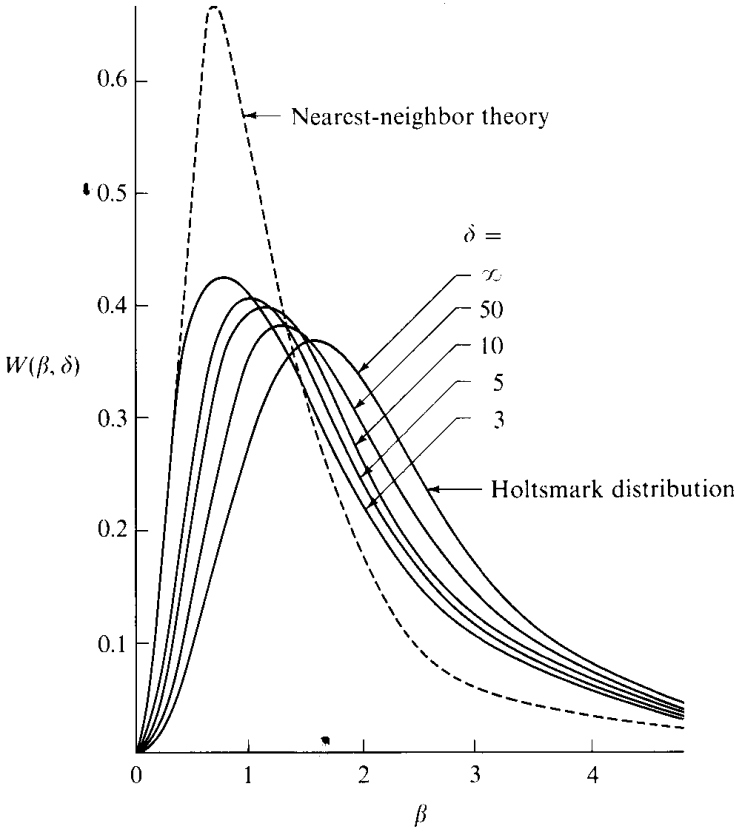

FIGURE 9-1
Probability distribution of field strength at a test point, including shielding effects; δ is the number of charged particles within the Debye sphere. From (**205**), by permission.

Hydrogen: Linear Stark Effect

- Each level degenerate with $2n^2$ sublevels.
- Perturbing field will separate sublevels.
- Observed profile is a superposition of components weighted by relative intensities and shifted by field probability function.
- $\Delta\lambda_{1/2} \approx 2.5\text{x}10^{-9}\alpha_{1/2}N_e^{2/3}$ where $\alpha_{1/2}$ is a half-width parameter widely used for plasma diagnostics (NIST).
- For Hα (n=2 to 3) in the Sun (P_e=20 dyne/cm^2, T=5800K), $\Delta\lambda_{\text{FWHM}}$=0.5 Å, i.e. a width 1000 times the natural width.
- Hot stars have very **high** electron pressures, so the Linear Stark effect greatly affects H I lines in hot stars (including white dwarfs), and is also relevant for hydrogenic ions (e.g. He II lines) in O stars.

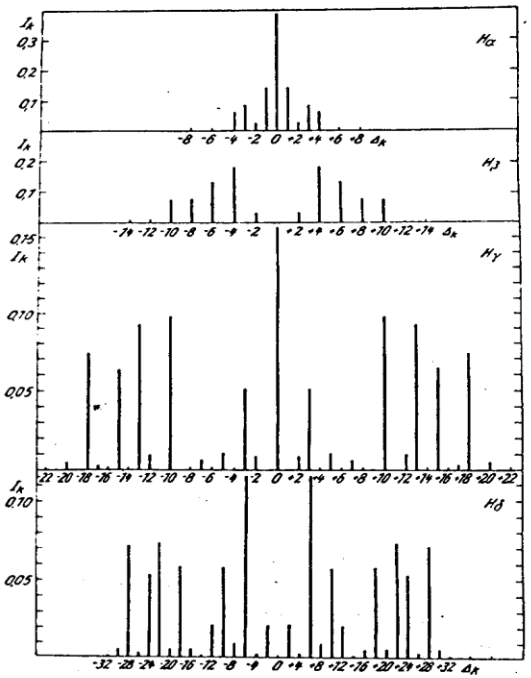

Fig. 11.1. The Stark effect splitting of the different Balmer lines (according to Unsöld, 1955, p. 320.)

Linear Stark broadening: examples (1)

Example of linear Stark broadening in early B stars – increased Hγ line width for increased pressure (this effect becomes significant for $T_{\rm eff}$>7500 K).

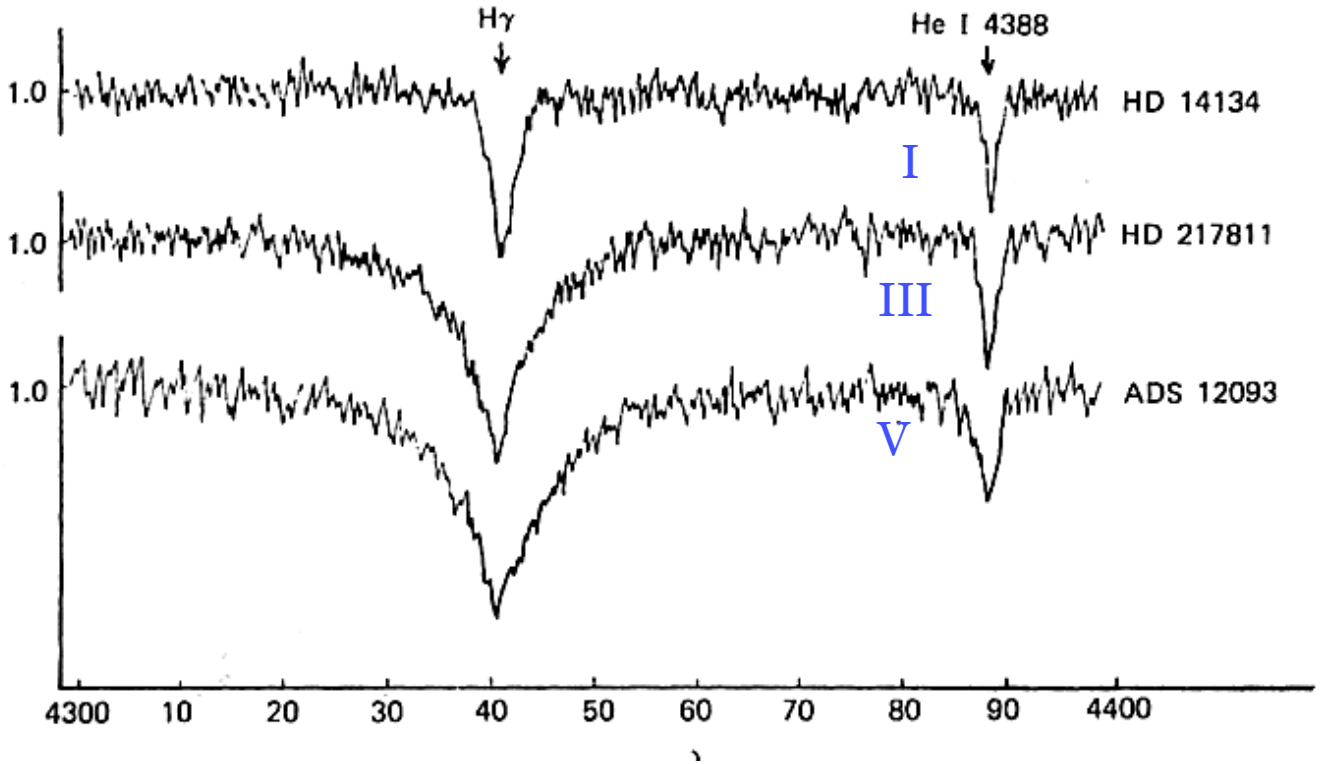

Linear Stark broadening: examples (2)

Vidal, Cooper & Smith (1973):

H I + p quasistatic approach;

H I + e collisional approximation – in a core

quasistatic approach - in wings

Observations

(solid line) and theory

(dash line)

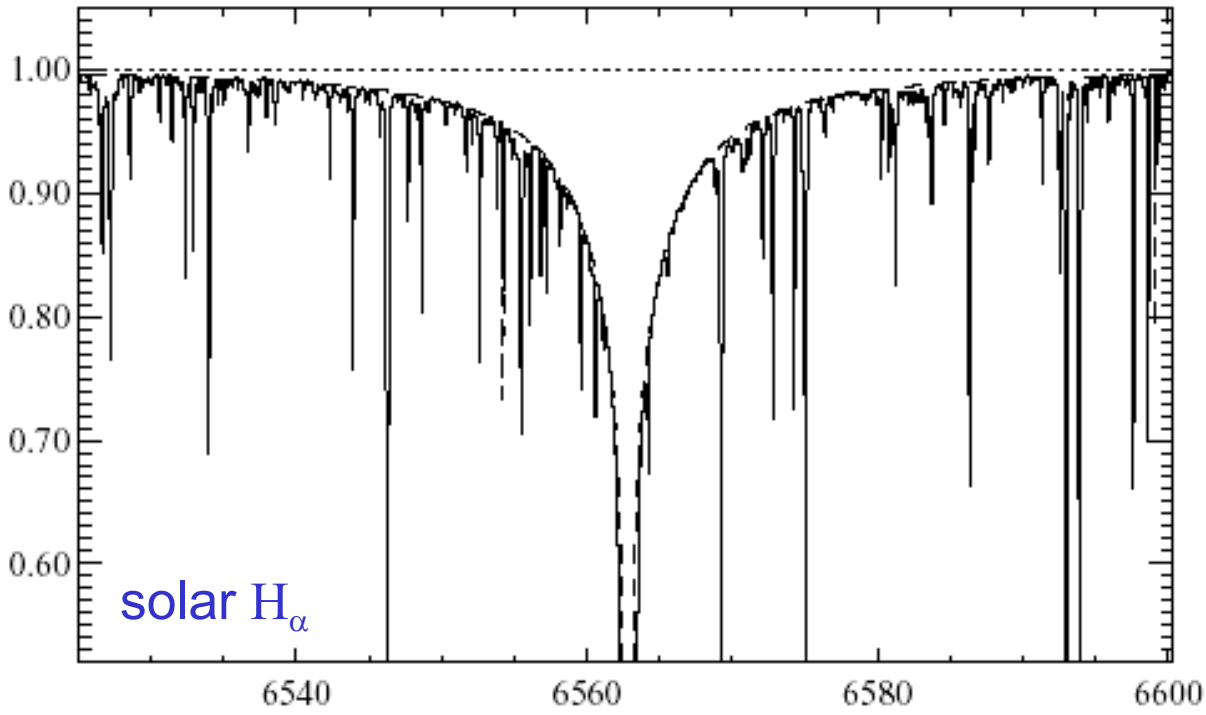

van der Waals broadening: example

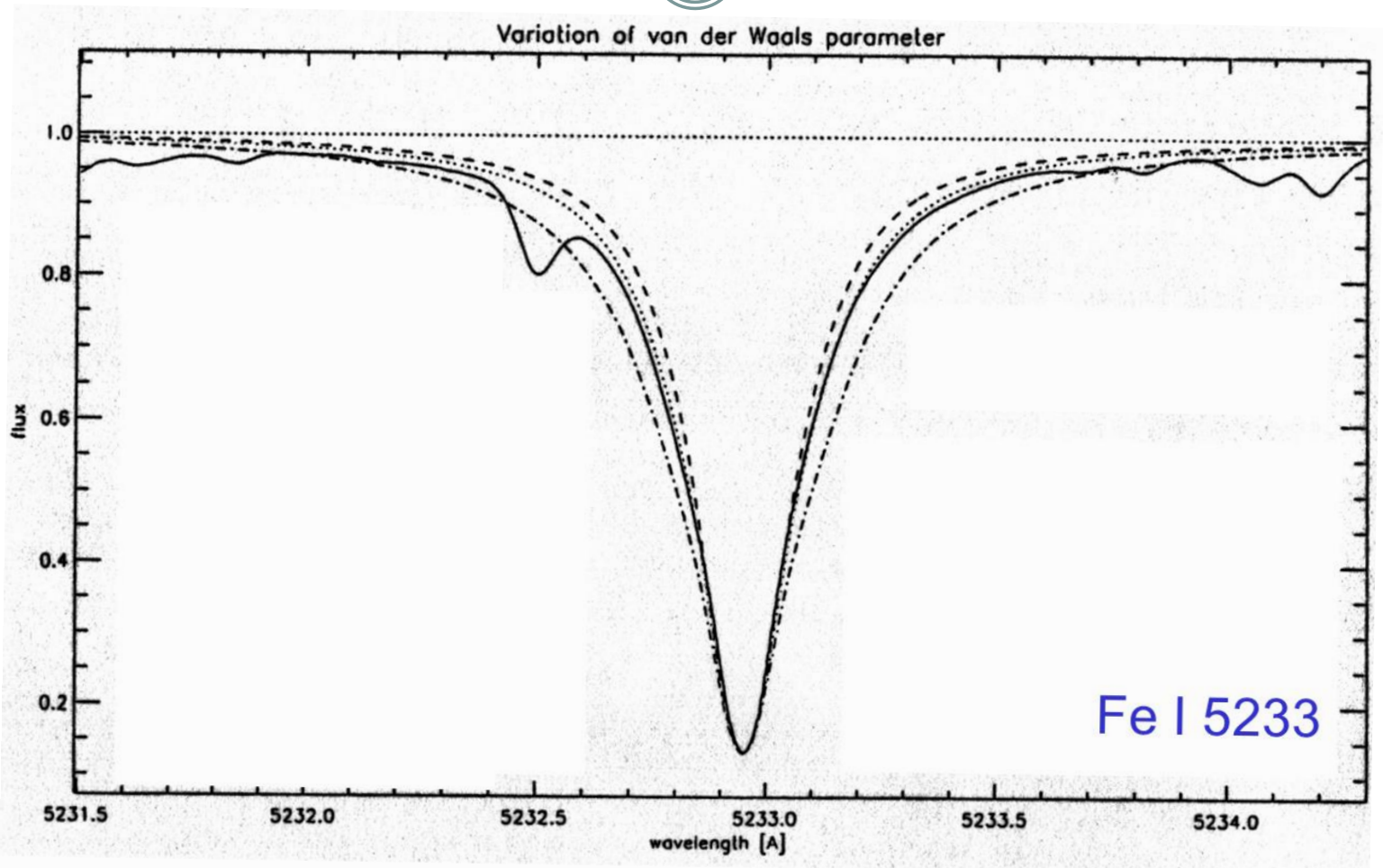

Example: log C_6 varies from -31.40 (top), -31.10 (middle), to -30.50 (bottom)

New Developments in the Theory of Pressure-Broadening

- Linear Stark broadening

Stehle & Hutcheon (1999, A&AS, 140, 93) – tables of Stark profiles

- van der Waals broadening

Anstee & O'Mara (1995, MNRAS, 276, 859) and following papers

$$\gamma_6 / 4\pi = N_H (4/\pi)^{\alpha/2} \Gamma\left((4-\alpha)/2\right) \mathrm{v}\, \sigma_0 (\mathrm{v}/\mathrm{v}_0)^{-\alpha}$$

σ_0, α - tabulated parameters

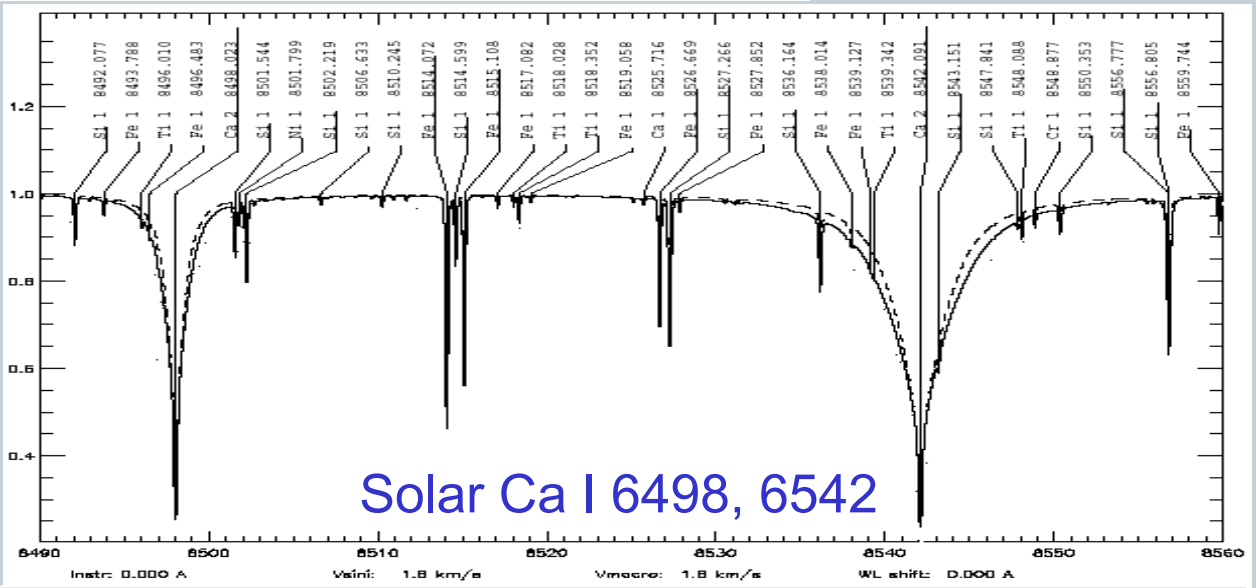

Additional material for self-study

Observations and Theory of *Anstee&O'Mara* are consistent!

Dash line – approximation of *Unsold* (1955)

♦ Resonance Broadening

Barklem et al. (2000, A&A, 363, 1091)

Influence of resonance broadening on the line profiles of H_α and H_β

♦ Quadratic Stark broadening

Papers by *Dimitrijevic et al.*

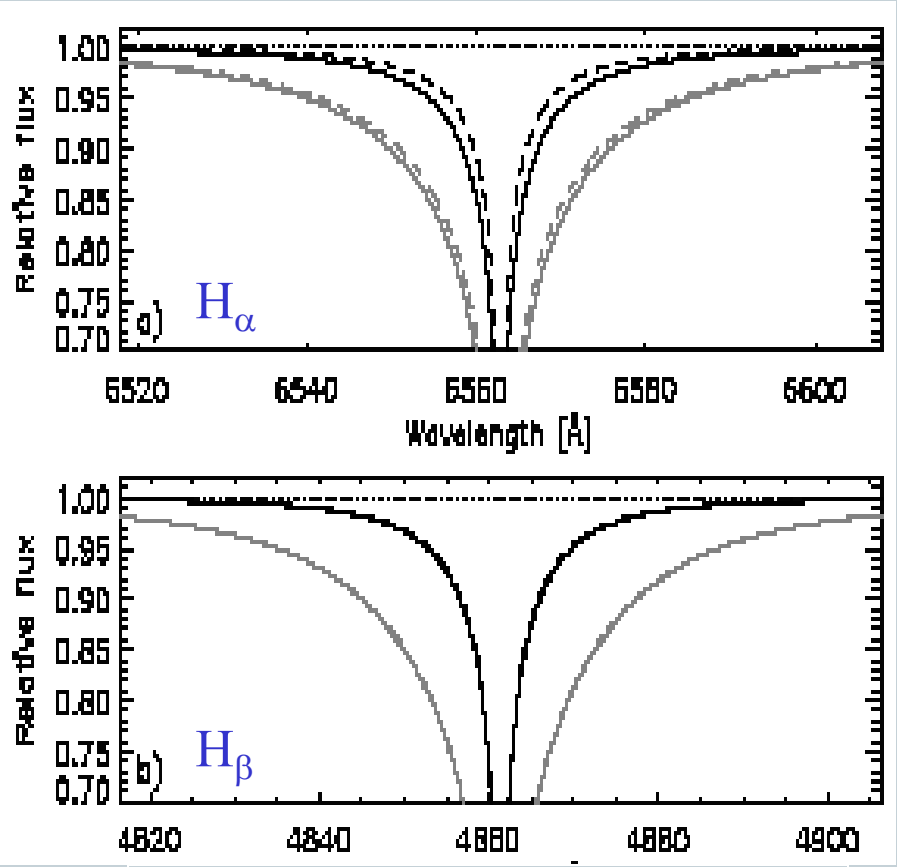

$T_{\rm eff} = 5780$ K, $\log g = 4.44$
$T_{\rm eff} = 7000$ K (grey)
Dash line:
Without resonance broadening

Additional material for self-study

Broadening of spectral lines

There are numerous broadening mechanisms which influence the apparent shape of spectral lines:

microscopic

1. Natural broadening
2. Thermal broadening
3. Microturbulence
   (treated like extra thermal broadening)
4. Collisions (important for strong lines)
5. Isotopic shift, hyperfine splitting (hfs)
   Zeeman effect

macro

6. Macroturbulence
7. Rotation
8. Instrumental broadening

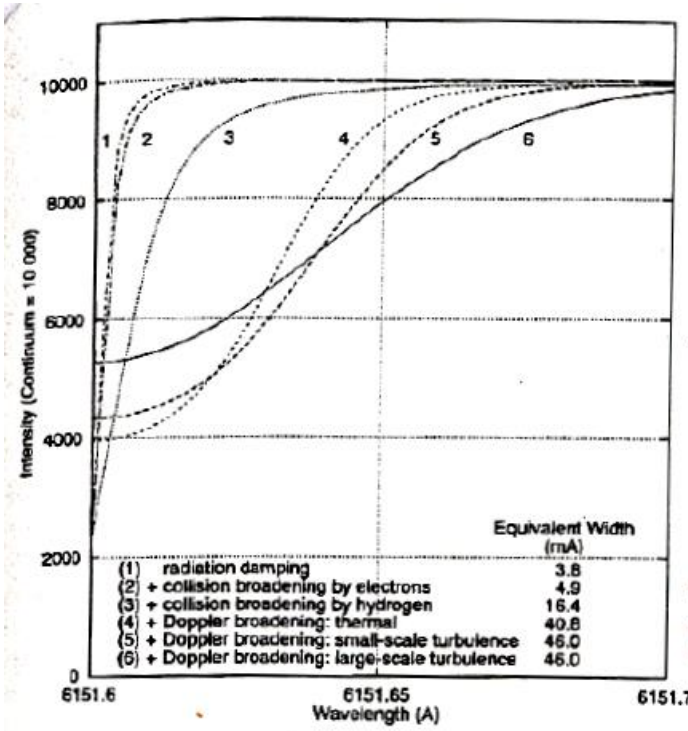

Holweger 1996

Other broadening mechanisms

- **Turbulent Broadening:** In addition to microscopic (thermal) and macroscopic (rotation) motions, there are other motions in stellar atmospheres which are introduced, operating on microscopic (**microturbulence**) and macroscopic (**macroturbulence**) scales, via convolutions with Gaussian velocity distribution

- **Isotope splitting:** Different isotopes have different nuclear mass and so slightly different term energies – the effect is greatest for hydrogen (e.g. deuterium vs hydrogen).

- **Zeeman splitting:** Magnetic fields split magnetically sensitive lines – at optical wavelengths the splitting is seen as line broadening, towards the IR the splitting becomes more noticeable since it increases as λ^2 versus λ for Doppler broadening.

Turbulent broadening

- Added to thermal broadening in quadrature. The Gaussian line profile (normalized to unity) remains.
  Recall the convolution of two Gaussian profiles!

$$\phi(\nu) = \frac{1}{\sqrt{\pi}\sqrt{\Delta\nu_D^2 + \xi_t^2}} \exp[-(\nu - \nu_0)^2 / (\Delta\nu_D^2 + \xi_t^2)]$$

  where ξ_t is a microturbulence velocity.

- Note that the broadening because of microturbulence does **not** depend on the mass of an atom!

Spectral line formation

EINSTEIN COEFFICIENTS

LINE PROFILES: NATURAL BROADENING

BROADENING OF SPECTRAL LINES

NATURAL LINE BROADENING:

THERMAL (DOPPLER) BROADENING

CONVOLUTION OF DIFFERENT BROADENING PROCESSES

PRESSURE BROADENING

INGIS-TELLER RELATION

ROTATIONAL AND INSTRUMENTAL BROADENING

Inglis-Teller relation

- Balmer lines, due to linear Stark broadening, overlap with each other close to the series limit, merging into a quasi-continuum at frequencies well below the nominal threshold.
- **If** linear Stark broadening is the dominant mechanism, one can estimate the N_e from the highest frequency Balmer line n_{max} that is still visible – the Inglis & Teller (1939) relation:

$$\log N_e = 23.26 - 7.5 \log n_{\max}^{Balmer}$$

Star	SpT	n_{max}	Log N_e
α Cyg	A2I	29	12.2
Sirius	A2V	18	13.8
τ Sco	B0V	14	14.6
White dwarf	DA	8	16.4

From Mihalas (1970)

Inglis-Teller in White Dwarfs

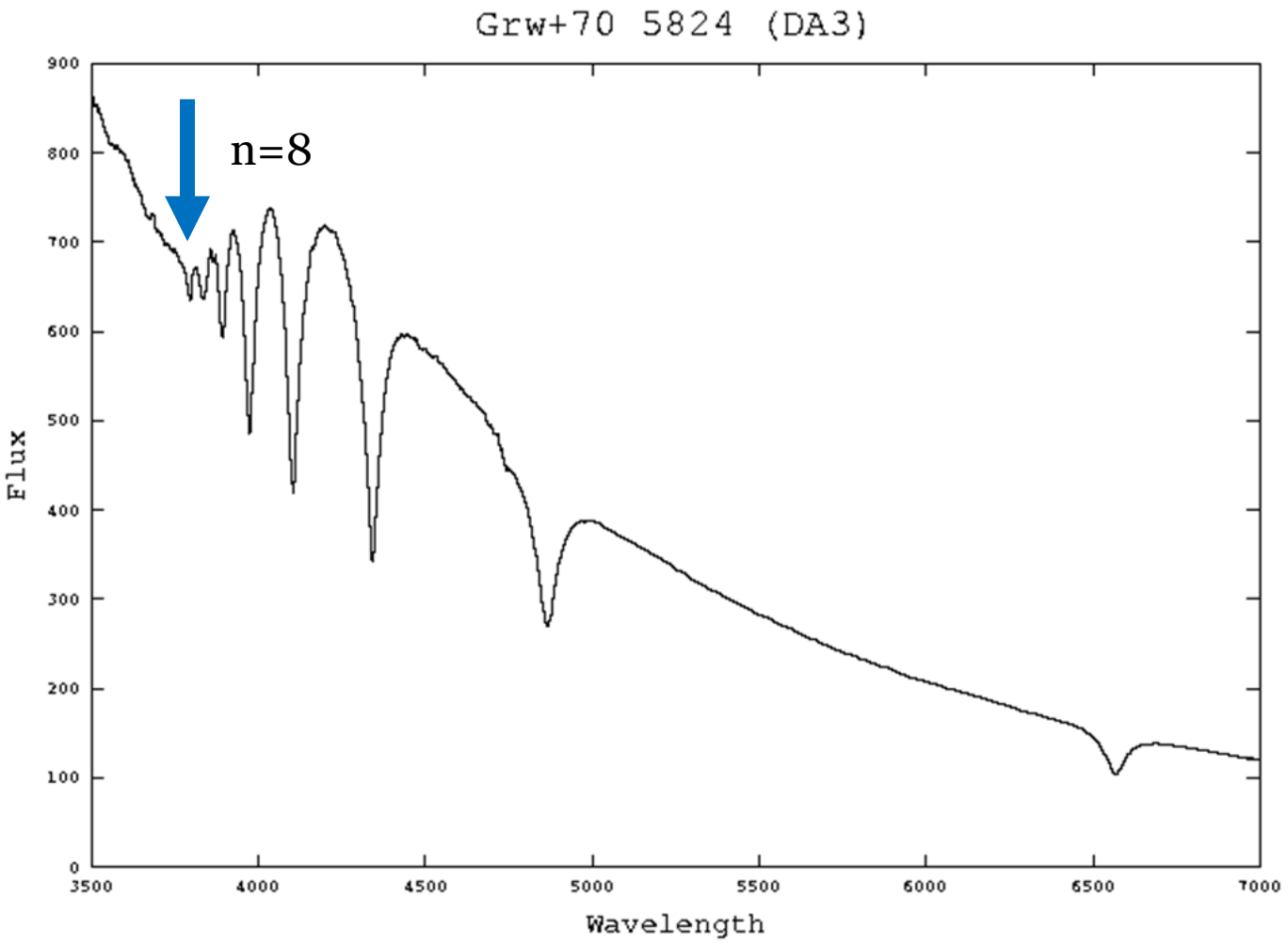

Spectral line formation

EINSTEIN COEFFICIENTS
LINE PROFILES: NATURAL BROADENING
BROADENING OF SPECTRAL LINES
NATURAL LINE BROADENING:
THERMAL (DOPPLER) BROADENING
CONVOLUTION OF DIFFERENT BROADENING PROCESSES
PRESSURE BROADENING
INGIS-TELLER RELATION
ROTATIONAL AND INSTRUMENTAL BROADENING

Rotational broadening

Thermal Doppler broadening describes the microscopic motion of individual particles in the atmosphere. The other scale extreme is **macroscopic** broadening of the lines caused by the **rotation** of the whole star. The maximum (critical) rotation velocity $V_c = \sqrt{(GM/R_e)}$ where R_e is the equatorial radius.

Successive synthetic models allowing for Doppler and Stark broadening are shown here for $V_{rot} \sin i$=0, 100, 200 km/s.

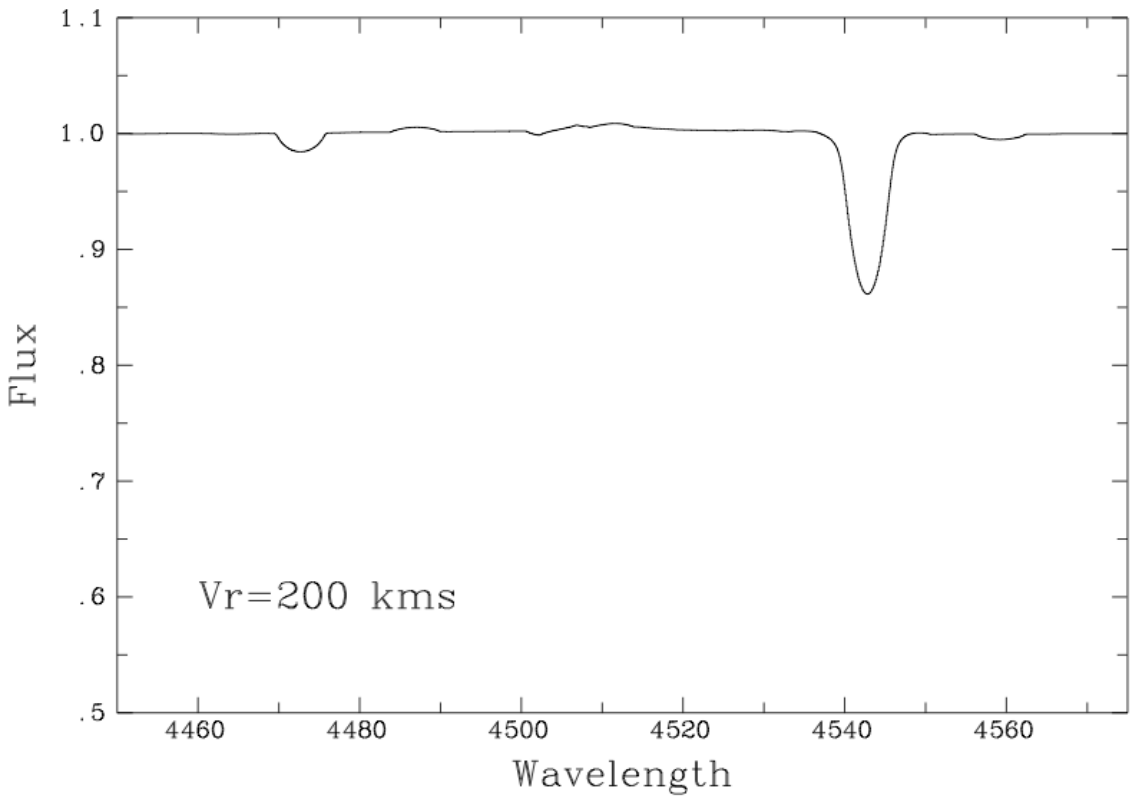

Rotational broadening

Successive synthetic models allowing for Doppler and Stark broadening are shown here for $V_{\rm rot} \sin i = 0$, 100, 200 km/s.

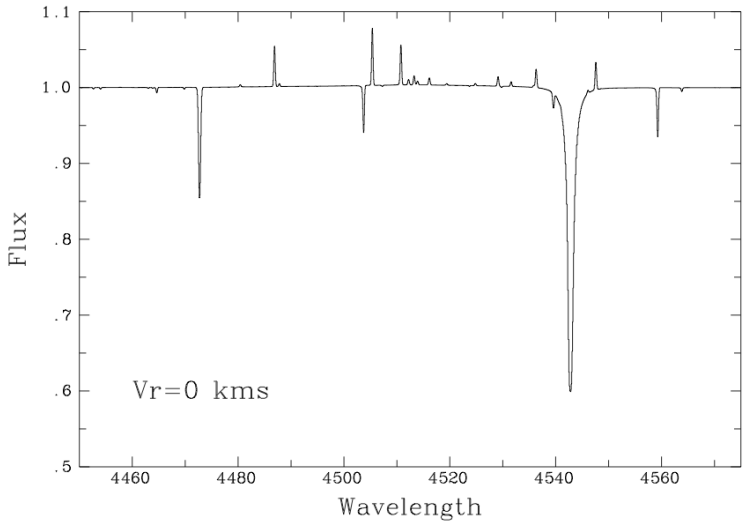

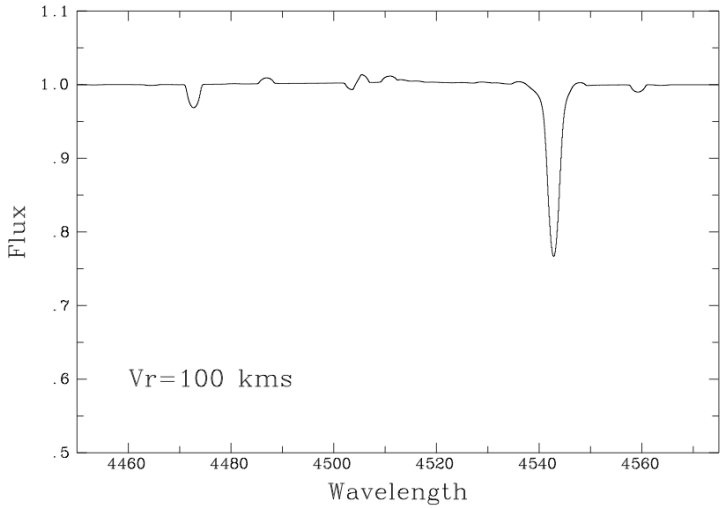

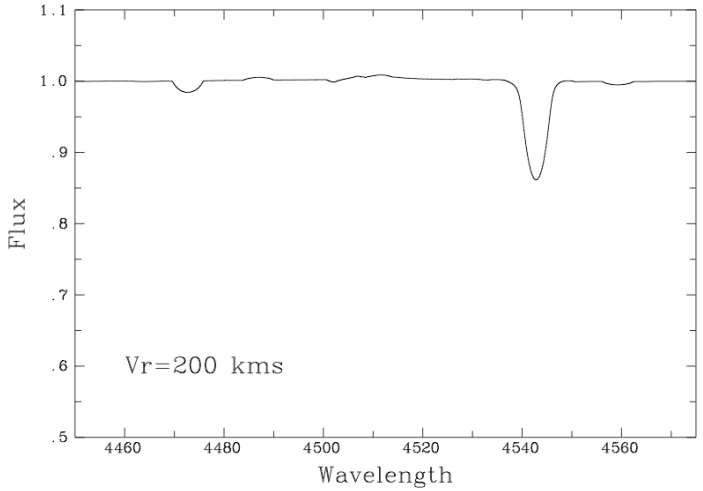

$V_{rot} \sin i$?

Many early-type OB stars are observed to be rotating rapidly (Be stars close to critical rotation), so this is the major broadening mechanism in these stars. Why $\sin(i)$? **Inclination is rarely known**, except for eclipsing binaries.

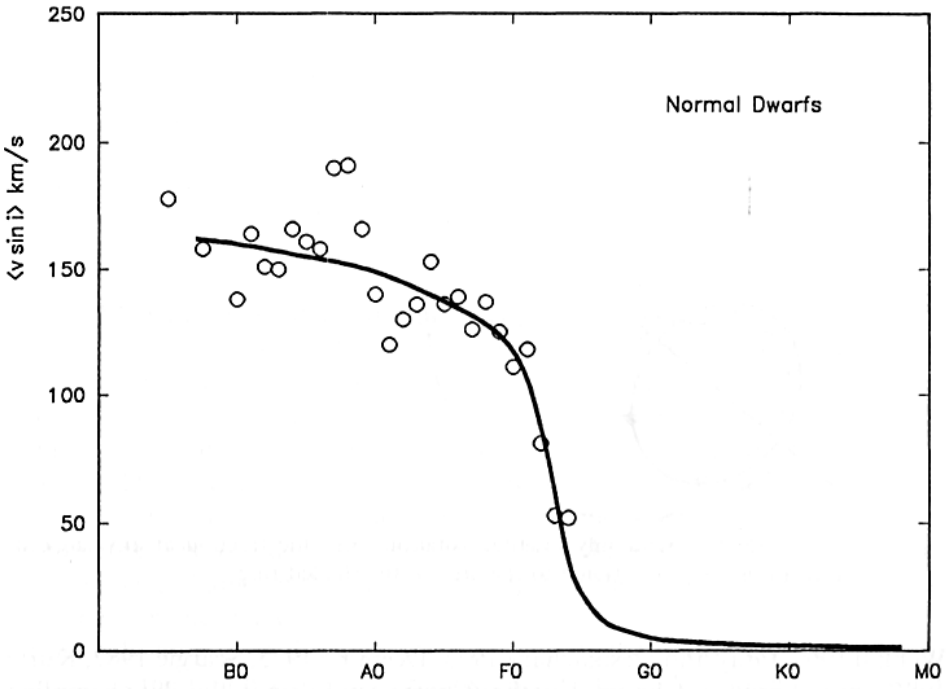

Fig. 17.16. The average rotation rates are shown for spectral intervals as a function of spectral type. (Data are from Uesugi and Fukuda (1982), Soderblom (1983), and Gray (1982b, 1984b).)

Instrumental Broadening

Any spectrograph used to observe a star has a finite resolution ($R=\lambda/\Delta\lambda$), regardless of the sharpness of the spectral line. For low resolution data (necessary when observing faint objects), this may affect the observed line profile more than everything else.

High (R=20,000),medium (R=2,000) and low (R=200) resolution Solar spectra at 2microns.

Faint stars with intrinsically narrow lines are generally broadened the most by the spectrograph!

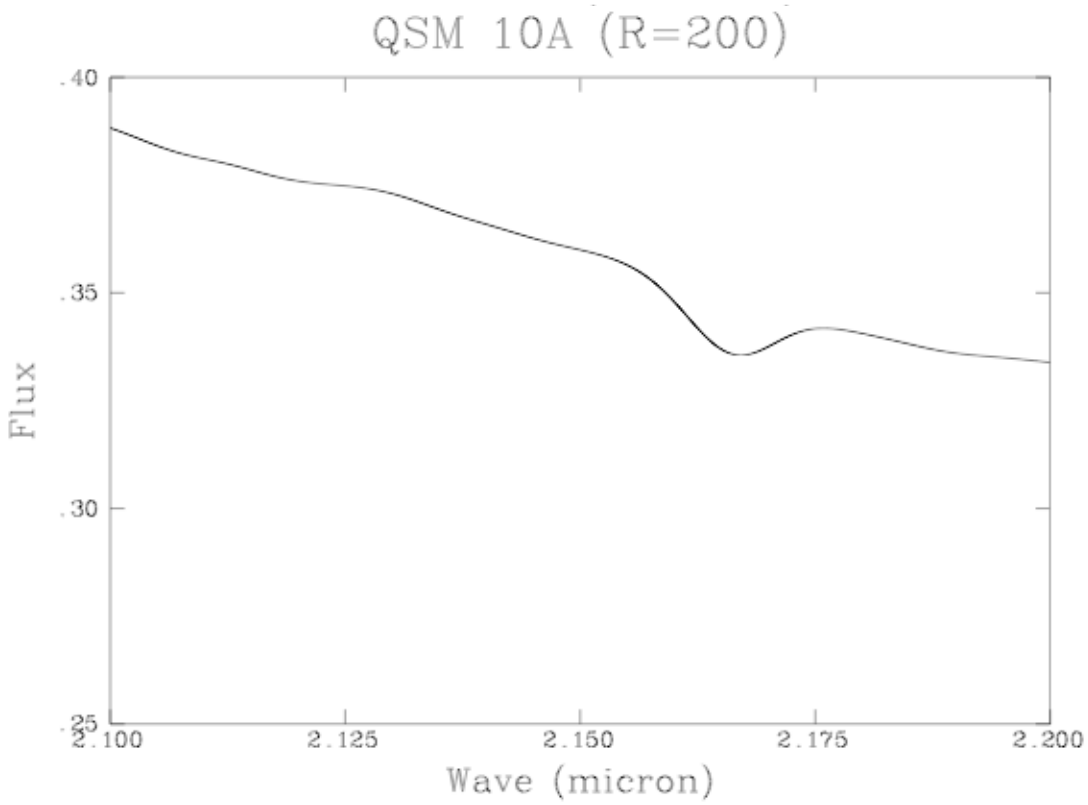

Instrumental Broadening

High (R=20,000), medium (R=2,000), and low (R=200) resolution Solar spectra at 2microns.

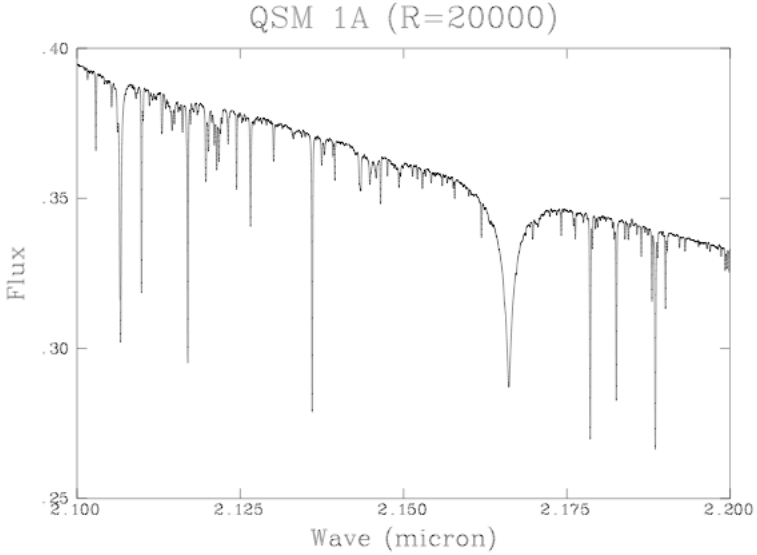

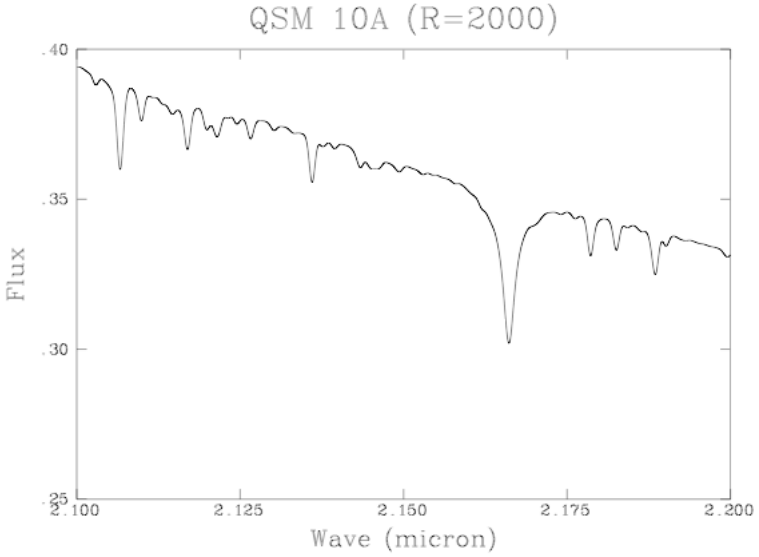

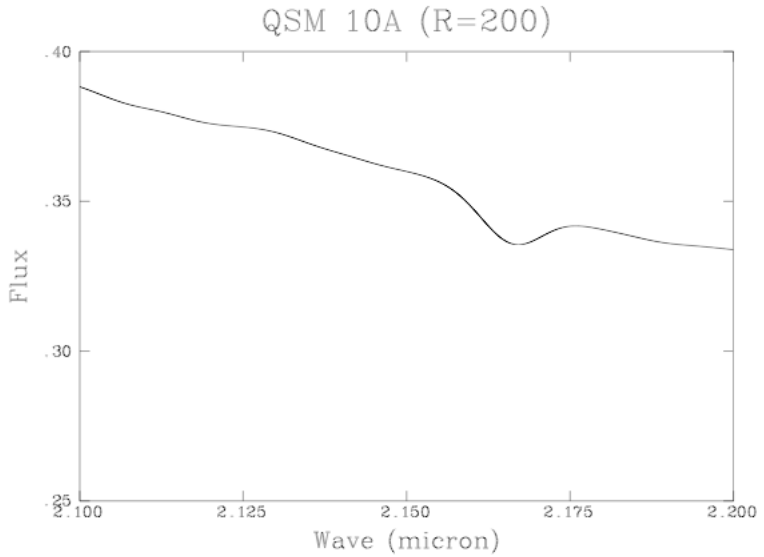

Summary

- Final profile is a convolution of all the key broadening processes.
- Convolution of Lorentzian profiles: $\Gamma_{total}=\Sigma\Gamma_i$
- Convolution of Lorentzian and Doppler broadening yields a Voigt profile.
- Pressure/collisional broadening via linear Stark broadening (only for hydrogenic ions), quadratic Stark broadening (interaction with electrons – hot stars) or Van der Waals broadening (interaction between neutral atoms – cool stars).
- Inglis-Teller relation allows estimate of N_e from overlapping Balmer lines in hot stars.
- Non-pressure broadening mechanisms include microscopic (thermal Doppler), macroscopic (rotational Doppler), turbulent, Zeeman, instrumental.
- Line profiles typically have characteristic Voigt profiles – Gaussian (thermal) cores and Lorenzian (pressure) wings.

Simple theory of line formation

SIMPLE LINE TRANSFER
SCHUSTER-SCHWARZSCHILD MODEL
THEORY OF LINE FORMATION
CURVE OF GROWTH

Schuster-Schwarzschild model

We now turn to the solution of the transfer equation for both line and continuum radiation. We will adopt the Schuster-Schwarzschild model, which assumes that the line is formed above the continuum and that continuous opacity plays only indirect role.

The total absorption coefficient within an arbitrary line is the sum of the line (α_L) and continuum (α_C) contributions i.e. $\alpha_\lambda = \alpha_L + \alpha_C$ as is the total emission coefficient ($\varepsilon_\lambda = \varepsilon_L + \varepsilon_C$). Hence,

$$S_\lambda = (\varepsilon_L + \varepsilon_C)/(\alpha_L + \alpha_C)$$

and

$$d\tau_\lambda = -(\alpha_L + \alpha_C)\, dz \qquad \tau_\lambda = \tau_L + \tau_C$$

So, we can write the transfer equation as usual:

$$\cos\theta \frac{dI_\lambda(\theta)}{d\tau_\lambda} = I_\lambda(\theta) - S_\lambda$$

Line source function

- We have seen earlier that the emergent flux from the stellar surface is π times the Source function at an optical depth of $2/3$:

$$F_\lambda(0) = \pi S_\lambda(\tau = 2/3)$$

- Across a line profile, α_λ varies, being larger towards the centre. The condition τ_λ=$2/3$ is true higher up in the atmosphere for λ near line centre and holds for progressively deeper layers for λ further into the wing.

- Assuming S_λ is a slowly varying function of λ (i.e. constant over the line width), $\pi S_\lambda(\tau_1 = 2/3) = F_\lambda(0)$ provides a mapping between F_λ as a function of λ and S_λ as a function of τ_λ

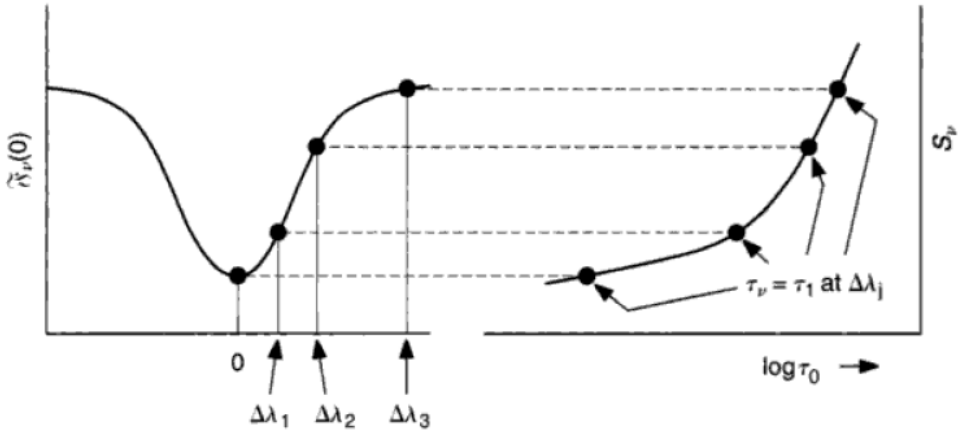

Theory of line formation

Because of larger absorption in the line, it is formed **higher** up in the atmosphere where T is lower **=>** absorption line.

$$\tau_\lambda = \tau_L + \tau_C$$

Consider **weak** lines: the layer $\tau_\lambda = 2/3$ is close to the layer with $\tau_C = 2/3$.

$$\alpha_L << \alpha_C \rightarrow \alpha_\lambda = \alpha_C (1 + \alpha_L / \alpha_C)$$

We can evaluate S_λ by a Taylor expansion around the point $\tau_C = \tau_\lambda$:

$$S_\lambda(\tau_\lambda = 2/3) \approx S_\lambda(\tau_C = 2/3) + \left.\frac{dS_\lambda}{d\tau_c}\right|_{\tau=2/3} \Delta\tau_C$$

$$\tau_\lambda / \tau_C = \alpha_\lambda / \alpha_C \rightarrow \tau_C = (\tau_L + \tau_C)\frac{\alpha_C}{\alpha_L + \alpha_C} \approx \frac{2}{3}\frac{\alpha_C}{\alpha_L + \alpha_C} \approx \frac{2}{3}\left(1 - \frac{\alpha_L}{\alpha_C}\right) \text{ for } \alpha_L << \alpha_C$$

$$\tau_C = \tau_\lambda + \Delta\tau_C = \frac{2}{3} + \Delta\tau_C \qquad \rightarrow \qquad \Delta\tau_C = -\frac{2}{3}\frac{\alpha_L}{\alpha_C}$$

Such a line is called optically thin.

Theory of line formation

$$S_\lambda(\tau_\lambda = 2/3) \approx S_\lambda(\tau_C = 2/3) - \frac{2}{3}\frac{\alpha_L}{\alpha_C}\frac{dS_\lambda}{d\tau_c}\bigg|_{\tau=2/3}$$

The line equivalent width is then (LTE: $S_\lambda = B_\lambda$)

$$W_\lambda = \int \frac{F_c - F_\lambda}{F_c} d\lambda = \int d\lambda \frac{B_\lambda(\tau_c = 2/3) - B_\lambda(\tau_\lambda = 2/3)}{B_\lambda(\tau_c = 2/3)}$$

$$W_\lambda = \int d\lambda \frac{dB_\lambda(\tau_c = 2/3)}{d\tau_c}\bigg|_{\tau_c=2/3} \left(\frac{2}{3}\frac{\alpha_L}{\alpha_C}\right) \frac{1}{B_\lambda(\tau_c = 2/3)} =$$

$$W_\lambda = \frac{2}{3}\int d\lambda \frac{d \ln B_\lambda(\tau_c = 2/3)}{d\tau_c}\bigg|_{\tau_c=2/3} \left(\frac{\alpha_L}{\alpha_C}\right)$$

Weakly depends on λ

$$W_\lambda = \frac{2}{3}\frac{1}{\alpha_C}\frac{d \ln B_\lambda(\tau_c = 2/3)}{d\tau_c}\bigg|_{\tau_c=2/3} \times \int_0^\infty \alpha_L d\lambda$$

If there is **no** temperature gradient with the temperature decreasing outwards, then there are **no** absorption lines in the spectrum.

The profile mimics the shape of α_L.
Line strength can be increased by decreasing the continuous absorption α_C or by increasing the line absorption α_L.

Theory of line formation

$$W_\lambda = \frac{2}{3}\frac{1}{\alpha_C}\left.\frac{d \ln B_\lambda(\tau_c = 2/3)}{d\tau_c}\right|_{\tau_c=2/3} \times \int_0^\infty \alpha_L d\lambda$$

$$\alpha_L = \sigma_L n, \qquad N = \int n\, dr = \frac{n}{\alpha_C}\int \alpha_C\, dr = \tau_c \frac{n}{\alpha_C} \approx \frac{2}{3}\frac{n}{\alpha_C} \rightarrow W_\lambda \propto N$$

For optically thin lines with $\alpha_L << \alpha_C$, $W_\lambda \propto N$

Strong lines

For $\alpha_L << \alpha_C$, the line is optically thin, and its strength increases proportionally with α_L / α_C. If $\alpha_L / \alpha_C > 1$, the line becomes optically thick, reaching a maximum depth R_λ. For very thick lines with $\alpha_L / \alpha_C = \infty$, the intensity in the line centre is given by the source function $S_\lambda(\tau_\lambda = 0)$, or $B_\lambda(\tau_\lambda = 0)$ in LTE. This is **not** zero since $T(\tau_\lambda = 0)$ is **non-zero**.

If non-LTE applies, when $S_\lambda \neq B_\lambda$, $S_\lambda(\tau_\lambda = 0)$ may tend towards zero, for instance, in resonance lines (arising from transitions between the ground states and the first energy level).

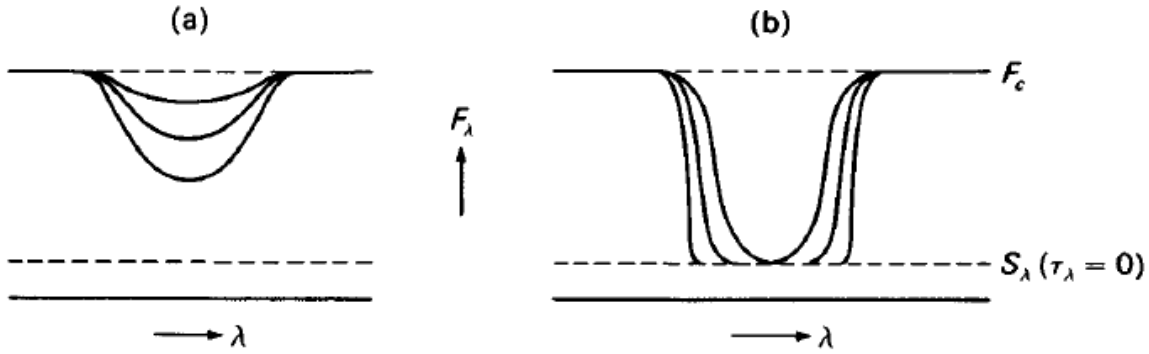

Fig. 10.12. Changes of the line profile with increasing κ_L/κ_c for (a) optically thin and (b) optically thick lines.

Curve of Growth

- The **Curve of growth** describes how the equivalent width (line strength) W_λ depends on the number of absorbing atoms or ions.
- For weak, optically thin lines, as the abundance doubles, the line equivalent width also doubles in strength:
  $W_\lambda \sim N$ – this is the LINEAR part of the curve of growth.
- As the abundance continues to increase, the Doppler core of the line becomes optically thick and saturates. The wings of the line, which are still optically thin, deepen, which occurs with little change in the line equivalent width and so produces a PLATEAU in the curve of growth, $W_\lambda \sim (\ln N)^{1/2}$.
- Ultimately, the damping wings become optically thick, increasing the equivalent width, $W_\lambda \sim (N)^{1/2}$. This is the DAMPING or SQUARE ROOT part of the curve of growth.

Curve of Growth

Curve of growth for the K line of Ca II. As N increases, the functional dependence of the equivalent width changes.

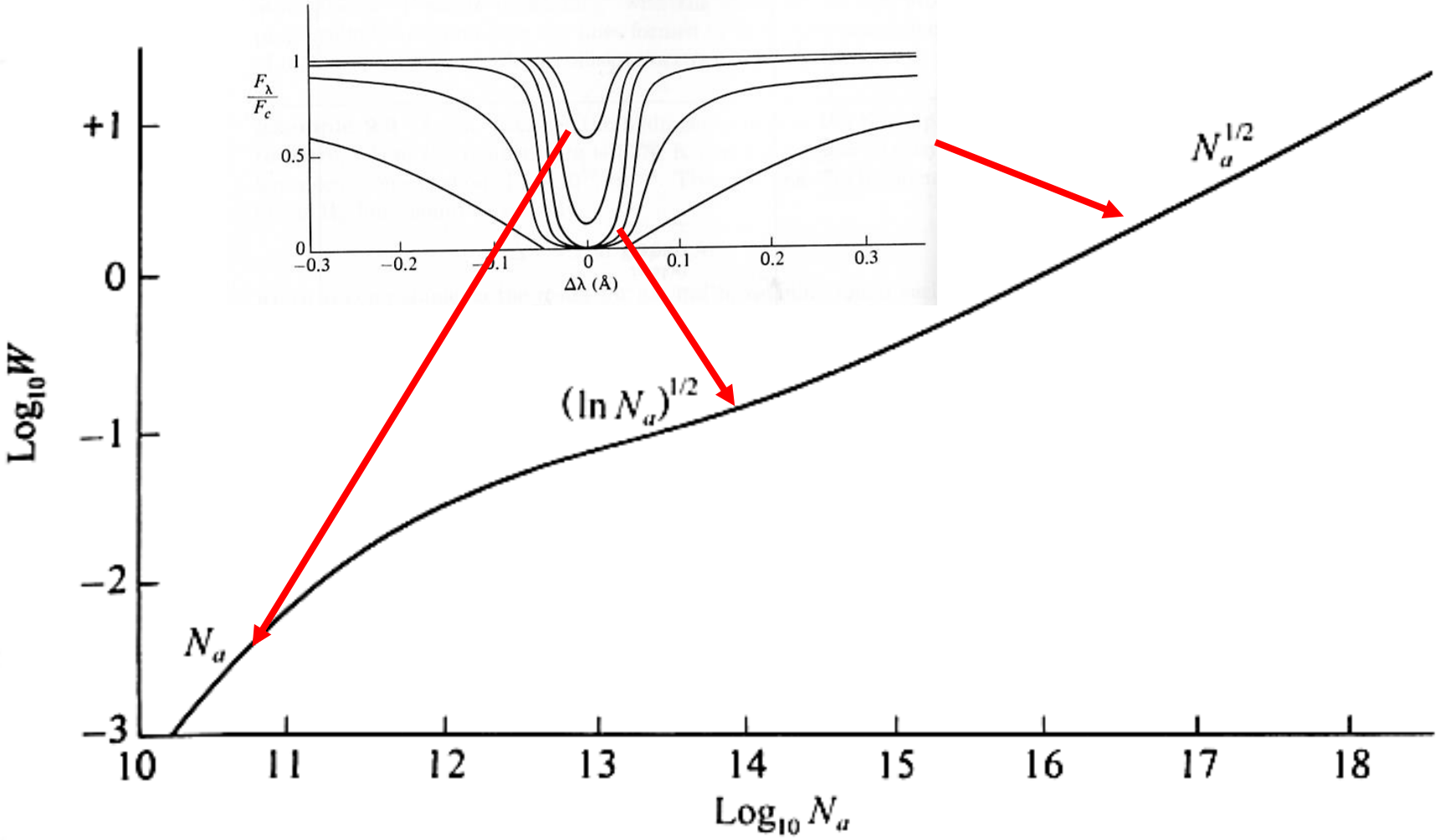

Methodology

- Using the curve of growth and a measured equivalent width we can derive the number of absorbing atoms.
- The Boltzmann and Saha equations convert this value into the total number of atoms of that element in the photosphere → abundance.
- To reduce errors, it is advisable to locate several lines on a curve of growth

Thermal and Pressure effects

The exact form of the curve of growth depends on the ratio of pressure to thermal broadening, $\alpha = \gamma / 2\Delta\lambda_D$.

For increasing Doppler line width, saturation occurs for larger W_λ, whilst the damping part will start earlier if α (i.e. γ) is larger.

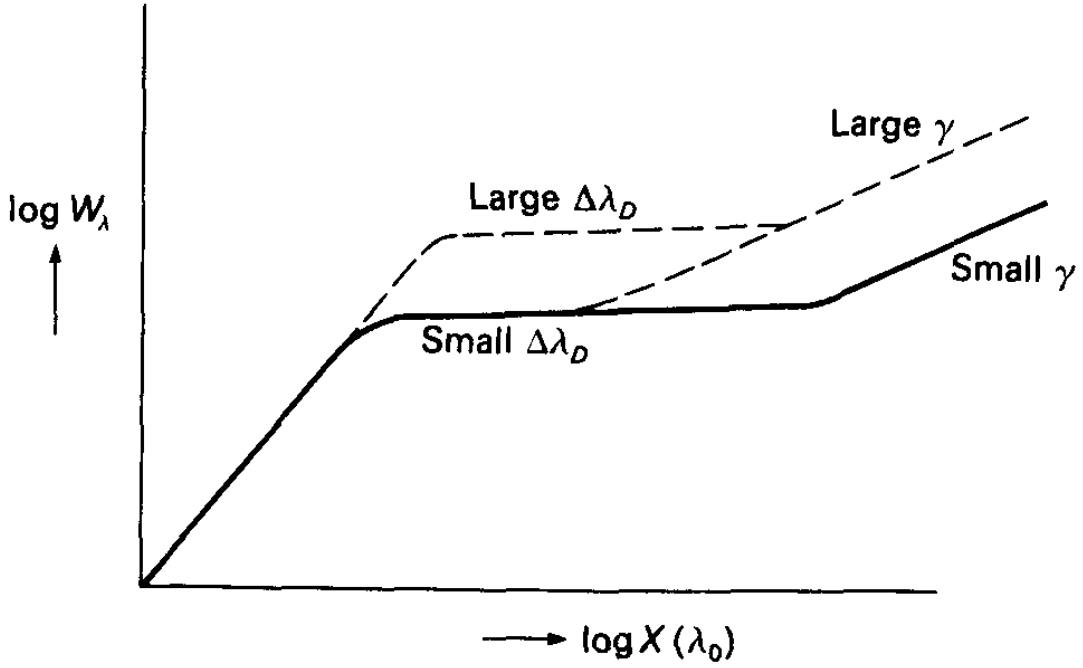

Transfer Equation including lines

SCATTERING IN LINES
THE MILNE-EDDINGTON MODEL
RESIDUAL FLUX OF THE LINE
ABSORPTION AND SCATTERING LINES
SCHUSTER MECHANISM FOR LINE EMISSION

Summary of simple line transfer

Simple line transfer:

The total absorption coefficient within an arbitrary line is the sum of the line (α_L) and continuum (α_C) contributions i.e. $\alpha_\lambda = \alpha_L + \alpha_C$ as is the total emission coefficient ($\varepsilon_\lambda = \varepsilon_L + \varepsilon_C$). Hence,

$$S_\lambda = (\varepsilon_L + \varepsilon_C)/(\alpha_L + \alpha_C)$$

and

$$d\tau_\lambda = -(\alpha_L + \alpha_C)\, dz \qquad \tau_\lambda = \tau_L + \tau_C$$

So, we can write the transfer equation as usual: $\cos\theta \frac{dI_\lambda(\theta)}{d\tau_\lambda} = I_\lambda(\theta) - S_\lambda$

The surface specific intensity and surface flux are obtained as previously.

$$I_\lambda(0,\theta) = \int_0^\infty S_\lambda(\tau_\lambda) e^{-\tau_\lambda \sec\theta} \sec\theta \; d\tau_\lambda$$

$$F_\lambda(0) = 2\pi \int_0^1 I_\lambda(0,\theta)\mu d\mu \qquad \mu = \cos\theta$$

Again, we need to know $S(\tau)$ to evaluate these integrals.

Scattering in lines

- Special case:
  Coherent scattering: $\nu_1 = \nu_2$
- Common case:
  2-level atom absorbs photon with frequency ν_1, re-emits photon with frequency ν_2; frequencies not exactly equal, because
  - levels a and b have non-vanishing energy width
  - Doppler effect because atom moves
- Non-coherent scattering requires a redistribution function

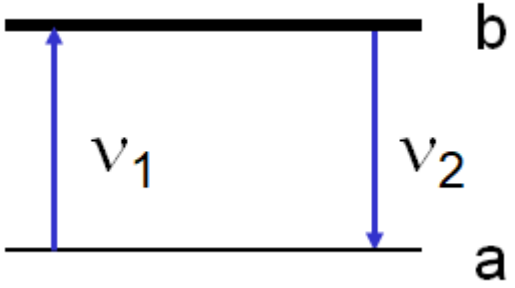

Transfer Equation including lines

Classical approach:

absorption of photons by line has two parts

1. (**1-ζ**) of absorbed photons are scattered
   (e^- returns to original state)
2. **ζ** of absorbed photons are destroyed
   (into thermal energy of gas)
   (for LTE: ζ =1)

Resonance lines (to/from the ground level)

A photon 1→2 returns back to the radiation field, thus dominates **Scattering**

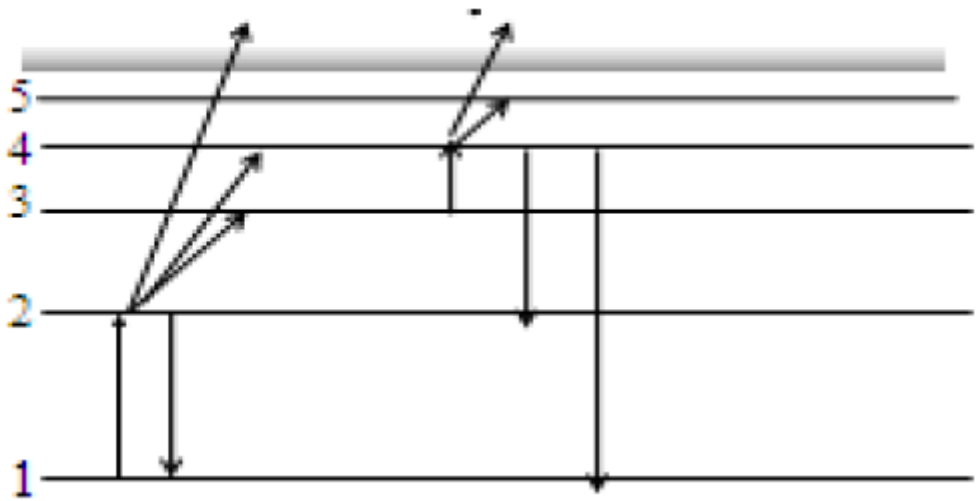

Subordinate lines (to/from higher levels)

A photon 3→4 disappears,

thus dominates **True absorption**

Scattering

- Pure Absorption and Thermal Emission:

$$S(\tau) = \frac{\varepsilon}{\alpha} \qquad \text{LTE: } \varepsilon_{th} = \alpha_{th} B(\tau)$$

- Pure Scattering:

For the case of pure scattering, the associated emission becomes completely insensitive to the thermal properties of the gas, and instead depends only on the local radiation field. If the scattering is roughly isotropic, the scattering emissivity ε_{sc} in any direction depends on both the opacity and the angle-averaged mean-intensity $\varepsilon_{sc} = \kappa_{sc} \rho J = \alpha_{sc} J$

This implies then that, for pure-scattering,

$$S(\tau) = J(\tau)$$

- Source Function for Scattering and Absorption:

The total opacity consists of both scattering and absorption, $\alpha \equiv \alpha_{abs} + \alpha_{sc}$

The total emissivity likewise contains both thermal and scattering components $\varepsilon = \varepsilon_{th} + \varepsilon_{sc} = \alpha_{th} B + \alpha_{sc} J$. The general source function

$$S(\tau) = \zeta B + (1 - \zeta) J(\tau)$$

absorption fraction $\zeta \equiv \dfrac{\alpha_{abs}}{\alpha_{abs} + \alpha_{sc}}$

The Milne-Eddington model (1)

Consider a case where at the given frequency the total opacity is a combination of both continuum and line processes:

Total absorption coefficient is $\alpha_\nu = \alpha_\nu^C + \alpha_\nu^L + \sigma$ ← scattering in the continuum

$= \alpha_\nu \times \phi_\nu =$ line opacity × line profile

The total optical depth is $d\tau_\nu = -(\alpha_\nu^C + \alpha_\nu^L + \sigma)\, ds$

(**larger** than in the continuum!)

The correponding emissivities $\varepsilon_\nu = \varepsilon_\nu^C + \varepsilon_\nu^L + \sigma J_\nu$

$S(\tau) = \frac{\varepsilon}{\alpha}$

$$\mu \frac{dI_\nu(\mu)}{d\tau_\nu} = I_\nu(\mu, \tau_\nu) - S_\nu(\tau_\nu)$$

Recall radiative transfer equation

$$\mu \frac{dI_\nu}{ds} = -\alpha_\nu I_\nu + \varepsilon_\nu$$

The Milne-Eddington model

Transfer equation:

$\varepsilon = \varepsilon_{th} + \varepsilon_{sc} = \alpha_{th} B + \alpha_{sc} J$

-absorbed +thermal +scattered

$$\mu \frac{dI_\nu}{ds} = -(\alpha_\nu^C + \alpha_\nu^L + \sigma) I_\nu + \varepsilon_\nu^C + \sigma J_\nu + \zeta \alpha_\nu^L B_\nu + (1-\zeta)\alpha_\nu^L J_\nu$$

+therm. line em. +scat. line emission (coherent)

Without dealing with the general case for the computation of all coefficients we assume:

- LTE in the continuum $\varepsilon_\nu^C = \alpha_\nu^C B_\nu(T)$
- scattering negligible in the continuum $\sigma \ll \alpha_\nu^C$

The following slides with light-grey backgrounds (like in this box) are for self-study. The derivation of equations will not be asked at the exam but will help understand the important results and conclusions.

The Milne-Eddington model (2)

$$\mu \frac{dI_\nu}{ds} = -(\alpha_\nu^C + \alpha_\nu^L) I_\nu + \alpha_\nu^C B_\nu + \zeta \alpha_\nu^L B_\nu + (1-\zeta)\alpha_\nu^L J_\nu$$

Using $\beta_\nu \equiv \frac{\alpha_\nu^L}{\alpha_\nu^C}$ $\qquad d\tau_\nu = -(\alpha_\nu^C + \alpha_\nu^L)\, ds = -\alpha_\nu^C (1+\beta_\nu)\, ds$

$$\mu \frac{dI_\nu}{d\tau_\nu} = I_\nu - B_\nu \frac{1+\zeta\beta_\nu}{1+\beta_\nu} - \frac{(1-\zeta)\beta_\nu}{1+\beta_\nu} J_\nu = I_\nu - \lambda_\nu B_\nu - (1-\lambda_\nu)\, J_\nu$$

destruction probability → $\lambda_\nu \equiv \frac{1+\zeta\beta_\nu}{1+\beta_\nu}$

$$\mu \frac{dI_\nu}{d\tau_\nu} = I_\nu - \lambda_\nu B_\nu - (1-\lambda_\nu)\, J_\nu$$

Milne-Eddington Equation. Solve at each frequency point across profile.

The Milne-Eddington model (3)

$$\mu \frac{dI_\nu}{d\tau_\nu} = I_\nu - \lambda_\nu B_\nu - (1 - \lambda_\nu) J_\nu$$

Milne-Eddington assumptions (for analytical solution):

1. β_ν, λ_ν and ζ are constant with depth
2. B_ν is linear in continuum optical depth: $B_\nu = a + b\tau_c$

$$d\tau_c = \frac{d\tau_\nu}{1 + \beta_\nu} \qquad \tau_c = \frac{\tau_\nu}{1 + \beta_\nu}$$

Also, the Eddington approximation $K_\lambda(\tau_\lambda) = \frac{1}{3} J_\lambda(\tau_\lambda)$

Recap: Eddington approximation

Lecture I-6

K-integral and radiation pressure

164

- K-integral is related to the radiation pressure: $K_\lambda = \frac{1}{4\pi}\oint I_\lambda \cos^2\theta \, d\omega$
- A photon has momentum $p_\lambda = E_\lambda / c$
- Consider photons transferring momentum to a solid wall.
  Force:

$$F = \frac{dp_{\lambda\perp}}{dt} = \frac{1}{c}\frac{dE_\lambda}{dt}\cos\vartheta$$

- Pressure: $dP_\lambda = \frac{F}{d\sigma} = \frac{1}{c}\frac{dE_\lambda \cos\vartheta}{dt \quad d\sigma} = \frac{1}{c} I_\lambda \cos^2\vartheta \; d\omega \, d\lambda$

$$I_\lambda = \frac{dE_\lambda}{\cos\theta \, d\lambda \, d\sigma \, d\omega \, dt}$$

$$P_{rad}(\lambda) = \frac{1}{c}\oint_{4\pi} I_\lambda \cos^2\vartheta \; d\omega = \frac{4\pi}{c} K_\lambda$$

Lecture II-18

Eddington approximation (1)

74

- Previously we have seen that for the determination of the flux the anisotropy in the radiation field is very important because in the flux integral the inward-going intensities are subtracted from the outward-going ones, due to the factor $\cos\theta$.
- But for K, a small anisotropy is unimportant because the intensities are multiplied by the factor $\cos^2\theta$, which does **not** change sign for inward and outward radiation.
- To evaluate K or c_2, we can approximate the radiation field by an isotropic radiation field of the mean intensity J: $I = J$ (by definition). From the definition of K_λ we obtain

$$4\pi \, K_\lambda = \oint I_\lambda(\tau_\lambda, \theta) \cos^2\theta \, d\omega = J_\lambda(\tau_\lambda) \oint \cos^2\theta \, d\omega = \frac{4\pi}{3} J_\lambda(\tau_\lambda)$$

or after division by 4π,

$$K_\lambda(\tau_\lambda) = \frac{1}{3} J_\lambda(\tau_\lambda)$$

$d\omega = \sin\theta \, d\theta \, d\varphi$

This approximation for the K-function is known as the **Eddington approximation**.

Recap: Moments of intensity

- The mean intensity J_λ is the directional average (over 4π steradians) of the specific intensity [0-th moment of intensity]:

$$J_\lambda \equiv \frac{1}{4\pi}\oint I_\lambda d\omega = \frac{2\pi}{4\pi}\int_{-1}^{1} I(\mu)\,d\mu = \frac{1}{2}\int_{-1}^{1} I(\mu)\,d\mu$$

- **Eddington** flux $H_{\lambda,,}$ is the directional average (over 4π steradians) of the projection of the specific intensity [1st moment of intensity]:

$$H_\lambda = \frac{1}{4\pi}\oint I_\lambda \cos\theta\, d\omega = \frac{2\pi}{4\pi}\int_{-1}^{1} I(\mu)\,\mu\, d\mu = \frac{1}{2}\int_{-1}^{1} I(\mu)\,\mu\, d\mu$$

F_λ - astrophysical flux
H_λ - Eddington flux
$F_\lambda = \pi F_\lambda = 4\pi H_\lambda$

- K-integral [2nd moment of intensity] :

$$K_\lambda = \frac{1}{4\pi}\oint I_\lambda \cos^2\theta\, d\omega = \frac{2\pi}{4\pi}\int_{-1}^{1} I(\mu)\,\mu^2\, d\mu = \frac{1}{2}\int_{-1}^{1} I(\mu)\mu^2 d\mu$$

The Milne-Eddington model (4)

$$\frac{1}{2}\int_{-1}^{+1} \ldots [\mu]\, d\mu \;\times\; \mu\frac{dI_\nu}{d\tau_\nu} = I_\nu - \lambda_\nu B_\nu - (1-\lambda_\nu) J_\nu \;\times\; \frac{1}{2}\int_{-1}^{+1} \ldots [\mu]\, d\mu$$

Multiply both sides by $d\mu$ and $\mu\, d\mu$ and integrate:

$$\frac{dH_\nu}{d\tau_\nu} = J_\nu - \lambda_\nu B_\nu - (1-\lambda_\nu) J_\nu = \lambda_\nu (J_\nu - B_\nu)$$

$$\frac{dK_\nu}{d\tau_\nu} = H_\nu = \frac{1}{3}\frac{dJ_\nu}{d\tau_\nu}$$

$\int_0^\infty \frac{dK_\lambda}{d\tau_\lambda} d\lambda = \frac{F(\tau)}{4\pi} = H(\tau)$

The third radiative equilibrium condition

F_λ - astrophysical flux
H_λ - Eddington flux
$F_\lambda = \pi F_\lambda = 4\pi H_\lambda$

Differentiate again

$$\frac{d^2K_\nu}{d\tau_\nu^2} = \lambda_\nu (J_\nu - B_\nu) = \frac{1}{3}\frac{d^2J_\nu}{d\tau_\nu^2}$$

← Eddington approximation

The Milne-Eddington model (5)

$$\frac{1}{3}\frac{d^2 J_\nu}{d\tau_\nu^2} = \lambda_\nu (J_\nu - B_\nu)$$

B_ν is linear in τ, so zero second derivative $\frac{d^2 B_\nu}{d\tau_\nu^2} = 0$

$$\frac{1}{3}\frac{d^2 J_\nu}{d\tau_\nu^2} = \frac{1}{3}\frac{d^2 (J_\nu - B_\nu)}{d\tau_\nu^2} = \lambda_\nu (J_\nu - B_\nu)$$

This can be integrated to give

$$J_\nu - B_\nu = \mathcal{A} e^{-\sqrt{3\lambda_\nu}\tau_\nu} + \mathcal{B} e^{\sqrt{3\lambda_\nu}\tau_\nu}$$

Apply boundary condition at depth:

$$\tau_\nu \to \infty \quad \Rightarrow \quad J_\nu \to B_\nu \quad \Rightarrow \quad \boldsymbol{\mathcal{B} = 0}$$

The Milne-Eddington model (6)

$J_\nu - B_\nu =$

Now a

From g

Lecture 19

Eddington approximation (3)

74

- Boundary condition: there is no flux going into the star, i.e. $I(0,\theta) = I^- = 0$ for $\pi/2 < \theta < \pi$
- We also assume that the outward intensity does not depend upon θ, i.e. $I(0,\theta) = I^+ = \text{const}$ for $0 < \theta < \pi/2$

$J_\lambda = \frac{1}{4\pi}\oint I_\lambda d\omega$ and $F_\lambda = \oint I_\lambda \cos\theta \, d\omega$

$d\omega = \sin\theta \, d\theta \, d\varphi$

- It gives $J(0) = \frac{1}{2}I^+ = \frac{1}{2\pi}F(0)$
- Hence $C = J(0) = F(0)/2\pi$ so:

τ=0

$S(\tau) = \frac{3}{4\pi}\tau F(0) + C = J(\tau)$

$S(\tau) = \frac{1}{\pi}(\frac{3}{4}\tau + \frac{1}{2})F(0)$

$$S(\tau) = \frac{3}{4\pi}(\tau + \frac{2}{3})F(0)$$

- To find the depth dependence of T, we also need to assume **LTE**.

$q(\tau)$ is a slowly varying function (Hopf function), with $q = 1/\sqrt{3}$ at τ=0

The Milne-Eddington model (6)

$$J_\nu - B_\nu = \mathcal{A} e^{-\sqrt{3\lambda_\nu}\tau_\nu} + \mathcal{B} e^{\sqrt{3\lambda_\nu}\tau_\nu}$$

Now apply boundary condition at surface:

$$\tau_\nu = 0 \quad \Rightarrow \quad J_\nu = B_\nu + \mathcal{A}$$

From grey atmosphere solution, get $J(\tau{=}0)$:

$$J(\tau) = \frac{3}{4\pi}[\tau + q(\tau)]F(0) = 3H(0 + \frac{1}{\sqrt{3}}) = \sqrt{3}H$$

The Milne-Eddington model (7)

$$J_\nu - B_\nu = \mathcal{A} e^{-\sqrt{3\lambda_\nu}\tau_\nu} + \mathcal{B} e^{\sqrt{3\lambda_\nu}\tau_\nu}$$

Now apply boundary condition at at surface:

$$\tau_\nu = 0 \quad \Rightarrow \quad J_\nu = B_\nu + \mathcal{A}$$

From grey atmosphere solution, get $J(\tau=0)$:

Eddington approximation (2)

- Inserting the Eddington approximation into the above equation we find

$$\frac{dK(\tau)}{d\tau} = \frac{1}{3}\frac{dJ(\tau)}{d\tau} = \frac{F(\tau)}{4\pi} = c_1$$

$$\frac{dJ(\tau)}{d\tau} = \frac{3}{4\pi}F(\tau)$$

$$\frac{dK(\tau)}{d\tau} = \frac{F(\tau)}{4\pi}$$

The Milne-Eddington model (8)

$$J_\nu - B_\nu = \mathcal{A} e^{-\sqrt{3\lambda_\nu}\tau_\nu} + \mathcal{B} e^{\sqrt{3\lambda_\nu}\tau_\nu}$$

Now apply boundary condition at at surface:

$$\tau_\nu = 0 \quad \Rightarrow \quad J_\nu = B_\nu + \mathcal{A}$$

From grey atmosphere solution, get $J(\tau{=}0)$:

$$J(\tau) = \frac{3}{4\pi}[\tau + q(\tau)]F(0) = 3H(0 + \frac{1}{\sqrt{3}}) = \sqrt{3}H$$

$$\frac{1}{3}\frac{dJ_\nu}{d\tau_\nu}\bigg|_{\tau_\nu=0} = H_\nu(0) = \frac{1}{\sqrt{3}}J_\nu(0)$$

From $B_\nu{=}a{+}b\tau_c$ $\quad J_\nu(\tau_c = 0) = B_\nu + \mathcal{A} = a{+}\mathcal{A} = \frac{1}{\sqrt{3}}\frac{dJ_\nu}{d\tau_\nu}\Big|_{\tau_\nu=0}$

The Milne-Eddington model (9)

$$J_\nu = B_\nu + \mathcal{A}e^{-\sqrt{3\lambda_\nu}\tau_\nu} = a + b\tau_c + \mathcal{A}e^{-\sqrt{3\lambda_\nu}\tau_\nu}$$

$$\left.\frac{1}{\sqrt{3}}\frac{dJ_\nu}{d\tau_\nu}\right|_{\tau_\nu=0} = \frac{1}{\sqrt{3}}\left[-\mathcal{A}\sqrt{3\lambda_\nu} + \frac{b}{1+\beta_\nu}\right] = a+\mathcal{A}$$

can now solve for $\mathcal{A}$!

$$\mathcal{A} = \frac{\frac{b}{1+\beta_\nu} - \sqrt{3}a}{\sqrt{3} + \sqrt{3\lambda_\nu}}$$

$$\tau_c = \frac{\tau_\nu}{1+\beta_\nu}$$

Define $p_\nu \equiv \frac{b}{1+\beta_\nu}$

$$J_\nu(\tau) = a + p_\nu\tau_\nu + \frac{p_\nu - \sqrt{3}a}{\sqrt{3} + \sqrt{3\lambda_\nu}}e^{-\sqrt{3\lambda_\nu}\tau_\nu}$$

The Milne-Eddington model (10)

Thus, we obtained the fully analytic solution for the mean intensity

$$J_\nu(\tau) = \underbrace{a + p_\nu \tau_\nu}_{B_\nu} + \frac{p_\nu - \sqrt{3}a}{\sqrt{3} + \sqrt{3\lambda_\nu}} e^{-\sqrt{3\lambda_\nu}\tau_\nu}$$

Thermalization depth

$$\tau_\nu \gtrsim \frac{1}{\sqrt{\lambda_\nu}}$$

$J_\nu \rightarrow B_\nu$

$J_\nu < B_\nu$ in outer parts of atmosphere

We can use this to obtain the emergent flux

$$H_\nu(0) = \frac{1}{\sqrt{3}} J_\nu(0) = \frac{a}{\sqrt{3}} + \frac{p_\nu - \sqrt{3}a}{3(1+\sqrt{\lambda_\nu})} = \frac{p_\nu + a\sqrt{3\lambda_\nu}}{3(1+\sqrt{\lambda_\nu})}$$

Residual flux of the line

$$H_\nu(0) = \frac{p_\nu + a\sqrt{3\lambda_\nu}}{3(1+\sqrt{\lambda_\nu})}$$

$B_\nu = a + b\tau_c \quad \beta_\nu \equiv \frac{\alpha_\nu^L}{\alpha_\nu^C} \quad \tau_c = \frac{\tau_\nu}{1+\beta_\nu}$

$$p_\nu \equiv \frac{b}{1+\beta_\nu} \qquad \lambda_\nu \equiv \frac{1+\zeta\beta_\nu}{1+\beta_\nu}$$

Residual flux (relative intensity)

$$r_\nu = \frac{F_\nu}{F_c} = \frac{H_\nu(0)}{H_c(0)}$$

for continuum H_c: $\beta_\nu = 0 \quad \Rightarrow \quad p_\nu = b \quad \lambda_\nu = 1$

$$H_c(0) = \frac{1}{3}\frac{(b + a\sqrt{3})}{2}$$

$$r_\nu = 2\frac{p_\nu + a\sqrt{3\lambda_\nu}}{(1+\sqrt{\lambda_\nu})(b+a\sqrt{3})}$$

Non-negligible scattering in continuum

$$H_\nu(0) = \frac{p_\nu + a\sqrt{3\lambda_\nu}}{3(1+\sqrt{\lambda_\nu})}$$

$B_\nu = a + b\tau_c \quad \beta_\nu \equiv \frac{\alpha_\nu^L}{\alpha_\nu^C} \quad \tau_c = \frac{\tau_\nu}{1+\beta_\nu}$

$$p_\nu \equiv \frac{b}{1+\beta_\nu} \quad \lambda_\nu \equiv \frac{\zeta^C + \zeta^L\beta_\nu}{1+\beta_\nu}$$

for continuum H_c: $\beta_\nu = 0 \quad \Rightarrow \quad p_\nu = b \quad \lambda_\nu = \zeta^C$

without proof

$$H_c(0) = \frac{(b + a\sqrt{3\zeta^C})}{3(1+\sqrt{\zeta^C})}$$

$$r_\nu = \left(\frac{p_\nu + a\sqrt{3\lambda_\nu}}{b + a\sqrt{3\zeta^C}}\right)\left(\frac{1+\sqrt{\zeta^C}}{1+\sqrt{\lambda_\nu}}\right)$$

Various special cases

$$r_\nu = 2\frac{p_\nu + a\sqrt{3\lambda_\nu}}{(1+\sqrt{\lambda_\nu})(b+a\sqrt{3})}$$

$$B_\nu = a + b\tau_c \qquad \beta_\nu \equiv \frac{\alpha_\nu^L}{\alpha_\nu^C} \qquad \tau_c = \frac{\tau_\nu}{1+\beta_\nu}$$

$$p_\nu \equiv \frac{b}{1+\beta_\nu} \qquad \lambda_\nu \equiv \frac{1+\zeta\beta_\nu}{1+\beta_\nu}$$

This general result contains interesting behaviours in various special cases:

a) case $\zeta = 1$ (LTE: pure absorption lines)

b) case $\zeta = 0$ (extreme non-LTE: pure scattering lines)

c) Schuster Mechanism: Line Emission from Continuum Scattering Layer

$$r_\nu = \left(\frac{p_\nu + a\sqrt{3\lambda_\nu}}{b + a\sqrt{3\zeta^C}}\right)\left(\frac{1+\sqrt{\zeta^C}}{1+\sqrt{\lambda_\nu}}\right)$$

Pure absorption lines (LTE)

$$r_\nu = 2\frac{p_\nu + a\sqrt{3\lambda_\nu}}{(1+\sqrt{\lambda_\nu})(b+a\sqrt{3})}$$

$$B_\nu = a + b\tau_c \qquad \beta_\nu \equiv \frac{\alpha_\nu^L}{\alpha_\nu^C} \qquad \tau_c = \frac{\tau_\nu}{1+\beta_\nu}$$

$$p_\nu \equiv \frac{b}{1+\beta_\nu} \qquad \lambda_\nu \equiv \frac{1+\zeta\beta_\nu}{1+\beta_\nu}$$

a) pure absorption in line: $\zeta = 1$

$$\lambda_\nu \equiv \frac{1+\zeta\beta_\nu}{1+\beta_\nu} = 1 \quad \Rightarrow \quad r_\nu = \frac{p_\nu + a\sqrt{3}}{b+a\sqrt{3}} = \frac{\frac{b}{1+\beta_\nu} + a\sqrt{3}}{b+a\sqrt{3}}$$

For strong lines: $\beta_\nu \gg 1$

$$r_\nu = \frac{a\sqrt{3}}{b+a\sqrt{3}} = \frac{a}{b/\sqrt{3}+a} = \frac{B_\nu(\tau_\nu = 0)}{B_\nu(\tau_\nu = 1/\sqrt{3})} \neq 0$$

For grey atmosphere, strongest lines:

$$S_\lambda(\tau_\lambda) = \frac{3}{4\pi}(\tau_\lambda + \frac{2}{3})F_\lambda(0)$$

a/b=2/3 → $r_\nu \approx 0.54$

Non-zero because we see B_ν at upper level with non-zero temperature

Thus, in LTE, the residual flux is non-zero even for strong absorption lines. However, resonance lines such as Na D have R~10^{-3} – 10^{-4}

Pure scattering lines (extreme NLTE)

$$r_\nu = 2\frac{p_\nu + a\sqrt{3\lambda_\nu}}{(1+\sqrt{\lambda_\nu})(b+a\sqrt{3})}$$

$$B_\nu = a + b\tau_c \qquad \beta_\nu \equiv \frac{\alpha_\nu^L}{\alpha_\nu^C} \qquad \tau_c = \frac{\tau_\nu}{1+\beta_\nu}$$

$$p_\nu \equiv \frac{b}{1+\beta_\nu} \qquad \lambda_\nu \equiv \frac{1+\zeta\beta_\nu}{1+\beta_\nu}$$

b) pure scattering in line: $\zeta = 0$

$$\lambda_\nu \equiv \frac{1+\zeta\beta_\nu}{1+\beta_\nu} = \frac{1}{1+\beta_\nu}$$

$$r_\nu = 2\frac{\frac{b}{1+\beta_\nu} + a\sqrt{\frac{3}{1+\beta_\nu}}}{(1+\sqrt{\frac{1}{1+\beta_\nu}})(b+a\sqrt{3})}$$

For strong lines: $\beta_\nu \gg 1$, $r_\nu \to 0$

Scattering removes all photons → no photon emerges from surface. Cores of strong scattering lines are **dark**!

The residual flux Rx vs frequency x

$\zeta = 1$ (LTE)

$\zeta = 0$ (non-LTE)

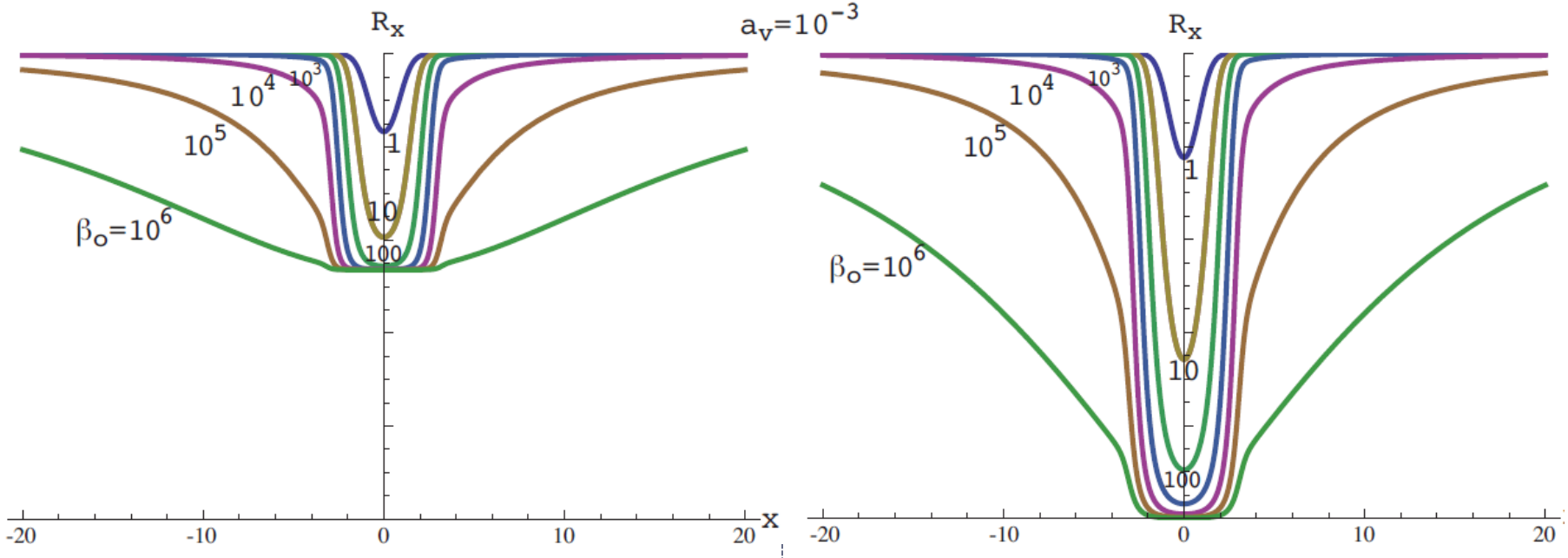

The residual flux Rx vs frequency x

$\zeta = 1$ (LTE)

$\zeta = 0$ (non-LTE)

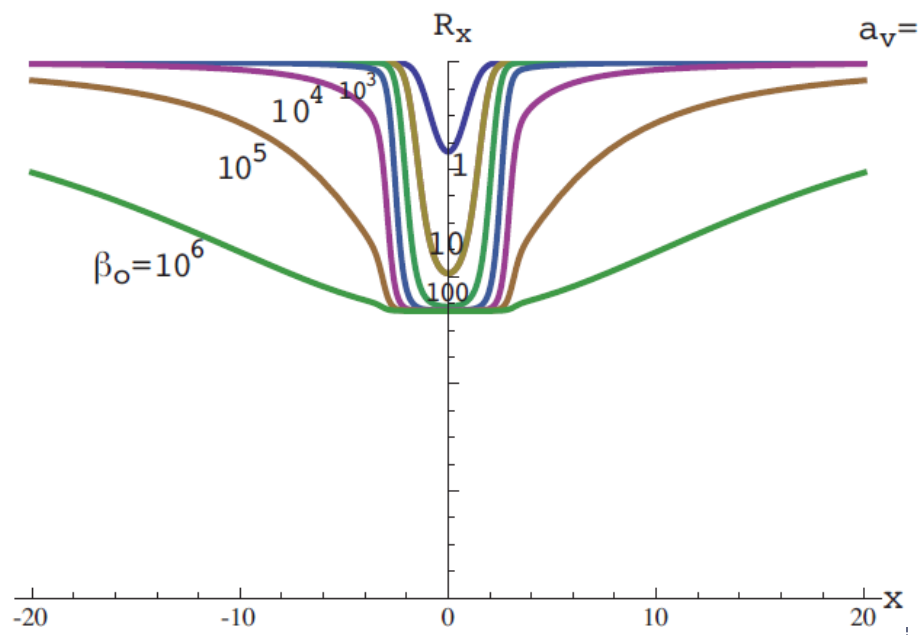

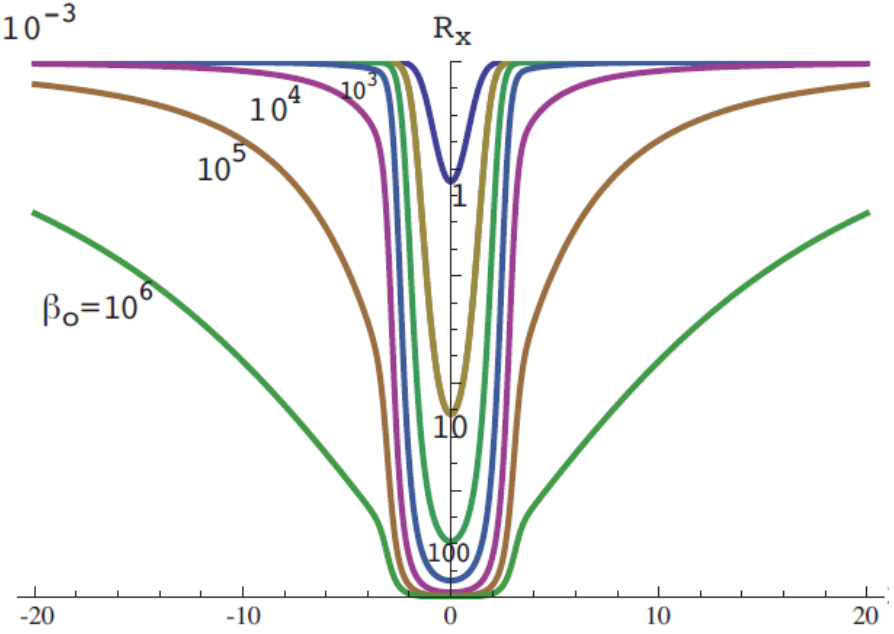

In LTE, the residual flux is non-zero even for strong absorption lines because we see the star surface with non-zero temperature.

In non-LTE, no photon emerges from surface due to scattering. Cores of strong scattering lines are **dark**!

Line emission from continuum scattering layer

$$r_\nu = \left(\frac{p_\nu + a\sqrt{3\lambda_\nu}}{b + a\sqrt{3\zeta^C}}\right)\left(\frac{1+\sqrt{\zeta^C}}{1+\sqrt{\lambda_\nu}}\right)$$

$$B_\nu = a + b\tau_c \qquad \beta_\nu \equiv \frac{\alpha_\nu^L}{\alpha_\nu^C} \qquad \tau_c = \frac{\tau_\nu}{1+\beta_\nu}$$

$$p_\nu \equiv \frac{b}{1+\beta_\nu} \qquad \lambda_\nu \equiv \frac{\zeta^C + \zeta^L\beta_\nu}{1+\beta_\nu}$$

c) pure scattering in continuum: $\zeta^C = 0$

$$\lambda_\nu \equiv \frac{\zeta^C + \zeta^L\beta_\nu}{1+\beta_\nu} = \frac{\zeta^L\beta_\nu}{1+\beta_\nu} \quad \Rightarrow \quad r_\nu = \frac{\frac{1}{1+\beta_\nu} + \frac{a}{b}\sqrt{3\lambda_\nu}}{1+\sqrt{\lambda_\nu}}$$

If the line opacity is also pure scattering, $\zeta^L = 0$, then $\lambda_\nu = 0$ $\quad r_\nu = \dfrac{1}{1+\beta_\nu} < 1$

always in absorption

But for $\zeta^L = 1$ and for strong lines $\beta_\nu \gg 1$ $\quad r_\nu \to \dfrac{\sqrt{3}a}{2b}$

For a weak temperature gradient with small b/a, can exceed unity, implying a net line emission instead of absorption.

Line profiles for Schuster model

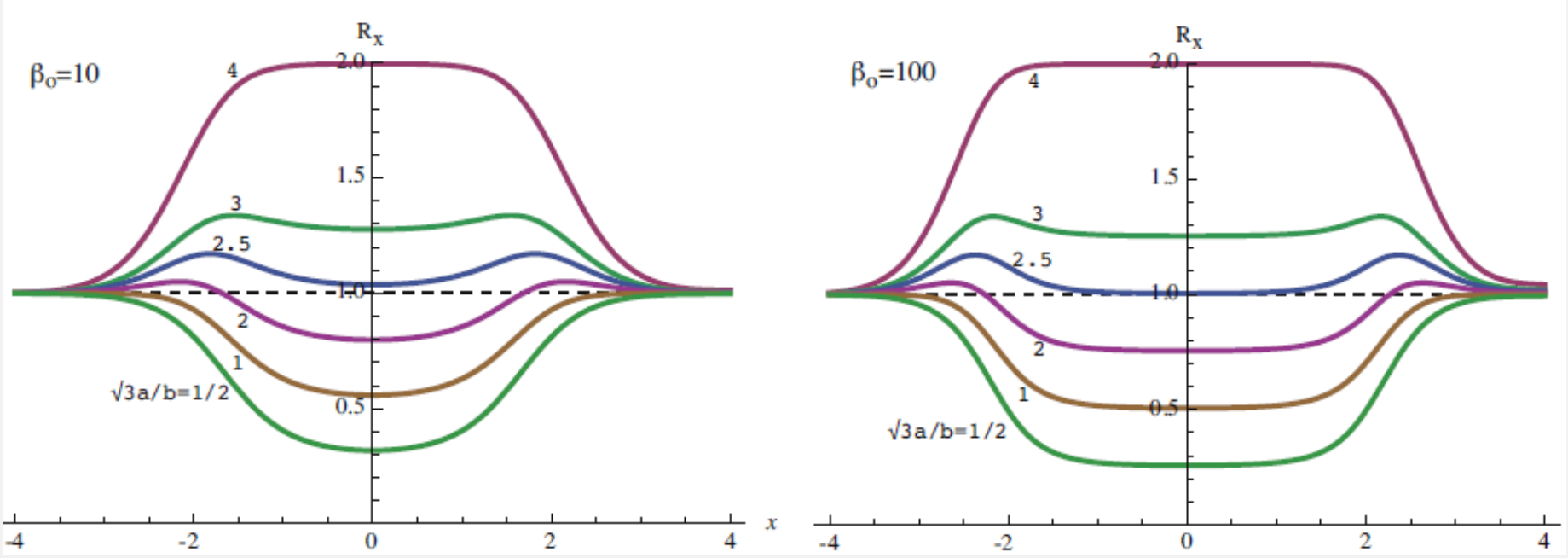

Scattering makes the continuum source function low near the surface, $S_c(0) - J_c(0) \ll B(0)$, which implies a weak continuum flux. The line can potentially be brighter, but only if the decline from the negative temperature gradient term is not too steep.

Summary

- We obtained Transfer Equation including lines and taking into account Scattering in lines.
- We solved it using the Milne-Eddington model.
- We then obtained Residual flux of the line.
- Finally, we discussed interesting special cases such as pure absorption and pure scattering lines.
- We also tried to explain emission lines applying Schuster mechanism for line emission.

Comparison of induced and spontaneous emission

There was a home work:

- When (at what temperatures, wavelengths) is spontaneous or induced emission stronger?

  Assume LTE (blackbody)

Spontaneous & Stimulated emission

Spontaneous emission

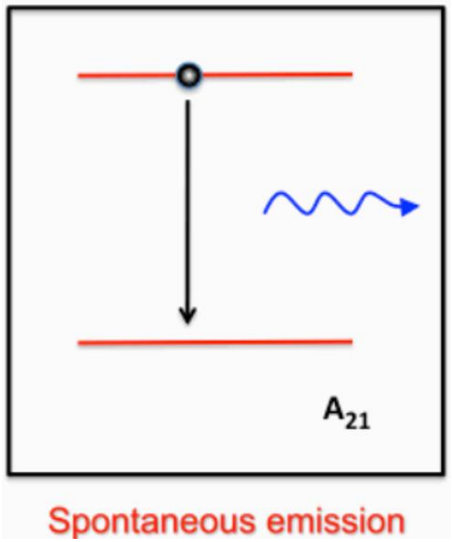

- The system goes from an upper level *u* to a lower level *l* spontaneously.
- Occurs independently of the radiation field.
- Emits **isotropically**.

Stimulated emission

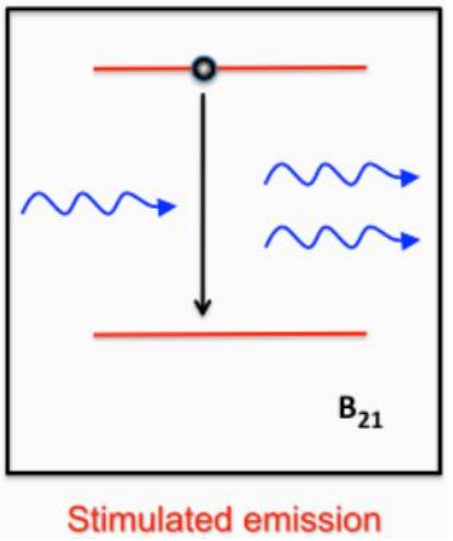

- The system goes from an upper level *u* to a lower level *l* stimulated by the presence of a radiation field ($h\nu$ corresponding to the energy difference between levels *u* and *l*).
- Stimulated emission occurs into the **same** state (frequency, direction, polarization) as the photon that stimulated the emission.

Relation between Einstein coefficients

$$\frac{A_{21}}{B_{21}} = \frac{2h\nu_{21}^3}{c^2} \quad \rightarrow \quad A_{21} = B_{21}\frac{2h\nu_{21}^3}{c^2}$$

$$\frac{g_1 B_{12}}{g_2 B_{21}} = 1 \quad \rightarrow \quad g_1 B_{12} = g_2 B_{21}$$

Einstein's coefficients concern the probability that a particle spontaneously emits a photon, the probability to absorb a photon, and the probability to emit a photon under the influence of another incoming photon.
Einstein's coefficients are valid for all radiation fields.

Induced and Spontaneous emission

When is spontaneous emission stronger?

Total amount of emitted photons per unit time at a given frequency is

Spontaneous emission: $\eta_{sp}=n_2A_{21}$

Stimulated emission: $\eta_{st}=n_2B_{21}J_\nu$

$$A_{21} = B_{21}\frac{2h\nu_{21}^3}{c^2}$$

$$g_1B_{12} = g_2B_{21}$$

$$\frac{\eta_{sp}}{\eta_{st}} = \frac{n_2A_{21}}{n_2B_{21}J} = \frac{2h\nu_{21}^3}{c^2J}$$

$$B_\nu(T) = \frac{2h\nu_{21}^3}{c^2}\left(e^{\frac{h\nu_{21}}{kT}} - 1\right)^{-1}$$

TE: blackbody, $J=B_\nu(T)$

$$\frac{\eta_{sp}}{\eta_{st}} = e^{\frac{h\nu_{21}}{kT}} - 1$$

$$e^{\frac{h\nu_{21}}{kT}} \geq 2 \quad \Rightarrow \quad h\nu_{21} \geq kT\ln 2 \quad \Rightarrow \quad \lambda_* \leq \frac{hc}{kT\ln 2} = \frac{2.076\times 10^8}{T}\text{ Å}$$

At wavelengths shorter than λ_* spontaneous emission is dominant

T=5777K → λ_*≈41000 Å λ_*=6563 Å → T≈31600K λ_*=4340Å → T≈48000K

Non-LTE

NON-LTE
STATISTICAL EQUILIBRIUM
TWO-LEVEL APPROXIMATION
THE LINE SOURCE FUNCTION
LTE VERSUS NON-LTE

From the previous lecture

$\zeta = 1$ (LTE)

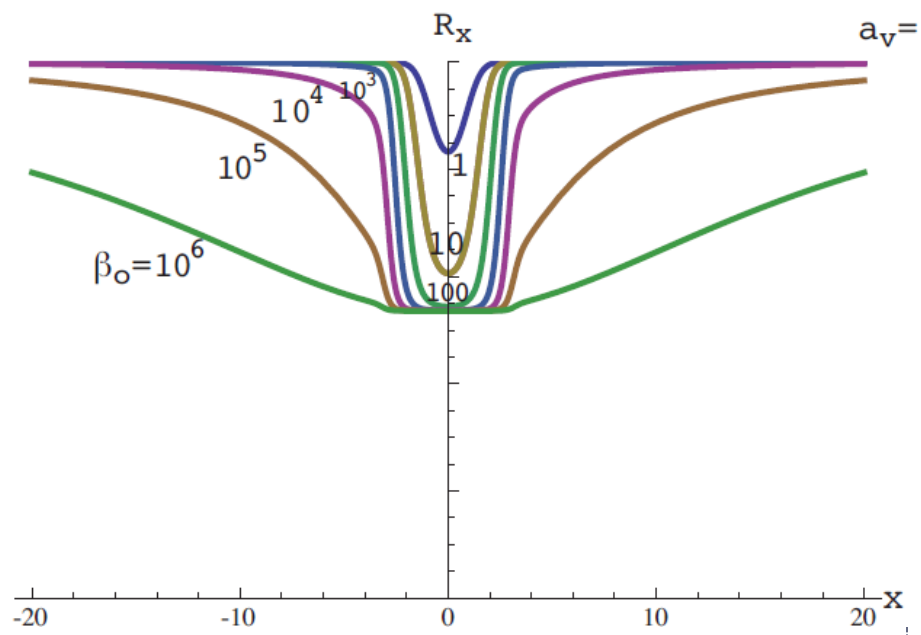

In LTE, the residual flux is non-zero even for strong absorption lines because we see the star surface with non-zero temperature.

$\zeta = 0$ (non-LTE)

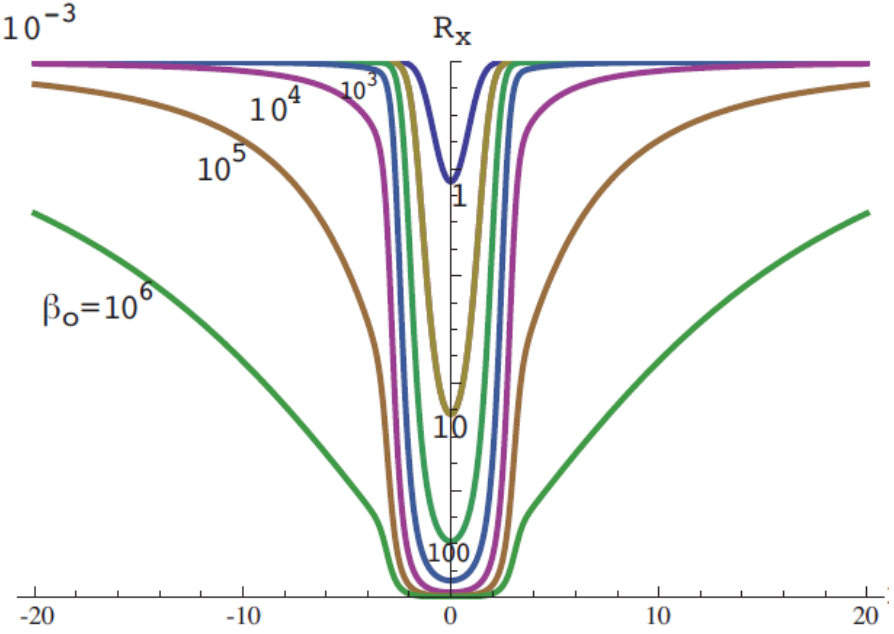

In non-LTE, no photon emerges from surface due to scattering. Cores of strong scattering lines are **dark**!

LTE versus non-LTE?

- Most studies of stellar atmospheres are performed under LTE, where the thermodynamic state of the plasma is described via the Saha-Boltzmann equation as a function of local T and N_e. However, LTE strictly holds only deep in the interior when collisions dominate, and the photon mean-free-path is small.

- For a more accurate physical description, the non-local nature of the radiation field and its interaction with the plasma must be accounted for. This requires consideration of the detailed atomic processes for excitation and ionization, as expressed in the rate equations of statistical equilibrium (non-LTE case).

- Departure coefficients b = pop(non-LTE)/pop(LTE)

What does non-LTE mean?

The level populations of atoms are governed by the rates of all (collisional and radiative) processes, by which an atom leaves a certain state i to some other state j (if bound) or k (if unbound) and vice versa.

Bound-bound	Bound-free
RADIATIVE	
Photoabsorption (R_{ij})	Photoionization (R_{ik})
Spontaneous + stimulated emission (R_{ji})	Spontaneous + stimulated recombination (R_{ki})
COLLISIONAL	
Excitation (C_{ij})	Ionization (C_{ik})
De-excitation (C_{ji})	Recombination (C_{ki})

The total upward rate $P_{ij}=C_{ij}+R_{ij}$, whilst the total downward rate is $P_{ji}=C_{ji}+R_{ji}$

LTE vs NLTE

- LTE: population numbers follow Saha-Boltzmann Equation
  $n_i = n_i(T, n_e)$
- NLTE: population numbers depend on radiation field
  $n_i = n_i(T, n_e, J)$
- Need to take into account the sum of all processes that decrease and increase population for a given level i:

$$\frac{d}{dt} n_i = \sum_{j \neq i} n_j P_{ji} - n_i \sum_{j \neq i} P_{ij}$$

In stellar atmospheres typically:
$dn_i / dt = 0$ (stationary)

Complete rate equations

For each atomic level i of each ion, of each chemical element we have:

$$-n_i\left[\sum_{j>i}\left(R_{ij}+C_{ij}\right)+\sum_{j<i}\left(R_{ij}+C_{ij}\right)\right]+\sum_{j>i}n_j\left(R_{ji}+C_{ji}\right)+\sum_{j<i}n_j\left(R_{ji}+C_{ji}\right)=\frac{dn_i}{dt}$$

- $\uparrow$ excitation and ionization
- $\leftarrow$ rates out of i
- $\downarrow$ de-excitation and recombination

- $\uparrow$ de-excitation and recombination
- $\leftarrow$ rates into i
- $\downarrow$ excitation and ionization

In steady-state, $dn_i/dt=0$

Statistical equilibrium

- Statistical equilibrium, also known as rate equations:

$$\frac{dn_i}{dt} = \sum_{j\neq i}^{N} n_j P_{ji} - n_i \sum_{j\neq i}^{N} P_{ij} =$$

$$= \sum_{j\neq i}^{N} n_j \left(R_{ji} + C_{ji}\right) + n_p (R_{ki} + C_{ki}) - n_i \sum_{j\neq i}^{N} \left(R_{ij} + C_{ij}\right) - n_i (R_{ik} + C_{ik}) = 0$$

Lines Recombination Lines Ionization

- Particle conservation: $\sum_{i=1}^{N} n_i = n_T$

- By "non-LTE", we refer to the solution of these equations of statistical equilibrium or rate equations. This is **much** more challenging computationally than LTE…
- Rate equations represent a non-linear system of equations, we look for the solution vector via linearization, based on Newton-Raphson iteration.

Two-level approximation

Let's consider schematic line-formation cases with easy solution.

Consider an atomic model with only **two** important levels: lower *l* and upper *u*.

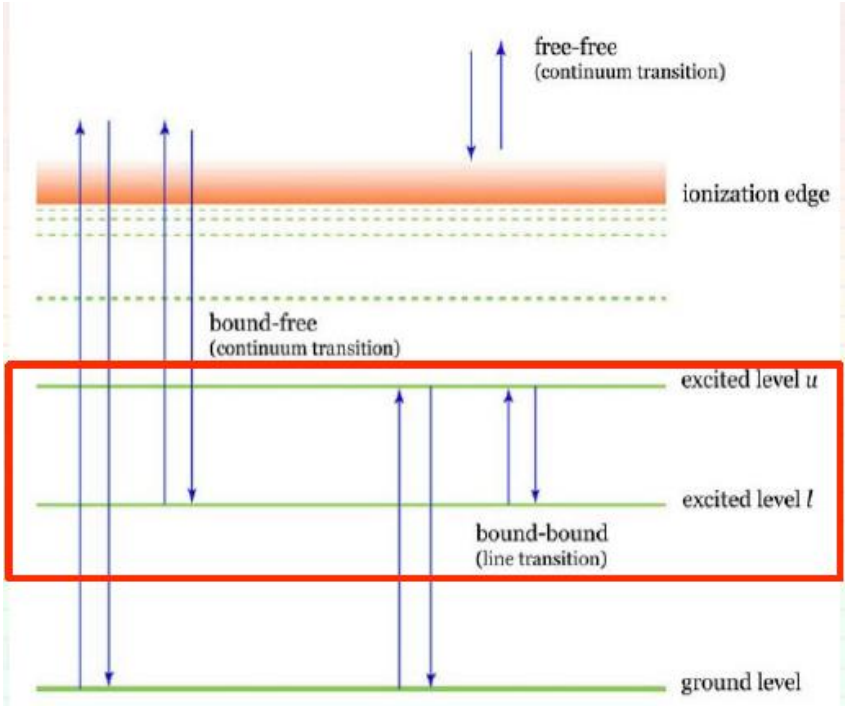

It is highly simplified:

not accurate, but provide insight into the mechanisms at work in real stellar atmospheres.
It well approximates the situation for some lines, *e.g.* resonance lines from the ground state.

Two-level approximation

Rate equations (statistical equilibrium: for a given level ***i*** the rate of transitions **out** = rate of transitions **in**)

$$n_i \sum_{j\neq i}^{N} (R_{ij} + C_{ij}) - n_i(R_{ik} + C_{ik}) = \sum_{j\neq i}^{N} n_j(R_{ji} + C_{ji}) + n_p(R_{ki} + C_{ki})$$

Lines | Ionization | Lines | Recombination

Consider two levels u and l: **isolating** the transitions between them:

$$n_l(R_{lu}+C_{lu}) + n_l \sum_{j\neq l,u} (R_{lj}+C_{lj}) + n_l(R_{lk}+C_{lk}) = n_u(R_{ul}+C_{ul}) + \sum_{j\neq l,u} n_j(R_{jl}+C_{jl}) + n_p(R_{kl}+C_{kl})$$

and **neglecting** all transitions involving $j \neq l,u$, plus recombinations/ionizations:

$$n_l(R_{lu} + C_{lu}) = n_u(R_{ul} + C_{ul})$$

Two-level approximation

$$n_l(R_{lu} + C_{lu}) = n_u(R_{ul} + C_{ul})$$

Einstein coefficients:
$n_l B_{lu} J_\nu = n_u A_{ul} + n_u B_{ul} J_\nu$

substituting for the *R* coefficients:

$$n_l\left(B_{lu}\int_0^\infty \varphi_\nu J_\nu d\nu + C_{lu}\right) = n_u\left(A_{ul} + B_{ul}\int_0^\infty \varphi_\nu J_\nu d\nu + C_{ul}\right)$$

Transition Probabilities: Radiative Processes

$$R_{ij} = B_{ij}\int_0^\infty \varphi_{ij}(\nu)\ J_\nu\, d\nu$$

Absorption

$$R_{ji} = A_{ji} + B_{ji}\int_0^\infty \varphi_{ij}(\nu)\ J_\nu\, d\nu$$

Spontaneous and stimulated Emission

Two-level approximation

$$n_l(R_{lu} + C_{lu}) = n_u(R_{ul} + C_{ul})$$

Einstein coefficients:
$n_l B_{lu} J_\nu = n_u A_{ul} + n_u B_{ul} J_\nu$

substituting for the *R* coefficients:

$$n_l\left(B_{lu}\int_0^\infty \varphi_\nu J_\nu d\nu + C_{lu}\right) = n_u\left(A_{ul} + B_{ul}\int_0^\infty \varphi_\nu J_\nu d\nu + C_{ul}\right)$$

Sanity check:
LTE case

assuming collision rates dominate over radiative rates $n_l C_{lu} = n_u C_{ul}$

remembering that $C_{lu} = \left(\frac{n_u}{n_l}\right)^* C_{ul} = \frac{g_u}{g_l} e^{-E_{ul}/kT} C_{ul}$

$$\Longrightarrow \quad n_l \frac{g_u}{g_l} e^{-E_{ul}/kT} C_{ul} = n_u C_{ul}$$

$$\Longrightarrow \quad \frac{n_u}{n_l} = \frac{g_u}{g_l} e^{-E_{ul}/kT} = \left(\frac{n_u}{n_l}\right)^{\mathrm{LTE}}$$

Calculation of the line source function

$$\alpha_\nu^{line} = (n_l B_{lu} - n_u B_{ul}) J_\nu \qquad \varepsilon_\nu^{line} = n_u A_{ul} J_\nu$$

$$S_\nu^{line} = \frac{\varepsilon_\nu^{line}}{\alpha_\nu^{line}} = \frac{n_u A_{ul}}{n_l B_{lu} - n_u B_{ul}} = \frac{A_{ul}}{\frac{n_l}{n_u} B_{lu} - B_{ul}}$$

Einstein Coefficients:

$$B_{lu} = \frac{g_u}{g_l} B_{ul} \qquad A_{ul} = \frac{2h\nu^3}{c^2} B_{ul}$$

$$S_\nu^{\text{line}} = \frac{2h\nu^3}{c^2} \frac{1}{\frac{n_l g_u}{n_u g_l} - 1}$$

Note: this is the general expression for the line source function in **NLTE**.
We have not made use of any equilibrium condition.
It is always valid (not only in 2-level approximation).
What is different in the general case, is how n_l and n_u are computed.

Calculation of the line source function

If we substitute $\frac{n_u}{n_l} = \frac{g_u}{g_l} e^{-E_{ul}/kT} = \left(\frac{n_u}{n_l}\right)^*$ $\qquad E = h\nu$

we recover the Planck function $S_\nu^{\text{line}} = \frac{2h\nu^3}{c^2} \frac{1}{e^{h\nu/kT} - 1} = B_\nu(T)$

For the 2-level atom we found $n_l(B_{lu} \int_0^\infty \varphi_\nu J_\nu d\nu + C_{lu}) = n_u(A_{ul} + B_{ul} \int_0^\infty \varphi_\nu J_\nu d\nu + C_{ul})$

$$\frac{n_l}{n_u} = \frac{1 + \frac{c^2}{2h\nu^3} \int \varphi_{\nu'} J_{\nu'} d\nu' + C_{ul}/A_{ul}}{\frac{g_u}{g_l} \left[\frac{c^2}{2h\nu^3} \int \varphi_{\nu'} J_{\nu'} d\nu' + e^{-h\nu/kT} C_{ul}/A_{ul}\right]}$$

Calculation of the line source function

Substituting n_l/n_u in S_ν:

$$S_\nu^{\text{line}} = \frac{2h\nu^3}{c^2}\frac{1}{\frac{n_l g_u}{n_u g_l} - 1}$$

$$S_\nu^{\text{line}} = \frac{2h\nu^3}{c^2}\frac{\frac{c^2}{2h\nu^3}\int \varphi_{\nu'} J_{\nu'} d\nu' + e^{-h\nu/kT} C_{ul}/A_{ul}}{1 + \frac{C_{ul}}{A_{ul}}(1 - e^{-h\nu/kT})} =$$

$$= \underbrace{\frac{1}{1 + \frac{C_{ul}}{A_{ul}}(1 - e^{-h\nu/kT})}}_{1 - \varepsilon} \int \varphi_{\nu'} J_{\nu'} d\nu' + \underbrace{\frac{2h\nu^3}{c^2}\frac{e^{-h\nu/kT} C_{ul}/A_{ul}}{1 + \frac{C_{ul}}{A_{ul}}(1 - e^{-h\nu/kT})}}$$

$$\frac{2h\nu^3}{c^2}\frac{1}{e^{h\nu/kT} - 1} \quad \underbrace{\frac{(1 - e^{-h\nu/kT}) C_{ul}/A_{ul}}{1 + \frac{C_{ul}}{A_{ul}}(1 - e^{-h\nu/kT})}}$$

$\downarrow$

$B_\nu(T)$

:= ε

The line source function (1)

scattering term

thermal term

$$S_\nu^{\text{line}} = (1-\epsilon)\int_0^\infty \varphi_{\nu'} J_{\nu'} d\nu' + \epsilon\, B_\nu(T) = \frac{\int_0^\infty \varphi_{\nu'} J_{\nu'} d\nu' + \epsilon'\, B_\nu(T)}{1+\epsilon'}$$

$$\epsilon := \frac{\left(1-e^{-h\nu/kT}\right) C_{ul}/A_{ul}}{1+\frac{C_{ul}}{A_{ul}}\left(1-e^{-h\nu/kT}\right)} = \frac{\epsilon'}{1+\epsilon'}$$

destruction probability

Photons are either destroyed into thermal pool or scattered photons are created in thermal processes

From the previous lecture:

$$\boldsymbol{S(\tau) = \zeta B + (1-\zeta)\, J(\tau)}$$

absorption fraction $\zeta \equiv \frac{\alpha_{\text{abs}}}{\alpha_{\text{abs}} + \alpha_{\text{sc}}}$

Now we obtained that Line source function has similar terms except that we also allow for non-coherent scattering

The line source function (2)

$$\epsilon := \frac{\left(1 - e^{-h\nu/kT}\right) C_{ul}/A_{ul}}{1 + \frac{C_{ul}}{A_{ul}}\left(1 - e^{-h\nu/kT}\right)} = \frac{\epsilon'}{1+\epsilon'}$$

$$S_\nu^{\text{line}} = (1-\epsilon)\int_0^\infty \varphi_{\nu'} J_{\nu'} d\nu' + \epsilon\, B_\nu(T) = \frac{\int_0^\infty \varphi_{\nu'} J_{\nu'} d\nu' + \epsilon'\, B_\nu(T)}{1+\epsilon'}$$

Deep layers: collisions dominate → ε' >> 1 or ε = 1 thermal term dominant

$C_{ul} \gg A_{ul}$ ε = 1 → $S_\nu = B_\nu(T)$ **LTE**

Higher layers: collisions non-important → ε'≈0 or ε = 0 scattering term dominant

$C_{ul} \ll A_{ul}$ $\varepsilon \approx 0$ → $S_\nu = \int \varphi_{\nu'} J_{\nu'} d\nu'$ **Extreme non-LTE**

From the previous lecture: $S_\nu = J_\nu$ for pure *coherent* scattering
now $S_\nu = \int \varphi_{\nu'} J_{\nu'} d\nu'$ *non-coherent* scattering

Transition probabilities: collisions

- probability of collision between atom/ion (cross section σ) and colliding particles in time dt: ~ σ v dt

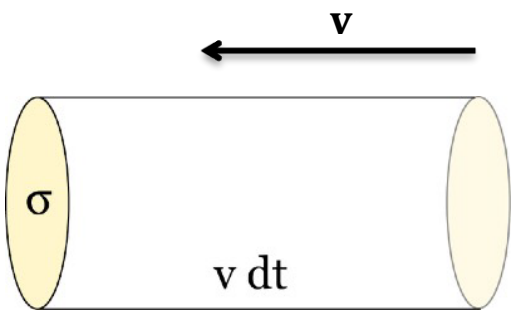

collision cylinder: all particles in that volume collide with target atom

- rate of collisions = flux of colliding particles relative to atom/ion (n_{coll} v) × cross section σ.

- for excitations: $$C_{ij} = n_{coll} \int_0^\infty \sigma_{ij}^{\mathrm{coll}}(v) v f(v) dv$$

- in a hot plasma free electrons dominate: $n_{coll} = n_e$

- f(v) dv is Maxwellian velocity distribution in stellar atmospheres established by e-e collisions.

Collisional rates (1)

For an electron with kinetic energy E exciting an atom

- Excitation:

$$C_{ij} = n_e \int_{E_{ij}}^{\infty} \sigma_{ij}(u) u f(u) du = n_e \int_{E_{ij}}^{\infty} \sigma_{ij}(E) \sqrt{\frac{2E}{m}} f(E) dE \propto \frac{n_e}{T^{3/2}} \int_{E_{ij}}^{\infty} \sigma_{ij}(E) e^{-E/kT} E\, dE \propto \frac{n_e}{T^{1/2}} e^{-E_{ij}/kT}$$

$$\sigma_{ij}(E) \propto 1/E$$

T is the kinetic temperature

- De-excitation:

$$C_{ji} = n_e \int_{0}^{\infty} \sigma_{ji}(u) u f(u) du = n_e \int_{0}^{\infty} \sigma_{ji}(E) \sqrt{\frac{2E}{m}} f(E) dE$$

where $f(E)$ is the (Maxwellian) energy distribution of the colliding particles.

- In TE, the principle of detailed balance gives

$$n_i C_{ij} = n_j C_{ji} \Rightarrow \frac{C_{ij}}{C_{ji}} = \frac{n_j}{n_i} = \frac{g_j}{g_i} e^{-E_{ij}/kT}$$

- Even if there is no TE, but we have a Maxwellian velocity distribution $\frac{C_{ij}}{C_{ji}} = \frac{g_j}{g_i} e^{-E_{ij}/kT}$

$$\frac{C_{ul}}{C_{lu}} = \frac{g_u}{g_l} e^{-(E_u - E_l)/kT}$$

Collisional rates (2)

$$\frac{C_{ul}}{C_{lu}} = \frac{g_u}{g_l} e^{-(E_u - E_l)/kT}$$

- Thus, if the excitations and de-excitations are due to collisions, the occupation numbers follow the Boltzmann formula for the kinetic temperature.
- We can conclude that in gases with high enough densities to make collisional excitations and de-excitations more important than the radiative processes, the occupation numbers follow the Boltzmann formula for the kinetic temperature.

- This means that the excitation temperature equals the kinetic temperature, which in turn means that the source function equals the Planck function for the kinetic temperature, which means

we have LTE.

Two-level approximation

- Moving outward in the photosphere scattering term dominates.
- At some point we reach the region where photons are being lost from the star (small optical depth)

→ J_ν decreases with height
→ S_ν decreases with height
→ absorption line

- line absorption coefficient larger at line center → see higher layers
- wings form in deeper layers than line core

Wing can form in LTE conditions whilst a line core in non-LTE

- 2-level atom is a special NLTE case
- In general, the coupling between J_ν, n_i and S_ν is far more complicated

NLTE: Occupation numbers (1)

We obtain a system of linear equations for n_i:

$$A \cdot \begin{pmatrix} n_1 \\ n_2 \\ \dots \\ n_p \end{pmatrix} = \mathbf{X}$$

Where matrix A contains terms:

$$\int_0^\infty \varphi_{ij}(\nu) \int_{4\pi} I_\nu(\omega) \frac{d\omega}{4\pi} d\nu$$

combine with equation of transfer:

$$\mu \frac{dI_\nu(\omega)}{dr} = -\kappa_\nu I_\nu(\omega) + \epsilon_\nu$$

$$\kappa_\nu = \sum_{i=1}^{N} \sum_{j=i+1}^{N} \sigma_{ij}^{\text{line}}(\nu) \left(n_i - \frac{g_i}{g_j} n_j \right) + \sum_{i=1}^{N} \sigma_{ik}(\nu) \left(n_i - n_i^* e^{-h\nu/kT} \right) + n_e n_p \sigma_{kk}(\nu, T) \left(1 - e^{-h\nu/kT} \right) + n_e \sigma_e$$

$$\epsilon_\nu = \dots$$

non-linear system of integro-differential equations

NLTE: Occupation numbers (2)

Iteration required:

radiative processes depend on radiation field

$$R_{ij} = B_{ij} \int_0^\infty \varphi_{ij}(\nu)\ J_\nu\, d\nu$$

radiation field depends on opacities

$$\mu \frac{dI_\nu(\omega)}{dr} = -\kappa_\nu I_\nu(\omega) + \epsilon_\nu$$

opacities depend on occupation numbers

$$\kappa_\nu^{\mathrm{b-f}} = n_l\ \sigma_{lk}(\nu)$$

requires database of atomic quantities: energy levels, transitions, cross sections

20...1000 levels per ion – 3-5 ionization stages per species – » 30 species

➔ fast algorithm to calculate radiative transfer required

LTE

LTE is a **good** approximation, if:

1) Collisional rates **dominate** for all transitions

$R_{ij} << C_{ij}$ so $P_{ij} (= R_{ij} + C_{ij}) \sim C_{ij}$

Since $C_{ij}/C_{ji} = (n_i/n_j)^*$

Solution of rate equations -> LTE

2) $J_\nu = B_\nu$ is a good approximation at all frequencies

$n_i R_{ij} = n_j R_{ji}$ so $n_i/n_j = (n_i/n_j)^*$

Solution of rate equations -> LTE

Non-LTE

LTE is a **bad** approximation, if:

1) Collisional rates are small
2) Radiative rates are large
3) Mean free path of photons is larger than that of electrons

- Large deviations from LTE may be expected for low density gas in which the radiation field deviates strongly from the Planck function for the kinetic temperature.
- Non-LTE needs to be considered for
  (a) hot stars, whose atmospheres are rapidly expanding
  (b) low density chromospheres and coronae of Solar-type stars
  (c) low $T_{\rm eff}$ of very cool stars (in which electron densities are low)
  (d) nebulae
  (e) ISM

Non-LTE effects in scattering

- Deep in the atmosphere, collisions are frequent, radiation field is close to Planck and populations follow Boltzmann law. → LTE.
- Close to the boundary, radiation can escape freely, density drops, collisional rates decrease, radiative rates are not enough to populate upper levels.
  As a result, the upper level can be underpopulated.
  Therefore, the source function deviates from Planck function.

- Even if the only scattering (no true absorption) occurs in the atmosphere, an absorption line forms.

LTE vs NLTE

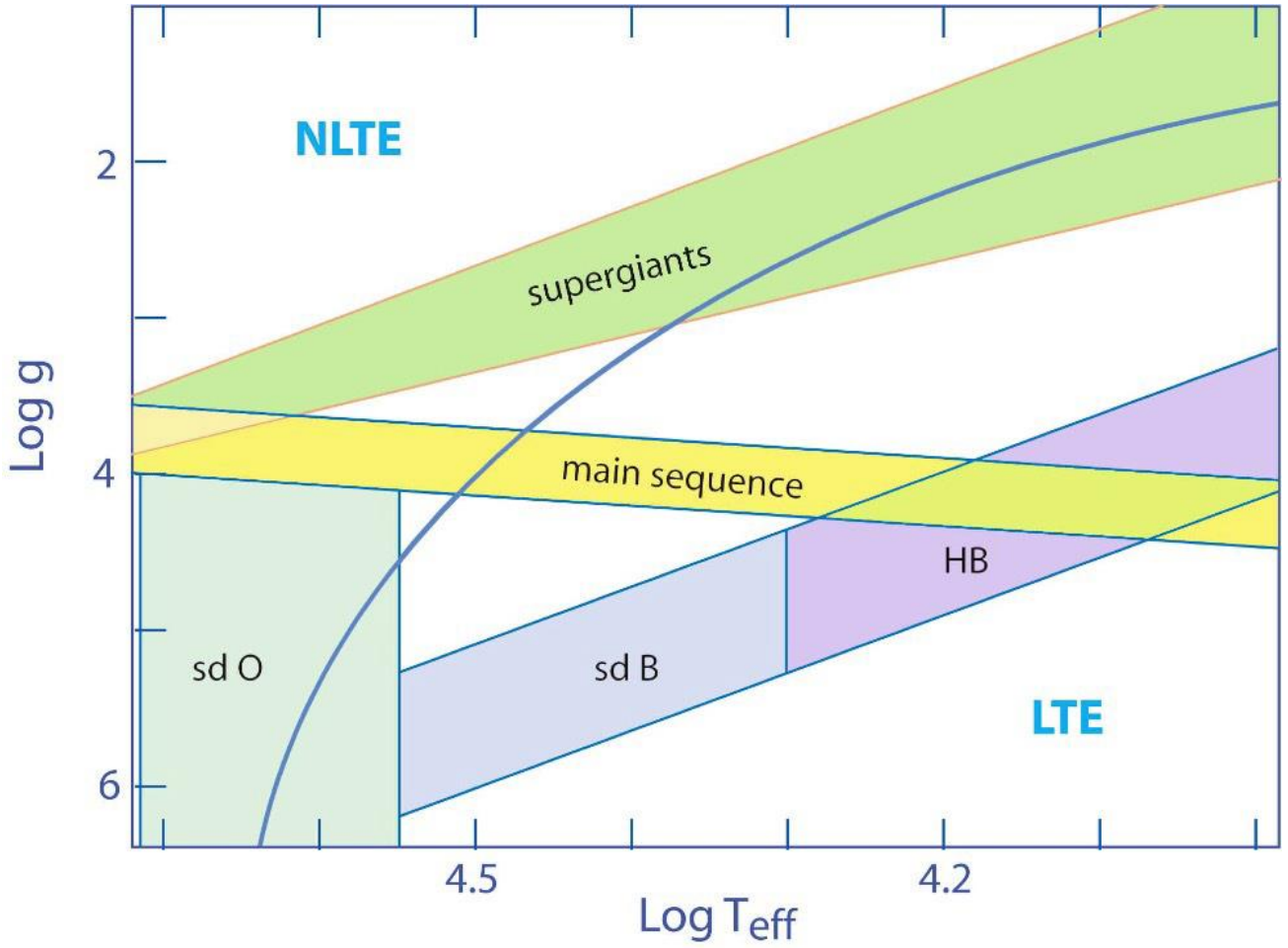
NLTE
supergiants
main sequence
HB
sd O
sd B
LTE
2
4
6
Log g
4.5
4.2
Log T_{eff}

Non-LTE in the Sun

- Chromosphere & corona in non-LTE, since the radiation field corresponds to a diluted Planck function for the effective temperature of the Sun, whilst the kinetic temperature in the coronae may be several 10^6 K.

- Photospheric departures from LTE occur.
  Weak lines of low-abundance species often show departures from LTE (e.g. they reverse to emission lines on the solar disc just inside the limb). Cores of strong lines may depart from LTE, while the wings may remain in LTE.

- Non-LTE is most relevant in the Solar context via inaccuracies in elemental abundances obtained with the LTE assumption (typically 0.05 dex), although effect is greatest from comparison between latest 3D vs earlier 1D models.

Solar Oxygen abundance

- Until recently, commonly adopted Solar oxygen abundance was log(O/H)+12=**8.93** suggested by analyses of [OI] 6300Å (Lambert 1978) and OH lines in IR using 1D LTE models.
- Asplund et al. (2004) has used 3D analyses of the [OI] and OH lines, revealing significant departures from LTE, indicating a much lower abundance of log(O/H)+12=**8.66**.
- Ar and Ne aren't seen in the Solar photosphere, so deduced from coronal material, relative to oxygen. The decrease in oxygen also causes Ar and Ne to be scaled down.

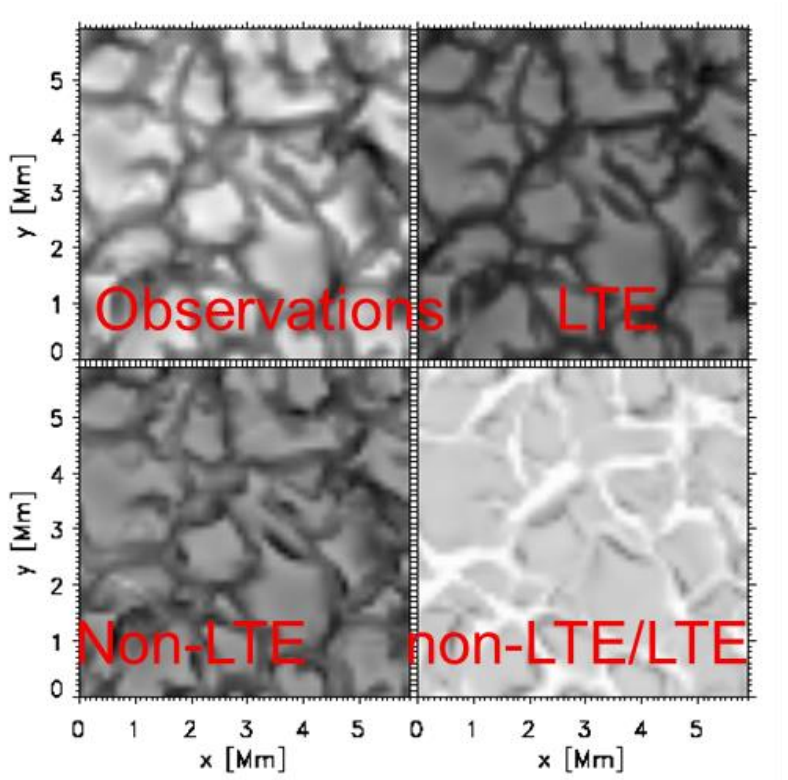

Consequences?

The Solar metal mass fraction **falls** from Z=0.019 to Z=0.013, reconciling some long-standing problems (e.g. agreement with local ISM abundances, e.g. Orion nebula), BUT there is now a helioseismology (sound speed, density below convective zone) discrepancy for the Sun, which can be reconciled in following ways:

- Missing opacity from OPAL calculations? Need 7% at log T=6.4, though new OP calculations suggest <2.5% missing in OPAL.
- Problems with diffusion in interior models?
- Problems with abundance of Ne (indirectly inferred from Ne/O in solar corona). Needs factor 3 increase!

Overall, experience from Solar analysis suggests that determination of stellar abundances may be less certain than is normally considered!

Non-LTE for hot stars

Radiation field is so intense in hot stars (O-type, OBA supergiants, WDs) that their populations are only weakly dependent on local (T_{eff}, N_e), consequently LTE represents a poor assumption.

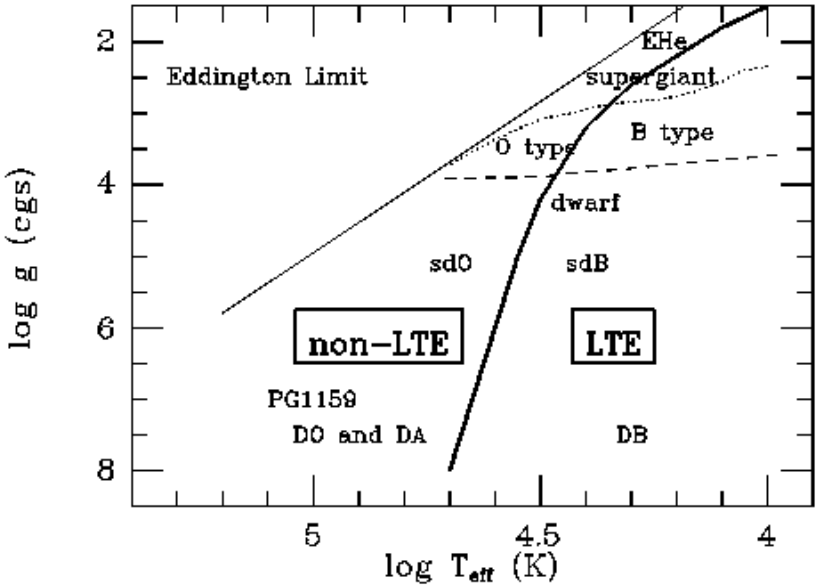

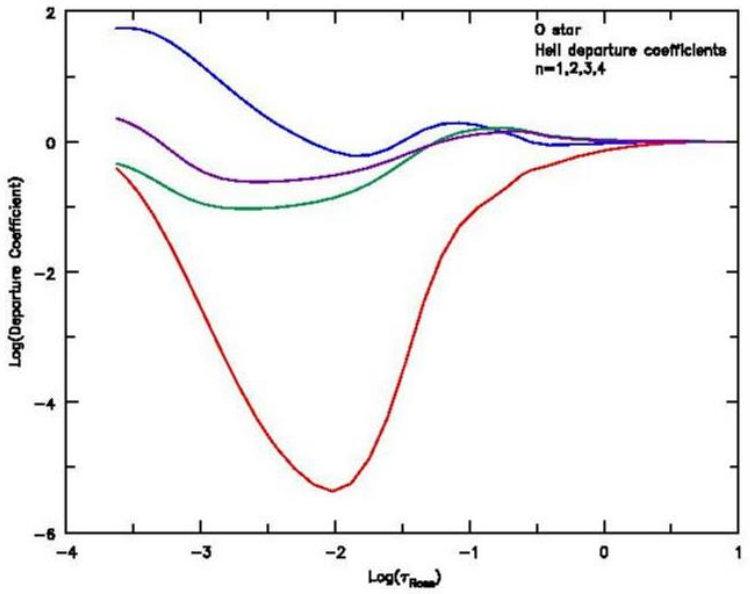

In O stars, LTE profiles are much too weak. Departure coefficients (non-LTE/LTE-pop) shown here for n=1,2,3,4 for HeII can differ greatly in wind and photosphere, making HeI & HeII lines *much* stronger.

LTE vs NLTE in hot stars

Difference between NLTE and LTE in Hγ line profile for an O-star model with T_{eff} = 45000K and log g = 4.5

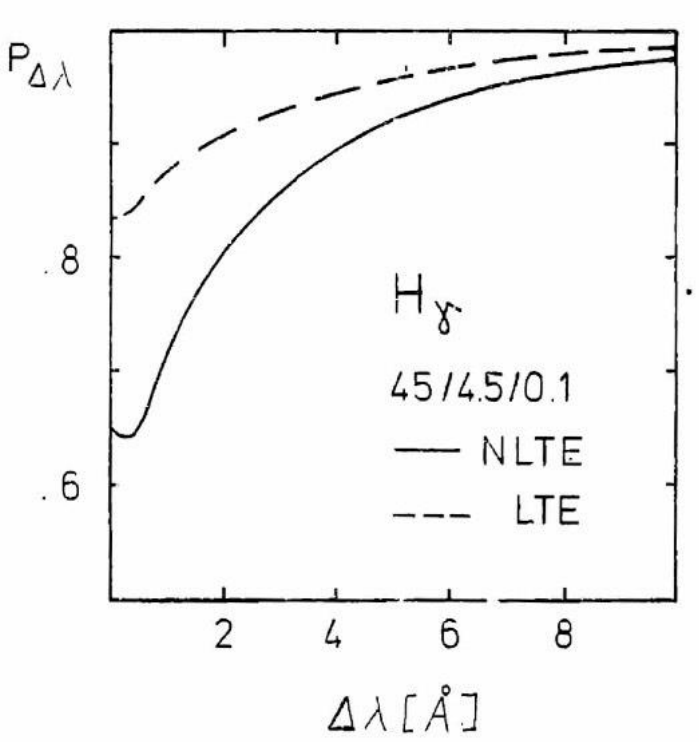

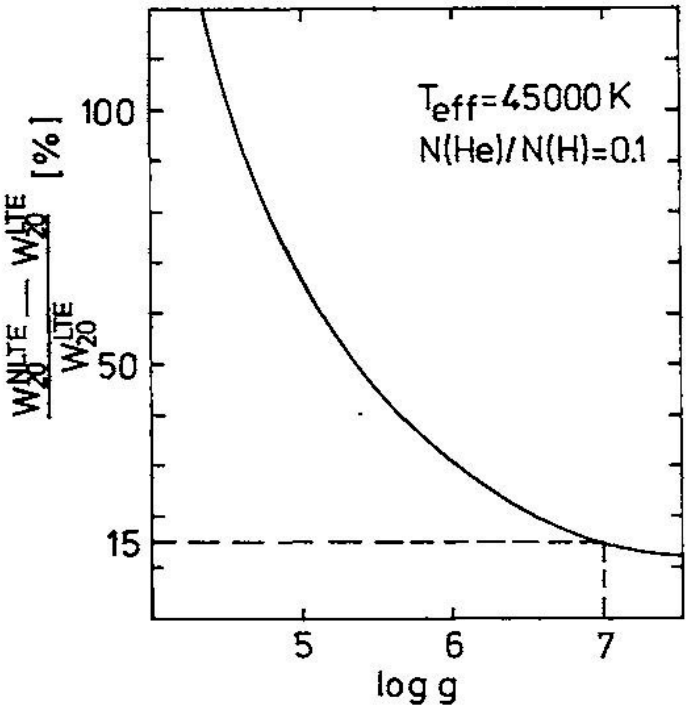

Difference between NLTE and LTE Hγ equivalent width as a function of log g for T_{eff} = 45,000 K for subluminous O stars

LTE vs NLTE: hydrogen lines in IR

Brackett lines

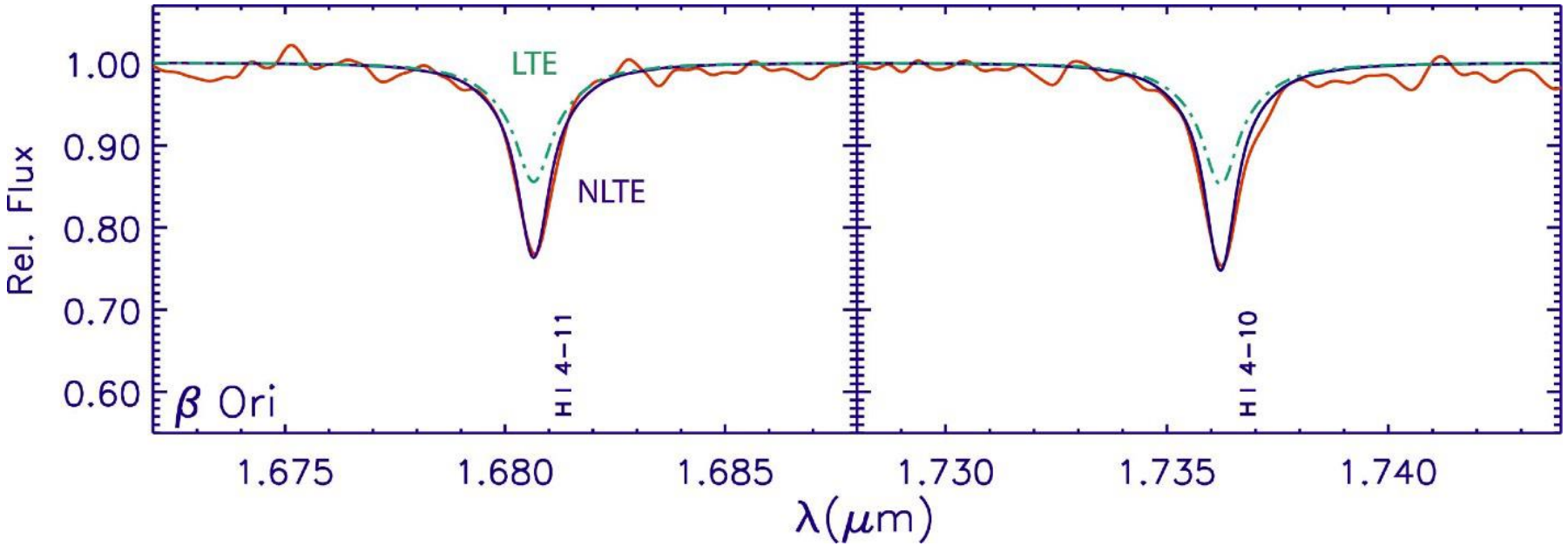

LTE vs NLTE: nitrogen lines

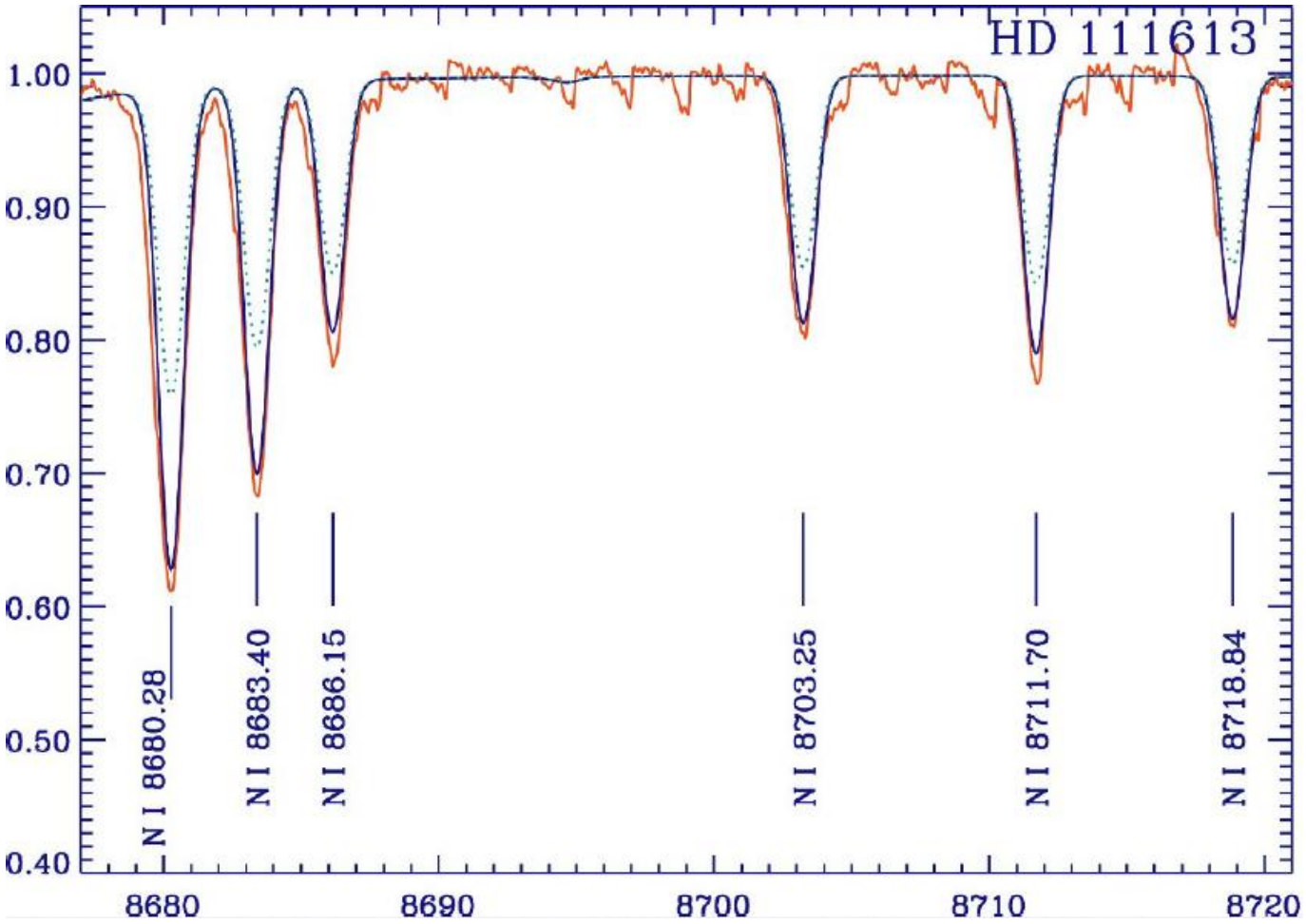

Non-LTE in OBA stars

- Hydrostatic equilibrium is invalid in OBA supergiants – their tenuous atmospheres lead to a drop in the line source function below LTE (Planckian) value.

- In the blue-violet spectra of B stars, some He I lines are formed in LTE, however red and IR lines are not collision dominated, instead photoionization-recombination processes dominate, so non-LTE is necessary.

- In A supergiants, reliable metal abundance determinations require non-LTE treatment – lines become stronger in non-LTE with corrections of up to factor of 10 for strong lines.

LTE vs NLTE in cool stars

LTE underpopulated

LTE overpopulated

LTE underpopulated

LTE overpopulated

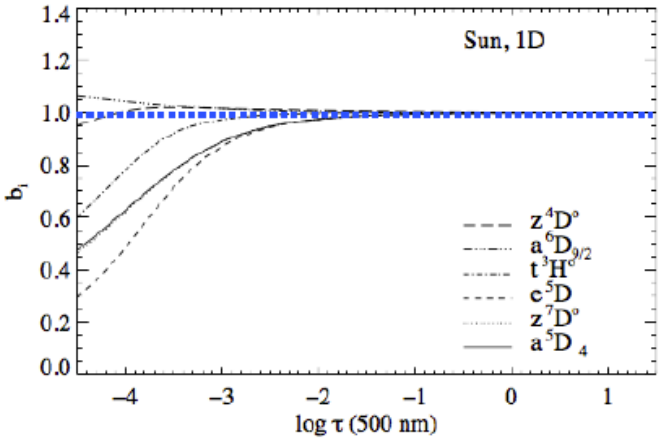

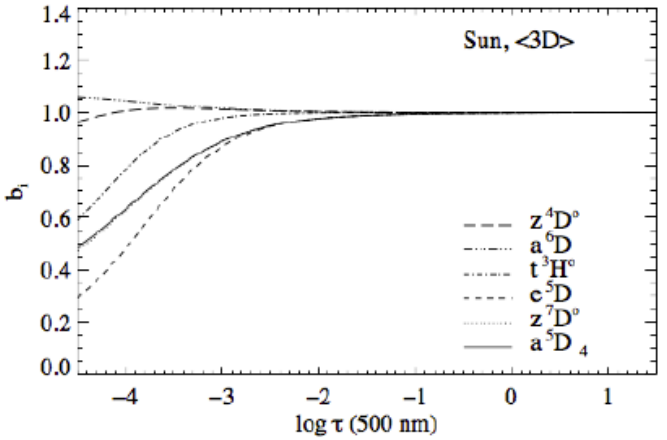

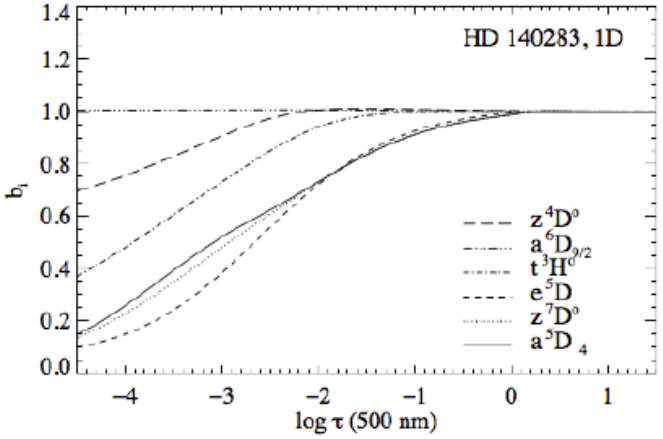

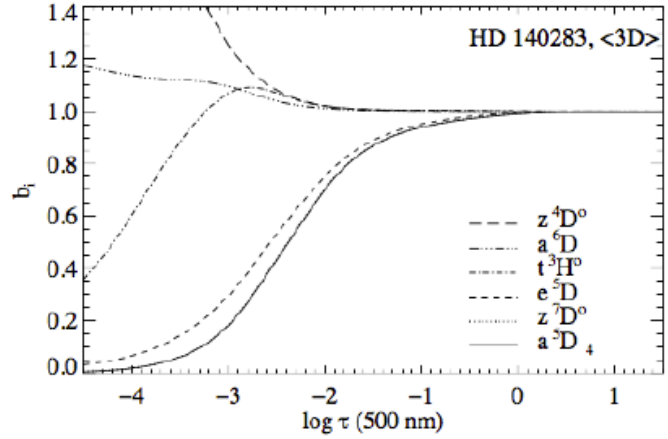

NLTE effects & stellar parameters

decreasing [Fe/H] (less metal line blocking)

decreasing log(g) (collisional processes become less important)

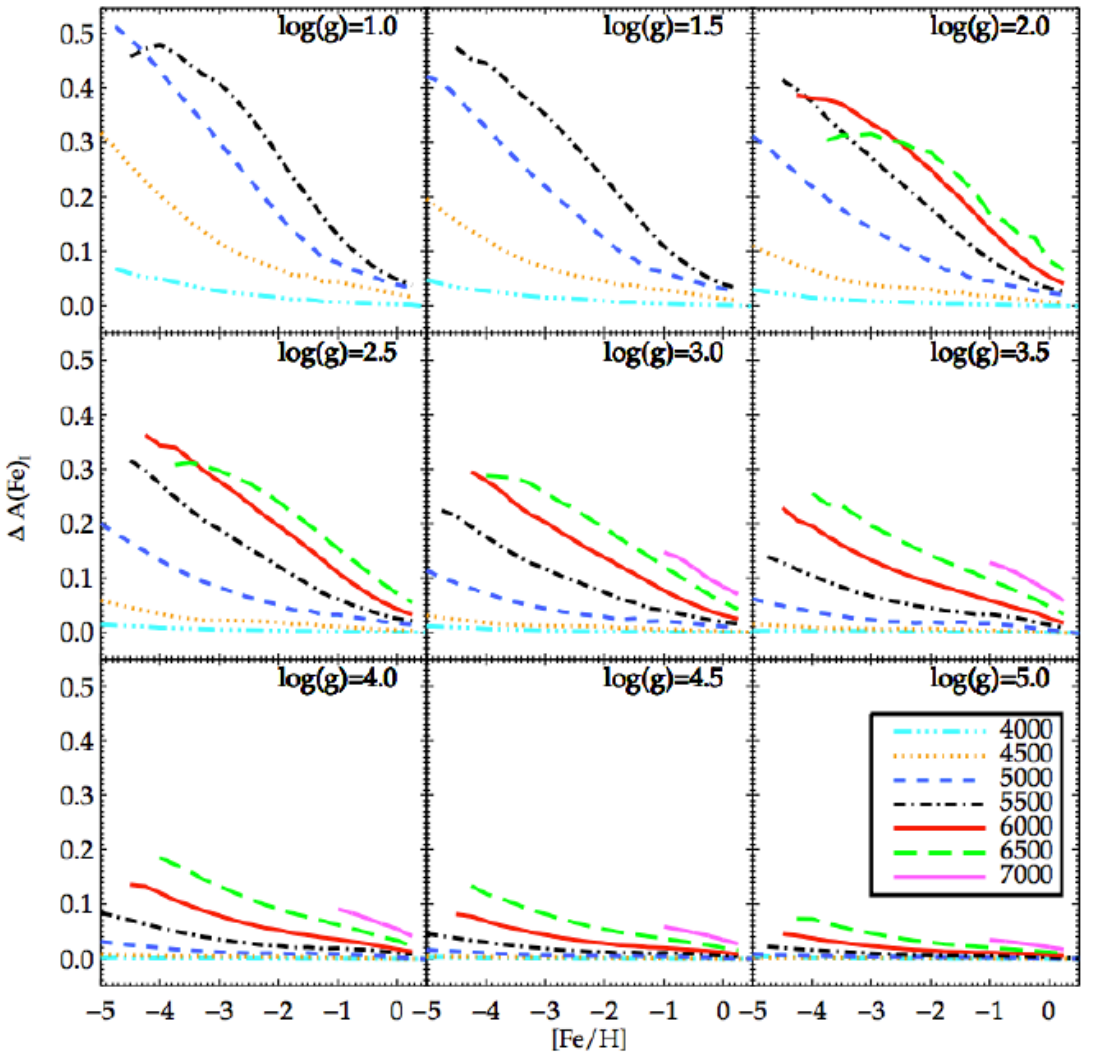

increasing temperature (radiative processes become more important)

Lind et al. 2014

Summary

- If LTE does not hold, Saha-Boltzmann no longer describes excitation and ionization conditions – need to solve rate equations for statistical equilibrium – much more complicated!

- Non-LTE is necessary for hot stars, coronae of cool stars, M-type stars (as well as in nebulae and ISM).

Spectral type sequence

Spectral Types: temperature sequence

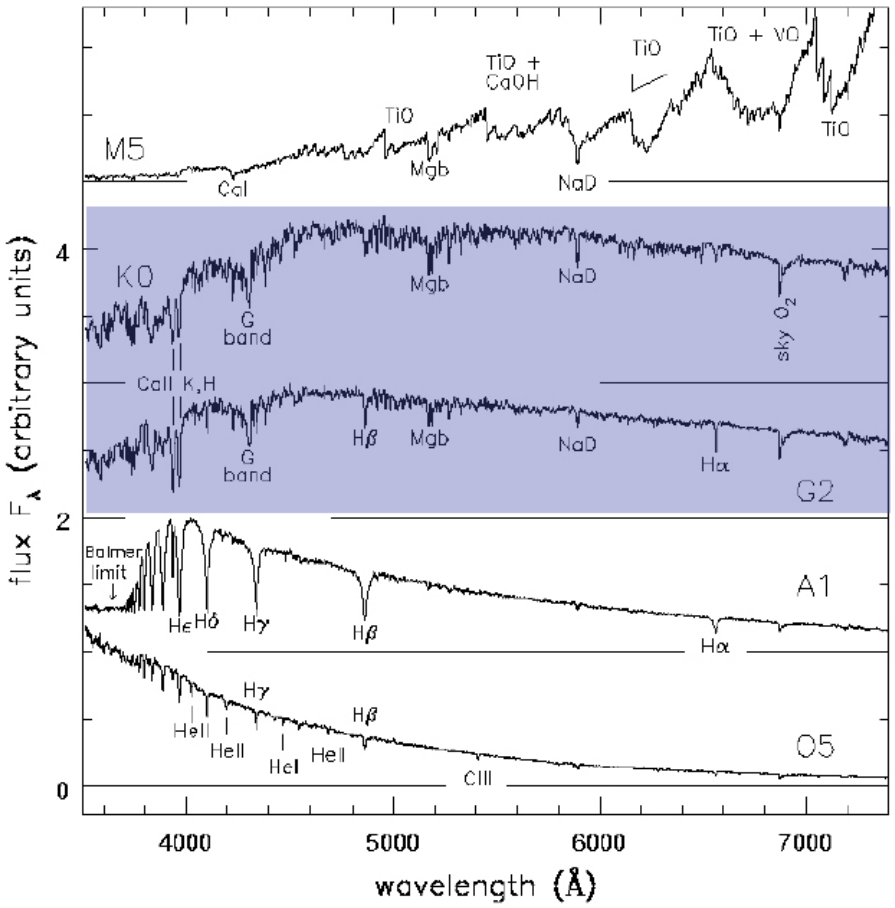

T ~ 4000K
Molecules!

Mainly neutral metal lines

T ~ 6000K
Ionised Metal lines

T < 11 000K
Dominated by neutral H

T ~ 30 000K
Highly ionised species

Line Broadenings

For example:
Stark Effect

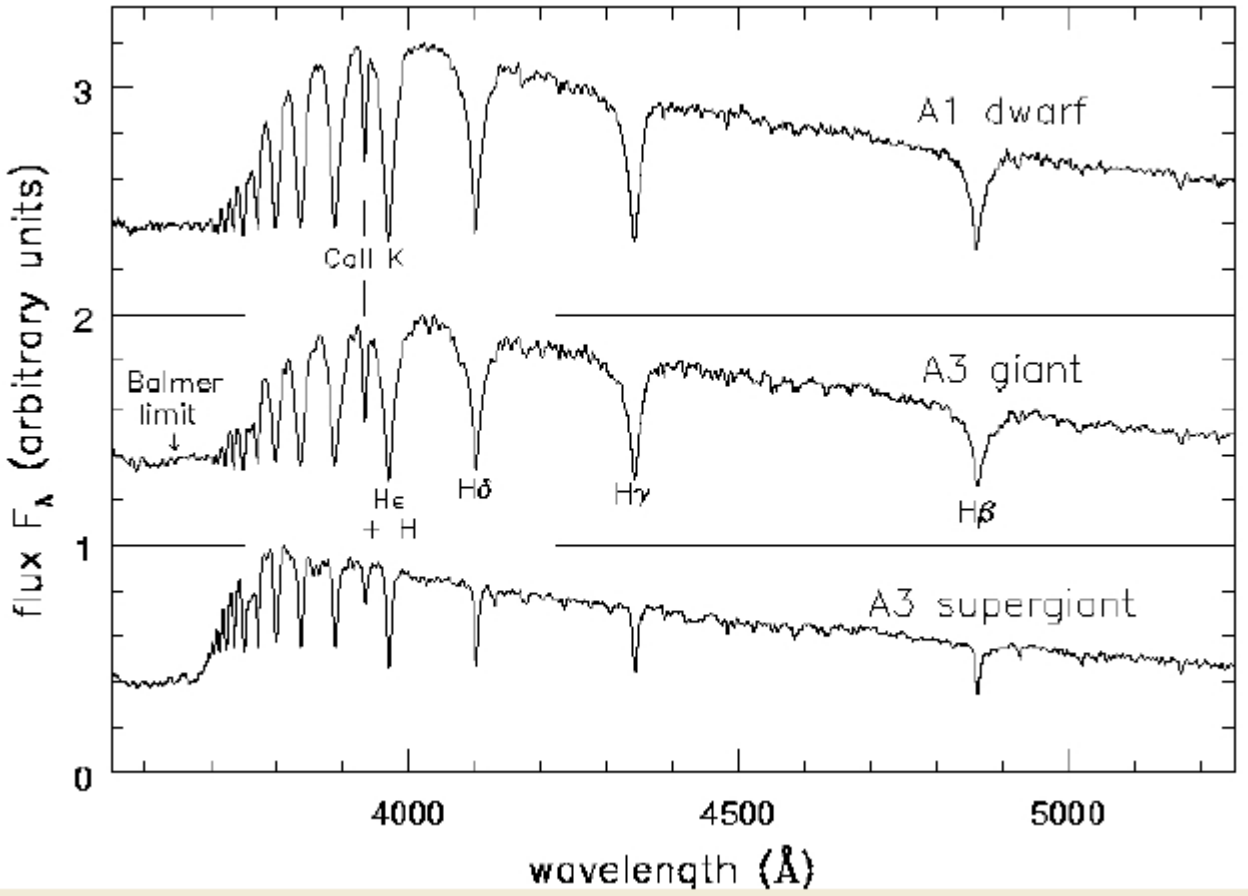

He and Metals

Metal are strongests when temperature is low enough that lower ionization stages are populated.
The metal lines become progressively stronger as the temperature cools and dominate in the F, G, K stars.

Helium is the second most abundant element, but only in the hottest stars (O and B) do He atoms show up in their excited levels where they can absorb visible light. For the very hottest O stars we also see HeII lines.

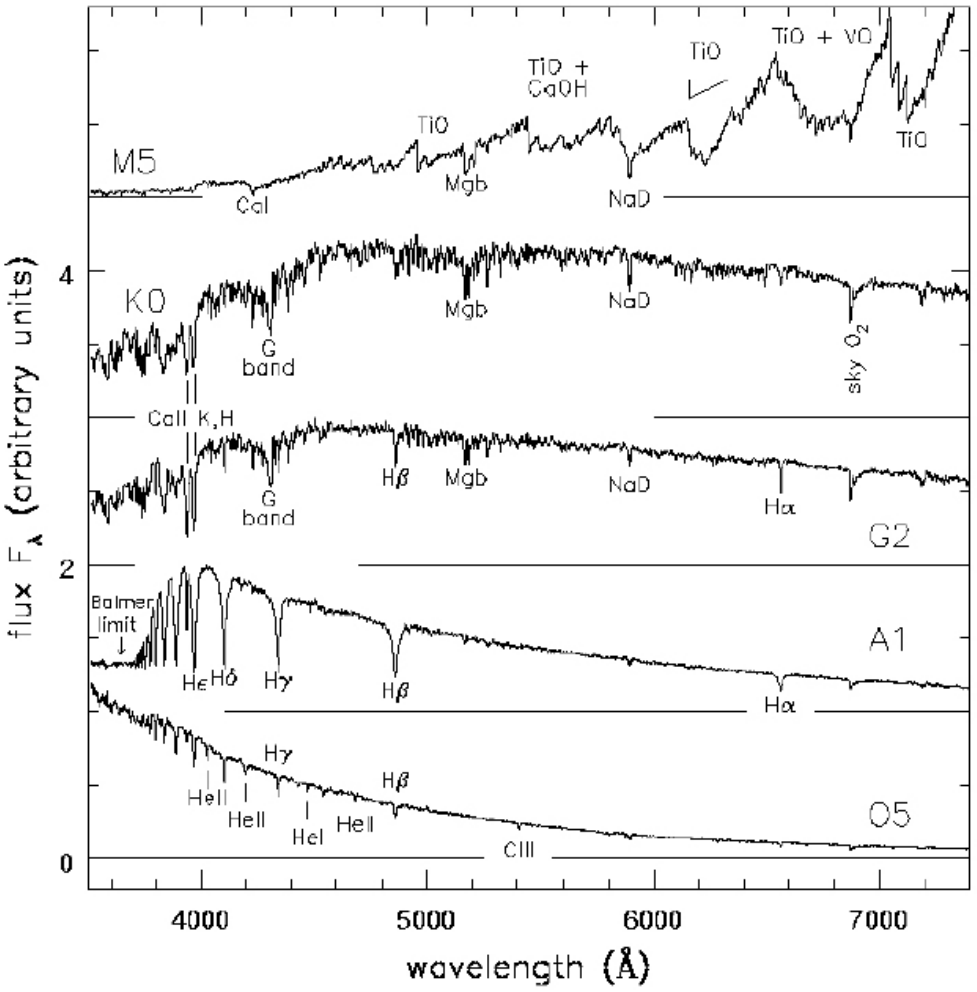

Molecular Bands

For very cool stars (M, L, T type) the atmospheres are sufficiently cool that simple molecules can form. These can absorb not only in electronic transitions, but also in vibrational and rotational modes. These create "bands" of absorption which can reduce the flux in vast portions of the spectrum. In M stars, TiO is a common important molecule. In L and T stars, other molecules such as CO, H_2O and CH_4 become important.

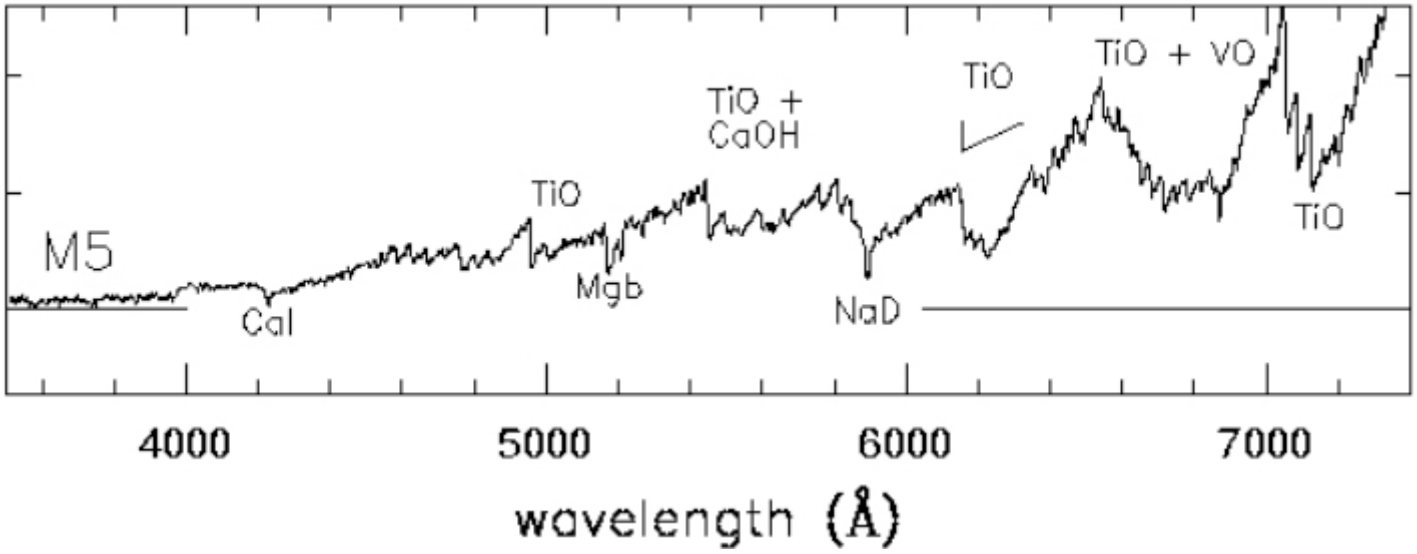

Relative Strength of Spectral Lines

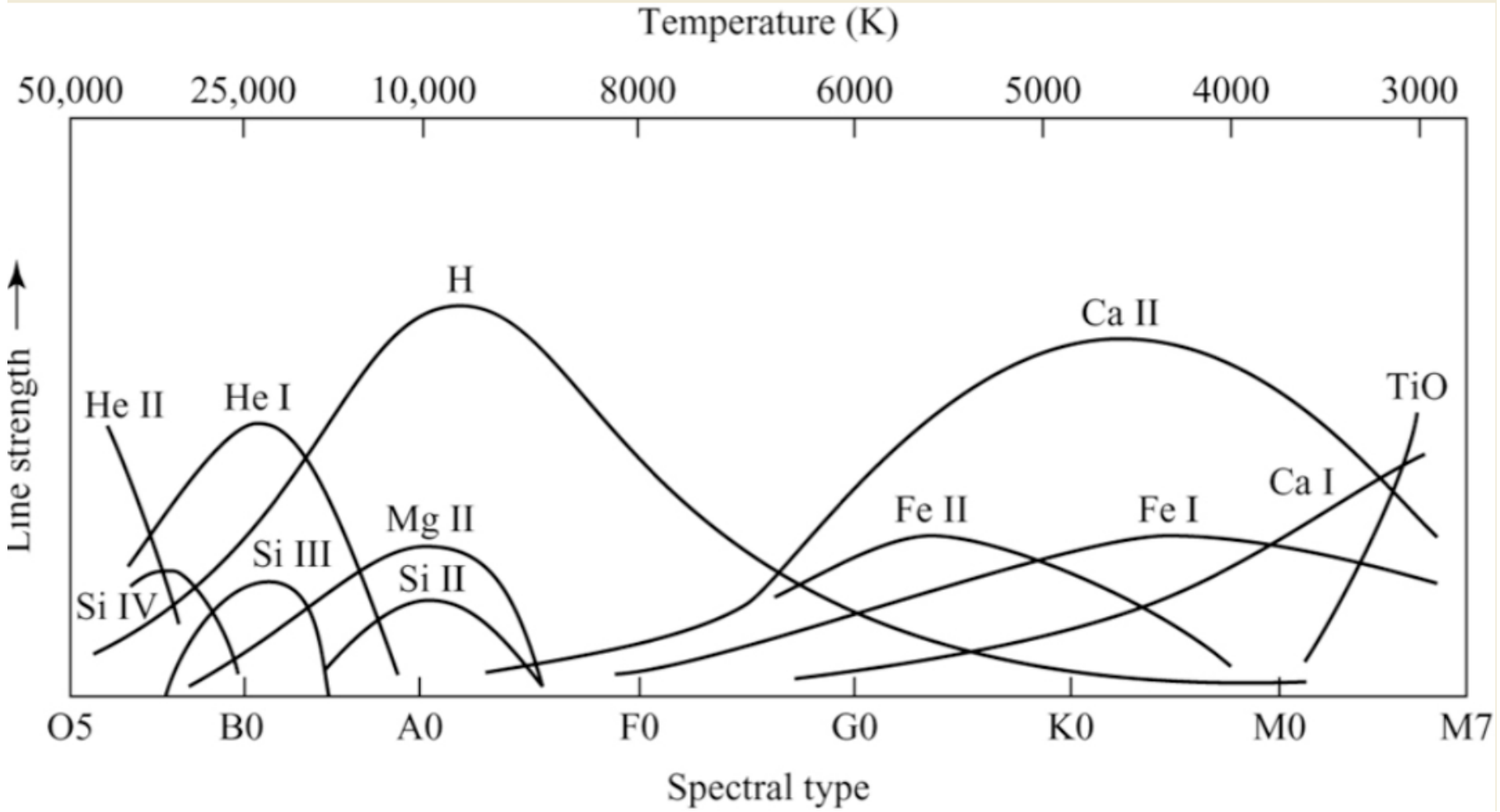

Spectral classification

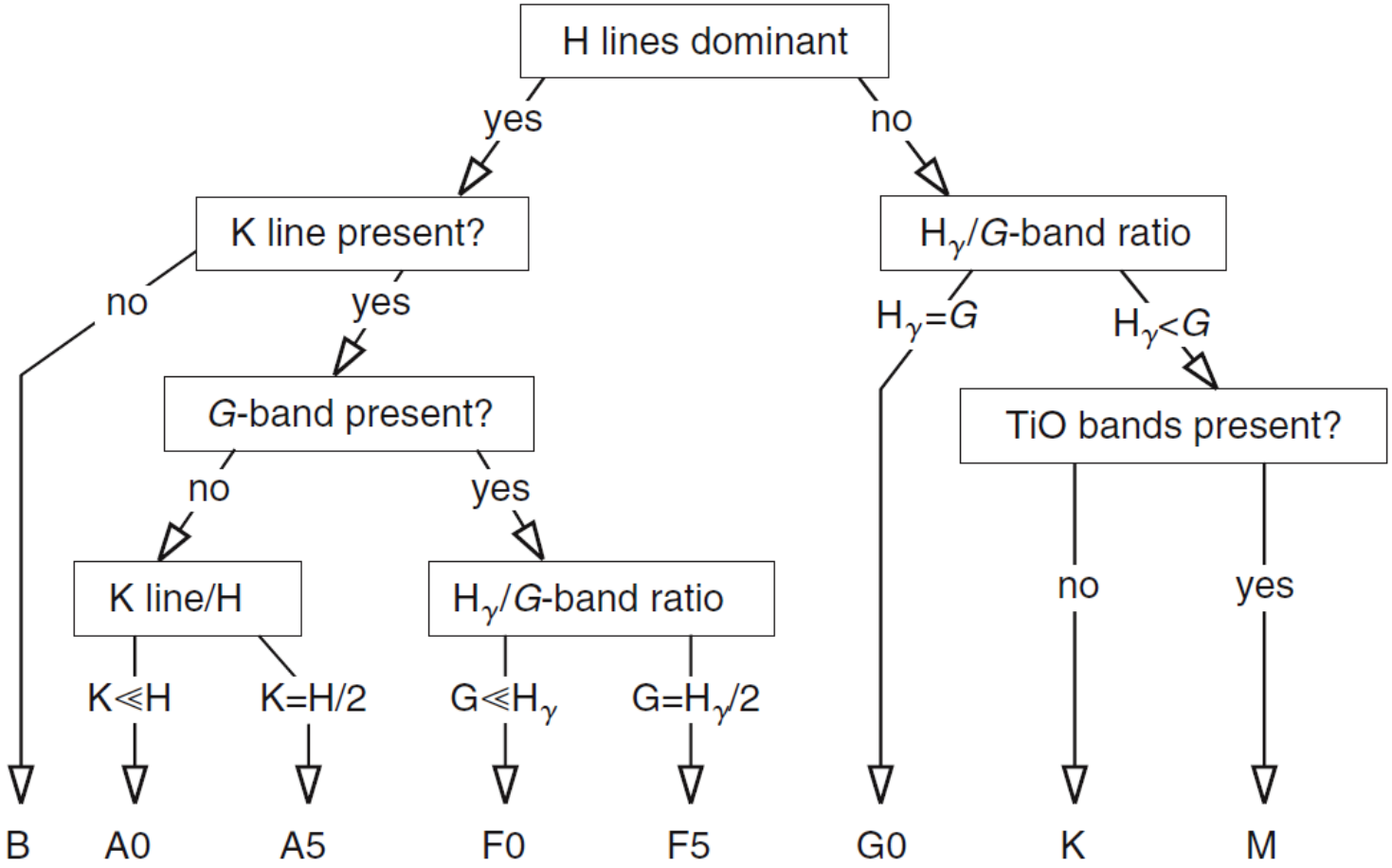

Towards the Model Photosphere

HYDROSTATIC EQUILIBRIUM
GAS PRESSURE
ELECTRON PRESSURE

Model atmospheres (example)

$\log \tau_0$	T (K)	$\log P_g$ (dyne/cm^2)	$\log P_e$ (dyne/cm^2)	$\log \kappa_0/P_e$ (cm^2/g per dyne/cm^2)	x (km)
Solar model, $S_0 = 1.0$, $\log g = 4.438$ cm/s^2					
−4.0	4310	2.87	−1.16	−1.22	−509
−3.8	4325	3.03	−1.02	−1.23	−476
−3.6	4345	3.17	−0.89	−1.24	−448
−3.4	4370	3.29	−0.78	−1.25	−422
−3.2	4405	3.41	−0.66	−1.26	−397
−3.0	4445	3.52	−0.55	−1.28	−373
−2.8	4488	3.64	−0.44	−1.30	−349
−2.6	4524	3.75	−0.33	−1.32	−325
−2.4	4561	3.86	−0.23	−1.33	−301
−2.2	4608	3.97	−0.12	−1.35	−277
−2.0	4660	4.08	−0.01	−1.37	−252
−1.8	4720	4.19	0.10	−1.40	−228
−1.6	4800	4.30	0.22	−1.43	−203
−1.4	4878	4.41	0.34	−1.46	−177
−1.2	4995	4.52	0.47	−1.50	−151
−1.0	5132	4.63	0.61	−1.55	−124
−0.8	5294	4.74	0.76	−1.60	−97
−0.6	5490	4.85	0.93	−1.66	−70
−0.4	5733	4.95	1.15	−1.73	−43
−0.2	6043	5.03	1.43	−1.81	−19
0.0	6429	5.10	1.78	−1.91	0
0.2	6904	5.15	2.18	−2.01	15
0.4	7467	5.18	2.59	−2.11	27
0.6	7962	5.21	2.92	−2.18	37
0.8	8358	5.23	3.16	−2.23	46
1.0	8630	5.26	3.32	−2.25	56
1.2	8811	5.29	3.42	−2.27	68
$S_0 = 0.7$, $\log g = 4.6$, normal abundances					
−4.0	3017	3.22	−2.12	−0.46	−246
−3.0	3111	3.89	−1.51	−0.53	−179

Usual assumptions to start with:

1. Plane parallel geometry, making all physical variables a function of only one space coordinate.
2. Hydrostatic equilibrium, meaning that the photosphere is not undergoing large scale-accelerations comparable to the surface gravity; there is no dynamically significant mass loss.
3. Structures such as granulation or star spots are negligible, or at least can be adequately represented by mean values of the physical parameters.
4. Magnetic fields are excluded.

Ideal gas

We require a knowledge of the **electron pressure** in order to use the Saha equation, which is related to the **gas pressure**. How do we calculate this in stellar atmospheres?

We start with **hydrostatic equilibrium**.

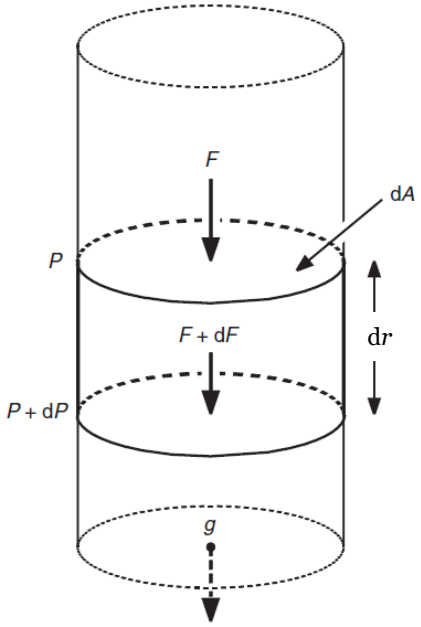

Forces acting upon the volume element of density $\rho(r)$ are gravity:

$$dF_g = -\frac{Gm(r)dm}{r^2} = -\frac{Gm(r)\rho(r)}{r^2}dAdr$$

plus buoyancy (pressure difference × area):

$$dF_P = -dPdA$$

Since the mass of the atmosphere is negligible compared to the stellar mass and the radius of the photosphere is negligible vs the stellar radius R,

$$dF_g = -\frac{Gm(r)\rho(r)}{R^2}dAdr = -g\rho(r)dAdr$$

since

$$g = \frac{Gm(R)}{R^2}$$

Hydrostatic equilibrium

Hydrostatic equilibrium is the balance between gravitational and pressure forces ($dF_g + dF_p = 0$). Then

$$\frac{dP}{dr} = -g\rho(r)$$

We can eliminate $\rho\,(r)$ with the ideal gas equation, $P_g = \frac{\rho kT}{\mu m_p} = \frac{\Re \rho T}{\mu}$

$$\frac{dP_g}{dr} = -g\,\frac{\mu(r)}{\Re\, T(r)} P_g(r)$$

where $\Re = \frac{k}{m_p} = 8.3\times10^7$ erg/mol/K is the gas constant

μ - mean molecular weight

Pressure Scale Height

We obtain

$$\frac{1}{P_g}\frac{dP_g}{dr} = \frac{d\ln P_g}{dr} = -\frac{g\mu(r)}{\Re T(r)}$$

For an idealized isothermal ($T(r)$=constant) atmosphere with $\mu(r)$=const, we can integrate this expression

$$P_g(r) = P_g(r_0)e^{-(r-r_0)g\mu/\Re T} = P_g(r_0)e^{-(r-r_0)/H}$$

where we have introduced the scale height H,

$$H = \frac{kT}{g\mu m_p} = \frac{\Re T}{g\mu}$$

i.e. gas pressure changes by a factor of **e** over a scale height.

For a (ficticious) atmosphere of constant density, corresponding to the gas pressure at the base of the real atmosphere, we can put the total mass of the real atmosphere into a layer of height H.

Examples

Betelgeuse	μ=1 (H)	T=3600K	Log g=0	H=4$R_\odot$
Sun	μ=1 (H)	T=6000K	Log g=4.4	H=200 km
Earth	μ=28 (N_2)	T=300K	Log g=3	H=9 km
White Dwarf	μ=0.5 (H^++N_e)	T=1.5x10^4 K	Log g=8	H=0.25 km
Neutron Star	μ=0.5 (H^++N_e)	T=10^6 – 10^7 K	Log g=15	H=2 mm

Gas Pressure $P_g(\rho)$

When using the Saha equation, we need T and P_g in a particular layer of the atmosphere, which can be described by geometric depth t or optical depth τ. Temperature dependence on average optical depth is known

$$T^4(\bar{\tau}) \approx \frac{3}{4}(\bar{\tau} + \frac{2}{3})T_{eff}^4$$

The average optical depth $d\bar{\tau} = -\kappa_R \rho \, dr$ may be expressed via the Rosseland mean opacity per unit mass (cm^2/g), κ_R.

Thus, we generally express the gas pressure as a function of optical depth. From hydrostatic equilibrium we obtain

$$\frac{dP_g}{dr} = -g\rho(r) \quad \Rightarrow \quad \frac{dP_g}{d\bar{\tau}} = \frac{g}{\kappa_R}$$

The gas pressure can now be obtained by integrating this differential equation, although in general κ_R, is a complicated function of temperature and pressure.

Integration of hydrostatic equation

- In the simplest case, assuming a constant mean opacity (which is not a very sensible approximation, but ok for electron scattering), with $\tau=0$ and $P_g=0$ at the surface:

$$P_g = \frac{g}{\kappa_R}\bar{\tau}$$

Knowing $T(\tau)$ for a given $T_{\rm eff}$, we can assume a value for κ_R, insert this into the above equation and compute a value for the gas pressure.

- More realistically, for this differential equation can be obtained the following formal solution (look at the Gray textbook):

$$P_{\rm g} = g^{2/3}\left(\frac{3}{2}\int_{-\infty}^{\log\tau_0}\frac{t_0 P_{\rm g}^{1/2}}{\kappa_0 \log e}\,{\rm d}\log t_0\right)^{2/3}$$

$$\frac{dP_g}{d\bar{\tau}} = \frac{g}{\kappa_R}$$

where κ_0 *is* the opacity at some reference wavelength (e.g. 5000Å).

Guess $P_g(\tau_0)$ for all τ_0 initially and then numerically evaluate the integral on the right for each τ_0 to obtain a better estimate of $P_g(\tau_0)$ on the left-hand side. Iterate this procedure.

Gravity dependence of P_g

$$P_g = g^{2/3}\left(\frac{3}{2}\int_{-\infty}^{\log\tau_0}\frac{t_0 P_g^{1/2}}{\kappa_0 \log e}\,\mathrm{d}\log t_0\right)^{2/3}$$

The pressure dependence inside the integral is weak and so

$$P_g \approx C(T)g^{2/3}$$

i.e. the gas pressure for a given optical depth increases with $g^{2/3}$.

Increasing the surface gravity the photosphere compresses, increasing all pressures.

For different stars we see down to $\tau = 2/3$, whose pressure varies approximately as $g^{2/3}$.

The larger the pressure, the greater the Rosseland mean opacity, so we see geometrically higher layers in stars with higher gravity.

Giants have deep atmospheres, dwarfs thin ones.

Electron pressure

So far, we have dealt with the gas pressure, but it is the **electron** pressure that is needed in the Saha equation.

We can generally say,

$$P_g = NkT$$

where N is the sum of all particles/cm^3 , and

$$P_e = n_e kT$$

with n_e=number of electrons/cm^3. Of course,

$$n_e = n^+ + 2n^{2+} + 3n^{3+} \text{ etc.}$$

In the simplest case of pure hydrogen,

$$N = N(\mathrm{H}) + N(\mathrm{H}^+) + n_e = N(\mathrm{H}) + 2N(\mathrm{H}^+) = P_g / kT$$

since from charge conservation $n_e = N(\mathrm{H}^+)$.

For ionized hydrogen, we find $P_e = 0.5 P_g$, For doubly ionized helium, $P_e = 2/3\ P_g$.

Given $N(\mathrm{H}^+) n_e / N(\mathrm{H}) = f(T)$ from Saha equation, we may solve for $N(\mathrm{H}^+) = n_e$ and $N(\mathrm{H})$, if T and P_g are known.

Numerical examples

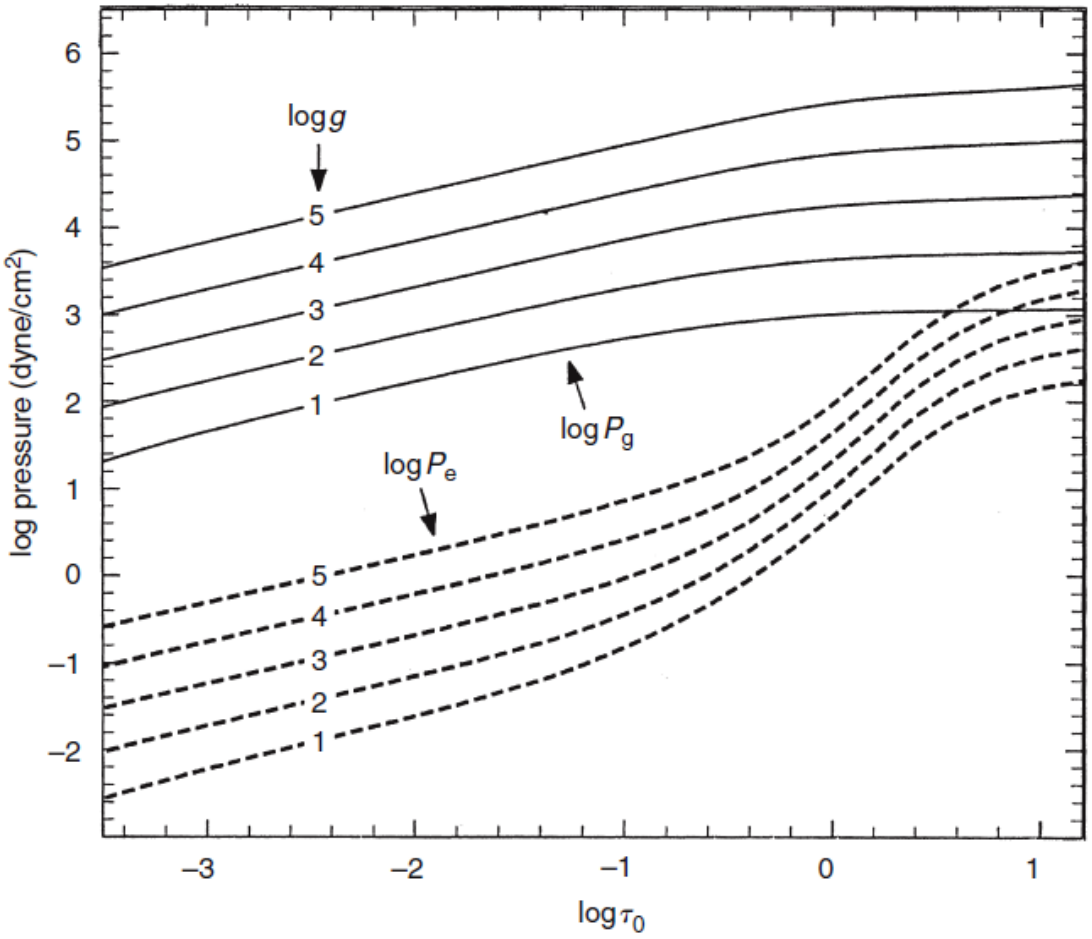

Numerical results show, that the gas pressure exponent is not 2/3, but ranges from 0.57 to 0.64 from shallow to deep layers.

The electron pressure dependence on gravity has two regimes, for cooler and hotter models.
For solar-type stars, approximately, $P_e^2 \propto P_g$, so an exponent of 1/3 predicted, while for hotter stars 2/3.

Numerical calculations show 0.48 to 0.33 from shallow to deep layers in the cooler model, and 0.53 to 0. 82 in the hotter model (Gray Fig. 9.13).

Role of Metals?

For a pure H atmosphere in the case of the Solar photosphere, the gas pressure greatly exceeds the electron pressure. Although metals are few in number, some are very easily ionized e.g. $Na/H=2\times10^{-6}$, $Mg/H=3\times10^{-5}$, $Al/H=2.7\times10^{-6}$, $Ca/H=2\times10^{-6}$, $Si/H=3\times10^{-5}$. These will **contribute** electrons to the atmosphere, increasing P_e and suppress ionization.

		Stage of ionization												
Atom		I	II	III	IV	V	VI	VII	VIII	IX	X	XI	XII	XIII	XIV
1	H	13.598 44													
2	He	24.587 41	54.417 78												
3	Li	5.391 72	75.640 18	122.454											
4	Be	9.322 63	18.211 16	153.897	217.713										
5	B	8.298 03	25.154 84	37.931	259.366	340.22									
6	C	11.260 30	24.383 32	47.888	64.492	392.08	489.98								
7	N	14.534 14	29.601 3	47.449	77.472	97.89	552.06	667.03							
8	O	13.618 06	35.117 30	54.936	77.413	113.90	138.12	739.29	871.41						
9	F	17.422 82	34.970 82	62.708	87.140	114.24	157.17	185.19	953.91	1 103.1					
10	Ne	21.564 54	40.963 28	63.45	97.12	126.21	157.93	207.28	239.10	1 195.8	1 362.2				
11	Na	5.139 08	47.286 4	71.620	98.91	138.40	172.18	208.50	264.25	299.9	1 465.1	1 648.7			
12	Mg	7.646 24	15.035 28	80.144	109.265	141.27	186.76	225.02	265.96	328.1	367.5	1 761.8	1 963		
13	Al	5.985 77	18.828 56	28.448	119.99	153.83	190.49	241.76	284.66	330.1	398.8	442.0	2 086	2 304	
14	Si	8.151 69	16.345 85	33.493	45.142	166.77	205.27	246.49	303.54	351.1	401.4	476.4	523	2 438	2 673
15	P	10.486 69	19.769 4	30.203	51.444	65.03	220.42	263.57	309.60	372.1	424.4	479.5	561	612	2 817
16	S	10.360 01	23.337 9	34.79	47.222	72.59	88.05	280.95	328.75	379.6	447.5	504.8	564	652	707
17	Cl	12.967 64	23.814	39.61	53.465	67.8	97.03	114.20	348.28	400.1	455.6	529.3	592	657	750
18	Ar	15.759 62	27.629 67	40.74	59.81	75.02	91.01	124.32	143.46	422.5	478.7	539.0	618	686	756
19	K	4.340 66	31.63	45.806	60.91	82.66	99.4	117.56	154.88	175.8	503.8	564.7	629	715	787
20	Ca	6.113 16	11.871 72	50.913	67.27	84.50	108.78	127.2	147.24	188.5	211.3	591.9	657	727	818
21	Sc	6.561 44	12.799 67	24.757	73.489	91.65	111.68	138.0	158.1	180.0	225.2	249.8	688	757	831
22	Ti	6.828 2	13.575 5	27.492	43.267	99.30	119.53	140.8	170.4	192.1	215.9	265.1	292	788	863
23	V	6.746 3	14.66	29.311	46.71	65.28	128.1	150.6	173.4	205.8	230.5	255.1	308	336	896
24	Cr	6.766 64	16.485 7	30.96	49.16	69.46	90.64	161.18	184.7	209.3	244.4	270.7	298	355	384
25	Mn	7.434 02	15.639 99	33.668	51.2	72.4	95.6	119.20	194.5	221.8	248.3	286.0	314	344	404
26	Fe	7.902 4	16.187 8	30.652	54.8	75.0	99.1	124.98	151.06	233.6	262.1	290.2	331	361	392
27	Co	7.881 0	17.083	33.50	51.3	79.5	103	131	160	186.2	276.2	305	336	379	411
28	Ni	7.639 8	18.168 84	35.19	54.9	75.5	108	134	164	193	224.6	321	352	384	430
29	Cu	7.726 38	20.292 40	36.841	55.2	79.9	103	139	167	199	232	266	369	401	435
30	Zn	9.394 05	17.964 40	39.723	59.4	82.6	108	136	175	203	238	274	311	412	454

Gas and electron pressures

To calculate the electron density properly, all low ionization energy species and their corresponding abundances should be included.

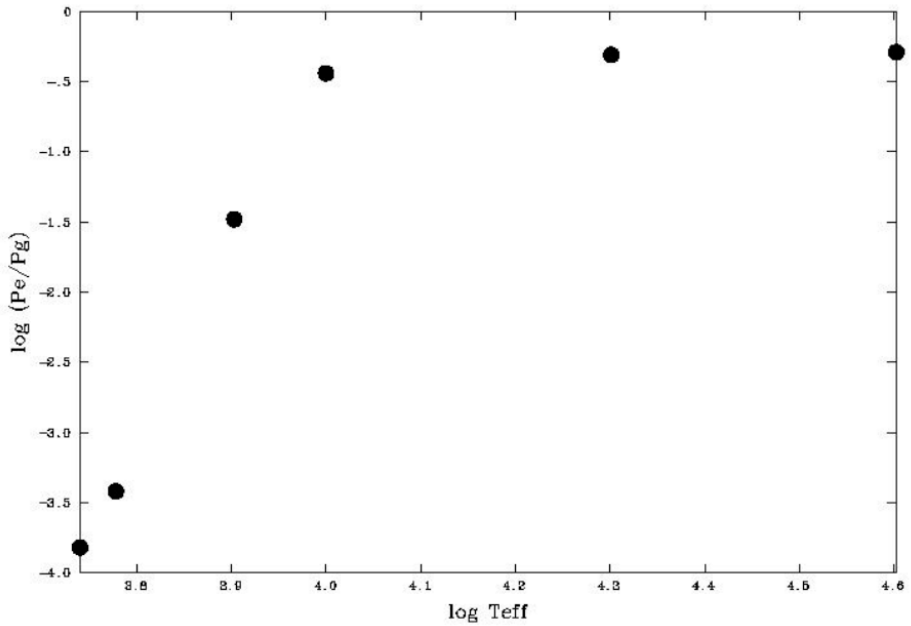

For ionized hydrogen, we find P_e=0.5P_g,
For doubly ionized helium, P_e=2/3 P_g.

Gas and electron pressures

$T_{\rm eff}$	Log g	Log $P_{\rm g}(\tau=2/3)$	Log $P_{\rm e}(\tau=2/3)$
5500	4	4.83	1.01
6000	4	4.76	1.34
8000	4	3.94	2.46
10000	4	3.03	2.59
20000	4	3.40	3.09
40000	4	3.58	3.29

Radiation Pressure, P_r

- Radiation may also have an effect on the pressure. Radiation is an inefficient carrier of momentum (velocities have the highest possible value), but when a photon is absorbed or scattered by matter, it imparts not only its energy to that matter, but also its momentum $h\nu/c$.

- Let's now recall the definition of the K-integral and Eddington approximation (Lectures 6-7).

Summary

- Hydrostatic equilibrium – P_g changes by a factor of e=2.71 over the scale height.
- $P_g(\rho)$ scales with $g^{1/2}$ in Solar-type stars.
  Dwarfs have high P_g & high mean opacities (thin atmospheres) whilst (super)giants have low P_g and low mean opacities (deep atmospheres).
- Increased P_e in Solar-type stars from readily ionized metals versus pure H case. Ratio of electron to gas pressure is strong function of T.

- **Radiation** may also have an effect on the pressure! We discussed it in previous lectures.

Measuring temperatures and surface gravities

DIRECT MEASUREMENT OF RADII

DETERMINING EFFECTIVE TEMPERATURE AND SURFACE GRAVITY

MODEL-INDEPENDENT METHODS

MODEL-DEPENDENT METHODS

ATMOSPHERIC MODELS

PHOTOMETRIC METHODS

SPECTROSCOPIC METHODS

Fundamental parameters

Stellar parameters:

- Luminosity (L)
- Mass (M)
- Radius (R)

In most cases, cannot be measured directly

Atmosphere parameters:

- Effective Temperature ($T_{\rm eff}$)
- Surface gravity ($\log g$)

Can help in measuring L & M

- Chemical composition (metallicity, element abundances)

~90% of stars in the Galaxy are "normal" (close to the Sun)

Surface Flux, Luminosity and T_{eff}

- Integral over frequency / wavelength at outer boundary (Surface Flux):

$$F_s = \int_0^\infty F_\lambda d\lambda$$

- Multiplied by stellar surface area yields the Luminosity, total energy radiated away by the star

$$L = 4\pi R^2 F_s$$

- The total energy arriving above the Earth's atmosphere is its observed flux, $F_\oplus$, corrected for the distance to the star d, neglecting interstellar absorption:

$$L = 4\pi d^2 F_\oplus \quad \rightarrow \quad F_s = F_\oplus (d/R)^2$$

- The Stefan-Boltzmann law, $F=\sigma T_{\text{eff}}^4$, or alternatively $L/4\pi R^2 = \sigma T_{\text{eff}}^4$ defines the "effective temperature" of a star, i.e. the temperature which a black body would need to radiate the same amount of energy as the star.

Model-independent methods (1)

Direct measurements:

$f_\oplus$ – the flux measured at the Earth ($F_\oplus$ - bolometric flux at the Earth)
F_S – the flux emitted from the stellar surface
d – the distance from us to the star
R – the radius of the star
θ – the angular radius of the star, R/d

Example:
$d = 1.3$ pc, $R = 700000$ km
$\theta = 0.004$ arcsec !!

$$4\pi d^2 F_\oplus = 4\pi R^2 F_S$$

We can relate this equation to the effective temperature

$$F_\oplus = \int_0^\infty f_\oplus(\nu)\, d\nu = \theta^2 \sigma T_{eff}^4$$

If θ is measured and the distance d is known, e.g. from parallax (Gaia, Hipparcos, etc.), then we can obtain R and L.

Inteferometric radii

- We have already introduced interferometry regarding limb darkening (Lecture 17).
- Several ground-based optical and IR interferometers are currently in operation.
- Reliable diameters generally restricted to nearby late-type giants with large angular radii on the sky.
- Radii of a few hundred stars are measured with an accuracy better than 10%.

- **VLTI** (Paranal, Chile): currently the most advanced optical/IR interferometer in operation. Combines large apertures of individual 8-m VLT telescopes with dedicated auxiliary 1.8-m telescopes.
- **Imaging Atmospheric Cherenkov Telescopes** (MAGIC, VERITAS, H.E.S.S., LST-1) are very promising.

The New Set at Paranal - The VLT, the VST Dome and the AT1

ESO PR Photo 02d/04 (30 January 2004) © European Southern Observatory

The AT1 Positioned Next to the VLTI Laboratory

ESO PR Photo 02b/04 (30 January 2004) © European Southern Observatory

Radii from other direct methods

- **Occultations**
  - Moon used as “knife-edge”
  - Diffraction pattern recorded as flux vs. time
  - Precision ~ 0.5 mas
  - A few hundred radii have been determined
- **Eclipsing binaries**
  - Photometry gives ratio of radii to semi-major axes. Useful simulation at http://www.midnightkite.com/binstar/StarLightPro.exe
  - Velocities from spectra give semi-major axes (i=90°)

Binary Masses

Accurate radii and masses can be obtained from analysis of photometric light curves (R, I) & spectroscopic orbit information ($M \sin^3 i$). If eclipsing $i \cong 90°$ → R, M.

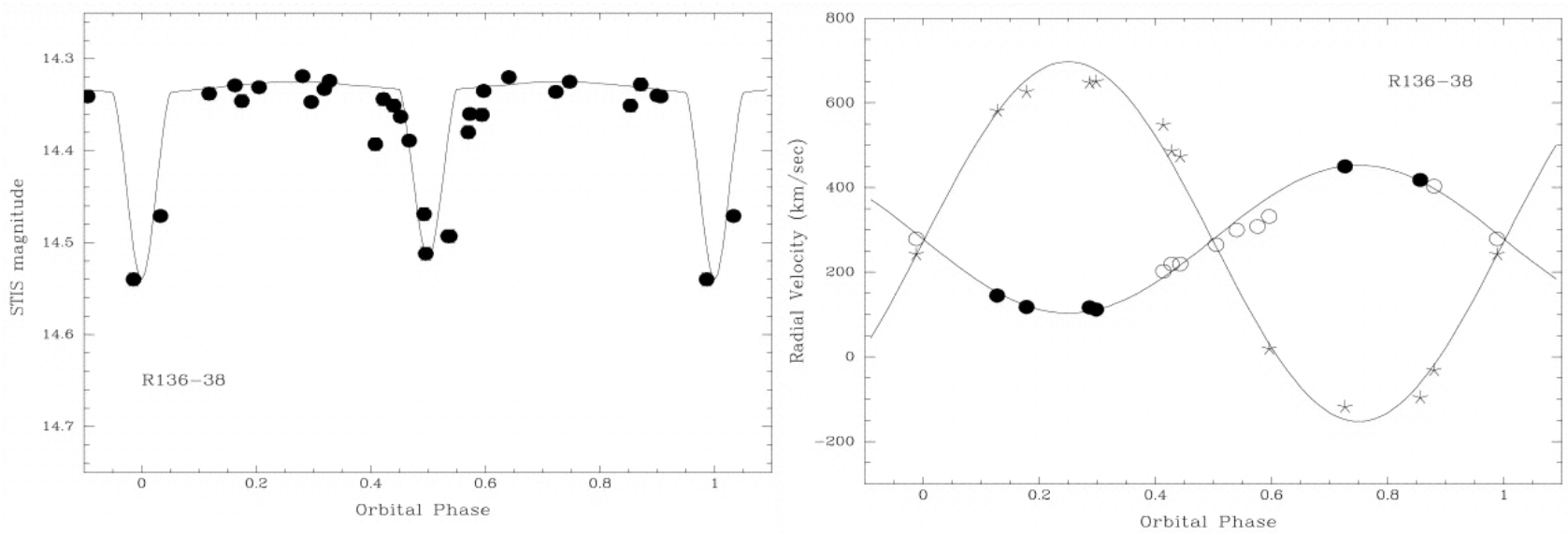

R136-38 (Massey et al. 2002, ApJ 565, 982) light curve analysis of O3V+O6V in LMC (P=3.4 day): 9.3$R_\odot$ (primary) 6.4$R_\odot$ (secondary)

Model-independent methods (2)

Direct measurements:

$$4\pi d^2 F_\oplus = 4\pi R^2 F_S \qquad g = \frac{GM}{R^2}$$

$$F_\oplus = \underbrace{\int_0^\infty f_\oplus(\nu)\, d\nu}_{} = \theta^2 \sigma T_{eff}^4$$

Difficult to reliably measure $F_\oplus$ because of interstellar absorption in UV (especially beyond the Lyman continuum)

Model-dependent methods

Using, e.g., model atmospheres and/or theoretical evolution tracks.

- $T_{\rm eff}$ from Bolometric Corrections
  - Lecture 16
- Log g from parallaxes

$$\log g/g_{\odot}=\log M/M_{\odot}+4\log T_{\rm eff}/T_{\rm eff,\odot}+0.4(M_{\rm bol}-M_{\rm bol,\odot})$$

- Method of IR fluxes (Blackwell & Shallis 1977)

$$4\pi d^2 F_{\oplus} = 4\pi R^2 F_S \quad \rightarrow \quad \frac{F_{\oplus}}{F_S} = \frac{R^2}{d^2} = \theta^2 = \frac{f_{\oplus}}{f_S}$$

$$T_{eff}^4 = \frac{F_{\oplus}}{\theta^2 \sigma}$$

Also correct for monochromatic fluxes

Alonso et al. : T_{eff}(IRFM) for 1000+ stars

Atmospheric Models

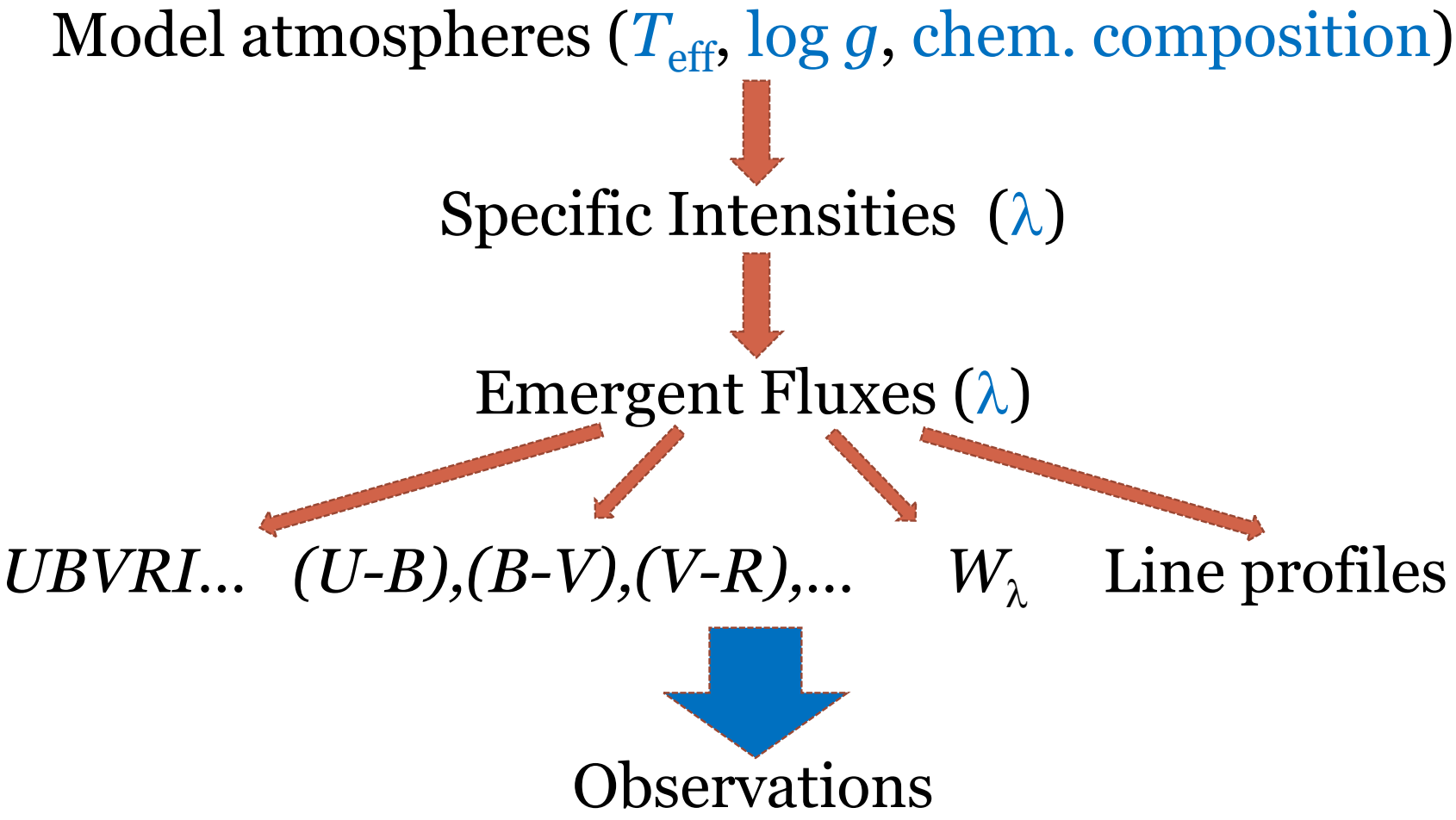

Atmospheric Models (1)

- For most stars, Kurucz LTE atmosphere models, accounting for “line blanketing” from metals, generally suffice http://kurucz.harvard.edu/grids.html
- For early-type stars, several non-LTE line blanketed models exist: TLUSTY http://tlusty.oca.eu for plane-parallel O stars, or for O stars with extended atmospheres WMbasic https://www.usm.uni-muenchen.de/people/adi/Programs/Programs.html
- For very late-type stars, opacity from molecules are important e.g. PHOENIX http://phoenix.astro.physik.uni-goettingen.de

Kurucz models

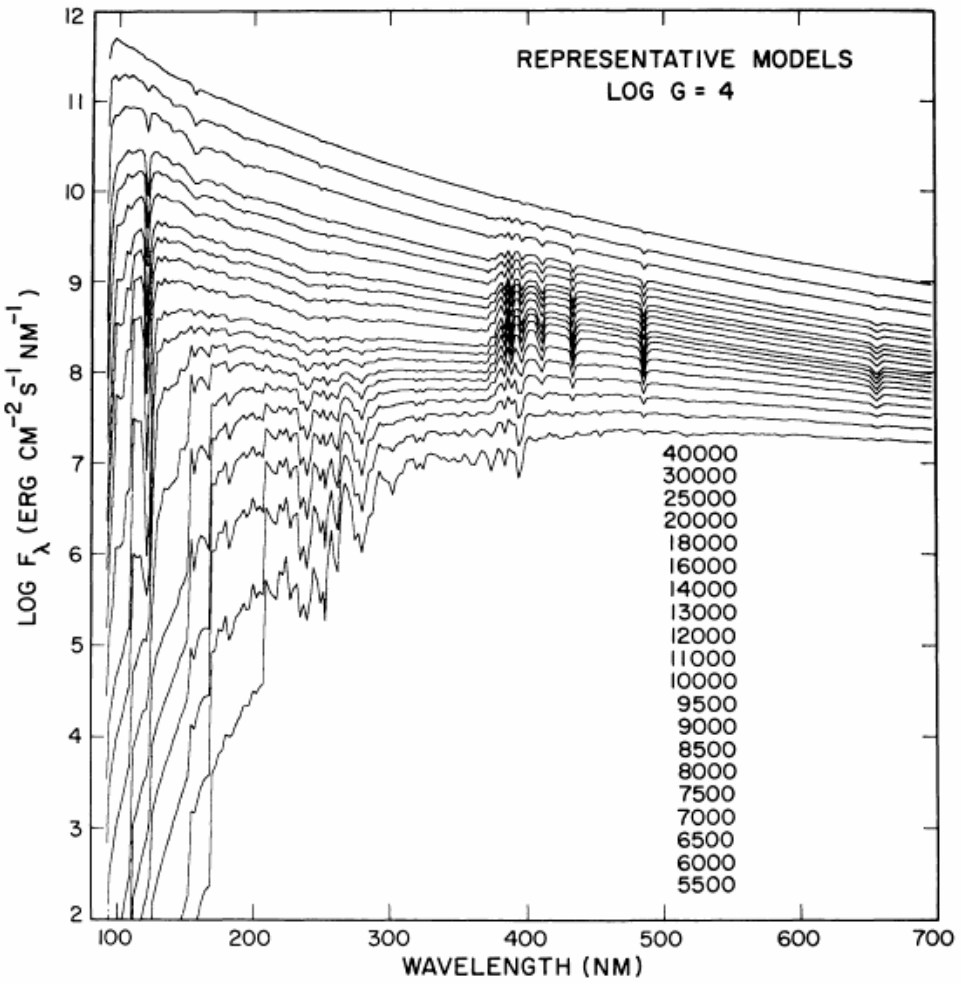

FIG. 16.—The flux F_λ redward of the Lyman limit as a function of T_{eff}

Atmospheric Models (2)

- To determine T_{eff} and $\log g$, one has to use spectral characteristics which are insensitive to chem. composition.
- At least one parameter should have a stronger dependence on T_{eff} than on $\log g$, and another one in the opposite way.
- The more parameters the better.

- If T_{eff} is fixed, then $g = \frac{GM}{R^2} = \frac{4\pi GM\sigma T_{eff}^4}{L}$ → $L \sim \frac{M}{g} T_{eff}^4$

  using $L \sim M^n$, we get $g \sim M^{(1-n)}$

g – a luminosity criterium

Photometric Methods

Alternative photometric systems to Johnson *UBV* are available – notably Strömgren (1963) *ubvy*.

These are narrower filters and are rather more useful in extracting $T_{\rm eff}$ and log g than *UBV*.

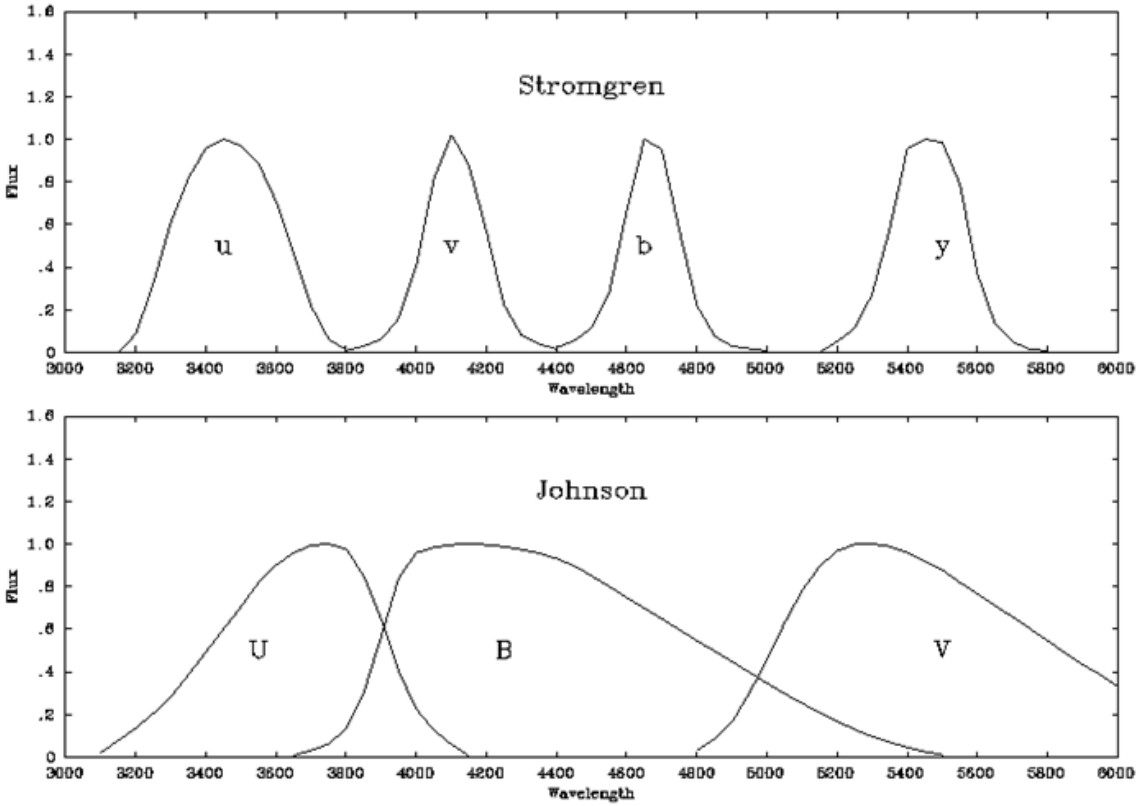

UBV versus uvby photometry

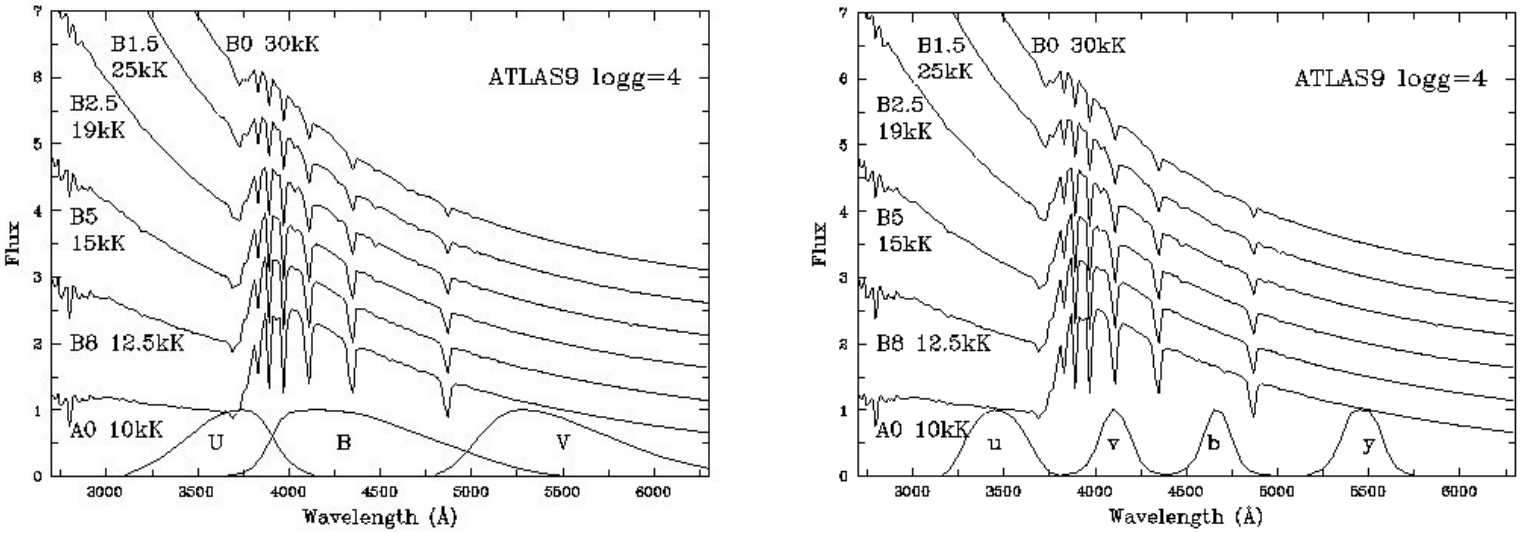

A comparison of synthetic Kurucz models for the Balmer jump in B dwarfs with the usual Johnson *UBV* filters (left) and Strömgren *ubvy* filters (right). The *U* filter is sensitive to radiation on both sides of the discontinuity, whilst the narrow Stromgren *u* filter samples light below 3647 & *v* filter samples light above, so the *u-v* colour provides $T_{\rm eff}$.

Photometric Methods

T_{eff} from photometry

- The slope of the Paschen continuum, F_{4000}/F_{7000}
- $c_1 = (u - v) - (v - b)$ for A0 stars and earlier
- $b - y$, $B - V$, $V - K$ for F stars and later

} $f(T_{\text{eff}})$

Photometric Methods

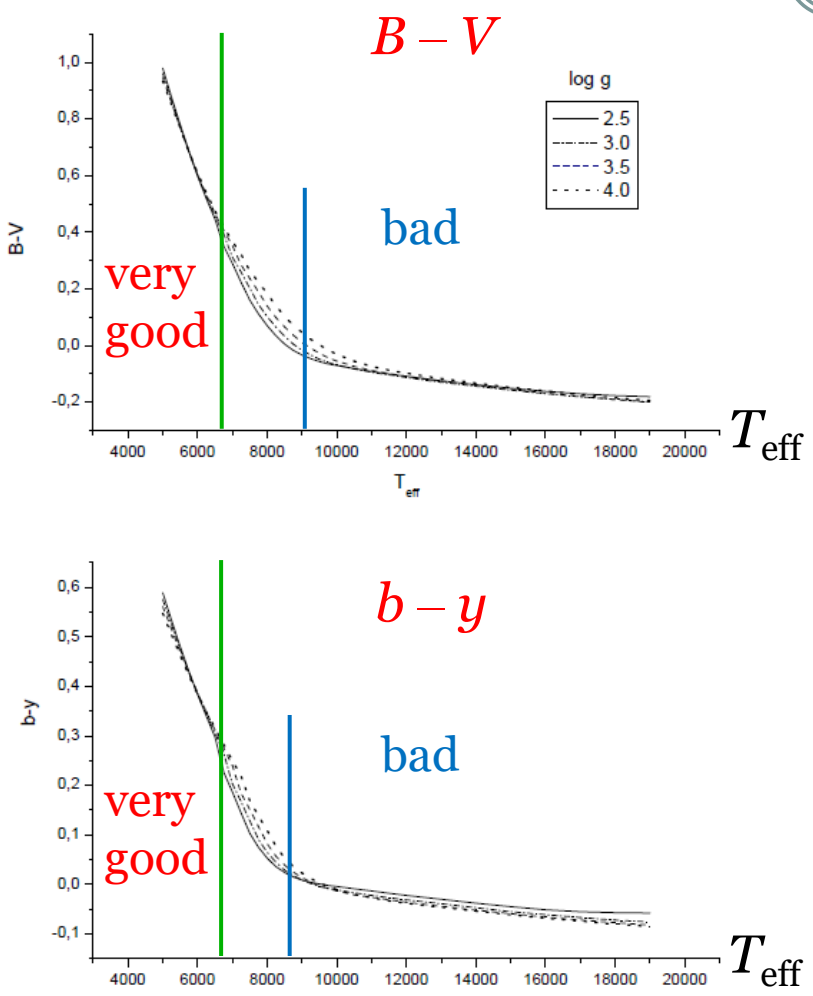

Kurucz atmosphere models

$c_1 = (u - v) - (v - b)$

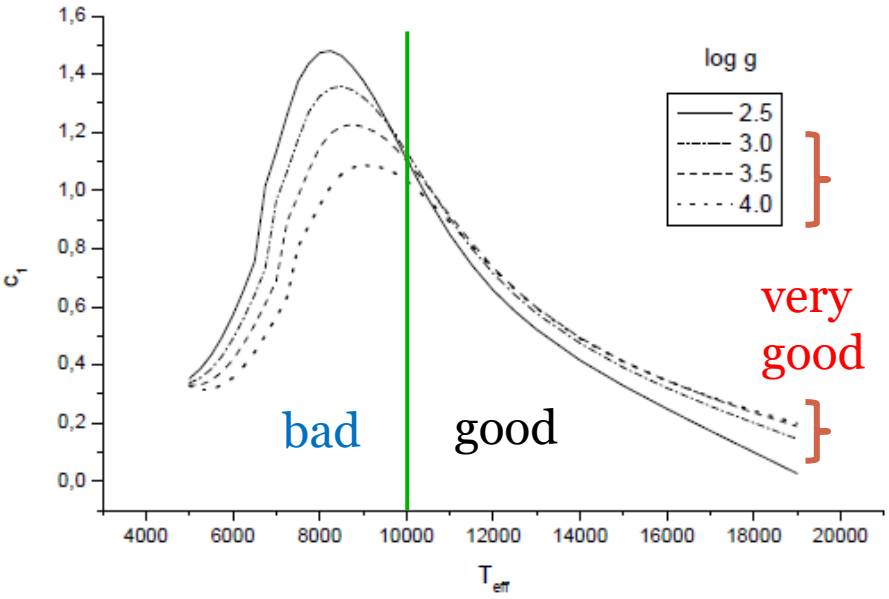

Temperatures from photometry

Observed *B*-*V* colour index generally allows T_{eff} for normal stars (0<*B*-*V*<1.5):

$$\log T_{eff} = 3.988 - 0.881(B-V) + 2.142(B-V)^2 - 3.614(B-V)^3 + 3.2637(B-V)^4 - 1.4727(B-V)^5 + 0.26(B-V)^6$$

Beyond this range most flux is originating in the UV or IR so *B*-*V* becomes insensitive to temperature.

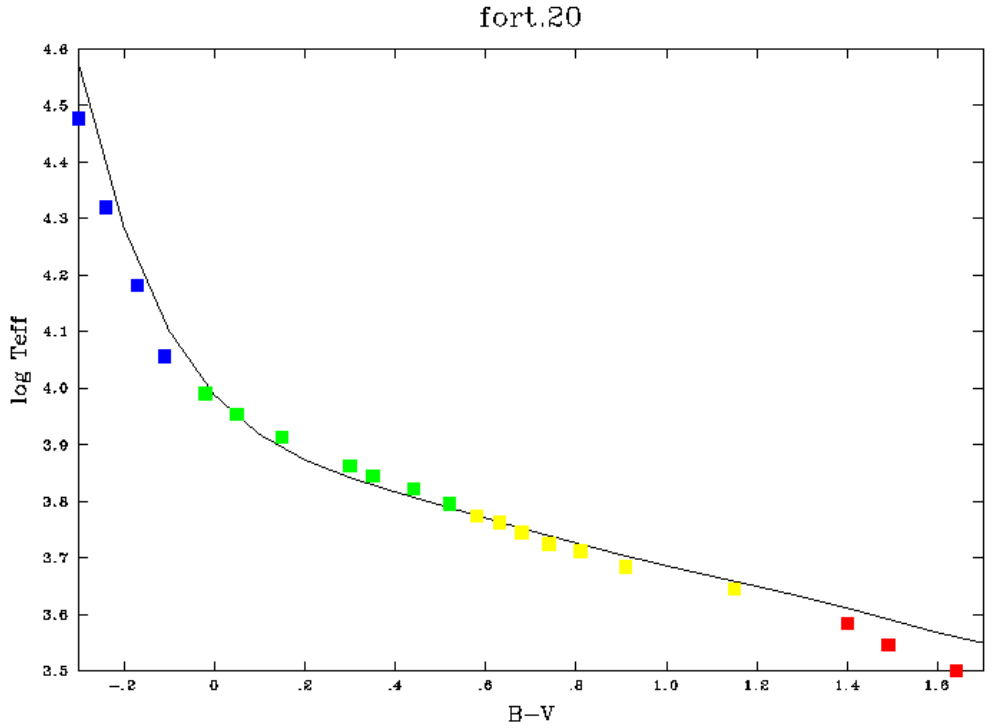

Spectroscopic methods

Equivalent Widths of Balmer lines

Good indicators of T_{eff} when T_{eff} <9000 K

If T_{eff} is higher, then indicators of log g.

Kurucz atmosphere models

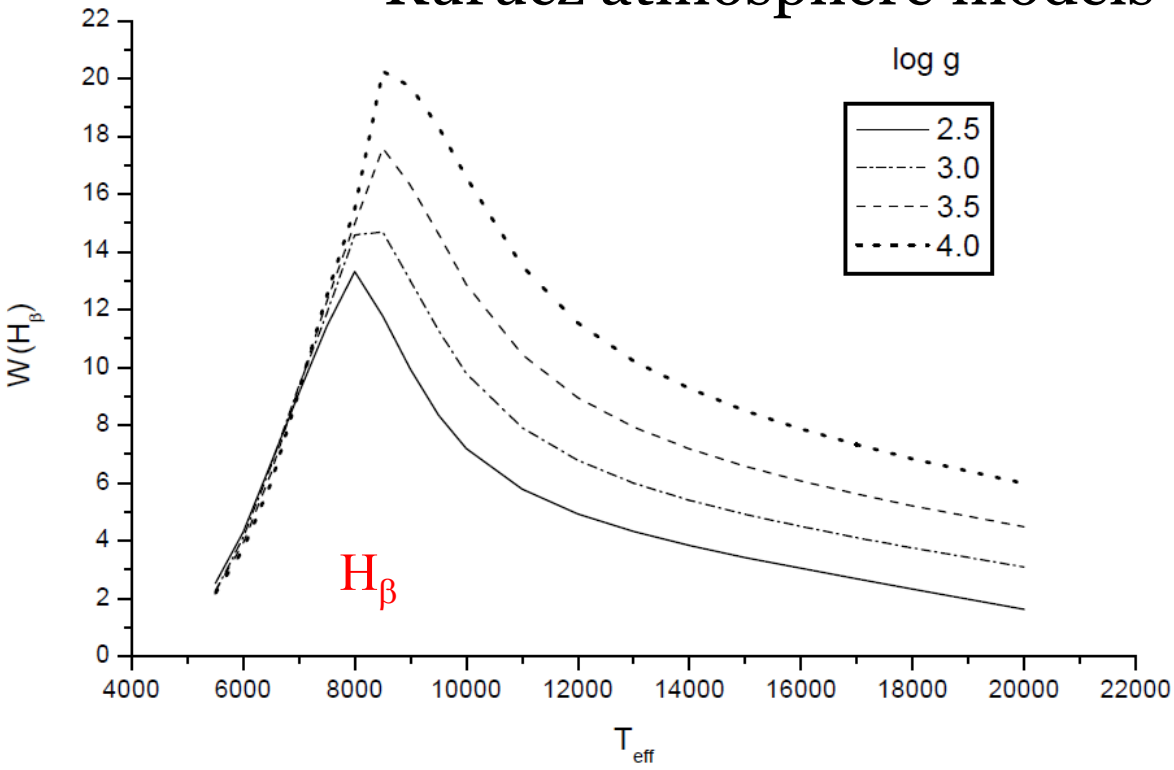

Spectroscopic methods

Wings of strong metal lines

Broadening:

Cool stars - **Van der Waals**

Hot stars - **Quadratic Stark**

Good indicators of g:

G, K, M stars: Na D, Ca I 4226, Mg I 5172, 5183

F, A, B stars: resonance lines Ca II, Mg II

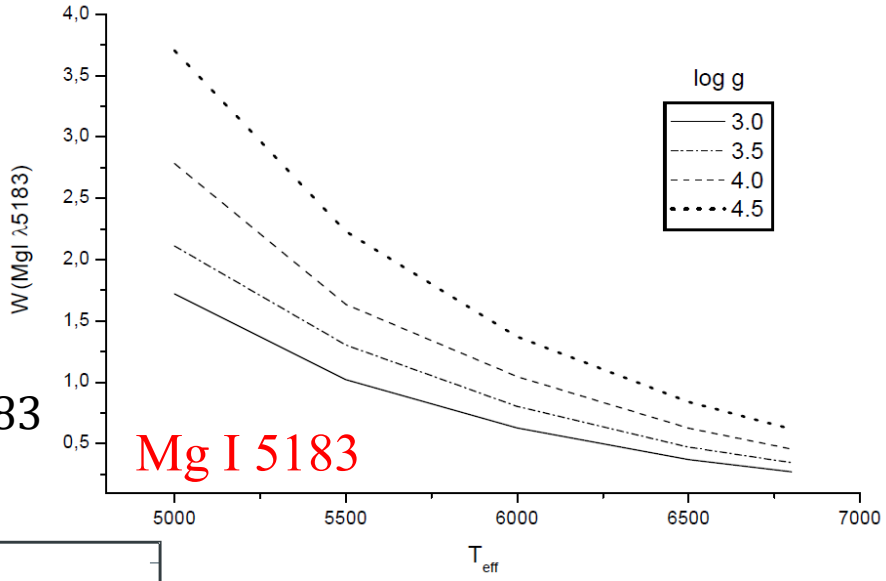

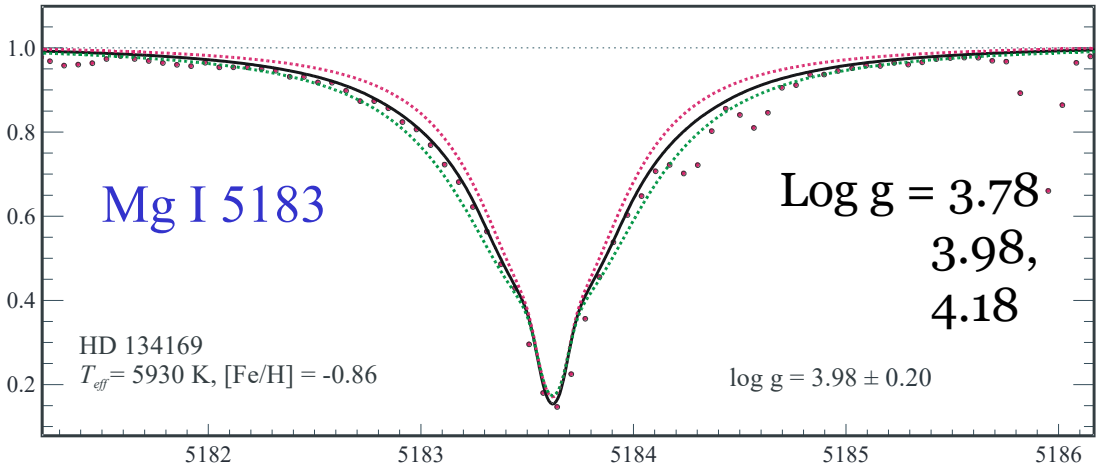

For example, Mg I 5183 is a good indicator of log g when T_{eff} <6000 K.

Spectroscopic methods

Equivalent Width ratios of species in two consecutive ionization states

G, K, M stars: Fe I and Fe II

O, B stars: He I and He II, Si III and Si IV

He I 4471/ He II 4511 can be an indicator of both $T_{\rm eff}$ and log g

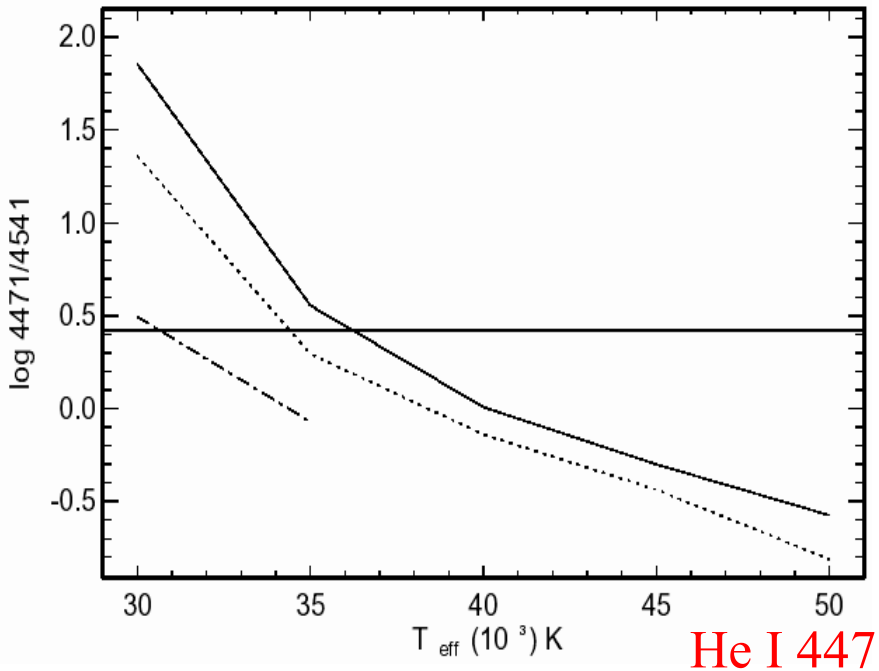

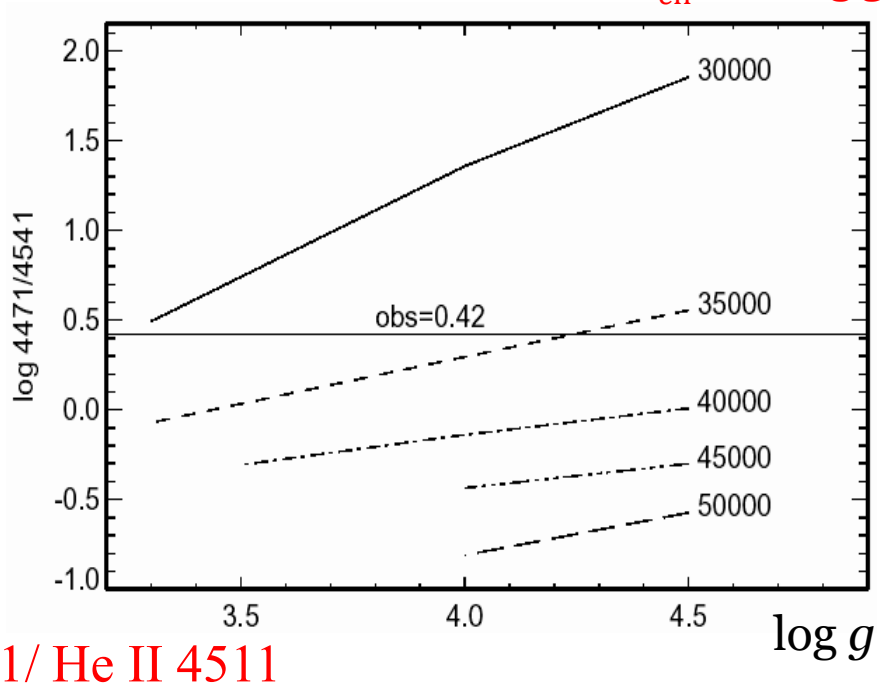

He I 4471/ He II 4511

Examples

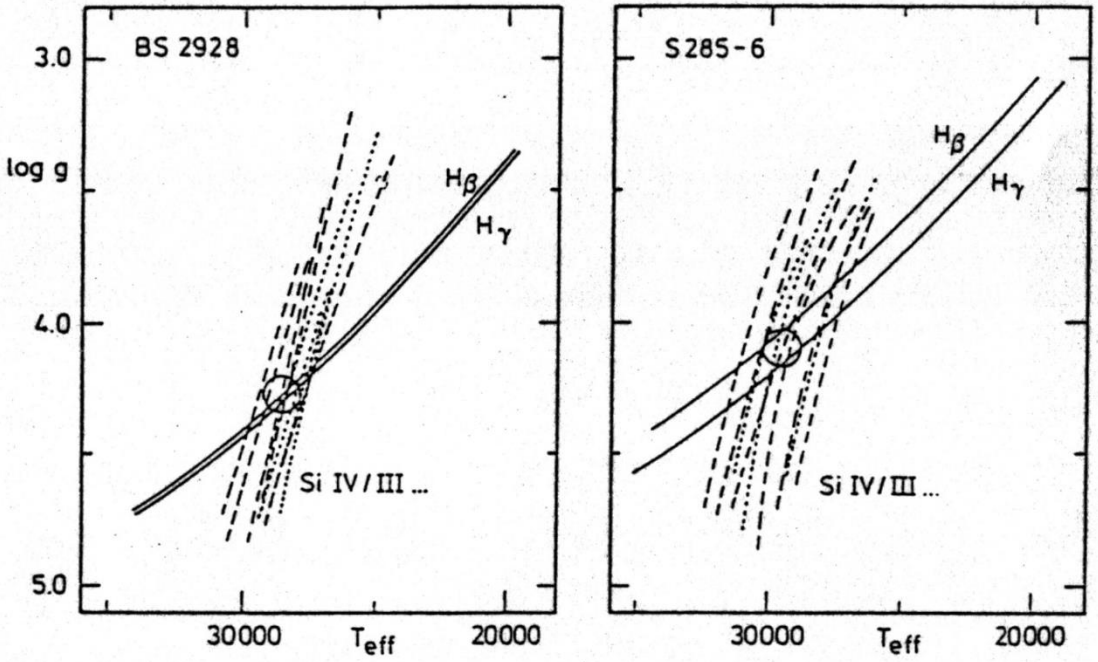

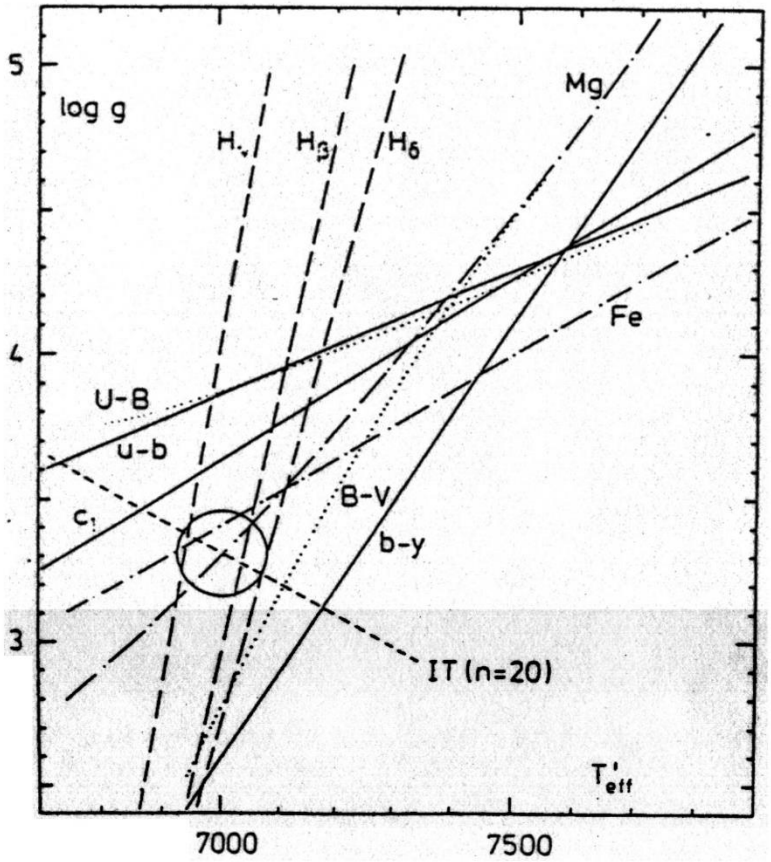

The different criteria for determining T_{eff} and $\log g$ are collected in the corresponding parameter plane with the final stellar parameters obtained from the mean intersection point

Summary

- Radii directly measured from interferometry (e.g. VLTI) if distance known from parallax (e.g. Gaia). Currently restricted to K & M giants.
- Masses/radii directly measured from close binaries. Otherwise, reliant upon models…
- Balmer jump sensitive to $T_{\rm eff}$ and $N_{\rm e}$ in F & G stars. (Discontinuity decreases with increasing $N_{\rm e}$ due to greater role of H^- ion)
- Balmer jump sensitive to $T_{\rm eff}$ in A & B stars (negligible role of H^- ion)
- Balmer jump absent in O stars (e.s. dominates opacity) so need to use line spectrum.